

THE UNIVERSITY OF HULL

**STABILISATION AND DESTABILISATION OF  
PICKERING EMULSIONS**

being a Thesis submitted for the Degree of Doctor of Philosophy in  
the University of Hull

by

Raojun Zheng  
MChem (Jiangnan University, China)

July 2020

## ACKNOWLEDGEMENTS

First and foremost, heartfelt thanks to my academic supervisor, Professor Bernard P. Binks. He has given me excellent guidance and constructive suggestions throughout the progress of this research. He has helped me a lot in improving the outline and the argumentation and correcting the grammatical errors for my every draft. This thesis could not be finished without your patient guidance. I am sincerely grateful to have had a wonderful time working with you.

I would like to thank my supervisors during my Master years, Professor Jianzhong Jiang and Professor Zhenggang Cui of Jiangnan University, China. They have continuously helped me with practical suggestions on conducting research work and encouraged me throughout my PhD project.

I also thank the China Scholarship Council for providing financial support to my PhD project.

Thanks to Niamh Turney who finished the experimental work on destabilisation of oil-in-water emulsions using solid particles as an MChem project. Niamh was well organized and did a fabulous job on experimental design and data collection, which helped a lot finishing this research. I would like to thank Mr. Timothy S. Dunstan for taking high-resolution SEM and cryo-SEM images.

Many thanks go to my colleagues and friends at the University of Hull for their help and friendship. Thanks go especially to Dr. Ana María Bago Rodríguez and Dr. Hui Shi for their guidance and fruitful discussions of my research work. I thank Dr. Jamie L. Stokes for his kind help in imaging particles at the planar oil-water interface.

Finally, I would like to express heartfelt gratitude to my family for their unconditional support and encouragement. Their love is always the source of my strength. Thanks particularly go to my other half, Lumin Fan, from whom I get tremendous love and comfort. Thanks also go to my best friend, Peiqian Li, for sharing news and gossip with me, and for enriching my life.

## ABSTRACT

In this thesis, the stabilisation and destabilisation of Pickering emulsions have been investigated. Organic electrolytes are added to hydrophilic silica and partially hydrophobic polystyrene latex particle dispersions to enable them to stabilise emulsions. A series of tetraalkylammonium salts ( $R_4NX$ , X is an anion) is added to aqueous dispersions of hydrophilic silica particles, with the alkyl chain (R) systematically increasing from 1 (methyl) to 4 (butyl). The adsorption of  $R_4N^+$  ions onto particle surface reduces the surface charge which increases the particle hydrophobicity. Consequently, the stability of oil-in-water (o/w) emulsions increases with salt concentration and the R chain length. In addition, we compare the arrangement of micron-sized silica particles at both curved droplet interfaces and at a planar oil-water interface in the presence of the butyl analogue.

Tetrapentylammonium bromide (TPeAB) and sodium thiocyanate (NaSCN) induce charge reversal of negatively charged sulfate ( $SO_4^-$ ) and positively charged amidine ( $C(NH)NH_3^+$ ) latex particles, respectively. However, charge reversal of particles hardly influences the type or stability of emulsions. Water-in-oil (w/o) emulsions are preferentially stabilised by both types of particles with dodecane. In systems with carboxyl latex particles, no charge reversal is induced by TPeAB at studied concentrations. However, emulsions invert from w/o to o/w upon increasing TPeAB concentration when PDMS (silicone oil) of viscosity 1 cS and 50 cS is used as the oil phase. It is intriguing that the surface charge of particles plays a minor role in the stabilization of emulsions whereas the hydrophobic polystyrene part dominates the emulsion type.

In addition, the destabilisation of both w/o and o/w Pickering emulsions using solid particles is explored. Destabilizers adsorb onto oil-water interfaces with the help of gentle stirring. If the particles are more wetted by the inner phase of droplets, the adsorbed particles traverse the interface entering the inner phase, which breaks the interface resulting in emulsion coalescence. Hence, monodispersed particles more wetted by the inner phase of droplets are preferred as the destabilizers. Overall, this research helps gain the understanding of particles at oil-water interface and expands the application of solid particles in the stabilization and destabilisation of emulsions.

## PUBLICATIONS AND PRESENTATIONS

The work contained within this thesis has given rise to the publications and contributed presentations as follows:

1. Zheng, R.; Binks, B.P. and Cui, Z. “Pickering emulsions of hydrophilic silica particles and symmetrical organic electrolytes”. *Langmuir* **2020**, *36*, 4619-4629.
2. Zheng, R. and Binks, B.P. “Pickering emulsions stabilised by hydrophobic polystyrene particles”. *J. Colloid Interface Sci.*, to be submitted (**2020**).
3. Zheng, R. and Binks, B.P. “Destabilisation of Pickering emulsions using solid particles”. *J. Colloid Interface Sci.*, to be submitted (**2020**).
4. Oral presentation: “Pickering emulsions stabilised by polystyrene particles”, University of Hull, Postgraduate Colloquium, 5 July 2019.
5. Poster presentation: “Pickering emulsions stabilised by polystyrene particles”, 33<sup>rd</sup> Conference of the European Colloid and Interface Society (ECIS), Leuven, 8-13 September 2019.
6. Poster presentation: “Pickering emulsions stabilised solely by hydrophilic silica particles in the presence of organic electrolytes”, 16<sup>th</sup> Conference of International Association of Colloid and Interface Science (IACIS), Rotterdam, 21-25 May 2018.

# CONTENTS

<b>ACKNOWLEDGEMENTS</b> .....	i
<b>ABSTRACT</b> .....	ii
<b>PUBLICATIONS AND PRESENTATIONS</b> .....	iii
<b>CONTENTS</b> .....	iv
<b>CHAPTER 1 - INTRODUCTION</b> .....	1
<b>1.1 Emulsions</b> .....	1
<i>1.1.1 Definition and type of emulsions</i> .....	1
<i>1.1.2 Phase inversion of emulsions</i> .....	2
<i>1.1.3 Destabilisation processes of emulsions</i> .....	3
<i>1.1.4 Surfactant as emulsifier</i> .....	7
<b>1.2 Stabilisation of Pickering emulsions</b> .....	9
<i>1.2.1 Free energy of particles adsorbing at an oil-water interface</i> .....	11
<i>1.2.2 Particle-particle interactions at oil-water interfaces</i> .....	13
<i>1.2.3 Factors affecting particle adsorption at an interface</i> .....	14
<i>1.2.4 Protocols of fabricating emulsions with hydrophilic particles</i> .....	16
1.2.4.1 Adjustment of pH in aqueous phase.....	16
1.2.4.2 Addition of indifferent salts in aqueous phase.....	17
1.2.4.3 Addition of organic salts .....	17
1.2.4.4 Addition of surfactant .....	18
1.2.4.5 Addition of oppositely charged particles or particles with different wettability .....	20
1.2.4.6 Addition of water-soluble oil .....	20
1.2.4.7 Addition of alcohol .....	21
1.2.4.8 <i>Ex situ</i> modification of particles .....	21
<b>1.3 Polystyrene latex colloids</b> .....	22
<i>1.3.1 Interactions of particles in colloidal suspensions</i> .....	22
<i>1.3.2 Charge reversal of polystyrene particles in electrolyte solutions</i> .....	26

<b>1.4 Destabilisation of Pickering emulsions</b> .....	27
1.4.1 <i>By adding fresh oil</i> .....	28
1.4.2 <i>By adding solute miscible with continuous phase</i> .....	29
1.4.3 <i>By adding surfactant</i> .....	30
<b>1.5 Presentation of thesis</b> .....	32
<b>1.6 References</b> .....	34
<b>CHAPTER 2 - EXPERIMENTAL</b> .....	45
<b>2.1 Materials</b> .....	45
2.1.1 <i>Particles</i> .....	45
2.1.1.1 Colloidal silica particles .....	45
2.1.1.2 Monodisperse silica particles .....	46
2.1.1.3 Fumed silica particles.....	46
2.1.1.4 Polystyrene latex particles .....	48
2.1.1.5 Zonyl MP 1100 and oligomeric tetrafluoroethylene (OTFE) particles .....	52
2.1.2 <i>Oils</i> .....	53
2.1.3 <i>Salts</i> .....	53
2.1.4 <i>Other materials</i> .....	53
<b>2.2 Methods</b> .....	54
2.2.1 <i>Preparation and characterisation of particle dispersions</i> .....	54
2.2.1.1 Measurement of zeta potential and particle size .....	54
2.2.1.2 Measurement of particle size by light diffraction .....	55
2.2.2 <i>Preparation and characterisations of emulsions</i> .....	55
2.2.2.1 Determining emulsion type .....	55
2.2.2.2 Monitoring emulsion stability .....	56
2.2.2.3 Optical microscopy .....	56
2.2.2.4 Measurement of droplet size by light diffraction.....	56
2.2.2.5 Cryogenic scanning electron microscopy .....	57

2.2.3	<i>Particles at a planar oil-water interface</i> .....	57
2.2.4	<i>Destabilisation of Pickering emulsions</i> .....	59
2.2.5	<i>Hydrophobisation of silica particles</i> .....	59
2.2.6	<i>Measurement of three-phase contact angle</i> .....	61
2.2.6.1	By sessile drop method .....	61
2.2.6.2	By gel-trapping technique .....	62
2.3	<b>References</b> .....	65
 <b>CHAPTER 3 - PICKERING EMULSIONS OF HYDROPHILIC SILICA PARTICLES AND SYMMERICAL ORGANIC ELECTROLYTES</b> .....		
3.1	<b>Introduction</b> .....	66
3.2	<b>Aqueous dispersion of silica particles</b> .....	68
3.3	<b>Emulsions stabilised by silica nanoparticles</b> .....	73
3.3.1	<i>Effect of salt concentration at a fixed particle concentration</i> .....	73
3.3.2	<i>Effect of particle concentration at a fixed salt concentration</i> .....	87
3.4	<b>Emulsions stabilised by micron-sized silica particles</b> .....	92
3.5	<b>Micron-sized silica particles at planar oil-water interfaces</b> .....	98
3.6	<b>Conclusions</b> .....	103
3.7	<b>References</b> .....	104
 <b>CHAPTER 4 - PICKERING EMULSIONS OF PARTIALLY HYDROPHOBIC POLYSTYRENE LATEX PARTICLES</b> .....		
4.1	<b>Introduction</b> .....	108
4.2	<b>Systems with sulfate latex particles</b> .....	110
4.2.1	<i>Aqueous dispersion of sulfate latex particles</i> .....	110
4.2.2	<i>Emulsions with dodecane as the oil phase</i> .....	115
4.3	<b>Systems with carboxyl latex particles</b> .....	124
4.3.1	<i>Aqueous dispersion of carboxyl latex particles at pH 11</i> .....	124
4.3.2	<i>Emulsions with dodecane at pH 11</i> .....	127
4.3.3	<i>Aqueous dispersion of carboxyl latex particles at pH 3</i> .....	132

4.3.4 <i>Emulsions with dodecane at pH 3</i> .....	135
4.3.5 <i>Emulsions with heptane at pH 11</i> .....	139
4.3.6 <i>Emulsions with 1 cS PDMS at pH 11</i> .....	144
4.3.7 <i>Emulsions with 50 cS PDMS at pH 11</i> .....	149
<b>4.4 Systems with amidine latex particles</b> .....	156
4.4.1 <i>Aqueous dispersion of amidine latex particles</i> .....	156
4.4.2 <i>Emulsions with dodecane as the oil phase</i> .....	159
<b>4.5 Conclusions</b> .....	166
<b>4.6 References</b> .....	168
<b>CHAPTER 5 - DESTABILISATION OF PICKERING EMULSIONS BY SOLID PARTICLES</b> .....	173
<b>5.1 Introduction</b> .....	173
<b>5.2 Destabilization of water-in-oil emulsions stabilized by polystyrene latex     particles</b> .....	174
5.2.1 <i>The effect of stirring on emulsions</i> .....	174
5.2.2 <i>By adding sub-micron silica particles</i> .....	178
5.2.2.1 <i>Addition of hydrophilic silica particles of varied size</i> .....	178
5.2.2.2 <i>Addition of 0.3 μm silica particles of varied concentration</i> .....	184
5.2.2.3 <i>Addition of 0.3 μm silica particles of varied hydrophobicity</i> ..	189
5.2.3 <i>By adding 2 μm hydrophilic silica particles</i> .....	196
5.2.3.1 <i>Destabilization at <math>\phi_w = 0.5</math></i> .....	196
5.2.3.2 <i>Destabilization at <math>\phi_w = 0.7</math></i> .....	204
5.2.3.3 <i>Possible mechanism of destabilization</i> .....	210
5.2.4 <i>By adding fumed silica particles</i> .....	223
5.2.4.1 <i>Effect of particle hydrophobicity</i> .....	223
5.2.4.2 <i>Effect of particle concentration</i> .....	229
<b>5.3 Destabilization of oil-in-water emulsions stabilized by fumed silica     particles</b> .....	235

5.3.1 Preparation of o/w emulsions stabilized by fumed silica particles	235
5.3.2 Destabilization by hydrophobic fumed silica particles	241
5.3.2.1 Effect of particle hydrophobicity	241
5.3.2.2 Effect of particle concentration	244
5.3.3 Destabilization by other hydrophobic particles	247
5.3.4 Destabilization by monodisperse silica particles	253
5.3.4.1 Addition of 0.3 $\mu\text{m}$ silica particles of varied hydrophobicity	253
5.3.4.2 Addition of 0.3 $\mu\text{m}$ silica particles of varied concentration	257
<b>5.4 Conclusions</b>	<b>260</b>
<b>5.5 References</b>	<b>261</b>
<b>CHAPTER 6 - SUMMARY OF CONCLUSIONS AND FUTURE WORK</b>	<b>264</b>
<b>6.1 Summary of conclusions</b>	<b>264</b>
<b>6.2 Future work</b>	<b>268</b>
<b>6.3 References</b>	<b>269</b>

## CHAPTER 1

### INTRODUCTION

#### 1.1 Emulsions

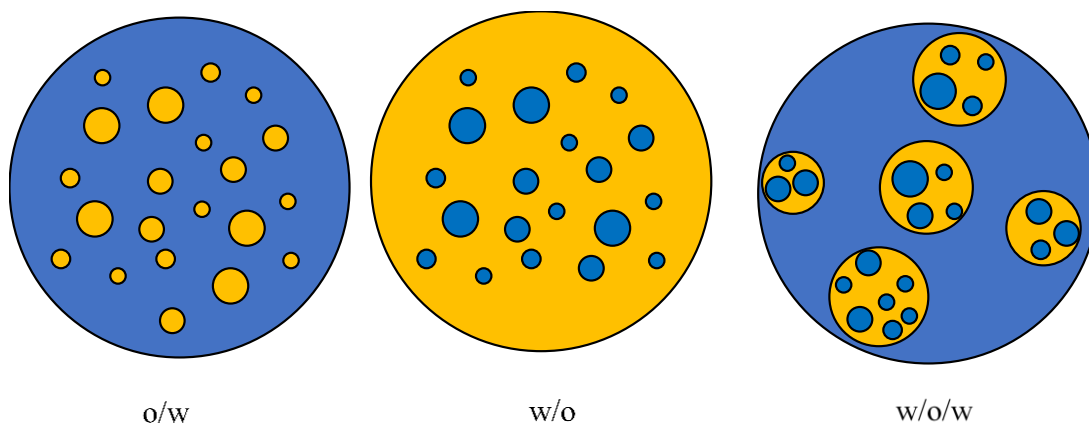
##### *1.1.1 Definition and type of emulsions*

An emulsion is a heterogeneous dispersion with one phase dispersed in a second immiscible liquid continuous phase as droplets.<sup>1</sup> Emulsions are widely encountered in our daily life, *e.g.* food emulsions such as mayonnaise and salad creams, personal care and cosmetics such as lotions and sunscreens.<sup>2</sup> In principle, emulsions can be classified into oil-in-water (o/w) and water-in-oil (w/o) type, depending on which phase is the dispersed phase, for example, oil droplets dispersed in water forms o/w emulsions.<sup>3</sup> A schematic of an o/w and w/o emulsion is shown in Figure 1.1. These two- phase systems are usually termed as simple emulsions. Multiple emulsions are complex systems consisting of more phases.<sup>4</sup> The simplest multiple emulsions are called double emulsions, which consist of three distinct phases. Typical double emulsions are water-in-oil-in-water (w/o/w) and oil-in-water-in-oil (o/w/o).<sup>4</sup> The former contains oil globules dispersed in water, with tiny water droplets dispersed inside the water globules. A schematic of w/o/w emulsion is also given in Figure 1.1. By contrast, o/w/o emulsions consist of tiny oil droplets entrapped within larger water globules, which are dispersed in a continuous oil phase. Multiple emulsions typically require two or more emulsifiers. For example, one surfactant of low hydrophile-lipophile balance (HLB) stabilising the inner water droplets, and the other one of high HLB stabilising the external oil globules.<sup>4</sup>

Generally, a typical emulsion formed from pure oil and water is milky white (as it scatters light) and the emulsion type can hardly be visually identified.<sup>5</sup> One simple method can help distinguish them, that is, the drop test.<sup>1</sup> When a drop of emulsion is added to a volume of either pure oil or pure water, a water continuous emulsion will be dispersed in water whereas an oil continuous emulsion will be dispersed in oil.<sup>1</sup> Another way is to measure the electrical conductivity of the emulsion, based on the fact that the conductivity of an emulsion is approximately equal to its continuous phase

and that an aqueous continuous phase displays higher conductivity than an oil one.<sup>3</sup> However, the above methods only determine the type of simple emulsions. For multiple emulsions, optical microscopy images are usually taken to confirm their structure.

**Figure 1.1.** Schematic of an oil-in-water (o/w), water-in-oil (w/o) and water-in-oil-in-water (w/o/w) emulsion.



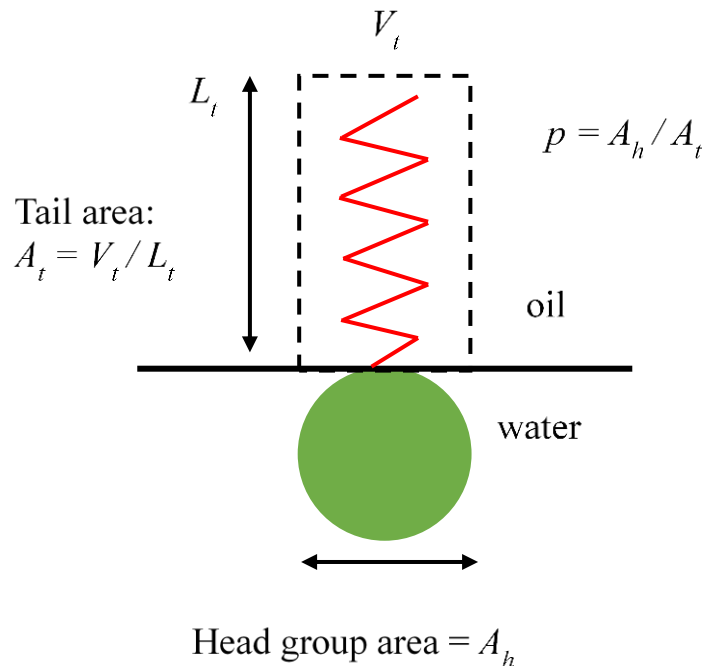
### 1.1.2 Phase inversion of emulsions

Phase inversion of emulsions means o/w emulsions converting to w/o or vice versa.<sup>3</sup> There are two primary ways of inducing phase inversion, namely, catastrophic inversion and transitional inversion.<sup>1</sup>

Catastrophic phase inversion is achieved by increasing the fraction of the dispersed phase, and a sudden change of emulsion type occurs at some point. This inversion occurs on systems with the characteristics of a catastrophe.<sup>1</sup> The preferred type of emulsion obtained during emulsification of a given oil and water mixture is dominated by the curvature that the emulsifier imparts to the oil-water interface.<sup>3</sup> For emulsions with surfactants as the stabiliser, the preferred curvature depends on the packing parameter ( $p$ ) of surfactant molecules at oil-water interface.<sup>3</sup> The  $p$  parameter is defined as the ratio of the area that the hydrophilic head group over the hydrophobic tail group subtended at the oil-water interface (see Figure 1.2). If  $p > 1$ , an o/w emulsion is preferred; if  $p < 1$ , then a w/o emulsion is preferred.<sup>3</sup> Catastrophic inversion is expected to occur more readily if the value of  $p$  is close to 1, in which case neither sign of curvature of the interface is strongly preferred.<sup>3</sup> In addition, the

catastrophic phase inversion is irreversible. The oil: water ratio for the inversion to occur when oil is added to water is not the same as when oil is added to water.<sup>1</sup>

**Figure 1.2.** Areas subtended by the head-group and tail of a surfactant molecule adsorbed at an oil-water interface, reproduced from ref. 3.



Transitional phase inversion is induced by gradually changing factors influencing the HLB of the system. For example, a change in temperature or salt concentration could invert a surfactant-stabilised o/w emulsion to a w/o emulsion, in which  $p$  changes from  $> 1$  to  $< 1$ . Transitional phase inversion is more common for emulsions.<sup>3</sup>

### 1.1.3 Destabilisation processes of emulsions

The droplet size of an ordinary emulsion lies in the range of several to tens of micrometers. There are also mini-emulsions in the range of 100 nm to 1  $\mu\text{m}$  and microemulsions with size  $< 100$  nm.<sup>3</sup> Macro- and mini-emulsions are considered thermodynamically unstable whereas microemulsions are thermodynamically stable. The free energy change  $\Delta G$  in going from a mixture of two liquids and forming an emulsion is given by:

$$\Delta G = \Delta A\gamma_{12} - T\Delta S_{conf} \quad (1.1)$$

where  $\Delta A$  is the change in interfacial area,  $\gamma_{12}$  is the interfacial tension between phase 1 and phase 2 at temperature  $T$  (in Kelvin) and  $\Delta S_{conf}$  is the configurational entropy change. The formation of an emulsion can be simply described as a sub-division of the dispersed phase into small droplets, during which the droplet number increases and  $\Delta S_{conf}$  is positive. In a system rendering pure water and pure oil as the components,  $\gamma_{12}$  is normally tens of  $\text{mN m}^{-1}$ , and the formation of an emulsion dramatically increases the interfacial area  $\Delta A$ , typically by a factor of  $10^4$  to  $10^5$ . However, the  $\Delta S_{conf}$  term is much lower in magnitude (and indeed is usually negligible) compared to the  $\Delta A\gamma_{12}$  term. Thus,  $\Delta G$  is positive and the emulsion is thermodynamically unstable, tending to revert to two bulk liquids, *i.e.* leading to phase separation.<sup>3,6</sup> Nevertheless, if there is surfactant in the system and the surfactant can reduce the interfacial tension to a sufficiently low value (ideally  $10^{-4}$  to  $10^{-2}$   $\text{mN m}^{-1}$ ), the  $\Delta A\gamma_{12}$  term will be relatively small thus allowing a negative  $\Delta G$  favoring spontaneous formation of microemulsions.<sup>6</sup>

As has been mentioned above, macroemulsions are thermodynamically unstable systems and tend to break in the absence of stabilisers. However, before breaking up, there are several processes that emulsion droplets will undergo, include creaming (or sedimentation), flocculation, coalescence and Ostwald ripening,<sup>5</sup> as illustrated in Figure 1.3.

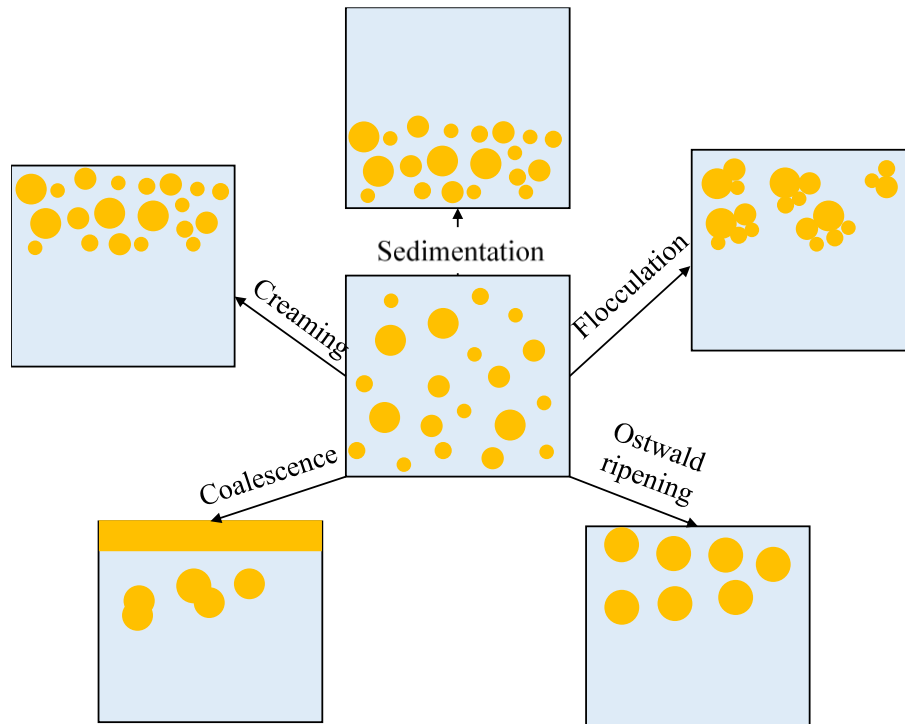
(a) Creaming (sedimentation)

Generally, there is a density difference between the two phases of an emulsion. Creaming is the process of droplets of lower density rising upward due to gravity or in a centrifuge to form a concentrated layer at the top of the sample. Sedimentation is the contrary, *i.e.* denser droplets submerge to the bottom. In this process, there is usually no change in the droplet size.<sup>1</sup> In a diluted emulsion, the speed ( $v_s$ ) of creaming (or sedimentation) of an isolated, spherical droplet is given by Stokes' Law:

$$v_s = \frac{2r^2(\rho_0 - \rho)g}{9\eta_0} \quad (1.2)$$

where  $r$  is the radius of the droplet,  $\rho_0$  and  $\rho$  are the density of the continuous phase and dispersed phase, respectively,  $g$  is the gravity acceleration and  $\eta_0$  is the viscosity of the continuous phase.<sup>1</sup> According to Equation 1.2, creaming (sedimentation) can be reduced by reducing the radius of the droplets, reducing the density difference between the two liquid phases or by increasing the viscosity of the continuous phase.<sup>1</sup>

**Figure 1.3.** Schematic destabilisation processes of an emulsion, redrawn from ref. 5.



(b) Flocculation

Flocculation refers to the formation of three-dimensional droplet aggregates driven by van der Waals attraction, but the interface between droplets does not rupture.<sup>1</sup> Flocculation increases the size of the droplet flocs and accelerates creaming or sedimentation in a gravitational field or centrifugal field, which is detrimental to the stability of the emulsion.

(c) Coalescence

Even though flocculation does not rupture the interface between droplets, it may produce a plane-parallel thin liquid film between them. In a film with no stabilising

moieties adsorbed at the surface, the thin film will drain continuously under the influence of inter-droplet van der Waals attraction resulting in a thinner film.<sup>3</sup> Subsequent vibration or oscillation finally ruptures the film, and as a consequence coalescence of the droplets occurs.<sup>3</sup> In the absence of stabilisers, droplet coalescence will continue until complete phase separation of the two constituent liquids occurs. In contrast, if there is stabiliser such as surfactant present, then the rate of droplet coalescence will be reduced.<sup>3</sup>

(d) Ostwald ripening

In a polydisperse system like an emulsion, smaller droplets will continue to dissolve while larger droplets constantly grow. As a result, emulsions may coarsen in size with time. This process, known as Ostwald ripening, indicates that even if coalescence does not occur in the system, the average droplet radius will increase resulting in reduced stability of the emulsion.<sup>1</sup> The mechanism of Ostwald ripening can be explained by the Kelvin equation:

$$\ln \frac{c_r}{c_0} = \frac{2\gamma V_m}{rRT} \quad (1.3)$$

where  $c_r$  is the aqueous phase solubility of oil ( $\text{m}^3 \text{m}^{-3}$ ) contained within a droplet of radius  $r$ ,  $c_0$  is the solubility of oil in the bulk phase,  $\gamma$  is the interfacial tension ( $\text{mN m}^{-1}$ ),  $V_m$  is the molar volume of oil ( $\text{m}^3 \text{mol}^{-1}$ ),  $R$  is the gas constant and  $T$  is the Kelvin temperature<sup>1</sup>. For a droplet with smaller radius, the solubility is higher. As a consequence, the smaller droplets dissolve and diffuse through the aqueous phase and enlarge bigger droplets.<sup>1</sup> The driving force of Ostwald ripening is associated with the existence of a pressure difference ( $\Delta P$ ) inside and outside the droplet, as given by the Laplace equation:

$$\Delta P = \frac{2\gamma}{r} \quad (1.4)$$

Equation 1.4 indicates that  $\Delta P$  is greater for the smaller droplets than for the larger ones.<sup>3</sup> Ostwald ripening is enhanced if the polydispersity of droplet size or the solubility of the molecules comprising the droplets in the continuous phase increases.

#### 1.1.4 Surfactant as emulsifier

It is extensively reported that pure oil and pure water can hardly stabilise emulsions, usually a third component known as an emulsifier is added to the system. Conventional emulsifiers are mainly amphiphilic compounds such as surfactants and amphiphilic polymers.<sup>5</sup> When surfactants are used as emulsifiers, there is usually a difference in the solubility of the surfactant molecule in the two liquid phases, considering the different hydrophilicity and lipophilicity of surfactants.

According to Bancroft's rule<sup>7</sup>, the phase with larger solubility of surfactant will become the continuous phase. Thus, o/w emulsions are obtained when water-soluble surfactants are used, whereas w/o emulsions are preferred when oil-soluble surfactants are used (exceptions exist however). The relative values of the hydrophilicity and lipophilicity of a surfactant can be characterized by the hydrophile-lipophile balance (HLB) number. Bancroft's rule<sup>7</sup> can be expressed as the HLB rule: when the surfactant has an HLB value of  $> 7$  (hydrophilic surfactant), o/w emulsion is preferable, otherwise when  $HLB < 7$  (lipophilic surfactant), w/o emulsion is more likely. When the HLB value of the surfactant is around 7, both types of emulsions are likely to be obtained but are generally unstable.<sup>8</sup>

The reasons why surfactants enhance the stability of an emulsion are summarized below:

##### (a) Lowering interfacial tension

A surfactant molecule contains both a polar and a non-polar part. When it dissolved in water, it tends to adsorb to the interface due to the hydrophobic effect: the hydrophobic moiety tends to keep away from water while the hydrophilic part remains in water.<sup>5</sup> Hence, surfactant molecules accumulate at the interface and form an oriented monolayer, until the critical micellization concentration (CMC) is reached. This process results in a decrease of the interfacial tension.<sup>5</sup>

##### (b) Forming an elastic interface film

Surfactant molecules adsorbing at the oil-water interface can form an oriented

monolayer interface film which can withstand a tangential stress.<sup>9</sup> That is, if surfactants adsorbed at the interface, when liquid flows along the interface, the flow tends to move the surfactant in the interface downstream thereby creating an interfacial tension gradient. In this way, lateral motion of the interface is prevented if a sufficiently large interfacial tension gradient is developed. The complement of the shear stress causing an interfacial tension gradient is the Marangoni effect: If for some reason an interfacial tension gradient exists, it will cause a shearing flow in the adjoining liquid.<sup>9</sup>

(c) Forming an intensive interfacial film

When the concentration of surfactant is lower than the CMC, the film strength will increase with surfactant concentration due to more molecules being available to adsorb at the interface. However, a highly purified surfactant cannot form a close-packed interfacial film. If a mixed surfactant is used, a mixed adsorption film can be formed at the interface, and the extent of adsorption can be greatly increased due to the interaction between different surfactants. Hence, the density and strength of the interfacial film can be increased, which increase the emulsion stability.<sup>8</sup>

(d) Forming an electrostatic or a steric barrier

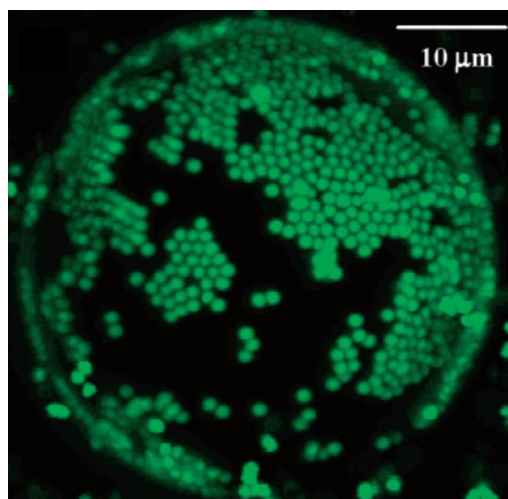
If the surfactant stabilising the emulsion is charged, the adsorption of charged species on the interface produces electrostatic repulsion. When two droplets get close to each other, the repulsion prevents them from being too close, thereby preventing flocculation and coalescence of the droplets.<sup>8</sup>

When nonionic surfactants or uncharged amphiphilic polymers are used as emulsifiers, the interfacial films are free of charge and thus do not produce an electrostatic barrier. However, these interface films will produce the so-called steric repulsion, which usually occurs when the two adsorbed layers overlap each other.<sup>8</sup> The distance is much smaller than the repulsive distance of the electric double layer, *i.e.* the two droplets are closer than that in the ionic surfactant systems.<sup>8</sup>

## 1.2 Stabilisation of Pickering emulsions

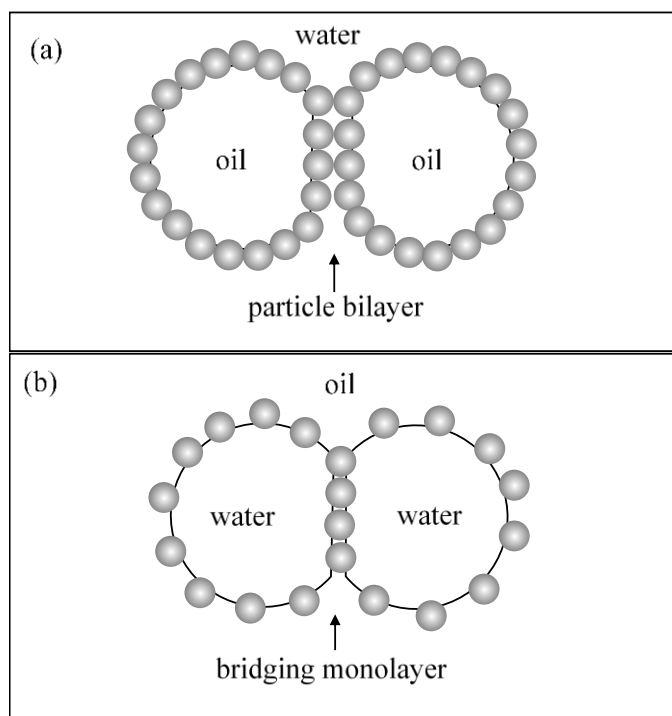
Pickering emulsions are emulsions stabilised by solid particles. The first report of such solid-stabilised emulsions is considered to be published by Pickering<sup>10</sup>. Although, according to his citation, Ramsden<sup>11</sup> reported an emulsion and a foam stabilised by protein particles four years earlier. Classical emulsions stabilised by surfactant usually have droplet diameters of several to tens of microns, whereas Pickering emulsions have droplet sizes from several micrometres to a few millimetres depending on the size of the particles used. Micron-sized solid particles can stabilise large droplets with a diameter of few millimetres.<sup>12</sup> General Pickering emulsions can be divided into o/w or w/o types,<sup>12-15</sup> which is similar to that of classical emulsions stabilised by surfactant. However, Pickering emulsions are not limited to o/w and w/o emulsions, oil-in-oil (o/o)<sup>16</sup> and water-in-water (w/w)<sup>17</sup> emulsions have recently aroused interest. The former consists of two immiscible oils (*e.g.* silicone oil + vegetable oil)<sup>16</sup>, while the latter consists of droplets of an aqueous phase dispersed into another immiscible aqueous phase.<sup>5,17</sup> Pickering emulsions not only retain the basic properties of classical emulsions, but also bring about specific properties, *e.g.* high stability to coalescence.<sup>12</sup> Adsorption of solid particles provides steric stability against coalescence. Figure 1.4 shows an oil droplet covered by sulfate treated polystyrene particles providing steric stability for the droplet.<sup>18</sup>

**Figure 1.4.** A three-dimensional fluorescent image of a poly(dimethylsiloxane)-in-water emulsion droplet stabilized by sulfate treated polystyrene particles. Reproduced from ref.18.



The mechanism for outstanding long-term stability of Pickering emulsions has been widely studied. In most systems, the steric mechanism accounts for it. As shown in Figure 1.5(a), particles adsorb around droplets forming close-packed monolayers and provide a robust physical barrier against coalescence. By contrast, emulsions stabilised at low surface coverage of particles have also been reported, and the bridging mechanism accounts for their stability.<sup>19-21</sup> In these emulsions, particles sparsely cover droplets but also accumulate in a dense monolayer bridging the droplets as illustrated in Figure 1.5(b). The sparse packing is due to strong long-range repulsion between highly hydrophobic particles, and the dense monolayer is induced by capillary attraction between particles caused by the deformed menisci around them.<sup>19</sup> Recently, it has been reported that bridging of droplets tends to occur in emulsions containing particles with a slight preference for the continuous phase.<sup>22</sup>

**Figure 1.5.** Two mechanisms of emulsion stabilisation by colloidal particles: (a) steric stabilisation of emulsion droplets covered with close packed particles, (b) bridging stabilisation of emulsion droplets covered with dilute particle monolayers. Reproduced from ref. 19.



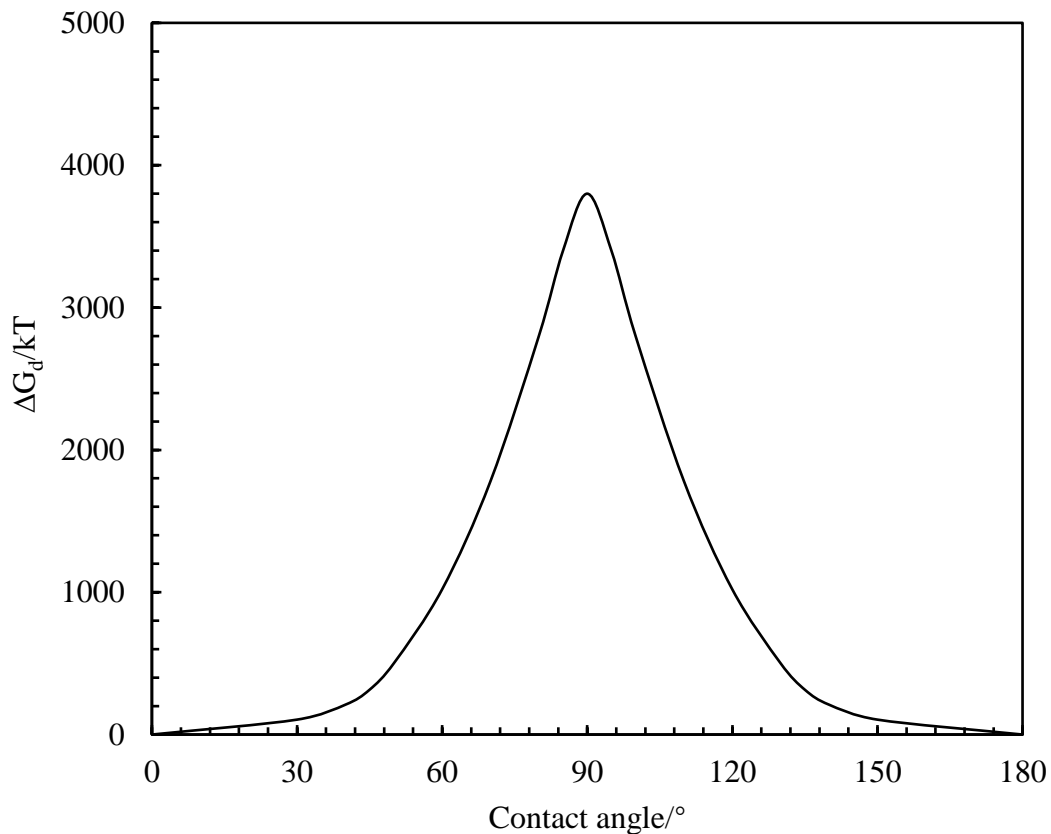
### 1.2.1 Free energy of particles adsorbing at an oil-water interface

For a spherical particle whose diameter ( $< 5 \mu\text{m}$ ) is much smaller than the emulsion droplet, the gravity of the particle is negligible.<sup>13</sup> When particles adsorb at an oil-water interface, the interface contact with particle can be treated as planar, the minimum energy needed for a particle of radius of  $r$  to detach from the interface of interfacial tension of  $\gamma_{ow}$  is given by the following equation:

$$\Delta G_d = \pi r^2 \gamma_{ow} (1 \pm \cos \theta)^2 \quad (1.5)$$

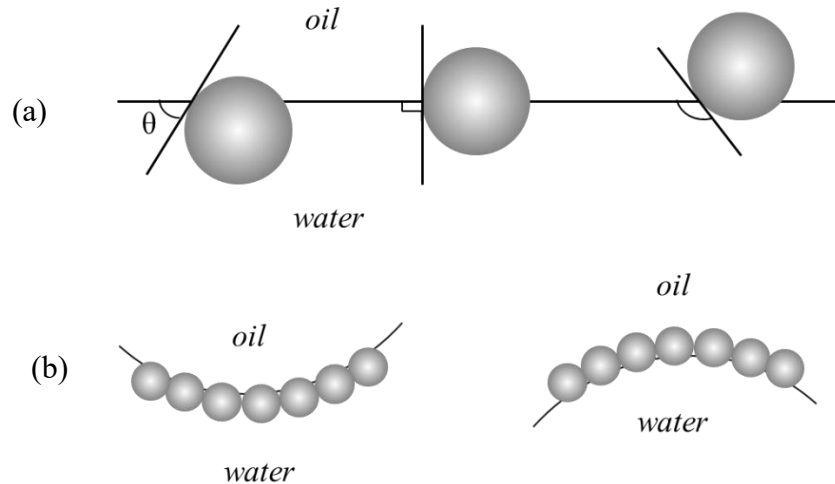
where  $\theta$  is the three-phase contact angle (usually measured into the aqueous phase and written as  $\theta_{o,w}$ ), “-” indicates that the particles enter the aqueous phase from the interface ( $0 \leq \theta \leq 90^\circ$ ), and “+” indicates that the particles enter the oil phase from the interface ( $90^\circ \leq \theta \leq 180^\circ$ ).<sup>6</sup> Figure 1.6 represents the dependence of the free energy of detachment ( $\Delta G_d$ ) on the contact angle of a spherical particle with  $r = 10 \text{ nm}$  and interfacial tension  $\gamma_{ow} = 50 \text{ mN m}^{-1}$  (typical of an alkane-water interface). Spherical particles with radius  $10 \text{ nm}$  and contact angle of  $10^\circ$  can hardly attach to the oil-water interface since their free energy of detachment is very small, approximately the thermal energy  $kT$  ( $k$  is the Boltzmann constant and  $T$  is the temperature).<sup>6</sup> On the other hand, very small particles ( $r < 0.5 \text{ nm}$ ) of the size comparable to most surfactant molecules are easily detached ( $< 10 kT$ ) and may not be effective as stabilisers.<sup>6</sup> However, for a particle with radius  $10 \text{ nm}$  and contact angle of  $90^\circ$ ,  $\Delta G_d$  is significantly higher ( $\sim 3800 kT$ ). Such particle will irreversibly adsorb at the oil-water interface providing superior stability for emulsions.<sup>6</sup>

**Figure 1.6.** Energy of particle detachment ( $\Delta G_d$ ) of a 10 nm particle from the oil-water interface with  $\gamma_{ow} = 50 \text{ mN m}^{-1}$  at 298 K as a function of the three-phase contact angle. Redrawn from ref. 6.



As described above, the energy needed for particle detachment from the interface rapidly increases when the three-phase contact angle gets closer to  $90^\circ$ . Therefore, for hydrophilic particles with  $\theta_{o,w} < 90^\circ$ , a larger portion of the particle would be submerged in water than in oil, and o/w emulsions are preferred, as illustrated in Figure 1.7. For hydrophobic particles with  $\theta_{o,w} > 90^\circ$ , the particle resides more in oil than in water, and w/o emulsions are preferred.<sup>15</sup>

**Figure 1.7.** (a) Position of a small spherical particle at a planar oil-water interface with a  $\theta_{o,w}$  less than  $90^\circ$  (left), equal to  $90^\circ$  (middle) and higher than  $90^\circ$  (right). (b) Corresponding probable position of particles at a curved oil-water interface. For  $\theta_{o,w} < 90^\circ$ , solid-stabilised o/w emulsions may form (left); for  $\theta_{o,w} > 90^\circ$ , solid-stabilised w/o emulsions may form (right). Reproduced from ref. 15.



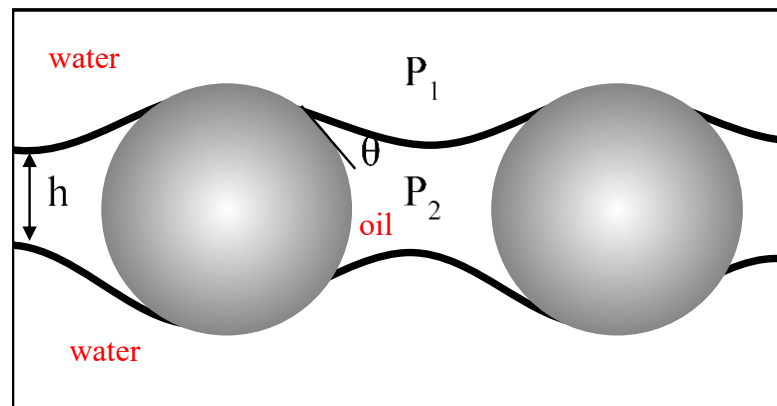
### 1.2.2 Particle-particle interactions at oil-water interfaces

When particles irreversibly adsorb to fluid-fluid interfaces, the interaction between particles is dependent on the particle characteristics as well as on the properties of the liquids forming the interface. The Derjaguin and Landau<sup>23</sup> and Verwey and Overbeek<sup>24</sup> (DLVO) model considers the interactions of particles in bulk liquids, which takes into account the electrostatic double layer repulsion and van der Waals attraction. The electrostatic double layer repulsion is due to the overlap of the electric double layers of particles, which is relatively short-range. The van der Waals attraction is instigated by an uneven electron distribution around the atoms creating a dipole, and by extension an asymmetrical charge distribution on a particle surface.<sup>25</sup> These interactions also apply to particles at oil-water interfaces.

On the other hand, for particles at fluid interfaces, due to partitioning of the particle surface between the two fluids, DLVO models do not capture the complete interaction between particles.<sup>26</sup> Long-range repulsion and capillary attraction are introduced. The long-range repulsive interactions are due to asymmetric charge dissociation in the polar liquid (*e.g.* water) and non-polar medium (oil or air), which leads to a dipole perpendicular to the interface.<sup>26</sup> Another source of long-range

repulsion is a small amount of residual surface charge at the oil-particle interface. As there is no charge in the oil phase, a small amount of charge is able to produce strong repulsion. Capillary attraction arises from the contact of particles with the fluid-fluid interface.<sup>27</sup> The pressure difference (Laplace pressure) inside ( $P_1$ ) and outside ( $P_2$ ) emulsion droplets results in a capillary pressure.<sup>28</sup> For emulsion droplets stabilised by the steric stabilisation mechanism, the oil-water interface is regarded as planar for adsorbed particles as the diameter of droplets is much larger than that of particles and the gravity of particles is negligible.<sup>27</sup> In this case, the capillary pressure equals zero. By contrast, for emulsions stabilised by the bridging mechanism, when particles adsorb at the interface of two neighbouring droplets, the laden particles deform the interface and create meniscus curvature on the interface (see Figure 1.8).<sup>28,29</sup> Increase of capillary pressure will result in an increase of meniscus curvature and a decrease of the separation of interfaces,  $h$ . The maximum capillary pressure indicates the threshold of film rupture, at which  $h$  equals zero. A higher maximum capillary pressure indicates a higher film stability to resist coalescence and also improved emulsion stability.<sup>28</sup>

**Figure 1.8.** Sketch of capillary attraction between particles at an oil-water interface. Reproduced from ref. 29.



### 1.2.3 Factors affecting particle adsorption at an interface

Successful preparation of stable emulsions requires particles adsorbing to the oil-water interface and then remaining there, which is the most common mechanism of emulsion stabilisation by solid particles.<sup>30</sup> The key factors involved in particle adsorption include the wettability, concentration, size and location of particles, pH and

the presence of electrolyte in the aqueous phase as well as oil polarity and other additives in the system.<sup>6</sup>

The wettability of particles which is reflected in the three-phase contact angle  $\theta_{o,w}$  can be a characterization of adsorption of particles onto interface.<sup>31</sup> When the particles are wetted equally by the oil and water phase ( $\theta_{o,w} \sim 90^\circ$ ), they can adsorb at the oil-water interface and form a coherent particle layer to prevent the droplet against coalescence. However, if the particles are either too hydrophilic ( $\theta_{o,w}$  is much lower than  $90^\circ$ ) or too hydrophobic ( $\theta_{o,w}$  is much higher than  $90^\circ$ ), they tend to remain dispersed in either the aqueous (low  $\theta_{o,w}$ ) or oil phase (high  $\theta_{o,w}$ ), respectively, and are not able to stabilise emulsions.<sup>13,31</sup>

Particle concentration is another factor affecting the stability of Pickering emulsions. Although there are reports showing that emulsion droplets can be stable against coalescence even with low surface coverage of droplets by particles, in most cases a high surface coverage is needed for emulsion stabilisation.<sup>6</sup> Limited coalescence is proposed to describe the effect of particle concentration.<sup>32-34</sup> Homogenization breaks one liquid into small droplets which will quickly coalesce until there are enough particles covering the droplet surface. This process results in growth of droplet size to a limiting value. If the total amount of particles is initially insufficient to fully cover the oil-water interfaces, the limited coalescence will give a relatively large droplet size.<sup>33</sup> Increase of initial particle concentration usually results in a decrease of final droplet size until coalescence is halted. Excess particles may increase emulsion stability by providing a three-dimensional network of particles surrounding droplets.<sup>6</sup> Arrested coalescence is another interesting phenomenon during the coalescence process of Pickering emulsions.<sup>35</sup> When two droplets collide and begin to coalesce, their complete merging into a single spherical drop can sometimes be arrested in an intermediate shape. The resultant arrested structure resembles a stable doublet that is a snapshot of an intermediate state of the coalescence process. The anisotropic Laplace stress within the arrested structure is balanced by the elastic modulus of the jammed interface and thus further relaxation of the arrested structure is halted. Arrested coalescence occurs within an intermediate surface coverage regime. If the droplets are completely covered by particles, their collision will result in total

stability, *i.e.*, non-coalescence. However, if the droplets are too sparsely covered by particles, their collision will lead to fully coalescence.<sup>35</sup>

#### 1.2.4 Protocols of fabricating emulsions with hydrophilic particles

A variety of particles, either inorganic or organic, have so far been studied as emulsion stabilisers. However, most particles, especially bare mineral particles, are usually very hydrophilic and unfavourable for the emulsification of non-polar oil.<sup>36</sup> Thus, efforts on tuning the wettability of hydrophilic particles to stabilise emulsions have been made in recent decades. Practically, people can control the wettability or flocculation of particles *via* modification of the surface chemistry or change the properties of the aqueous phase or the oil phase. Recently, Binks summarized the present strategies developed to tune the surface activity of particles, including adjustment of pH in the aqueous phase, addition of salt to the aqueous phase, addition of organic salt to the oil phase, addition of surfactant, addition of oppositely charged particles, addition of water-soluble oil, addition of alcohol and by *ex situ* modification of particles, some of which can also tune the flocculation of particles.<sup>37</sup>

##### 1.2.4.1 Adjustment of pH in aqueous phase

For particles containing ionizable surface groups such as -SiOH, -COOH or -NH<sub>2</sub>, altering the surface charge *via* changing the pH will change the wettability of particles, thus influencing the properties of emulsions they stabilise.<sup>37</sup> At pH values around the isoelectric point (IEP) of the solid, particles lose most of their surface charge and are able to adsorb at oil-water interfaces to stabilise emulsions. In contrast, at pH values far from the IEP, particles are highly charged and fully wetted by water, thus unable to stabilise emulsions.<sup>38-42</sup> In many cases, the influence of pH on the properties of an emulsion is reversible and pH-responsive emulsions can be designed. Double hydroxide (LDHs) particles,<sup>42</sup> hydroxyapatite nanoparticles,<sup>43</sup> Ludox CL silica particles<sup>44</sup> and fibrous palygorskite clay particles<sup>45</sup> have been used in pH stimulus-responsive Pickering emulsions. In addition, partially hydrophobic silica particle-stabilised w/o emulsions can be inverted from water-in-toluene to toluene-in-water by simply increasing the pH of the aqueous phase from 6 to 12.5.<sup>40</sup>

#### 1.2.4.2 Addition of indifferent salts in aqueous phase

Addition of salts to the aqueous phase is frequently employed to enable particles to stabilise emulsions.<sup>38,46-48</sup> The presence of salts on one hand suppresses the electrostatic repulsion between particles,<sup>49</sup> on the other hand they tend to flocculate particles in the aqueous phase promoting the formation of a particle network and enhancing the aggregation of emulsion drops.<sup>50-52</sup> These two functions synergistically promote the formation and stability of particle-stabilised emulsions.<sup>46</sup> However, extensive flocculation of particles induced by salts could lead to destabilisation of emulsions.<sup>38</sup> Compared with monovalent electrolytes like NaCl, multivalent electrolytes might have a more distinct effect on the stability of emulsions, given their significantly lower critical flocculation concentration.<sup>38</sup>

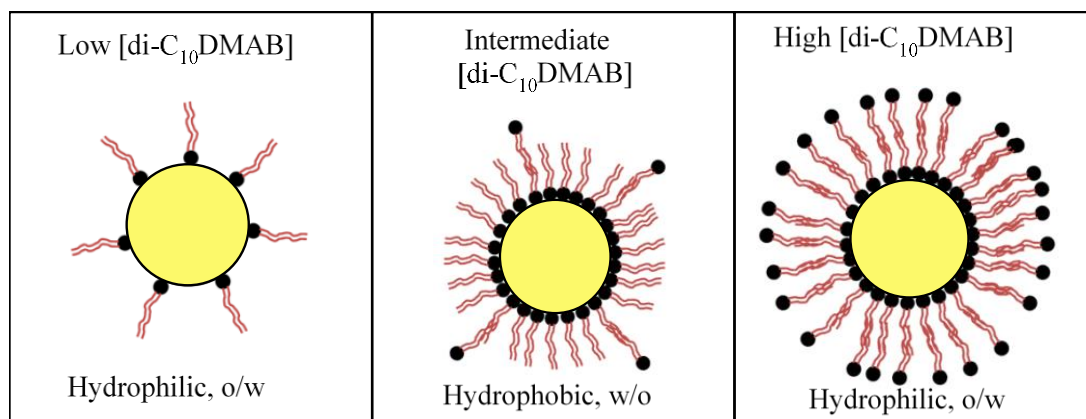
#### 1.2.4.3 Addition of organic salts

Recently, it was reported that metal nanoparticles can be driven to an oil-water interface by adding a “promoter”, which is an organic salt containing oppositely charged ions to that of the particles.<sup>53,54</sup> Therefore, addition of organic salts could be another effective protocol to enable hydrophilic particles to stabilise emulsions. Binks and Lumsdon explored the addition of tetraethylammonium bromide (TEAB) in water on the stability of emulsions.<sup>38</sup> In comparison to the cases of indifferent electrolytes such as NaCl, the mechanism of this organic salt influencing the stability of an emulsion is quite different. At low salt concentrations, it is due to the “hydrophobic” adsorption of TEA<sup>+</sup> ions onto neutral, undissociated silanol groups without displacing hydrated protons; whereas at high salt concentrations, there is a competition between TEA<sup>+</sup> ions and protons adsorbing directly onto negative, dissociated sites.<sup>38</sup> Some non-surface active amphiphiles can also serve as modifiers for particles. Akartuna and co-workers developed a versatile method that allows turning the hydrophobicity of many kinds of hydrophilic particles by adsorbing short chain carboxylic acids.<sup>55</sup> In addition, particles modified by 8-hydroxyquinoline (8-HQ)<sup>56</sup>, short-chain aliphatic amines<sup>57</sup>, methyl orange<sup>58</sup>, octyl gallate<sup>59</sup>, asphaltenes<sup>60</sup> and palmitic acid<sup>61</sup> in the stabilisation of different Pickering emulsions have been reported.

#### 1.2.4.4 Addition of surfactant

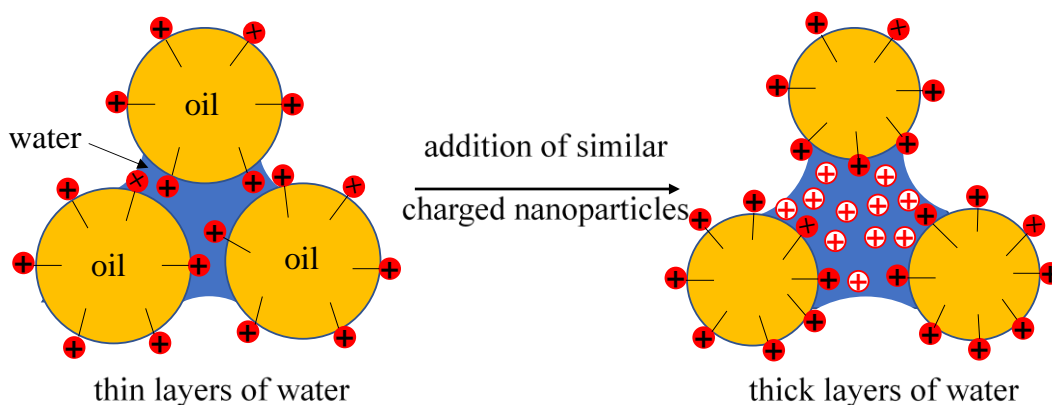
Modification of particle surface wettability by adding surfactants has been extensively studied, a process named *in situ* surface activation, enabling particles to become surface-active. Numerous examples have been presented in which surfactant was used to tune the hydrophilicity as well as the surface charge of particles and control the stability of Pickering emulsions.<sup>62-64</sup> Nonionic surfactants adsorb to hydrophilic particle surface and increase their hydrophobicity, consequently increasing the stability of emulsions. By electrostatic adsorption, oppositely charged surfactants to that of particles synergistically enhance the stability of emulsions. Binks *et al.* reported double inversion of an o/w emulsion by using a cationic surfactant diacyldimethylammonium bromides (di-C<sub>10</sub>DMAB).<sup>63,64</sup> Without any surfactant, silica particles are highly charged and unable to stabilise emulsions. In the presence of di-C<sub>10</sub>DMAB at low concentrations, positively charged surfactant headgroups adsorb on the surface of the nanoparticles, exposing the hydrophobic tails. But the limited adsorption of surfactant still exposes mostly the silica surface, which results in formation of o/w emulsions (left sketch in Figure 1.9). When the surfactant concentration increases to a particular value, the particle surface is tightly covered by hydrophobic tails, raising the particle hydrophobicity and giving w/o emulsions (center sketch). Further increase of di-C<sub>10</sub>DMAB concentration results in bilayer adsorption of surfactant molecules *via* chain-chain interaction in alkyl chains, now with positively charged headgroups toward the solution and favour o/w emulsions again (right sketch). Pickering emulsions can even be made stimuli-responsive in the presence of specific surfactants.<sup>64-67</sup>

**Figure 1.9.** Schematic of the effect of surfactant concentration on the adsorption of surfactant on particle surfaces and its influence on particle wettability and emulsion type. Reproduced from ref. 64.



Recently, Xu *et al.*<sup>68</sup> proposed another stabilisation mechanism of o/w emulsions containing a mixture of ionic surfactant and like-charged nanoparticles. Emulsion droplets are sparsely coated by ionic surfactant molecules. The addition of similarly charged nanoparticles in the aqueous phase repels surfactant molecules from the aqueous phase and promote their adsorption to oil-water interfaces. As illustrated in Figure 1.10, the adsorption of surfactant at the oil-water interface is slightly enhanced by particles through electrostatic repulsion, which reduces the interfacial tension and endows droplets with charge such that they repel other droplets and particles.

**Figure 1.10.** Sketch of enhanced stabilisation of surfactant-stabilised emulsions in the presence of similarly charged nanoparticles. Reproduced from ref. 68.



#### 1.2.4.5 Addition of oppositely charged particles or particles with different wettability

Addition of oppositely charged particles or particles with different hydrophobicity has been also effective in rendering particles to stabilise emulsions. Charged particles can interact strongly with oppositely charged particles. Abend and co-workers<sup>69</sup> were among the first researchers combining two kinds of oppositely charged particles to stabilise emulsions. They found that the combination of negatively charged bentonite and positively charged magnesium aluminum hydroxide further increased the coalescence stability of the emulsion. This was attributed to the build-up of a three-dimensional network of particles in the continuous phase, which reduced the mobility of emulsion droplets. The heteroaggregation of the particles lowered the net charge of the system and resulted in an increase of the hydrophobicity.<sup>70-75</sup> Saha *et al.*<sup>76</sup> mixed two phases containing hydrophilic nanoparticles in water and hydrophobic nanoparticles in oil, respectively. The attractive interactions between the hydrophilic and hydrophobic particles cause them to assemble at the oil-water interfaces into Janus-like clusters that effectively stabilise emulsions. Other examples using particles with different hydrophobicity to stabilise Pickering emulsions can also be found in the literature.<sup>77,18</sup>

#### 1.2.4.6 Addition of water-soluble oil

Many reports have demonstrated that highly hydrophilic particles cannot stabilise emulsions when a non-polar oil was used.<sup>30,72</sup> However, when a polar oil is used, or a water-soluble oil is added to the aqueous phase or oil phase, stabilisation of o/w Pickering emulsions by fully hydrophilic silica nanoparticles is achievable. Frelichowska *et al.* prepared Pickering emulsions using oils with different polarity and found that when polar oils were used, emulsions stable to coalescence were successfully fabricated with 6 wt.% silica in the aqueous phase, whereas emulsions of oils with lower polarity were not stable.<sup>78</sup> Binks and Yin added adipate oils to aqueous dispersions of hydrophilic fumed silica particles, which made the emulsions they stabilised stable to coalescence.<sup>36</sup> Due to the formation of H-bonds between the carbonyl group of oil molecules and the hydroxyl group on particle surfaces, adipate oils are able to adsorb onto particle surfaces and modify the surface hydrophobicity of

particles. Ridel *et al.*<sup>79</sup> reported a similar phenomenon using non-aggregated bare silica particles and diisopropyl adipate.

#### 1.2.4.7 Addition of alcohol

Addition of alcohol into the system can also drive charged hydrophilic particles to the oil-water interface, although reports on this are limited and mainly related to gold nanoparticles. Reincke and co-workers reported the phenomenon that gold nanocrystals spontaneously form a monolayer at the heptane-water interface by addition of ethanol to the aqueous phase.<sup>80</sup> The addition of ethanol to the sol decreases the surface charge of gold particles due to competitive adsorption of ethanol molecules, which displace the citrate or gold-chloride anions from the gold surface. Similarly, Park *et al.*<sup>81,82</sup> described the formation of 2-dimensional films consisting of highly ordered gold nanoparticles by adding 1-dodecanethiol into the oil and ethanol into the oil-water interface. The addition of ethanol decreases the interfacial energy, entrapping nanoparticles to the hexane-water interface. Then the 1-dodecanethiol in the hexane *in situ* coats onto nanoparticle surfaces, which converts the residual electrostatic repulsion between particles into van der Waals interaction. Although the reports above are all about the formation of planar nanoparticle films, the methodology can be applied to the stabilisation of Pickering emulsions. For example, Kubowicz *et al.*<sup>83</sup> prepared o/w emulsions stabilised by gold nanoparticles coated by hexane and undecanol ligand at a relative ratio of 1:6. The mixed-monolayer coating tuned the wettability of the particles and enabled them to stabilise Pickering emulsions.

#### 1.2.4.8 *Ex situ* modification of particles

Apart from *in situ* modification of hydrophilic particles as described above, researchers tried modifying the particles beforehand. For example, increasing the hydrophobicity of hydrophilic particles by surface coating, then employing them to stabilise Pickering emulsion. Such a protocol named *ex situ* modification has been extensively investigated. Silanizing reagents such as dichlorodimethylsilane (DCDMS) has been widely employed for the hydrophobization of particles. Silica particles can be hydrophobized to different extents by reacting with DCDMS at different concentrations, which results in different percentages of silanol groups and

dimethyldichlorosilane groups on particle surfaces.<sup>84-90</sup> Silane reagents can also coat other particle surfaces such as titanium dioxide and Fe<sub>3</sub>O<sub>4</sub>.<sup>91-93</sup>

### 1.3 Polystyrene latex colloids

A colloid is defined as a disperse system with one phase dispersed into another; the typical size of a colloidal particle is 5 nm to 5 μm.<sup>3</sup> Most colloidal dispersions are thermodynamically unstable as colloidal particles continually collide with each other due to Brownian motion, and as a result particles may associate.<sup>94</sup> The interactions between colloidal particles have been extensively studied theoretically and experimentally. Surfactant-free monodisperse polystyrene latices have long been considered as suitable model systems to study the fundamental properties of colloidal particles. These particles are spherical, monodisperse and usually have clean surfaces. The latex particles are stabilised by the electrical repulsion introduced by the charged groups on the surface which are covalently linked to the polymer molecules.<sup>95</sup>

#### 1.3.1 Interactions of particles in colloidal suspensions

The stability of aqueous colloidal dispersions is dependent on the interaction between particles. The DLVO theory considered the inter-particle interaction in the simplest manner, *i.e.* two spherical particles with the same radius in a diluted suspension.<sup>94</sup> The theory takes into account the attractive van der Waals force and the repulsive electrostatic forces between charged particles as they approach each other. The van der Waals interaction is a sum of the dipole-dipole force (Keesom force), dipole-induced dipole force (Debye force) and the dispersion force (London force).<sup>27</sup> The dispersion force is instigated by fluctuating dipoles due to the motion of the electrons in any atom, and this is the main source of attraction between colloidal particles. The van der Waals attraction is a long-range interaction which is comparable to the radii of colloidal particles. The attractive potential energy is directly proportional to particle radius ( $a$ ), a material constant, *i.e.* the Hamaker constant ( $A$ ), and is inversely proportional to the distance of separation ( $h$ ).<sup>3</sup> When the particle separation is small ( $h \ll 2a$ ), the attractive potential energy can be expressed as:

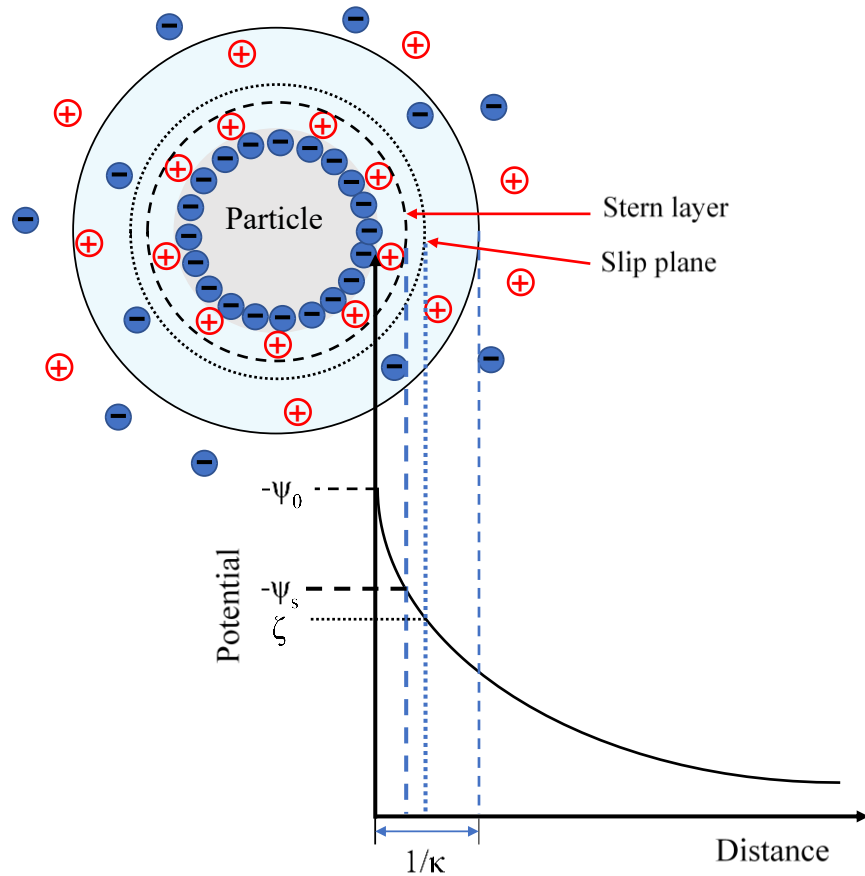
$$V_A = -\frac{Aa}{12h} \quad (1.6)$$

The Hamaker constant used in the calculation of the attractive potential is a geometric mean of that of the particle ( $A_p$ ) and that of the medium ( $A_m$ ) with respect to their values in vacuum,<sup>3</sup> as illustrated in the following equation:

$$A = (\sqrt{A_p} - \sqrt{A_m})^2 \quad (1.7)$$

Electrical repulsion is a result of the overlap of electrical double layers of particles, which is a key mechanism for the stabilisation of colloidal particles.<sup>3,27</sup> Electrical double layer theory has been developed to describe the electrical repulsive interaction between particles. The surface charge of particles arises from dissociation of surface groups or adsorption of ions from the solution. Particles will attract oppositely charged ions (counterions) to neutralize their surface charge, with the adsorbed counterions forming an electrical double layer around particles. Figure 1.11 illustrates the electrical double layer for a negatively charged particle along with the potential curve. The electrical double layer can be divided into two layers, *i.e.* a Stern layer and a diffuse layer.<sup>94</sup> The former contains a layer of counterions strongly bound to the surface and the latter contains counterions distributed freely in the solution. The thickness of the diffuse layer is characterized by the Debye length ( $1/\kappa$ ). The potential of the particle surface is termed as  $\psi_0$ , which can hardly be measured experimentally. A slip plane defines the region where the fluid moves together with the particles when an electrical field is applied in the solution. The potential at this plane is called the zeta potential ( $\zeta$ ) and is experimentally accessible.<sup>94</sup> When two particles approach each other, their electrical double layers overlap and the repulsive force hinders particles aggregating.

**Figure 1.11.** Schematic of the electrical double layer of a positively charged surface.  $\psi_0$  is the potential at the surface,  $\psi_s$  is the potential at the Stern layer and  $\zeta$  is the potential at the slip plane. Reproduced from ref. 94.



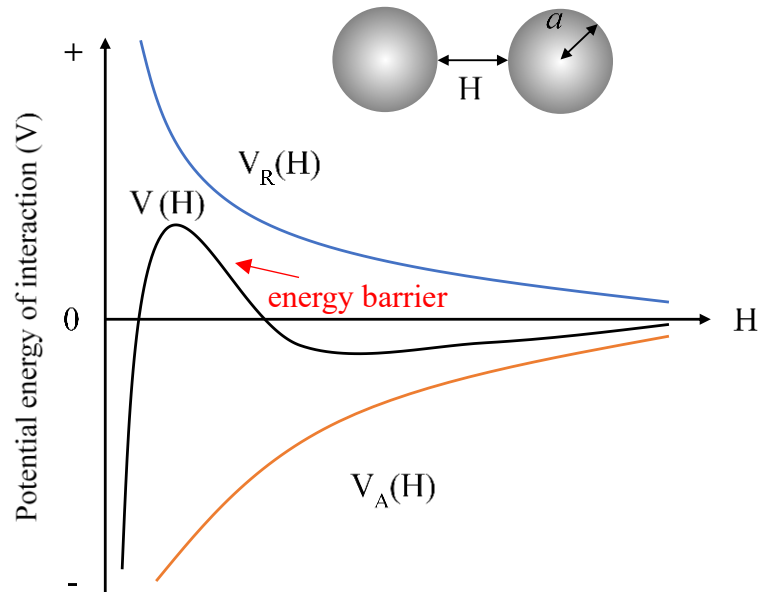
The total interaction between two particles is the combination of the van der Waals interaction energy and the electrical repulsive interaction energy, which can be expressed by:

$$V(H) = V_R(H) + V_A(H) \quad (1.8)$$

where  $V(H)$  represents the total interaction energy,  $V_R(H)$  and  $V_A(H)$  are the repulsive and attractive energy of two colloidal particles at separation  $H$ , respectively.<sup>3</sup> Figure 1.12 shows the potential energy curves of  $V(H)$ ,  $V_R(H)$  and  $V_A(H)$  against  $H$ . The curve of  $V(H)$  is a linear superposition of  $V_R(H)$  and  $V_A(H)$  which leads to a maximum in the curve. This maximum is known as the energy barrier and provides kinetic stability to a dispersion.<sup>3</sup> When two particles come together, it will result in aggregated particles if they collide with sufficient energy to overcome the barrier. Larger energy

barrier provides longer stability of the system.<sup>3</sup>

**Figure 1.12.** An example of the potential curves for the repulsive electrostatic interaction energy  $V_R(H)$ , the attractive van der Waals interaction energy  $V_A(H)$  and the total interaction  $V(H)$  of two colloidal particles of radius  $a$  at separation  $H$ . Reproduced from ref. 3.



An increase of electrolyte concentration will result in a reduction of the energy barrier due to screening of the electrical double layer. A critical coagulation concentration (C.C.C.) is introduced when there is no energy barrier and the inter-particle force is zero.<sup>3</sup> At C.C.C., the coagulation of the particles is controlled by diffusion and collisions of particles will result in coagulation. The valency of the counterions has a significant impact on the stability of charged colloids and the Shultz-Hardy rule formalized that the C.C.C. of an electrolyte decreases inversely proportional to the sixth power of the valency of the counterion.<sup>3</sup>

The classical DLVO theory successfully explains the behavior and the stability of many colloid systems. However, it fails to explain some phenomena where the coagulation behavior of particles is affected by the size of counterions with the same valency.<sup>96,97</sup> Non-DLVO forces are hence employed in the explanation of these phenomena, which can be distinguished into two cases: hydration forces and hydrophobic forces. Hydration forces occur between hydrophilic surfaces and arise

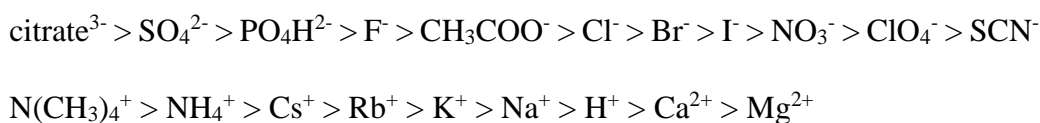
whenever water molecules strongly bind to a surface containing hydrophilic groups.<sup>27</sup> They are short-range repulsive forces. In contrast, hydrophobic forces are mediated by structural changes in the thin water layer between hydrophobic surfaces; they are attractive forces and longer range than hydration forces (up to 100 nm).<sup>27</sup>

### *1.3.2 Charge reversal of polystyrene particles in electrolyte solutions*

It has been widely accepted that the stability of colloid particles in aqueous dispersions is due to the presence of surface charge on particles. The presence of electrolytes in the aqueous phase will screen the surface charge and decrease the magnitude of the zeta potential. In the case of polystyrene latex particles, some electrolyte ions may specifically adsorb on particle surfaces, neutralizing the surface charge and even induce charge reversal of these particles. The surface charge of amidine (C(NH)NH<sub>2</sub>) latex particles changed from positive to negative on addition of poly(acrylic acid).<sup>98,99</sup> An analogous situation has been reported by Yu and co-workers in the mobility of anionic polystyrene sulfate latex particles in the presence of cationic poly(vinylamine).<sup>100</sup> Van den Hoven and Bijsterbosch observed charge reversal of negatively charged polystyrene latex particles induced by tetraamylammonium cations.<sup>101</sup> In addition, the highly symmetrical monovalent anion tetrapenylborate (Ph<sub>4</sub>B<sup>-</sup>)<sup>102</sup> and cation tetraphenyl arsonium (Ph<sub>4</sub>As<sup>+</sup>)<sup>103</sup> induces charge inversion of amidine polystyrene particles and sulfonated polystyrene particles, respectively. By comparing the experimental results with DLVO theory, Behrens and co-workers found that for the aggregation properties of carboxyl latex particles, classical DLVO theory was successfully applied at relatively low ionic strength ( $\leq 10$  mM).<sup>104</sup> However, at higher ionic strength, discrepancies between theory and experiment are observed. Maxima of the pair energy between particles were observed at surface separations of only a few Å, where non-DLVO forces have been observed.<sup>104</sup> Non-DLVO forces (*e.g.* structural forces or hydrophobic interaction forces) between colloidal particles have been widely involved in explaining the mechanism of charge reversal.<sup>103,105-107</sup> When organic counterions accumulate near the colloid surface, the hydrophobic groups adsorb onto the hydrophobic latex surface due to the hydrophobic effect.

In addition to organic electrolytes, some inorganic salts were also reported to induce charge reversal of polystyrene particles. Elimelech and O'Melia found that sulfate polystyrene latex particles in a trivalent salt (LaCl<sub>3</sub>) show lower mobility than

that in monovalent (KCl) and divalent (CaCl<sub>2</sub>) salts.<sup>108</sup> Although according to DLVO theory, trivalent cations are more effective in reducing the electrokinetic potential of colloidal particles than bivalent or monovalent cations, the charge reversal induced by LaCl<sub>3</sub> at high concentrations is beyond the framework of the theory.<sup>108</sup> Schneider *et al.* conducted similar investigations and found that at high concentrations of both Mg<sup>2+</sup> and La<sup>3+</sup> counterions accumulate at the very proximity of the particle surface leading to charge reversal.<sup>107</sup> Some theoretical simulations predict that charge inversion is possible to be induced by monovalent ions in the case of big ions due to steric effects, which is indeed observed experimentally. For example, monovalent ions (ClO<sub>4</sub><sup>-</sup> and SCN<sup>-</sup>) were reported to induce charge inversion of cationic amidine polystyrene latex particles.<sup>102</sup> The mechanism of charge reversal induced by inorganic ions was suggested to lie in ion-specific effects which was firstly observed in protein precipitation experiments that ions with the same valency induce different stabilisation power of protein solutions.<sup>109-112</sup> This ion specificity was also found in a wide range of phenomena (surface tension, colloid stability, etc.), in which ions consistently follow the same sequence, *i.e.* the Hofmeister series:



where anions (cations) to the left of Cl<sup>-</sup> (Na<sup>+</sup>) are customarily referred to as kosmotropic (chaotropic) ions and anions to the right of Cl<sup>-</sup> (Na<sup>+</sup>) as chaotropic (kosmotropic) ions.<sup>109</sup> Chaotropic ions break the water structure while kosmotropic ions promote the formation of water structure.<sup>110</sup>

#### 1.4 Destabilisation of Pickering emulsions

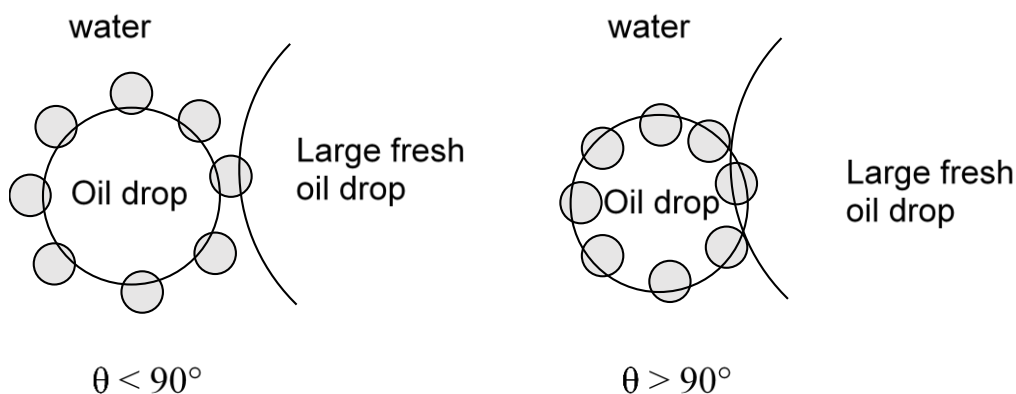
It is well-known that Pickering emulsions are extensively used in a variety of industries, however, in some processes such as enhanced oil recovery, mineral processing and pollution control, demulsification of such emulsions is also important. Mechanical protocols such as centrifugation have been used in industry to break such emulsions. However, the equipment and operating costs are fairly high.<sup>113</sup> To make emulsions stable or unstable on demand, particles are designed to attach or detach from oil-water interfaces by tuning the prevailing conditions. Employing these particles in emulsification, Pickering emulsions responsive to external stimuli such as

pH change, external electric field and magnetic field have been prepared. A comprehensive review on stimuli-responsive emulsions has been given by Tang *et al.*<sup>114</sup> Although a variety of stimuli mechanism have been developed, the application of emulsions responsive to specific stimulus is relatively narrow. For a general emulsion which is unresponsive to any stimulus, a relatively universal destabilisation method is required. Recently, Whitby and Wanless published a review on the destabilisation of Pickering emulsions and summarized the strategies to detach particles from fluid interfaces, which includes altering particle wettability, competitive displacement of particles at fluid interfaces, flocculating drops and particles, transferring mass between the liquid phases such as promoting Ostwald ripening and inducing coalescence of droplets by shear or compressive stress.<sup>115</sup> Herein, we focus on the destabilisation of Pickering emulsions by addition of an extra component to the emulsion.

#### *1.4.1 By adding fresh oil*

Yan and Masliyah investigated demulsification of oil-in-water emulsions stabilised by kaolinite clay particles ( $d = 0.2 \mu\text{m}$ ) by addition of fresh oil.<sup>116</sup> When fresh oil is added to mineral oil (Bayol-35)-in-water emulsions under gentle stirring, large fresh oil droplets are formed. Owing to the biwettable nature of the stabilising solids, they also have a tendency to adsorb at the new surface of the fresh oil droplet (see Figure 1.13). For hydrophilic particles ( $\theta < 90^\circ$ ), at the equilibrium position, only a smaller volume fraction of the particle remains in the oil phase and the emulsion droplets need not contact the large fresh oil droplets. Thus, the collision does not lead to a contact between interfaces of the two oil droplets and consequently no coalescence would occur. However, if the solids contact angle is higher than  $90^\circ$ , for equilibrium partitioning both the emulsion droplet and the large fresh oil droplet have a tendency to engulf a larger volume fraction of the particle. Consequently, the two oil droplets come into contact for possible coalescence. Therefore, the large fresh oil droplet acts as a scavenger which engulfs the small emulsion droplet. The larger the solids contact angle, the easier the engulfing process will be. The demulsification is enhanced with increasing mixing time, increasing the amount of fresh oil and increasing the clay contact angle. The increase in the rotational speed of the stirrer also enhances the collision rate and consequently increases the demulsification efficiency.<sup>117</sup>

**Figure 1.13.** Schematics showing the collision between a solids-stabilised oil droplet and a large fresh oil droplet. Reproduced from ref.116.



#### 1.4.2 By adding solute miscible with continuous phase

Malloggi *et al.* prepared emulsions stabilised by hydrophobic silica particles (using trimethyloxysilane) and destabilised them by addition of solvent miscible with the continuous phase.<sup>118</sup> When water was used as the aqueous phase, oil-in-water emulsions were obtained. The destabilisation of the emulsion can be achieved by addition of a short-chain alcohol (C<sub>1</sub>-C<sub>4</sub>). The addition of an amount of miscible solvent between 10% and 20% is generally sufficient to trigger the coalescence. Vigorous stirring or increasing the amount of miscible solvent enhances the destabilisation.<sup>118</sup> Similarly, hexadecane-in-water emulsions stabilised by yeast were destabilised by *iso*-butanol. A concentration of 10% (v/v) of *iso*-butanol resulted in a recovery of 96% initial oil.<sup>119</sup> It was proposed that the presence of polar and nonpolar moieties in the structure of alcohols shifts the kinetic equilibrium of emulsions. The alcohol molecules destabilise the emulsions by displacing surfactants from the interface. However, this mechanism applies for the destabilisation of surfactant-stabilised emulsions. The mechanism of the destabilisation of particle-stabilised emulsions by adding short chain alcohols is unclear.

Whitby *et al.* investigated destabilisation in emulsions of water drops coated by organoclay particles in organic solvents.<sup>120</sup> The clay particle surfaces are modified with waxy hydrocarbons and stabilise water-in-toluene emulsions. Destabilisation of the emulsion is induced by diluting the emulsions in polar solvents such as isopropyl

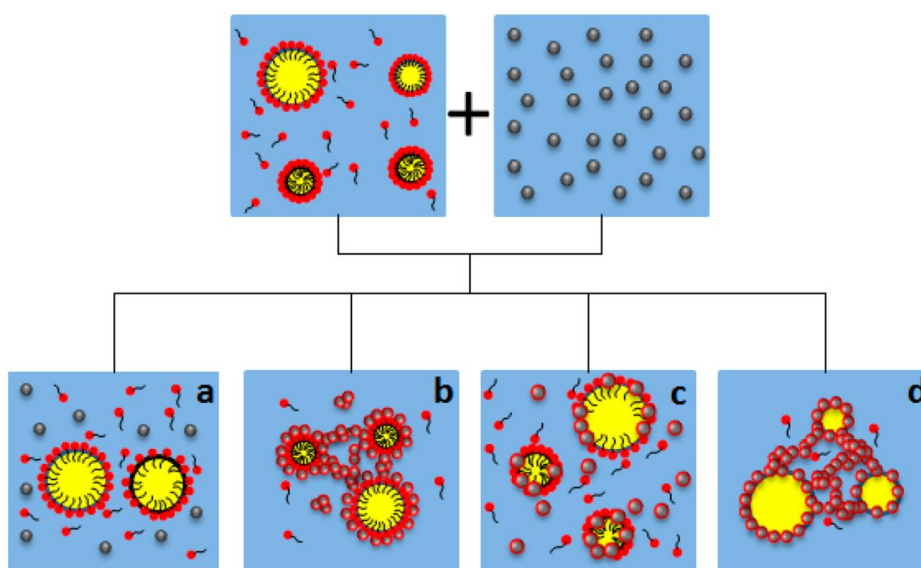
myristate (IPM), ethyl myristate and undecanol. If the emulsions are diluted in a poor-quality solvent such as IPM, the drops are destabilised due to flocculation. Aggregating drops tend to stick to each other, and the clusters assemble together into random networks of deformed drops. Rupture of the interfacial layer produces particle flocs and uncoated, unstable water drops that settle out of the emulsions. The drops coalesce if their particle coatings detach from the drop surfaces. The clay particle flocculation can be varied systematically in the emulsions by controlling the proportion of polar solvent in the organic phase. Akartuna *et al.* reported similar method of coalescing pairs of surfactant-stabilised water-in-fluorocarbon oil droplets by addition of a poor solvent for the surfactant.<sup>121</sup>

#### 1.4.3 By adding surfactant

Katepalli *et al.* observed detachment of particles from droplet surfaces of Pickering emulsions when surfactant is added to the prepared emulsions, although the detachment does not destabilise the emulsions.<sup>122</sup> Similarly, Whitby *et al.* found that the rate and extent of creaming and flocculation of the drops were enhanced when diluting dodecane-in-water emulsions stabilised by partially hydrophobized silica particles in surfactant at concentrations above the critical micelle concentration (CMC).<sup>123</sup> Furthermore, Vashisth and co-workers added surfactant to dodecane-in-water emulsions stabilised by silica nanoparticles. Complete displacement of particles by surfactant was observed upon application of shear.<sup>124</sup> It is speculated that surfactant adsorption occurs in the pores of the close packed particle layer. Perhaps the development of surface tension gradients as surfactant molecules adsorb on the drop surfaces enables particle detachment as drops collide during mixing. Once there is sufficient surfactant adsorption at the drop surfaces to enable drop fragmentation, then the faster rate of surfactant diffusion and adsorption at the interface will result in the fresh interface created being stabilised by surfactant molecules. Zhao *et al.* investigated demulsification of a Pickering emulsion to control solute release from water droplets.<sup>125</sup> Water-in-canola oil emulsions were stabilised by a high-melting surfactant glycerol monostearate (GMS), which forms interfacial crystalline shells around droplets upon cooling. Addition of a nonionic surfactant, sorbitan monooleate, permitted salt release due to gradual displacement of the interfacially adsorbed GMS layer by surfactant whose adsorption to the interface was energetically favoured.<sup>125</sup>

On the other hand, replacement of surfactant molecules by particles at emulsion droplet surfaces was observed by Katepalli and Bose.<sup>126</sup> They investigated the influence of negatively charged fumed silica on emulsions stabilised by anionic, cationic and nonionic surfactants. Addition of a particle suspension to the sodium dodecyl sulfate-stabilised emulsions showed no effect on emulsion stability. For emulsions stabilised with Triton X-100 (nonionic), an increase in droplet size with an increase in particle concentration was observed. Nonionic surfactants with ethoxylated groups can form hydrogen bonds with hydroxyl groups on silica surfaces. As the particle concentration increases, more surfactant becomes adsorbed on particle surfaces depleting surfactant from the interfaces. The loss of the stabilising amphiphile results in droplet coarsening. Strong attractive electrostatic interactions dominate between silica particles and cetyltrimethylammonium bromide (CTAB). As a result, the addition of fumed silica particles to CTAB-stabilised emulsions resulted in droplet coalescence and phase separation of oil and water or formation of particle-coated droplets, depending on the concentration of silica particles. Figure 1.14 shows the possible results of adding silica particles to different surfactant-stabilised emulsions. A follow-on report was published by Katepalli and co-workers regarding the effect of particle hydrophilicity on surfactant-stabilised emulsions.<sup>127</sup> The addition of partially hydrophobic fumed silica particles at relatively high concentrations resulted in phase separation of emulsions. Surface tension and interfacial tension measurements showed significant depletion of the surfactant from the aqueous phase in the presence of these particles.

**Figure 1.14.** Possible end states of adding colloidal particles to surfactant stabilised emulsions. (a) Emulsion remains stabilised by surfactant on weak or no particle-surfactant interactions; (b) Emulsion stabilised by particle-coated surfactant droplets on strong particle-surfactant interaction under gentle mixing; (c) Breaking of emulsion on strong particle-surfactant interaction under vortex mixing; (d) Particle network stabilised emulsion on strong particle-surfactant interaction and high concentration of particles. Reproduced from ref.126.



## 1.5 Presentation of thesis

The aim of this research is to understand the adsorption and desorption of solid particles at oil-water interfaces. Investigations have been mainly conducted on Pickering emulsions stabilised by different particle types. The arrangement of silica particle monolayers at planar oil-water interfaces has also been studied to compare with the same particles adsorbing at droplet surfaces. Chapter 2 describes all the experimental materials and methods used throughout this research. Chapter 3 concerns octane-in-water emulsions stabilised by hydrophilic silica particles in the presence of symmetrical organic electrolytes added to water. It contains four main investigations, namely, the behavior of silica nanoparticles in aqueous dispersions in the presence of electrolytes, emulsions stabilised by nano-sized silica particles, emulsions stabilised by micron-sized silica particles and the arrangement of micron-sized particles at a

planar octane-water interface. For emulsions stabilised by silica particles, the effect of electrolyte concentration as well as particle concentration on the stabilisation of emulsions has been investigated.

Chapter 4 investigates emulsions stabilised by nano-sized polystyrene (PS) latex particles with three different surface groups (sulfate, amidine and carboxyl) which endow particles with positive ( $-\text{C}(\text{NH})\text{NH}_3^+$ ) or negative ( $-\text{SO}_4^-$  and  $-\text{COO}^-$ ) charge. Particles are received in aqueous dispersion but possess hydrophobic surfaces. The presence of oppositely charged electrolytes to that of particles reduces the surface charge and even induces charge reversal of particles, which promotes the stability of emulsions stabilised by these particles. This chapter is divided into three main topics; systems with sulfate latex particles, systems with carboxyl latex particles and systems with amidine latex particles. In each system, the effect of electrolyte concentration on the stability and type of emulsions has been investigated. In addition, the three-phase contact angle of each type of particle (micron-sized) at a planar oil-water interface has been measured using the gel-trapping technique (GTT).

Chapter 5 explores the destabilisation of Pickering emulsions using solid particles. Firstly, the destabilisation of water-in-dodecane emulsions stabilised by carboxyl latex particles and destabilised by silica particles is described. Monodisperse silica particles of varied size as well as fumed silica particles were used as destabiliser. The effect of particle size, particle concentration and particle hydrophobicity on the efficiency of destabilisation has been studied. In addition, the mechanism of destabilisation of w/o emulsions by silica particles has been deduced. Secondly, the destabilisation of oil-in-water emulsions stabilised by fumed silica particles and destabilised by solid particles is presented. Fumed silica particles of varied hydrophobicity, monodisperse oligotetrafluoroethylene (OTFE) and polytetrafluoroethylene (PTFE) particles as well as monodisperse silica particles of varied hydrophobicity have been employed as the destabiliser. Similarly, the effect of particle hydrophobicity and particle concentration on the destabilisation efficiency has been investigated.

Chapter 6 is a summary of the thesis. The conclusions of each chapter are presented along with suggestions for future work.

## 1.6 References

1. Binks, B.P. *Modern Aspects of Emulsion Science*, Royal Society of Chemistry, Cambridge, **1998**, ch. 1, pp. 1-48.
2. Tadros, T.F. *Emulsion science and technology: a general introduction*, Wiley-VCH, Weinheim, **2009**, ch.1, pp.1-56.
3. Cosgrove, T. *Colloid Science: principles, methods and applications*, John Wiley & Sons Ltd, Chichester, **2010**, ch.6, pp.117-134.
4. Aserin, A. *Multiple emulsion: technology and applications*, John Wiley & Sons Ltd, Hoboken, **2008**, ch.1, pp.1-27.
5. Tadros, T.F. *Applied Surfactants: principles and applications*, WILEY-VCH, Weinheim, **2006**, ch. 6, pp. 115-186.
6. Binks, B.P. and Horozov, T.S. *Colloidal Particles at Liquid Interfaces*, Cambridge University Press, Cambridge, **2006**, ch. 6, pp.186-224.
7. Bancroft, W.D. The theory of emulsification, *J. Phys.Chem.***1913**, *17*, 501-519.
8. Rosen, M.J. and Kunjappu, J.T. *Surfactants and Interfacial Phenomena*, John Wiley & Sons Ltd, Hoboken, **2012**, pp. 336-391.
9. Becher, P. *Encyclopedia of Emulsion Technology*, Marcel Dekker, New York, **1996**, volume 4, pp. 1-62.
10. Pickering, S.U. Cxcvi.-emulsions. *J. Chem. Soc.* **1907**, *91*, 2001-2021.
11. Ramsden, W. Separation of solids in the surface-layers of solutions and 'suspensions'(observations on surface-membranes, bubbles, emulsions, and mechanical coagulation).-Preliminary account. *Proc. Roy. Soc.* **1904**, *72*, 156-164.
12. Chevalier, Y.; Bolzinger, M.A. Emulsions stabilized with solid nanoparticles: Pickering emulsions. *Colloids Surf. A* **2013**, *439*, 23-34.
13. Aveyard, R.; Binks, B.P. and Clint, J.H. Emulsions stabilised solely by colloidal particles. *Adv. Colloid Interface Sci.* **2003**, *100*, 503-546.
14. Hunter, T.N.; Pugh, R.J.; Franks, G.V. and Jameson, G.J. The role of particles in stabilising foams and emulsions. *Adv. Colloid Interface Sci.* **2008**, *137*, 57-81.
15. Binks, B.P. Particles as surfactants-similarities and differences. *Curr. Opin. Colloid Interface Sci.* **2002**, *7*, 21-41.

16. Binks, B.P. and Tyowua, A.T. Oil-in-oil emulsions stabilised solely by solid particles. *Soft Matter* **2016**, *12*, 876-887.
17. Esquena, J. Water-in-water (W/W) emulsions. *Curr. Opin. Colloid Interface Sci.* **2016**, *25*, 109-119.
18. Tarimala, S. and Dai, L.L. Structure of microparticles in solid-stabilized emulsions. *Langmuir* **2004**, *20*, 3492-3494.
19. Horozov, T.S. and Binks, B.P. Particle-Stabilized Emulsions: A Bilayer or a Bridging Monolayer? *Angew. Chem. Int. Ed.* **2006**, *118*, 787-790.
20. Xu, H.; Lask, M.; Kirkwood, J. and Fuller, G. Particle bridging between oil and water interfaces. *Langmuir* **2007**, *23*, 4837-4841.
21. French, D.J.; Brown, A.T.; Schofield, A.B.; Fowler, J.; Taylor, P. and Clegg, P.S. The secret life of Pickering emulsions: particle exchange revealed using two colours of particle. *Sci. Rep.* **2016**, *6*, 1-9.
22. French, D.J.; Taylor, P.; Fowler, J. and Clegg, P.S. Making and breaking bridges in a Pickering emulsion. *J. Colloid Interface Sci.* **2015**, *441*, 30-38.
23. Derjaguin, B. and Landau, L.D. Theory of the stability of strongly charged lyophobic sols and of the adhesion of strongly charged particles in solutions of electrolytes. *Acta Physicochim. USSR* **1941**, *14*, 633-662.
24. Verwey, E.J.W. and Overbeek, J.T.G. *Theory of the stability of lyophobic colloids*, Elsevier, Amsterdam, **1948**.
25. Butt, H.J. and Kappl, M., *Surface and Interfacial Forces*, John Wiley & Sons Ltd, Weinheim, **2018**, ch. 3, pp. 43-98.
26. Park, B.J.; Ngai, T.; Zhao, H.; Bon, S.A.; Clegg, P.; Wang, C.; Nonomura, Y.; Biggs, S.; Norton, I. and Xu, Z., *Particle-stabilized Emulsions and Colloids: formation and applications*, Royal Society of Chemistry, Cambridge, **2014**, ch. 2, pp. 8-44.
27. Butt, H.J. and Kappl, M., *Surface and Interfacial Forces*, John Wiley & Sons Ltd, Weinheim, **2018**, ch. 5, pp. 131-166.
28. Denkov, N.; Ivanov, I.; Kralchevsky, P. and Wasan, D. A possible mechanism of stabilization of emulsions by solid particles. *J. Colloid Interface Sci.* **1992**, *150*, 589-593.
29. Kaptay, G. On the equation of the maximum capillary pressure induced by solid particles to stabilize emulsions and foams and on the emulsion stability diagrams. *Colloids Surf. A* **2006**, *282*, 387-401.

30. Binks, B.P. and Whitby, C.P. Nanoparticle silica-stabilised oil-in-water emulsions: improving emulsion stability. *Colloids Surf. A* **2005**, *253*, 105-115.
31. Maestro, A.; Guzmán, E.; Ortega, F. and Rubio, R.G. Contact angle of micro- and nanoparticles at fluid interfaces. *Curr. Opin. Colloid Interface Sci.* **2014**, *19*, 355-367.
32. Wiley, R. Limited coalescence of oil droplets in coarse oil-in-water emulsions. *J. Colloid Sci.* **1954**, *9*, 427-437.
33. Arditty, S.; Whitby, C.P.; Binks, B.P.; Schmitt, V. and Leal-Calderon, F. Some general features of limited coalescence in solid-stabilized emulsions. *Eur. Phys. J. E* **2003**, *11*, 273-281.
34. Whitesides, T.H. and Ross, D.S. Experimental and theoretical analysis of the limited coalescence process: stepwise limited coalescence. *J. Colloid Interface Sci.* **1995**, *169*, 48-59.
35. Pawar, A.B.; Caggioni, M.; Ergun, R.; Hartel, R.W. and Spicer, P.T. Arrested coalescence in Pickering emulsions. *Soft Matter*, **2011**, *7*, 7710-7716.
36. Binks, B.P. and Yin, D.Z. Pickering emulsions stabilized by hydrophilic nanoparticles: *in situ* surface modification by oil. *Soft Matter* **2016**, *12*, 6858-6867.
37. Binks, B.P. Colloidal particles at a range of fluid-fluid interfaces. *Langmuir* **2017**, *33*, 6947-6963.
38. Binks, B.P. and Lumsdon, S.O. Stability of oil-in-water emulsions stabilised by silica particles. *Phys. Chem. Chem. Phys.* **1999**, *1*, 3007-3016.
39. Wang, H.Z.; Singh, V. and Behrens, S.H. Image charge effects on the formation of Pickering emulsions. *J. Phys. Chem. Lett.* **2012**, *3*, 2986-2990.
40. Binks, B.P. and Lumsdon, S.O. Effects of oil type and aqueous phase composition on oil-water mixtures containing particles of intermediate hydrophobicity. *Phys. Chem. Chem. Phys.* **2000**, *2*, 2959-2967.
41. Amalvy, J.I.; Armes, S.P.; Binks, B.P.; Rodrigues, J.A. and Unali, G.F. Use of sterically-stabilised polystyrene latex particles as a pH-responsive particulate emulsifier to prepare surfactant-free oil-in-water emulsions. *Chem. Comm.* **2003**, 1826-1827.
42. Yang, F.; Niu, Q.; Lan, Q. and Sun, D.J. Effect of dispersion pH on the formation and stability of Pickering emulsions stabilized by layered double hydroxide particles. *J. Colloid Interface Sci.* **2007**, *306*, 285-295.

43. Fujii, S.; Okada, M. and Furuzono, T. Hydroxyapatite nanoparticles as stimulus-responsive particulate emulsifiers and building block for porous materials. *J. Colloid Interface Sci.* **2007**, *315*, 287-296.
44. Li, J. and Stover, H.D.H. Doubly pH-Responsive Pickering emulsion. *Langmuir* **2008**, *24*, 13237-13240.
45. Lu, J.; Tian, X.X.; Jin, Y.L.; Chen, J.; Walters, K.B. and Ding, S.J. A pH responsive Pickering emulsion stabilized by fibrous palygorskite particles. *Appl. Clay Sci.* **2014**, *102*, 113-120.
46. Yang, F.; Liu, S.Y.; Xu, J.; Lan, Q.; Wei, F. and Sun, D.J. Pickering emulsions stabilized solely by layered double hydroxide particles: The effect of salt on emulsion formation and stability. *J. Colloid Interface Sci.* **2006**, *302*, 159-169.
47. Horozov, T.S.; Binks, B.P. and Gottschalk-Gaudig, T. Effect of electrolyte in silicone oil-in-water emulsions stabilised by fumed silica particles. *Phys. Chem. Chem. Phys.* **2007**, *9*, 6398-6404.
48. Zhang, J.C.; Li, L.; Wang, J.; Sun, H.G.; Xu, J. and Sun, D.J. Double inversion of emulsions induced by salt concentration. *Langmuir* **2012**, *28*, 6769-6775.
49. Paunov, V.N.; Binks, B.P. and Ashby, N.P. Adsorption of charged colloid particles to charged liquid surfaces. *Langmuir* **2002**, *18*, 6946-6955.
50. Ashby, N.P. and Binks, B.P. Pickering emulsions stabilised by Laponite clay particles. *Phys. Chem. Chem. Phys.* **2000**, *2*, 5640-5646.
51. Fuma, T. and Kawaguchi, M. Rheological responses of Pickering emulsions prepared using colloidal hydrophilic silica particles in the presence of NaCl. *Colloids Surf. A* **2015**, *465*, 168-174.
52. Whitby, C.P.; Fischer, F.E.; Fornasiero, D. and Ralston, J. Shear-induced coalescence of oil-in-water Pickering emulsions. *J. Colloid Interface Sci.* **2011**, *361*, 170-177.
53. Konrad, M.P.; Doherty, A.P. and Bell, S.E. Stable and uniform SERS signals from self-assembled two-dimensional interfacial arrays of optically coupled Ag nanoparticles. *Anal. Chem.* **2013**, *85*, 6783-6789.
54. Xu, Y.K.; Konrad, M.P.; Lee, W.W.Y.; Ye, Z.W. and Bell, S.E.J. A method for promoting assembly of metallic and nonmetallic nanoparticles into interfacial monolayer films. *Nano Lett.* **2016**, *16*, 5255-5260.

55. Akartuna, I.; Studart, A.R.; Tervoort, E.; Gonzenbach, U.T. and Gauckler, L.J. Stabilization of oil-in-water emulsions by colloidal particles modified with short amphiphiles. *Langmuir* **2008**, *24*, 7161-7168.
56. Haase, M.F.; Grigoriev, D.; Moehwald, H.; Tiersch, B. and Shchukin, D.G. Encapsulation of amphoteric substances in a pH-sensitive Pickering emulsion. *J. Phys.Chem. C* **2010**, *114*, 17304-17310.
57. Li, W.; Yu, L.; Liu, G.; Tan, J.; Liu, S. and Sun, D. Oil-in-water emulsions stabilized by Laponite particles modified with short-chain aliphatic amines. *Colloids Surf. A* **2012**, *400*, 44-51.
58. Li, W.; Zhao, C.H.; Tan, J.J.; Jiang, J.J.; Xu, J. and Sun, D.J. Roles of methyl orange in preparation of emulsions stabilized by layered double hydroxide particles. *Colloids Surf. A* **2013**, *421*, 173-180.
59. Sturzenegger, P.N.; Gonzenbach, U.T.; Koltzenburg, S. and Gauckler, L.J. Controlling the formation of particle-stabilized water-in-oil emulsions. *Soft Matter* **2012**, *8*, 7471-7479.
60. Yan, N.X. and Masliyah, J.H. Adsorption and desorption of clay particles at the oil-water interface. *J. Colloid Interface Sci.* **1994**, *168*, 386-392.
61. Santini, E.; Guzman, E.; Ferrari, M. and Liggieri, L. Emulsions stabilized by the interaction of silica nanoparticles and palmitic acid at the water-hexane interface. *Colloids Surf. A* **2014**, *460*, 333-341.
62. Pichot, R.; Spyropoulos, F. and Norton, I. O/W emulsions stabilised by both low molecular weight surfactants and colloidal particles: The effect of surfactant type and concentration. *J. Colloid Interface Sci.* **2010**, *352*, 128-135.
63. Binks, B.P. and Rodrigues, J.A. Double Inversion of Emulsions By Using Nanoparticles and a Di-Chain Surfactant. *Angew. Chem. Int. Ed.* **2007**, *46*, 5389-5392.
64. Binks, B.P.; Isa, L. and Tyowua, A.T. Direct Measurement of Contact Angles of Silica Particles in Relation to Double Inversion of Pickering Emulsions. *Langmuir* **2013**, *29*, 4923-4927.
65. Amalvy, J.I.; Unali, G.F.; Li, Y.; Granger-Bevan, S.; Armes, S.P.; Binks, B.P.; Rodrigues, J.A. and Whitby, C.P. Synthesis of sterically stabilized polystyrene latex particles using cationic block copolymers and macromonomers and their application as stimulus-responsive particulate emulsifiers for oil-in-water emulsions. *Langmuir* **2004**, *20*, 4345-4354.

66. Jiang, J.H.; Zhu, Y.; Cui, Z.G. and Binks, B.P. Switchable Pickering emulsions stabilized by silica nanoparticles hydrophobized *in situ* with a switchable surfactant. *Angew. Chem. Int. Ed.* **2013**, *52*, 12373-12376.
67. Zhu, Y.; Jiang, J.Z.; Liu, K.H.; Cui, Z.G. and Binks, B.P. Switchable Pickering emulsions stabilized by silica nanoparticles hydrophobized *in situ* with a conventional cationic surfactant. *Langmuir* **2015**, *31*, 3301-3307.
68. Xu, M.; Jiang, J.; Pei, X.; Song, B.; Cui, Z. and Binks, B.P. Novel oil-in-water emulsions stabilised by ionic surfactant and similarly charged nanoparticles at very low concentrations. *Angew. Chem. Int. Ed.* **2018**, *130*, 7864-7868.
69. Abend, S.; Bonnke, N.; Gutschner, U. and Lagaly, G. Stabilization of emulsions by heterocoagulation of clay minerals and layered double hydroxides. *Colloid. Polym. Sci.* **1998**, *276*, 730-737.
70. Binks, B.P.; Liu, W.H. and Rodrigues, J.A. Novel stabilization of emulsions *via* the heteroaggregation of nanoparticles. *Langmuir* **2008**, *24*, 4443-4446.
71. Wang, S.; He, Y.J. and Zou, Y. Study of Pickering emulsions stabilized by mixed particles of silica and calcite. *Particuology* **2010**, *8*, 390-393.
72. Whitby, C.P.; Fornasiero, D. and Ralston, J. Structure of oil-in-water emulsions stabilised by silica and hydrophobised titania particles. *J. Colloid Interface Sci.* **2010**, *342*, 205-209.
73. Barg, S.; Binks, B.P.; Wang, H.L.; Koch, D. and Grathwohl, G. Cellular ceramics from emulsified suspensions of mixed particles. *J. Porous Mater.* **2012**, *19*, 859-867.
74. Nallamilli, T.; Mani, E. and Basavaraj, M.G. A Model for the prediction of droplet size in Pickering emulsions stabilized by oppositely charged particles. *Langmuir* **2014**, *30*, 9336-9345.
75. Nallamilli, T.; Binks, B.P.; Mani, E. and Basavaraj, M.G. Stabilization of Pickering emulsions with oppositely charged latex particles: Influence of various parameters and particle arrangement around droplets. *Langmuir* **2015**, *31*, 11200-11208.
76. Saha, A.; John, V.T. and Bose, A. *In situ* assembly of hydrophilic and hydrophobic nanoparticles at oil-water interfaces as a versatile strategy to form stable emulsions. *ACS Appl. Mater. Interfaces* **2015**, *7*, 21010-21014.
77. Briggs, T. Emulsions with finely divided solids. *Ind. Eng. Chem.* **1921**, *13*, 1008-1010.

78. Frelichowska, J.; Bolzinger, M.A. and Chevalier, Y. Pickering emulsions with bare silica. *Colloids Surf. A* **2009**, *343*, 70-74.
79. Ridel, L.; Bolzinger, M.A.; Gilon-Delepine, N.; Dugas, P.Y. and Chevalier, Y. Pickering emulsions stabilized by charged nanoparticles. *Soft Matter* **2016**, *12*, 7564-7576.
80. Reincke, F.; Hickey, S.G.; Kegel, W.K. and Vanmaekelbergh, D. Spontaneous assembly of a monolayer of charged gold nanocrystals at the water/oil interface. *Angew. Chem. Int. Ed.* **2004**, *43*, 458-462.
81. Park, Y.K.; Yoo, S.H. and Park, S. Assembly of highly ordered nanoparticle monolayers at a water/hexane interface. *Langmuir* **2007**, *23*, 10505-10510.
82. Park, Y.K. and Park, S. Directing close-packing of mid-nanosized gold nanoparticles at a water/hexane interface. *Chem. Mater.* **2008**, *20*, 2388-2393.
83. Kubowicz, S.; Daillant, J.; Dubois, M.; Delsanti, M.; Verbavatz, J.M. and Mohwald, H. Mixed-monolayer-protected gold nanoparticles for emulsion stabilization. *Langmuir* **2010**, *26*, 1642-1648.
84. Binks, B.P. and Rodrigues, J.A. Types of phase inversion of silica particle stabilized emulsions containing triglyceride oil. *Langmuir* **2003**, *19*, 4905-4912.
85. Binks, B.P. and Lumsdon, S.O. Influence of particle wettability on the type and stability of surfactant-free emulsions. *Langmuir* **2000**, *16*, 8622-8631.
86. Binks, B.P.; Fletcher, P.D.I.; Holt, B.L.; Beaussoubre, P. and Wong, K. Phase inversion of particle-stabilised perfume oil-water emulsions: experiment and theory. *Phys. Chem. Chem. Phys.* **2010**, *12*, 11954-11966.
87. Gautier, F.; Destribats, M.; Perrier-Cornet, R.; Dechezelles, J.F.; Giermanska, J.; Heroguez, V.; Ravaine, S.; Leal-Calderon, F. and Schmitt, V. Pickering emulsions with stimuable particles: from highly- to weakly-covered interfaces. *Phys. Chem. Chem. Phys.* **2007**, *9*, 6455-6462.
88. Giermanska-Kahn, J.; Schmitt, V.; Binks, B.P. and Leal-Calderon, F. A new method to prepare monodisperse pickering emulsions. *Langmuir* **2002**, *18*, 2515-2518.
89. Frelichowska, J.; Bolzinger, M.A. and Chevalier, Y. Effects of solid particle content on properties of o/w Pickering emulsions. *J. Colloid Interface Sci.* **2010**, *351*, 348-356.

90. Chen, J.; Zhou, X.R.; Ge, H.Y.; Wang, D.Z.; Liu, H.S. and Li, S. Preparation and performance of nano-SiO<sub>2</sub> stabilized Pickering emulsion type sizing agent for glass fiber. *Polym. Compos.* **2016**, *37*, 334-341.
91. Zhou, J.; Wang, L.J.; Qiao, X.Y.; Binks, B.P. and Sun, K. Pickering emulsions stabilized by surface-modified Fe<sub>3</sub>O<sub>4</sub> nanoparticles. *J. Colloid Interface Sci.* **2012**, *367*, 213-224.
92. Qiao, X.Y.; Zhou, J.; Binks, B.P.; Gong, X.L. and Sun, K. Magnetorheological behavior of Pickering emulsions stabilized by surface-modified Fe<sub>3</sub>O<sub>4</sub> nanoparticles. *Colloids Surf. A* **2012**, *412*, 20-28.
93. Zhang, Q.; Bai, R.X.; Guo, T. and Meng, T. Switchable Pickering emulsions stabilized by awakened TiO<sub>2</sub> nanoparticle emulsifiers using UV/Dark actuation. *ACS Appl. Mater. Interfaces* **2015**, *7*, 18240-18246.
94. Schramm, L.L., *Emulsions, Foams, and Suspensions: fundamentals and applications*, John Wiley & Sons Ltd, Weinheim, **2006**, ch.5, pp.117-154.
95. Midmore, B. and Hunter, R. The effect of electrolyte concentration and co-ion type on the  $\zeta$ -potential of polystyrene latices. *J. Colloid Interface Sci.* **1988**, *122*, 521-529.
96. Quesada-Pérez, M.; González-Tovar, E.; Martín-Molina, A.; Lozada-Cassou, M. and Hidalgo-Álvarez, R. Ion size correlations and charge reversal in real colloids. *Colloids Surf. A* **2005**, *267*, 24-30.
97. Zimehl, R. and Lagaly, G., Coagulation of latex dispersions by inorganic salts: structural effects in *Polymers as Colloid Systems*, Springer, Berlin, **1985**, pp 28-36.
98. Sadeghpour, A.; Szilágyi, I. and Borkovec, M. Charging and aggregation of positively charged colloidal latex particles in presence of multivalent polycarboxylate anions. *Z. Phys. Chem.* **2012**, *226*, 597-612.
99. Szilágyi, I.; Sadeghpour, A. and Borkovec, M. Destabilization of colloidal suspensions by multivalent ions and polyelectrolytes: From screening to overcharging. *Langmuir* **2012**, *28*, 6211-6215.
100. Yu, W.; Bouyer, F. and Borkovec, M. Polystyrene sulfate latex particles in the presence of poly (vinylamine): absolute aggregation rate constants and charging behavior. *J. Colloid Interface Sci.* **2001**, *241*, 392-399.

101. Van den Hoven, T.J. and Bijsterbosch, B. Streaming currents, streaming potentials and conductances of concentrated dispersions of negatively-charged, monodisperse polystyrene particles. *Colloids Surf.* **1987**, 22, 171-185.
102. Calero, C.; Faraudo, J. and Bastos-González, D. Interaction of monovalent ions with hydrophobic and hydrophilic colloids: Charge inversion and ionic specificity. *J. Am. Chem. Soc.* **2011**, 133, 15025-15035.
103. Martín-Molina, A.; Calero, C.; Faraudo, J.; Quesada-Pérez, M.; Travesset, A. and Hidalgo-Álvarez, R. The hydrophobic effect as a driving force for charge inversion in colloids. *Soft Matter* **2009**, 5, 1350-1353.
104. Behrens, S.H.; Christl, D.I.; Emmerzael, R.; Schurtenberger, P. and Borkovec, M. Charging and aggregation properties of carboxyl latex particles: Experiments *versus* DLVO theory. *Langmuir* **2000**, 16, 2566-2575.
105. Sugimoto, T.; Nishiya, M. and Kobayashi, M. Electrophoretic mobility of carboxyl latex particles: effects of hydrophobic monovalent counter-ions. *Colloid Polym. Sci.* **2017**, 295, 2405-2411.
106. Smith, A.M.; Maroni, P. and Borkovec, M. Attractive non-DLVO forces induced by adsorption of monovalent organic ions. *Phys. Chem. Chem. Phys.* **2018**, 20, 158-164.
107. Schneider, C.; Hanisch, M.; Wedel, B.; Jusufi, A. and Ballauff, M. Experimental study of electrostatically stabilized colloidal particles: Colloidal stability and charge reversal. *J. Colloid Interface Sci.* **2011**, 358, 62-67.
108. Elimelech, M. and O'Melia, C.R. Effect of electrolyte type on the electrophoretic mobility of polystyrene latex colloids. *Colloids Surf.* **1990**, 44, 165-178.
109. López-León, T.; Ortega-Vinuesa, J.L. and Bastos-González, D. Ion-specific aggregation of hydrophobic particles. *Chem. Phys. Chem.* **2012**, 13, 2382-2391.
110. López-León, T.; Jódar-Reyes, A.B.; Bastos-González, D. and Ortega-Vinuesa, J.L. Hofmeister effects in the stability and electrophoretic mobility of polystyrene latex particles. *J. Phys. Chem. B* **2003**, 107, 5696-5708.
111. Schwierz, N.; Horinek, D. and Netz, R.R. Anionic and cationic Hofmeister effects on hydrophobic and hydrophilic surfaces. *Langmuir* **2013**, 29, 2602-2614.

112. Oncsik, T.; Trefalt, G.; Borkovec, M. and Szilagyi, I. Specific ion effects on particle aggregation induced by monovalent salts within the Hofmeister series. *Langmuir* **2015**, *31*, 3799-3807.
113. Yan, N. and Masliyah, J.H. Demulsification of solids-stabilized oil-in-water emulsions. *Colloids Surf. A* **1996**, *117*, 15-25.
114. Tang, J.T.; Quinlan, P.J. and Tam, K.C. Stimuli-responsive Pickering emulsions: recent advances and potential applications. *Soft Matter* **2015**, *11*, 3512-3529.
115. Whitby, C. and Wanless, E. Controlling Pickering emulsion destabilisation: a route to fabricating new materials by phase inversion. *Materials* **2016**, *9*, 626.
116. Yan, Y. and Masliyah, J.H. Solids-stabilized oil-in-water emulsions: scavenging of emulsion droplets by fresh oil addition. *Colloids Surf. A* **1993**, *75*, 123-132.
117. Yan, N. and Masliyah, J.H. Characterization and demulsification of solids-stabilized oil-in-water emulsions Part 2. Demulsification by the addition of fresh oil. *Colloids Surf. A* **1995**, *96*, 243-252.
118. Malloggi, F.; Thill, A. and Fouilloux, S., Method for destabilizing a Pickering emulsion. *Commissariat a l'Energie Atomique et aux Energies Alternatives, Paris (FR)* **2017**, US 9579616 B2.
119. Furtado, G.F.; Picone, C.S.; Cuellar, M.C. and Cunha, R.L. Breaking oil-in-water emulsions stabilized by yeast. *Colloids Surf. B* **2015**, *128*, 568-576.
120. Whitby, C.P.; Anwar, H.K. and Hughes, J. Destabilising Pickering emulsions by drop flocculation and adhesion. *J. Colloid Interface Sci.* **2016**, *465*, 158-164.
121. Akartuna, I.; Aubrecht, D.M.; Kodger, T.E. and Weitz, D.A. Chemically induced coalescence in droplet-based microfluidics. *Lab on a Chip* **2015**, *15*, 1140-1144.
122. Katepalli, H.; John, V.T. and Bose, A. The response of carbon black stabilized oil-in-water emulsions to the addition of surfactant solutions. *Langmuir* **2013**, *29*, 6790-6797.
123. Whitby, C.P.; Fornasiero, D. and Ralston, J. Effect of adding anionic surfactant on the stability of Pickering emulsions. *J. Colloid Interface Sci.* **2009**, *329*, 173-181.

124. Vashisth, C.; Whitby, C.P.; Fornasiero, D. and Ralston, J. Interfacial displacement of nanoparticles by surfactant molecules in emulsions. *J. Colloid Interface Sci.* **2010**, *349*, 537-543.
125. Zhao, X.; Huang, B.; El-Aooiti, M. and Rousseau, D. Demulsification to control solute release from Pickering crystal-stabilized water-in-oil emulsions. *J. Colloid Interface Sci.* **2018**, *509*, 360-368.
126. Katepalli, H. and Bose, A. Response of surfactant stabilized oil-in-water emulsions to the addition of particles in an aqueous suspension. *Langmuir* **2014**, *30*, 12736-12742.
127. Katepalli, H.; Bose, A.; Hatton, T.A. and Blankschtein, D. Destabilization of oil-in-water emulsions stabilized by non-ionic surfactants: effect of particle hydrophilicity. *Langmuir* **2016**, *32*, 10694-10698.

## CHAPTER 2

### EXPERIMENTAL

This chapter describes the materials and experimental methods used throughout this research.

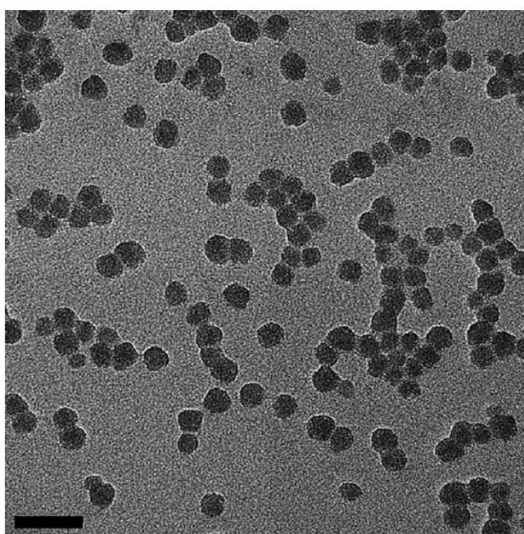
#### 2.1 Materials

##### 2.1.1 Particles

###### 2.1.1.1 Colloidal silica particles

Ludox® HS-30 colloidal silica particles were purchased from Aldrich. They were received as a 30 wt.% alkaline dispersion of synthetic amorphous silica in water; the pH of the dispersion is 9.8. The particles are spherical and relatively monodisperse with an average diameter of  $\sim 15$  nm<sup>1</sup> and a surface area of  $\sim 220$  m<sup>2</sup>/g (given by the manufacturer). A transmission electron microscopy (TEM) image is shown in Figure 2.1.

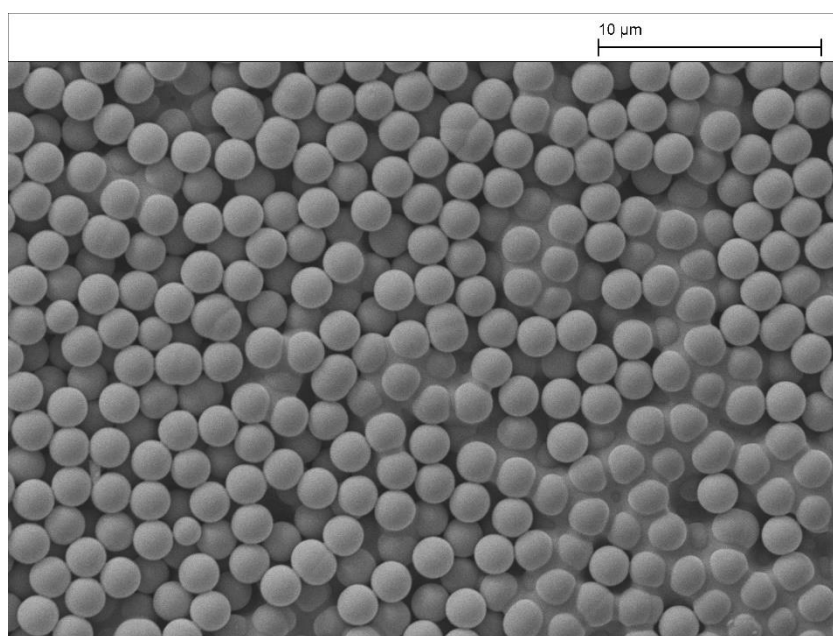
**Figure 2.1.** Transmission electron microscopy (TEM) image of 0.1 wt.% Ludox HS-30 particles in water at pH = 9.8. Scale bar = 50 nm. Taken from ref. 1.



### 2.1.1.2 Monodisperse silica particles

ÅngströmSphere™ monodisperse silica particles with diameters ranging from 0.3  $\mu\text{m}$  to 2  $\mu\text{m}$  were synthesised by Fiber Optic Center Int. (USA) and supplied by Blue Helix (UK). They were received as a white powder with purity > 99.9%. The scanning electron microscopy (SEM) of the particles with a quoted diameter of 2  $\mu\text{m}$  is shown in Figure 2.2.

**Figure 2.2.** Scanning electron microscopy (SEM) of monodisperse silica particles with a quoted diameter of 2  $\mu\text{m}$ . The average particle diameter calculated from the image is  $1.83 \pm 0.04 \mu\text{m}$ .

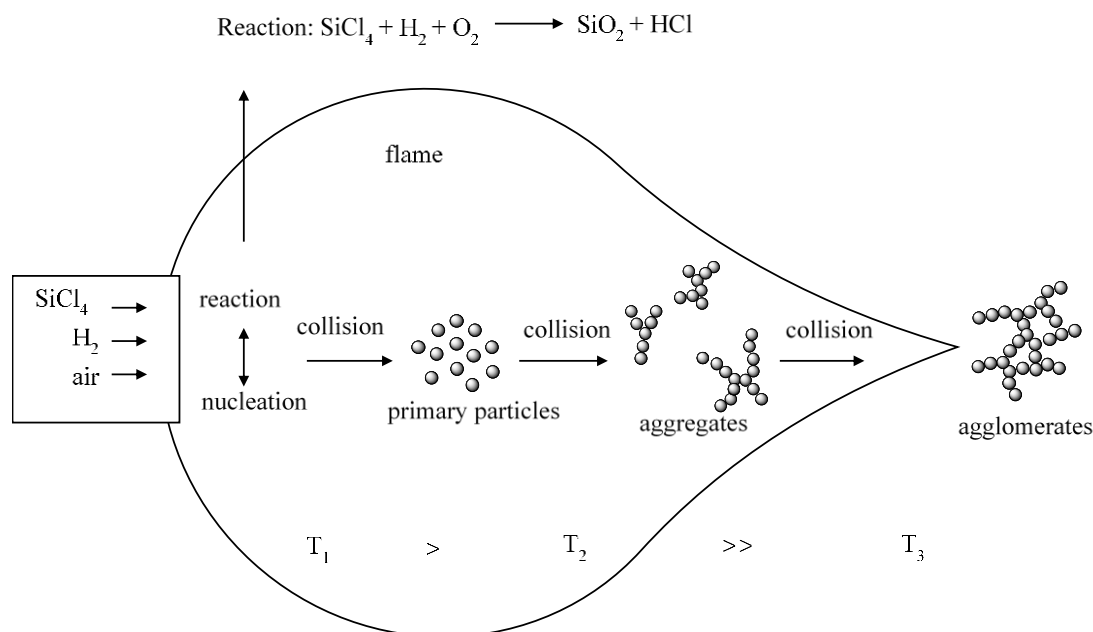


### 2.1.1.3 Fumed silica particles

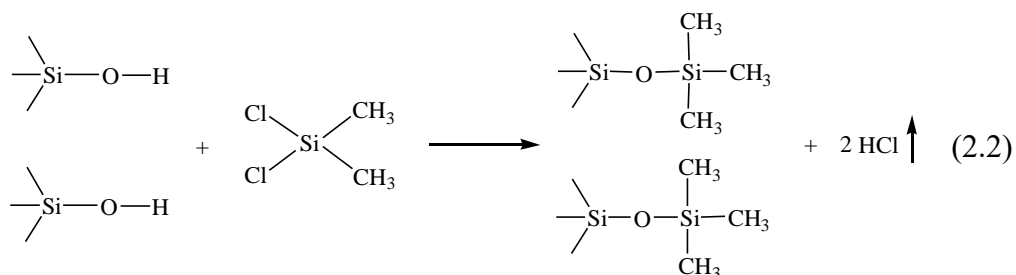
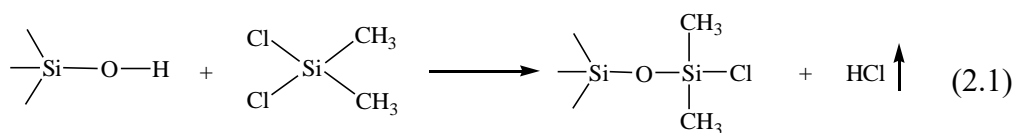
Fumed silica particles with different hydrophobicities were kindly provided by Wacker-Chemie in Burghausen (Germany). Raw silica particles were produced by burning silicon tetrachloride in an oxygen-hydrogen flame.<sup>2</sup> Primary particles of diameter about 20 nm are formed at high flame temperatures due to collision and coalescence of proto particles. At lower temperature, primary particles collide and partially fuse, leading to the formation of stable particle aggregates with diameter in the range of 100 nm. The silica aggregates leave the flame and cool, but they still collide. Consequently, agglomerates of aggregates with size larger than 5  $\mu\text{m}$  are

formed. Fumed silica exhibits a smooth non-microporous surface, which is hydrophilic owing to surface silanol groups (SiOH) and its oxide nature. Figure 2.3 shows the schematic process of producing fumed silica in a flame.

**Figure 2.3.** Production of fumed silica in a flame process. Reproduced from ref. 2.



Hydrophobic fumed silica particles are prepared by reacting hydrophilic silica with reactive silanes, *e.g.* chlorosilanes or hexamethyldisilazane.<sup>3,4</sup> Barthel reported silylation of fumed silica by spraying dichlorodimethylsilane (DCDMS) onto the carefully fluidized and stirred silica in the presence of molar amounts of water, followed by drying at 300 °C for 1 h.<sup>5</sup> This reaction proceeds monofunctionally to form chlorodimethylsiloxy and difunctionally to form dimethylsiloxy groups on the particle surface, as illustrated in equations (2.1) and (2.2). The chlorodimethylsiloxy and dimethylsiloxy groups cover the silica surface like a monolayer, without significantly altering the particle diameter.<sup>3</sup> For the fumed silica used in this research, carbon content (%C) was determined using a Leco CS/244 Carbon/Sulfur Elemental Analysis (USA), the silanol content on the silica surface was determined by acid-base titration and the relative content of silanol groups after surface modification was determined by dividing the silanol content of the modified silica by that of the hydrophilic silica (100% SiOH).



#### 2.1.1.4 Polystyrene latex particles

Three types of surfactant-free polystyrene latex particles with different functional groups (sulfate, amidine or carboxyl groups) on their surface were purchased from Invitrogen Corp. (Thermo Fisher Scientific) and received as aqueous dispersions. Sulfate ( $\text{SO}_4^-$ ) latex particles were received at a particle concentration of 8 w/v%, amidine ( $\text{C}(\text{NH})\text{NH}_3^+$ ) and carboxyl ( $\text{COO}^-$ ) latex particles were received at 4 w/v%. According to the manufacturer, amidine latex particles were made by surfactant-free emulsion polymerization using an amidine-functionalized initiator, whereas sulfate and carboxyl latex particles were made by adding a modified styrene (terminal styrene) at the end of the reaction. These latex particles are cleaned by dialysis against deionised water in order to remove unreacted monomer, initiator and by-products formed during the reaction until the conductance is close to that of deionised water. The particles are stabilized against aggregation by covalently linked charged groups (sulfate, carboxyl, amidine). The charged ends take up about 5% of the particle surface area, allowing about 95% free for placing other molecular species. Hence, the surface of particles is very hydrophobic. Figure 2.4 shows the schematic of latex particles with different surface functional groups. Figure 2.5 shows the SEM of three types of latex particles of micron-size in diameter.

**Figure 2.4.** Schematic representations of polystyrene latex particles with different surface functional groups: (a) sulfate, (b) amidine and (c) carboxyl.

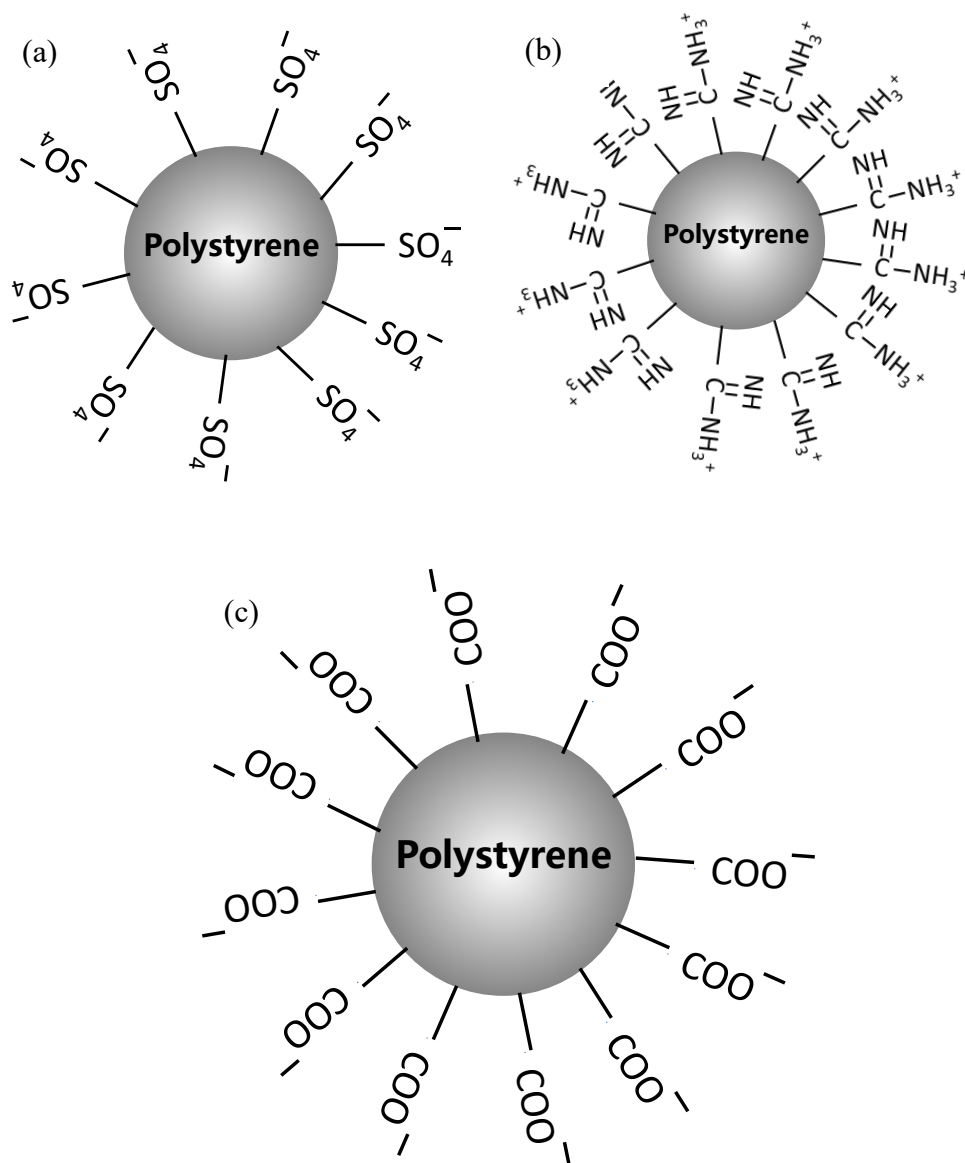
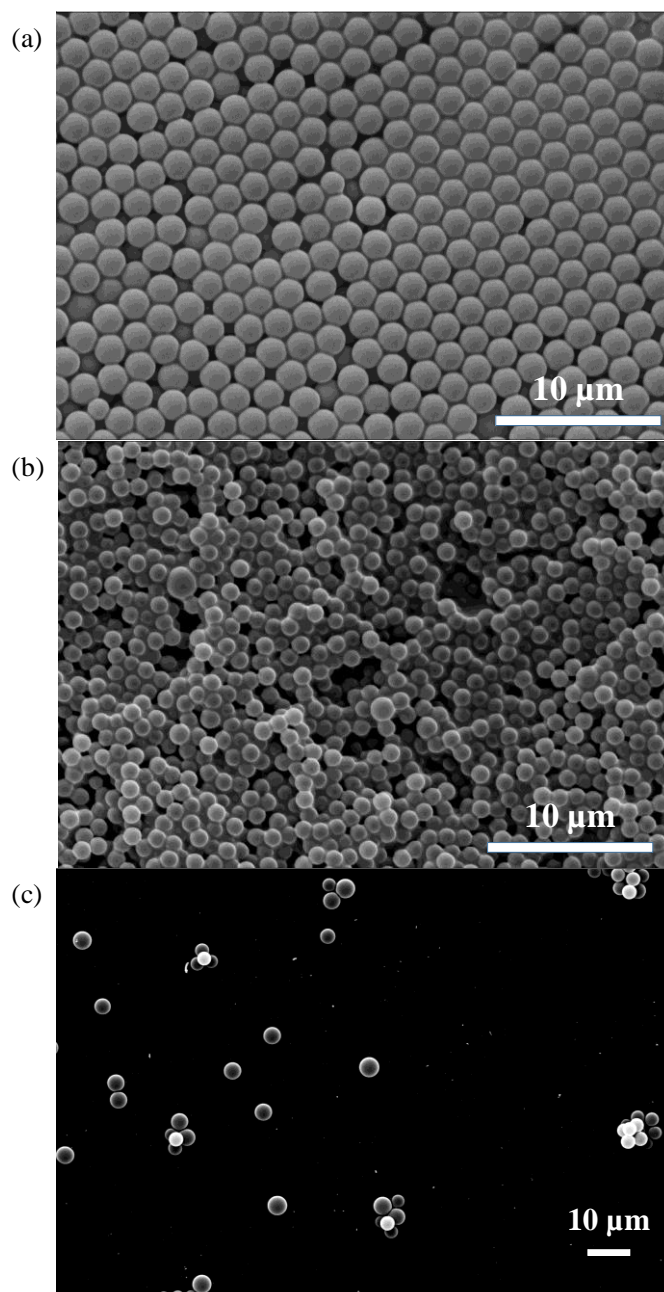


**Figure 2.5.** SEM of (a) sulfate latex particles (diameter = 2  $\mu\text{m}$ ), (b) amidine latex particles (diameter = 1  $\mu\text{m}$ ) and (c) carboxyl latex particles (diameter = 3.5  $\mu\text{m}$ ). Particles were coated by gold. The mean diameter calculated from the images is  $1.80 \pm 0.09 \mu\text{m}$  in (a),  $1.04 \pm 0.02 \mu\text{m}$  in (b) and  $3.56 \pm 0.55 \mu\text{m}$  in (c).



The latex particles were characterised by the manufacturer and some properties are listed in Table 2.1. The particle diameter is measured by TEM. More than 500 particles are measured, and the average diameter is reported. The specific surface area

(SSA) is defined as the total surface area of all the microspheres in 1 g of sample and is given in units of cm<sup>2</sup>/g. It is calculated using equation 2.3.

$$SSA = \frac{\text{Area}}{\text{Volume } \rho_p} = \frac{\pi D^2}{\frac{\pi}{6} D^3 \rho_p} = \frac{6}{D \rho_p} \quad (2.3)$$

where D is the diameter of particle (μm), ρ<sub>p</sub> is the density of polystyrene particle which is 1.055 g/cm<sup>3</sup>.

The surface charge density (σ) is determined by acid-base conductometric titration. Particles are first carefully cleaned using an ion-exchange column to remove ions that affect the real surface charge density, then the latex particles were titrated with either a strong acid or base. The equivalence point (E<sub>t</sub>) of the titration is determined conductometrically and is found as the number of micro-equivalents of base or acid used to neutralize 1 g of polymer (μeq/g). The titration equivalence point is converted into surface charge density using the following equation.

$$\sigma = \frac{E_t}{SSA} F \quad (2.4)$$

where F is the Faraday constant (F = 96,485 Coulombs per equivalent).

The area per charged group is calculated using SSA divided by the number of charged groups per gram using Avogadro's number (N<sub>A</sub>) to convert the number of equivalents to number of charged groups:

$$A = \frac{SSA}{E_t N_A} \quad (2.5)$$

where A is the area per charged group (Å<sup>2</sup>).

**Table 2.1.** Properties of sulfate latex, amidine latex and carboxyl latex particles supplied by the manufacturer.

<b>Particle surface group</b>	<b>Diameter/<math>\mu\text{m}</math></b>	<b>Number of surface groups per particle</b>	<b>Parking area per surface group/<math>\text{\AA}^2</math></b>	<b>Surface charge density/<math>\text{mC/m}^2</math></b>
Sulfate	$0.25 \pm 0.008$	$6.8 \times 10^3$	2906	-6
	$1.9 \pm 0.052$	$1.8 \times 10^6$	637	-25
Amidine	$0.22 \pm 0.010$	$1.2 \times 10^5$	122	+132
	$1.0 \pm 0.044$	$3.1 \times 10^6$	103	+156
Carboxyl	$0.21 \pm 0.007$	$1.1 \times 10^5$	123	-103
	$3.6 \pm 0.55$	$3.3 \times 10^7$	124	-129

#### 2.1.1.5 Zonyl MP 1100 and oligomeric tetrafluoroethylene (OTFE) particles

Zonyl MP1100 particles were made by DuPont and supplied by E&E Ltd. (UK). They were received as a white, free-flowing, polytetrafluoroethylene (PTFE) powder. Zonyl MP1100 particles are fairly monodisperse with a diameter of approximately 0.3  $\mu\text{m}$ , with smooth surfaces and round in shape. Oligotetrafluoroethylene (OTFE) particles were supplied by Central Glass Co. Ltd. (Japan). They are almost spherical with a diameter of  $\sim 1.3 \mu\text{m}$ . They were used to destabilize Pickering emulsions in Chapter 5.

### 2.1.2 Oils

The oils described here were used to stabilise emulsions. Octane ( $\geq 99\%$ ), dodecane ( $\geq 99\%$ ), heptane ( $\geq 99\%$ ), polydimethylsiloxane (PDMS) of viscosity 1.0 cS and 50 cS (25 °C) were purchased from Sigma-Aldrich. Prior to use, each oil was columned twice through chromatographic alumina (Merck kGaA, particle size: 0.063-0.200 mm) to remove polar impurities.

### 2.1.3 Salts

The salts described here were added as electrolytes to aqueous dispersions of particles for the purpose of emulsion preparation. Tetramethylammonium nitrate (TMA $\text{NO}_3$ ,  $> 96\%$ ), tetraethylammonium nitrate (TEA $\text{NO}_3$ ,  $> 98\%$ ), tetrapropylammonium bromide (TPAB,  $> 99\%$ ), tetrabutylammonium nitrate (TBA $\text{NO}_3$ , 97%), tetrapentylammonium bromide (TPeAB,  $\geq 99\%$ ) and sodium thiocyanate (NaSCN,  $\geq 99.99\%$ ) were purchased from Sigma Aldrich. Potassium chloride (KCl,  $> 99\%$ ) and potassium nitrate (KNO $_3$ ,  $> 99\%$ ) were purchased from Fisher Scientific. All of the salts were used as received.

### 2.1.4 Other materials

Water was purified using an Elga Prima reverse osmosis unit and then treated with a Milli-Q reagent system (Millipore) until a resistivity of 18 M $\Omega$  cm was reached. Sodium hydroxide (NaOH, Fisher Scientific,  $> 98.6\%$ ) and hydrochloric acid (HCl, Fisher Scientific, 37.4%, analytical grade) were used to adjust the pH of particle dispersions and salt solutions in this research. NaOH was also used to hydroxylate glass substrates for contact angle measurements and hydrophobization of glass slides. Potassium hydroxide (Fisher Scientific, laboratory reagent grade) and 2-propanol (Honeywell,  $\geq 99.5\%$ ) were used to prepare Base-Bath cleaning solution to clean glass vessels. 2-propanol was also used to aid particle spreading at an oil-water interface. Ethanol (VWR Chemicals, 100%) and chloroform (Fisher Scientific,  $> 99\%$ ) were used to clean equipment and silica particles or glass slides.

Dodecyltrimethylammonium bromide (C $_{12}$ TAB,  $\sim 99\%$ ) and hexadecyltrimethylammonium bromide (C $_{16}$ TAB,  $> 99\%$ ), both purchased from

Sigma-Aldrich, were used to prepare control emulsions in combination with Ludox HS-30 silica particles.

Cyclohexane (Fisher Scientific,  $\geq 99.5\%$ ) and dichlorodimethylsilane (DCDMS, Sigma-Aldrich,  $\geq 99.5\%$ ) were used for the hydrophobisation of silica particles and glass slides in section 2.2.5.

Gellan gum (CPKelco (USA), food grade), acetonitrile (Honeywell,  $\geq 99.9\%$ ), PDMS Sylgard 184 elastomer (Dow Corning) and ethylenediaminetetraacetic acid disodium salt (EDTA disodium salt, Sigma-Aldrich, 99-101% by titration) were used to determine contact angles using the gel-trapping technique in section 2.2.6.2.

## **2.2 Methods**

### *2.2.1 Preparation and characterisation of particle dispersions*

Aqueous dispersions of Ludox HS-30 silica nanoparticles and polystyrene latex particles were prepared by diluting stock dispersions with Milli-Q water. Aqueous dispersions of micron-sized silica particles and fumed silica particles were prepared by dispersing a known mass of silica powder into 5 cm<sup>3</sup> of Milli-Q water using a high intensity ultrasonic vibracell processor (Sonics & Materials, tip diameter 0.3 cm), operating at 11 W for 2 min with cooling using ice. Aqueous electrolyte solutions of various concentrations were then added before adjusting the solution pH using acid (0.1 M HCl) or base (0.5 M NaOH). The pH was measured using a Jenway-3510 pH Meter with an InLab Flex-Micro electrode (Mettler-Toledo Ltd).

#### *2.2.1.1 Measurement of zeta potential and particle size*

The zeta potential of particles was measured at 25 °C with a Zetasizer Nanoseries Nano ZS (Malvern Instruments) equipped with a 4 mW He-Ne laser beam operating at  $\lambda = 633$  nm. Measurements were conducted by introducing a universal dip cell (ZEN1002, Malvern Instruments) inside a plastic disposal cuvette (1 cm path length). The samples were 0.1 wt.% particle dispersions in the presence of the corresponding electrolyte. Three measurements with 12 runs each were conducted for each sample.

The size distribution of Ludox HS-30 silica particles was measured at 25 °C with the same instrument under a scattering angle of 173°.

#### 2.2.1.2 Measurement of particle size by light diffraction

The volume weighted particle diameter distribution of polystyrene latex particles was determined using a Malvern Mastersizer 2000 fitted with a small volume sample dispersion unit. Samples were measured in Milli-Q water. About 200 µL of particle dispersion was diluted in 120 mL water in the dispersion unit, stirred at 1500 rpm. The refractive index of polystyrene particles is 1.591 at 590 nm and 20 °C. The size range was 0.02 µm to 2000 µm and the analysis model was the General Purpose Spherical Model. Three measurements were conducted for each sample.

#### 2.2.2 *Preparation and characterisations of emulsions*

The required volumes of aqueous particle dispersion and oil were added to a screw-cap glass vial with an inside diameter of 1.6 cm and height of 7.2 cm. The two phases were emulsified using an IKA Ultra Turrax T 25 homogenizer with an 8 mm head and operating at 13,000 rpm for 2 min. All the experiments were conducted at room temperature ( $22 \pm 1^\circ\text{C}$ ) unless otherwise stated.

##### 2.2.2.1 Determining emulsion type

The emulsion type was inferred from the drop test. A small sample of emulsion was added into water or the oil used to prepare the emulsion. If the emulsion can be dispersed in water, then it is oil-in-water (o/w); if it is dispersed in oil, then the emulsion type is water-in-oil (w/o).

The conductivity of the emulsion was measured by a Jenway Model 4510 Bench conductivity meter immediately after homogenization. The conductivity meter was calibrated with 0.01 M KCl solution. If the emulsion conductivity is close to that of the aqueous phase, then the emulsion type is o/w. However, if the emulsion conductivity is close to that of oil, then the emulsion type is w/o.

#### 2.2.2.2 Monitoring emulsion stability

Photos of the obtained emulsions were taken immediately after preparation and with time to visually evaluate their stability. For o/w emulsions, the stability of the emulsions to creaming was determined by monitoring the position of the clear water/emulsion interface; the stability of an emulsion to coalescence was determined by monitoring the position of the oil/emulsion interface. In contrast, for w/o emulsions, the stability to sedimentation was assessed by monitoring the position of the clear oil/emulsion interface, whilst the stability to coalescence was assessed by monitoring the position of the clear water/emulsion interface.

#### 2.2.2.3 Optical microscopy

Optical microscopy images of the prepared emulsions were taken using an Olympus BX-51 microscope fitted with a DP70 digital camera and Image-Pro Plus 5.1 software (Media Cybernetics). The emulsion was diluted 10 times with the corresponding continuous phase, then a diluted emulsion drop was placed on a glass slide (Fisher Scientific) and observed under the microscope. The mean droplet diameter as well as the error in the form of standard deviation was calculated from the droplets of emulsions on digital micrographs with Image J 1.47v. If the number of droplets on an image was less than 50, all the droplets were used. If the number of droplets on an image was larger than 50, then at least 50 droplets were used.

#### 2.2.2.4 Measurement of droplet size by light diffraction

Resembling the measurement of particle size by light diffraction, the volume weighted droplet diameter distribution of oil-in-water emulsions with silica nanoparticles and octane was determined using a Malvern Mastersizer 2000 instrument. Samples were measured in corresponding tetraalkylammonium salt ( $R_4NX$ , X is an anion) solutions at the same concentrations as that in emulsions. During the measurement, about 150  $\mu\text{L}$  of emulsion was diluted in 120 mL water or  $R_4NX$  solutions in the dispersion unit, stirred at 1500 rpm. The refractive index of  $R_4NX$  solutions at various concentrations was determined using a refractometer equipped with a sodium lamp unit (Bellingham Stanley Ltd.) beforehand. The refractive index of the dispersed octane drops was 1.38.

#### 2.2.2.5 Cryogenic scanning electron microscopy

Cryogenic scanning electron microscopy (cryo-SEM) measurements were carried out on selected emulsion samples in the following way. A small volume of emulsion was pipetted onto a channelled aluminium stub to form a dome and plunged into nitrogen slush for 2 min. The frozen sample was transferred to a Quorum Technologies preparation chamber at  $-145\text{ }^{\circ}\text{C}$ . A scalpel was used to fracture the frozen sample exposing a freshly cut surface. The sample was transferred to the cold stage in the SEM instrument ( $-140\text{ }^{\circ}\text{C}$ ) and sublimed at  $-90\text{ }^{\circ}\text{C}$  for 20 minutes. Then the sample was transferred back to the Quorum preparation chamber and coated with 2 nm of platinum. It was then examined with a Carl Zeiss Evo-60 SEM with a LaB6 emitter at a beam current of  $40\text{ }\mu\text{A}$ , an accelerating voltage of 15 kV and probe current of 35 pA using the secondary electron detector. Energy dispersive X-ray (EDX) elemental maps were also stored and processed using an Oxford X-max 80 X-ray detector equipped with Oxford Inca software. For spot analysis, data was collected for 45 sec, for mapping data was collected for 30 frames.

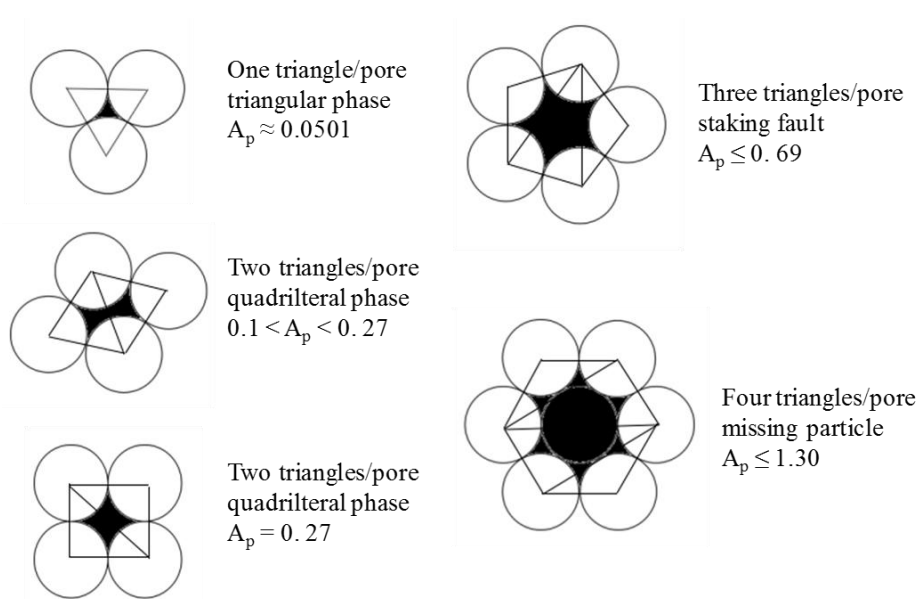
#### 2.2.3 *Particles at a planar oil-water interface*

Monolayers of silica particles of  $2\text{ }\mu\text{m}$  in diameter were formed by spreading particles at the octane-water interface. The spreading suspension was prepared by dispersing 0.05 g of  $2\text{ }\mu\text{m}$  diameter silica particles in 5 g of 50:50 (by vol.) aqueous solution of 2-propanol (IPA) using a high-intensity ultrasonic vibracell processor (Sonics & Materials, tip diameter 0.3 cm), operating at 11W for 2 min with cooling using ice.  $5\text{ cm}^3$  of aqueous solution and  $2\text{ cm}^3$  of octane was added into a glass petri dish with an inside diameter of 4 cm (area,  $12.6\text{ cm}^2$ ) and height of 1 cm. The aqueous phase was either Milli-Q water or  $\text{TBANO}_3$  solutions at different concentrations at pH  $\sim 10$ . Then a small amount of spreading suspension ( $\sim 180\text{ }\mu\text{L}$ ) containing about 1 wt.% particles was injected close to the octane-water interface from the oil layer using a 100  $\mu\text{L}$  syringe (SGE Analytical Science). The particles spread at the interface with the help of IPA and form a monolayer. The small amount of IPA dissolving into the water phase does not change the interfacial tension by much.<sup>6</sup> Prior to the experiments, Base-Bath cleaning solution was prepared by dissolving 50 g potassium hydroxide in 100 mL water in a beaker. After cooling down to room temperature, the solution was added

to 1 L of 2-propanol. The vessels were immersed in Base-Bath cleaning solution overnight to remove any organics. The syringe was immersed in ethanol and put in an ultrasonic bath for 15 min.

The monolayers were observed from the top using a Nikon Optiphot-2 microscope fitted with extra-long working distance objectives and a CCD camera (TK 1381, JVC). The images were recorded by a VCR and processed with Image-Pro Plus 7.0 software. The Delaunay triangulation procedure<sup>7</sup> is used to estimate the structural irregularities of the monolayers. This procedure generates a triangulation of a point set within which no point falls in the circumcircle (circle that passes through all three vertexes) of any triangle in the triangulation.<sup>7</sup> Different particle arrangements in the lattice can be identified by the pore area between particles. At hexagonal close packing with the smallest pore area, one equilateral triangle will be sufficient to envelop the pore between three particles. At quadrilateral packing with larger pores, two triangles will be needed. Three triangles often refers to stacking faults and four triangles usually corresponds to a missing particle in the structure.<sup>8</sup> A schematic illustration of packing types is given in Figure 2.6.

**Figure 2.6.** Schematic illustration of different particle packing types together with the associated number of Delaunay triangles. The pores are shaded black, and the normalized pore area,  $A_p$ , is included. Reproduced from ref. 8.



#### 2.2.4 Destabilisation of Pickering emulsions

Prior to destabilization processes, initial emulsions were prepared and left quiescently for a specific period of time. A known amount of destabilizer (various types of solid particle) was added into the emulsions and stirred with a PTFE magnetic bar (Fisherbrand, 12 mm × 4.5 mm, cylindrical shape with Pivot ring) at 300 rpm on a Thermo Scientific Variomag Poly 15 magnetic stirrer. Photos of the emulsions were taken along stirring time to visually evaluate the stability of emulsions. Microscopy images of emulsions were taken after the process of destabilization.

#### 2.2.5 Hydrophobisation of silica particles

In Chapter 5, monodisperse silica particles of different hydrophobicity will be used to destabilize Pickering emulsions. These particles were produced by hydrophobizing the surface of hydrophilic silica particles with a silanising agent, dichlorodimethylsilane (DCDMS).

Prior to hydrophobisation, clean volumetric flasks were pre-treated to hydrophobise the inner surface by sealing the flasks overnight with 0.5 cm<sup>3</sup> DCDMS. The flasks were cleaned using chloroform and ethanol three times to remove excess DCDMS then left to dry naturally. The pre-treatment hydrophobized the inner surface of the flasks so that hydrophobisation will not take place on addition DCDMS solution which would have alter the concentration of DCDMS. Then DCDMS in cyclohexane at concentrations from 1×10<sup>-6</sup> M to 0.1 M were prepared in 50 cm<sup>3</sup> pre-treated volumetric flasks.

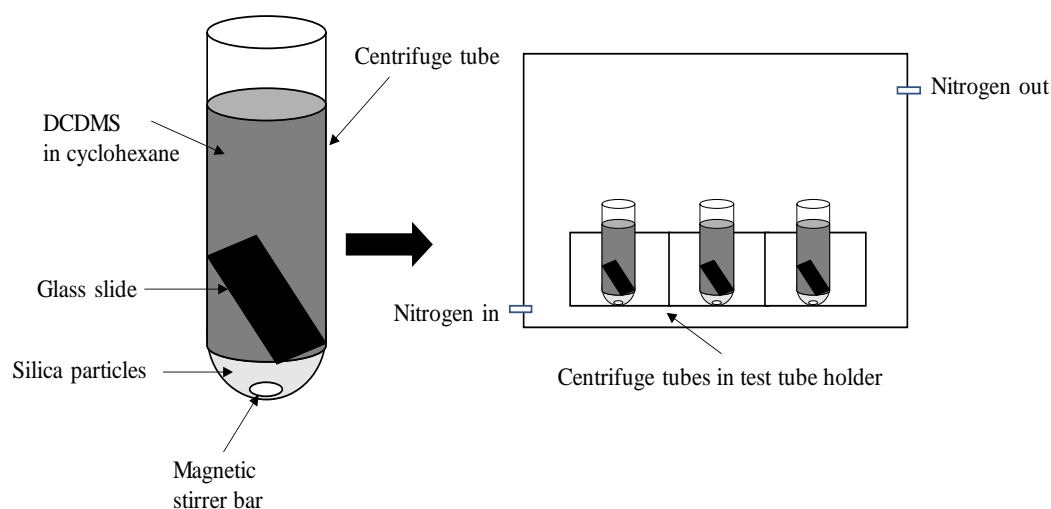
Oak Ridge Teflon® centrifuge tubes (Nalgene) were used for the silanisation reaction and subsequent cleaning. These tubes are resistant to many chemicals including toluene and chloroform while also able to withstand temperatures up to 200 °C and high centrifugation speeds. Silica particles were sonicated in ethanol for 10 min then centrifuged at 8000 rpm for 10 min. Ethanol was then removed and replaced with Milli-Q water, followed by sonication for 10 min and centrifuged for 10 min. This process was repeated three times. Finally, particles were dried in an oven (Advantage-Lab) at 100 °C overnight.

To get an approximate measurement of the degree of hydrophobicity of the silica particles after the procedure, glass microscope slides were treated simultaneously in the same solutions for the duration of the procedure. As the materials are similar an idea of the contact angle can be determined with sessile water drops on the microscope slides. Prior to use, small pieces (2.5 cm × 2 cm) of microscope slides (Fisher Scientific) were hydroxylated with 30 wt.% NaOH solution for 24 hours, and washed with Milli-Q water, then dried with compressed air.<sup>9,10</sup>

Each sample vessel contained 1 g of pre-cleaned and oven-dried silica particles and a small piece of glass substrate to be treated. Approximately 30 cm<sup>3</sup> of DCDMS in cyclohexane solution was added to each vessel. A PTFE magnetic stirrer bar was used to keep the particles dispersed during the procedure. The vessels were placed in a test tube rack on a Thermo Scientific Variomag Poly 15 magnetic stirrer, which was placed in a nitrogen atmosphere under a box. Figure 2.7 shows the schematic of the setup for the hydrophobisation process. The system was put in a fume cupboard throughout the reaction.

After one hour, 4 cm<sup>3</sup> of ethanol was added to each vessel to react with the remaining DCDMS. The slides were removed, rinsed in chloroform and then sonicated in a fresh volume of chloroform. The chloroform was washed off by sonicating in ethanol and then the slides were dried in the oven. The particle dispersion was centrifuged at 8000 rpm for 10 min and then the cyclohexane was removed. After this they were sonicated in chloroform for 10 min and then centrifuged, followed by sonication in ethanol for 10 min then centrifuged, which was repeated three times.

**Figure 2.7.** Schematic of the experimental setup used for the hydrophobisation of silica particles and microscope slides.



## 2.2.6 Measurement of three-phase contact angle

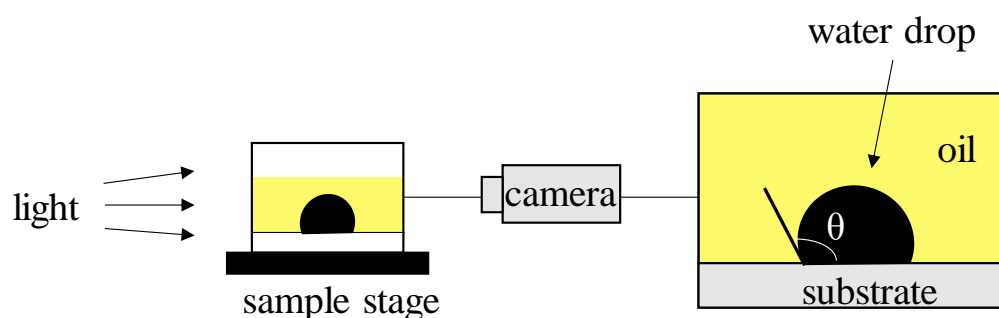
### 2.2.6.1 By sessile drop method

In order to measure the three-phase contact angle of Ludox HS-30 silica particles at octane-water interfaces, 30 wt.% NaOH solution treated glass substrates were used to mock the surface of particles. Batches of tetraalkylammonium salt solutions at different concentrations were prepared, the pH of each solution was adjusted to  $\sim 10$  as it was the pH of Ludox HS-30 silica dispersions used to stabilise emulsions. The measurement was through the aqueous phase at the oil-water-glass substrate interface. A Krüss Drop Shape Analysis 10 instrument was used to observe the side-on profile of sessile liquid drops (as illustrated in Figure 2.8). The glass slide was immersed in octane inside a rectangular cuvette (Hellma®) with inside size of  $30 \times 30 \times 30$  mm. A drop of water or tetraalkylammonium salt solution ( $\sim 5 \mu\text{L}$ ) was placed onto the glass surface using a  $25 \mu\text{L}$  MicroVolume syringe (SGE Analytical Science). The bevel tip of the needle on the syringe was adjusted to blunt by cutting the tip and unblocking with a line. The advancing contact angle was determined with circle fitting method after equilibration of 5 minutes. Afterward, a small amount of liquid in the drop was extracted with the same syringe until the contact line of the water drop with the glass slide shrinks, and the receding contact angle was determined. Three measurements were conducted for each sample. The three-phase contact angle of glass microscope

slides which were hydrophobized simultaneously with silica particles were determined using the same way.

For Zonyl MP 1100 and OTFE particles, the three-phase contact angle was measured with the same sessile drop method by loading water drops on compressed particle disks. Particle disks with a diameter of 13 mm and thickness of 2 mm were prepared by compressing 400 mg of particle powder in a steel die using a hydraulic press (Research and Industrial Instrument Co.) under a pressure of  $10^9 \text{ N m}^{-2}$ .

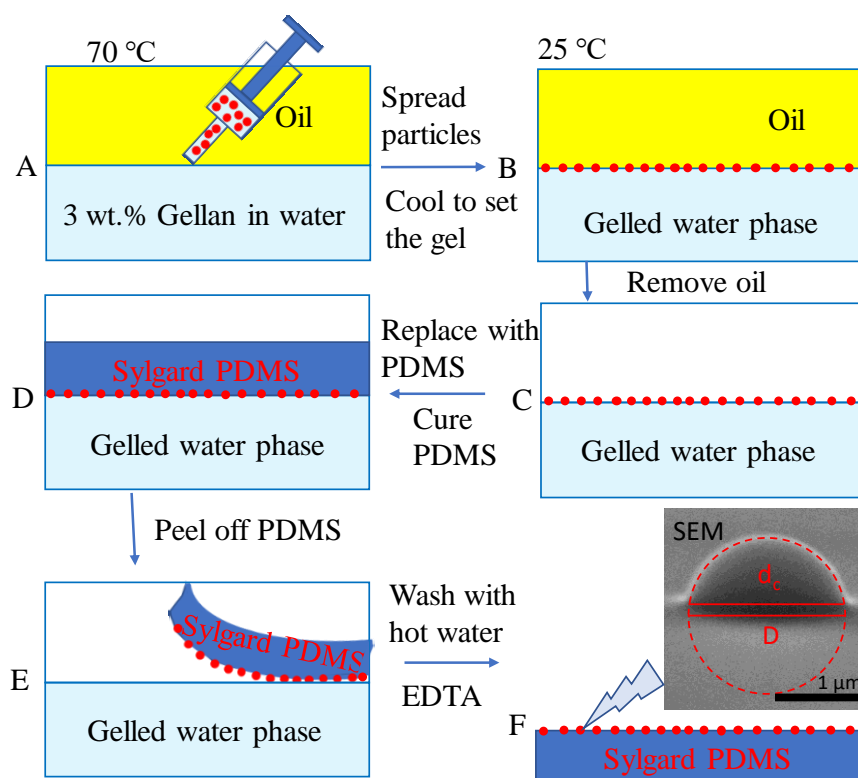
**Figure 2.8.** Schematic of Kruss DSA 10 instrument for contact angle measurement with sessile drop method.



#### 2.2.6.2 By gel-trapping technique

The gel trapping technique (GTT) was used to measure the three-phase contact angle of latex particles at oil-water interfaces. GTT is based on spreading the particles at an oil-water interface and subsequently gelling the aqueous phase with a non-adsorbing polysaccharide (Gellan gum).<sup>10</sup> With the particle monolayer trapped on the surface of the aqueous gel, the oil is removed and replaced by PDMS elastomer, which allows the particles to embed within the PDMS. Peeling the PDMS layer from the gelled aqueous phase, particles embedded within PDMS can be imaged with high resolution SEM. The position of the particles relative to the PDMS surface and the diameter of the contact line of particles with the PDMS surface can be determined from the SEM images, which gives information on the particle contact angle at the oil-water interface.<sup>10</sup> Figure 2.9 shows a schematic diagram of the method. It is applicable for particle diameters ranging from several hundred nanometers to several hundred micrometers.

**Figure 2.9.** Schematic diagram of the GTT for determining contact angles of microparticles at an oil-water interface. Reproduced from ref. 10.



Prior to use, gellan gum was purified by passing a hot solution twice through a pre-activated C18-silica chromatographic column. Gellan gum powder was dispersed in Milli-Q water at 95 °C in a water bath for 30 min to form a 0.5 wt.% solution. C18-silica chromatographic column (Phenomenex) was pre-activated using an acetonitrile-water mixture (80 : 20) and flushed several times with hot Milli-Q water. The 0.5 wt.% gellan solution was then passed twice through the pre-activated C18-silica chromatographic column connected to a vacuum filtration set. The latter was heated using a hair dryer from outside during the filtration of the hot gellan solution to prevent its gelation inside the column. Finally, after purification, the gellan solution was dried by evaporation until a dry solid was obtained.

Batches of salt solutions at varied concentrations were prepared at the required pH. Subsequently, a known amount of purified gellan solid was added to the solutions and heated to 95 °C in a water bath for 30 min to obtain 3 wt.% gellan-salt solutions. These gellan-salt solutions were then kept in an oven at 70 °C for further use.

Aqueous suspensions of latex particles at 1 wt.% were prepared by mixing stock dispersions with 2-propanol (50:50 by vol.) which was used as a spreading solvent. Oil was pre-warmed up to 70 °C to match the temperature of the purified gellan solution. 2.5 mL of hot 3 wt.% gellan-salt solution was poured into a pre-heated plastic Petri dish of diameter 35 mm (Thermo Fisher Scientific) and the same amount of pre-heated oil was carefully introduced on top of the gellan solution. A small sample (typically 10  $\mu$ L) of latex particle suspension in spreading solvent was carefully spread at the oil-water interface using a 100  $\mu$ L syringe. The Petri dish including the sample was kept at room temperature for 1 h until gelling of the aqueous phase. Afterwards the oil phase was decanted off and its residue was carefully removed from the edge of the Petri dish using tissue paper. Sylgard PDMS was mixed in a ratio of 10:1 (by mass) with its curing agent and centrifuged at 3000 rpm for 5 min to remove any air bubbles formed during mixing. Subsequently, 2.5 g of Sylgard PDMS was carefully layered over the gelled aqueous phase with the particle monolayer to avoid trapping of air bubbles and was cured at least for 48 h at room temperature. After peeling off the solidified Sylgard PDMS layer with the particles, the samples were incubated in hot aqueous solutions (95 °C) of 20 mM of EDTA disodium salt, 20 mM sodium hydroxide and Milli-Q water for 5 min, respectively, to wash off the gellan residues from the Sylgard PDMS surface. A Carl Zeiss EVO-60 SEM with a secondary electron detector was used to image the particle monolayers on Sylgard PDMS at a voltage of 20 kV and a probe current of 100 pA. Before imaging, samples were coated with  $\sim$ 10 nm carbon layer (spectrally pure graphite) by using an Edwards High Vacuum evaporator. The three-phase contact angles of the sulfate latex particles were determined from the SEM micrographs of the Sylgard PDMS micro-casts with particles at the oil-water interface using the following analysis:

- (i) If the particle contact line diameter  $d_c$  was below the particle equatorial diameter (hydrophilic particles,  $\theta < 90^\circ$ ), the contact angle  $\theta$  was determined from the relationship:

$$\sin\theta = d_c/D \quad (2.6)$$

- (ii) For hydrophobic particles,  $\theta > 90^\circ$ , whose contact line is above the particle equatorial diameter, the contact angle was calculated by:

$$\sin(\pi - \theta) = d_c/D \quad (2.7)$$

### 2.3 References

1. Binks, B.P.; Kirkland, M. and Rodrigues, J.A. Origin of stabilisation of aqueous foams in nanoparticle-surfactant mixtures. *Soft Matter* **2008**, *4*, 2373-2382.
2. Auner, N. and Weis, J. *Organosilicon chemistry ii: From molecules to materials* VCH Verlagsgesellschaft mbH, Weinheim, **1995**, ch. 91, pp. 761-778.
3. Tripp, C. and Hair, M. Reaction of chloromethylsilanes with silica: a low-frequency infrared study. *Langmuir* **1991**, *7*, 923-927.
4. Hair, M.L. and Hertl, W. Reactions of chlorosilanes with silica surfaces. *J. Phys. Chem.* **1969**, *73*, 2372-2378.
5. Barthel, H. Surface interactions of dimethylsiloxy group-modified fumed silica. *Colloids Surf. A* **1995**, *101*, 217-226.
6. Bonales, L.; Rubio, J.; Ritacco, H.; Vega, C.; Rubio, R. and Ortega, F. Freezing transition and interaction potential in monolayers of microparticles at fluid interfaces. *Langmuir* **2011**, *27*, 3391-3400.
7. Hansen, P.H.; Rödner, S. and Bergström, L. Structural characterization of dense colloidal films using a modified pair distribution function and Delaunay triangulation. *Langmuir* **2001**, *17*, 4867-4875.
8. Rödner, S.C.; Wedin, P. and Bergström, L. Effect of electrolyte and evaporation rate on the structural features of dried silica monolayer films. *Langmuir* **2002**, *18*, 9327-9333.
9. Binks, B.P.; Dyab, A.K.F. and Fletcher, P.D.I. Contact angles in relation to emulsions stabilised solely by silica nanoparticles including systems containing room temperature ionic liquids. *Phys. Chem. Chem. Phys.* **2007**, *9*, 6391-6397.
10. Paunov, V.N. Novel method for determining the three-phase contact angle of colloid particles adsorbed at air-water and oil-water interfaces. *Langmuir* **2003**, *19*, 7970-7976.

## CHAPTER 3

### PICKERING EMULSIONS OF HYDROPHILIC SILICA PARTICLES AND SYMMERICAL ORGANIC ELECTROLYTES

#### 3.1 Introduction

At high pH, bare silica particles are not an effective Pickering emulsion stabiliser of non-polar oils with water due to their high surface charge. Internal or external protocols will be needed to render such hydrophilic particles to stabilize emulsions. As has been summarized in section 1.2.5, addition of salts to the aqueous phase is a widely reported protocol to enable hydrophilic particles to stabilise emulsions. Relatively high concentrations of salt cause particle aggregation however and may lead to an increase in viscosity of the aqueous phase contributing to increased emulsion stability.<sup>1,2</sup> In addition, the majority of work involves adding non-adsorbing, indifferent salts,<sup>3-5</sup> whereas little work has been reported on the use of organic salts to enable hydrophilic particles to stabilise Pickering emulsions.<sup>6</sup> For organic electrolytes which contain an ionic hydrophilic atom bonded to more hydrophobic alkyl chains, this ion may adsorb at particle surfaces, altering both the surface charge and surface potential. Symmetrical tetraalkylammonium salts,  $R_4NX$  where R is an alkyl group and X is an anion like bromide or nitrate, have been found to adsorb on silica particles, raising the isoelectric point and causing particle coagulation.<sup>6-8</sup> For salts of R group  $C_1$ ,  $C_3$  and  $C_5$ , it was argued that  $R_4N^+$  ions adsorb on both neutral SiOH groups due to their hydrophobic character and charged  $SiO^-$  groups *via* electrostatic attraction (site binding).<sup>7</sup> Also, it was found that the adsorbed amount of  $R_4N^+$  on silica increased with salt concentration and with R chain length ( $C_1$ - $C_3$ ).<sup>8</sup> Here, it was claimed that adsorption was not on  $SiO^-$  groups but on more hydrophobic Si-O-Si siloxane bridges.

Recently, it was reported that nanoparticles including  $TiO_2$ ,  $SiO_2$  and metallic Ag or Au were promoted to planar oil-water interfaces by adding salts with hydrophobic ions of opposite charge to the nanoparticles.<sup>9,10</sup> The salts, *e.g.* tetrabutylammonium nitrate, referred to as promoters, were added from the oil phase and were claimed not to adsorb directly on particle surfaces but, being located near the oil-water interface, enabled particle adsorption by screening the Coulombic repulsion between the

negatively charged surfaces of particles in the oil phase. A similar hydrophobic screening effect was reported in the formation of gold nanoparticle films in the presence of tetramethylammonium ions from water.<sup>11</sup> However, although these particles were able to adsorb at planar oil-water interfaces, they were found unable to stabilise Pickering emulsions.<sup>11</sup> Therefore, it is interesting to see how the particles behave with respect to emulsion stabilization when such organic salts are added to the aqueous phase. Although Binks and Lumsdon<sup>5</sup> briefly investigated emulsions stabilised by fumed silica particles in the presence of tetraethylammonium bromide, no systematic work such as varying the chain length of the alkyl group (R) has been carried out. It has been well documented that surfactants with opposite charge to that of the particles initially adsorb on particle surfaces *via* electrostatics increasing the particle hydrophobicity<sup>12-14</sup> and enabling Pickering emulsion stabilisation.<sup>15</sup> Tetraalkylammonium bromides of relatively long hydrophobic chain are also surface-active at air-water<sup>16</sup> and oil-water<sup>17</sup> interfaces and their surface activity increases with alkyl chain length, although it is weaker than that of single- or double-chained surfactants with the same number of carbon atoms.<sup>18</sup> Therefore, it is also interesting to determine the transition between electrolyte and surfactant of similar structures with respect to the stabilization of Pickering emulsions with hydrophilic particles.

This chapter has systematically investigated Pickering emulsions stabilised by hydrophilic silica particles (nm or  $\mu\text{m}$ -sized) in the presence of tetraalkylammonium salts ( $\text{R}_4\text{NX}$ , X is an anion) of increasing R chain length, *i.e.* tetramethylammonium nitrate (TMANO<sub>3</sub>), tetraethylammonium nitrate (TEANO<sub>3</sub>), tetrapropylammonium bromide (TPAB) and tetrabutylammonium nitrate (TBANO<sub>3</sub>). The influence of R chain length and salt concentration as well as the concentration of particles on emulsion stability has been studied. These emulsions were also compared with those stabilised by a mixture of silica particles and cationic surfactant ( $\text{RMe}_3\text{NX}$ ) containing a similar number of carbon atoms as that in  $\text{R}_4\text{NX}$  salts. Finally, for micron-sized particles, their arrangement at emulsion drop interfaces and planar oil-water interfaces in the presence of TBANO<sub>3</sub> was also compared.

### 3.2 Aqueous dispersion of silica particles

Prior to studying the properties of emulsions, the properties of Ludox HS-30 silica dispersions upon addition of  $R_4NX$  salts were characterised in terms of size and zeta potential by dynamic light scattering.

Figure 3.1 shows the appearance of 2 wt.% silica dispersions with increasing concentration of the four  $R_4NX$  salts ( $TMANO_3$ ,  $TEANO_3$ , TPAB and  $TBANO_3$ ) at pH 10 after 24 h. Both particle and salt concentrations mentioned throughout this research for the purpose of preparing emulsions are relative to the mass of aqueous dispersions. As can be seen, all dispersions are bluish and no flocculation is observed up to 0.1 M salt. Figure 3.2 is a plot of the average particle diameter as a function of salt concentration. Since the diameter in pure water is 21.6 nm, it is clear that salt addition does not lead to any significant increase in particle size (reflecting aggregates), consistent with the absence of visual flocculation. The results agree with earlier findings in which no flocculation was observed in hydrophilic fumed silica dispersions at pH 10 on addition of TEAB up to 0.2 M.<sup>5</sup>

The isoelectric point for silica particles in water is around pH 2. At pH 10, the particles are highly negatively charged due to dissociation of silanol (SiOH) groups, which renders the dispersion stable. According to DLVO theory for charge-stabilised colloidal particles, the electrostatic potential at the surface of a particle is the most important parameter controlling colloid stability. It is commonly known that addition of electrolytes can reduce the electrostatic potential by compressing the electrical double layer resulting in coagulation of the particles. This applies to inorganic, non-adsorbing electrolytes which do not alter the surface charge of the particles. However, for organic electrolytes, one of the ions in the electrolyte may adsorb preferentially at the particle surface altering both the surface charge and electrostatic potential. The latter has been shown with the adsorption of  $R_4N^+$  ions on silica particles.<sup>6-8</sup> Binks and Lumsdon<sup>5</sup> reported the flocculation of Aerosil 200 silica particles upon addition of tetraethylammonium bromide (TEAB). At pH 10, particles remained dispersed irrespective of salt concentration. However, at intermediate pH (6), the particles were dispersed at low salt concentration, flocculated between 0.003 and 0.6 M and re-

dispersed above 0.7 M.<sup>5</sup> Flocculation was attributed to preferential adsorption of  $R_4N^+$  ions onto particle surfaces.

The zeta potentials of these particles in the presence of the four  $R_4NX$  salts are shown in Figure 3.3. The value in pure water is -34 mV. On addition of salt, the magnitude of the zeta potential gradually decreases with increasing salt concentration. In addition, salts with longer hydrophobic chain length are more effective in reducing the zeta potential (TBANO<sub>3</sub> and TPAB). The decrease of the zeta potential is likely due to the adsorption of  $R_4N^+$  ions on particle surfaces. Up to 0.05 M salt, all zeta potential values are negative indicating that adsorption of ions in  $R_4NX$  salts does not neutralise all the charge. It was suggested that adsorbed  $R_4N^+$  ions occupy a significantly larger surface area than the silanol group, such that a single ion may adsorb over more than one negative site preventing complete neutralization even with a monolayer of adsorbed ions.<sup>7</sup> For comparison, the zeta potential of silica particles in KNO<sub>3</sub> were also measured. This salt does not change the zeta potential up to a salt concentration of 0.01 M, in contrast to the findings for silica particles around neutral pH in the presence of NaCl where it decreases linearly with the logarithm of the counter-ion concentration.<sup>19</sup> The results are in line with those of Oh *et al.*<sup>20</sup> in the case of KCl at pH 8.

**Figure 3.1.** Appearance of 2 wt.% Ludox HS-30 silica nanoparticle dispersions in (a) TMANO<sub>3</sub>, (b) TEANO<sub>3</sub>, (c) TPAB and (d) TBANO<sub>3</sub> solutions of different concentrations (given) at pH 10 and 24 h after preparation.

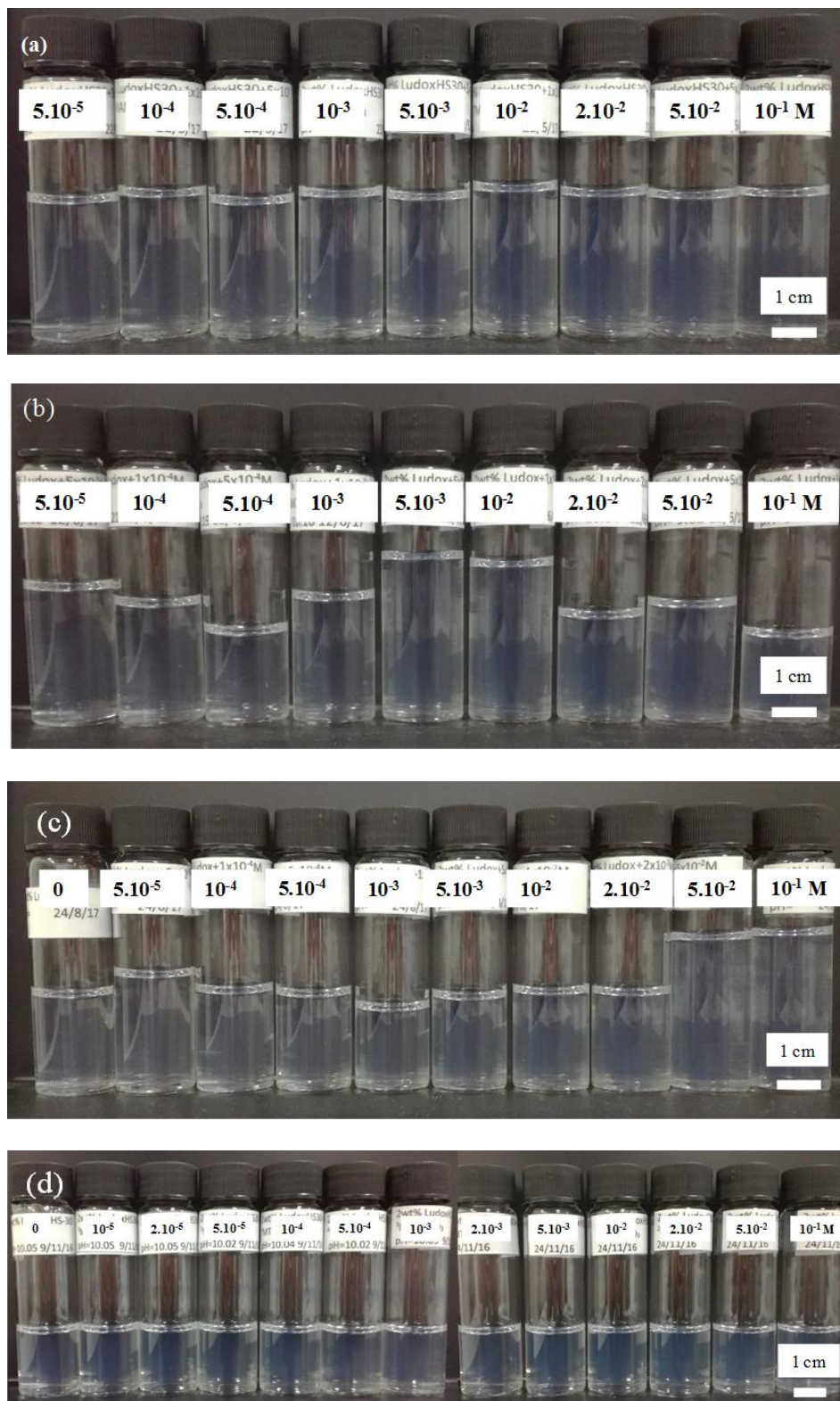


**Figure 3.2.** Average diameter of Ludox HS-30 silica particles at different R<sub>4</sub>NX salt concentrations for 0.1 wt.% dispersions at pH 10. Dashed line indicates the diameter in pure water.

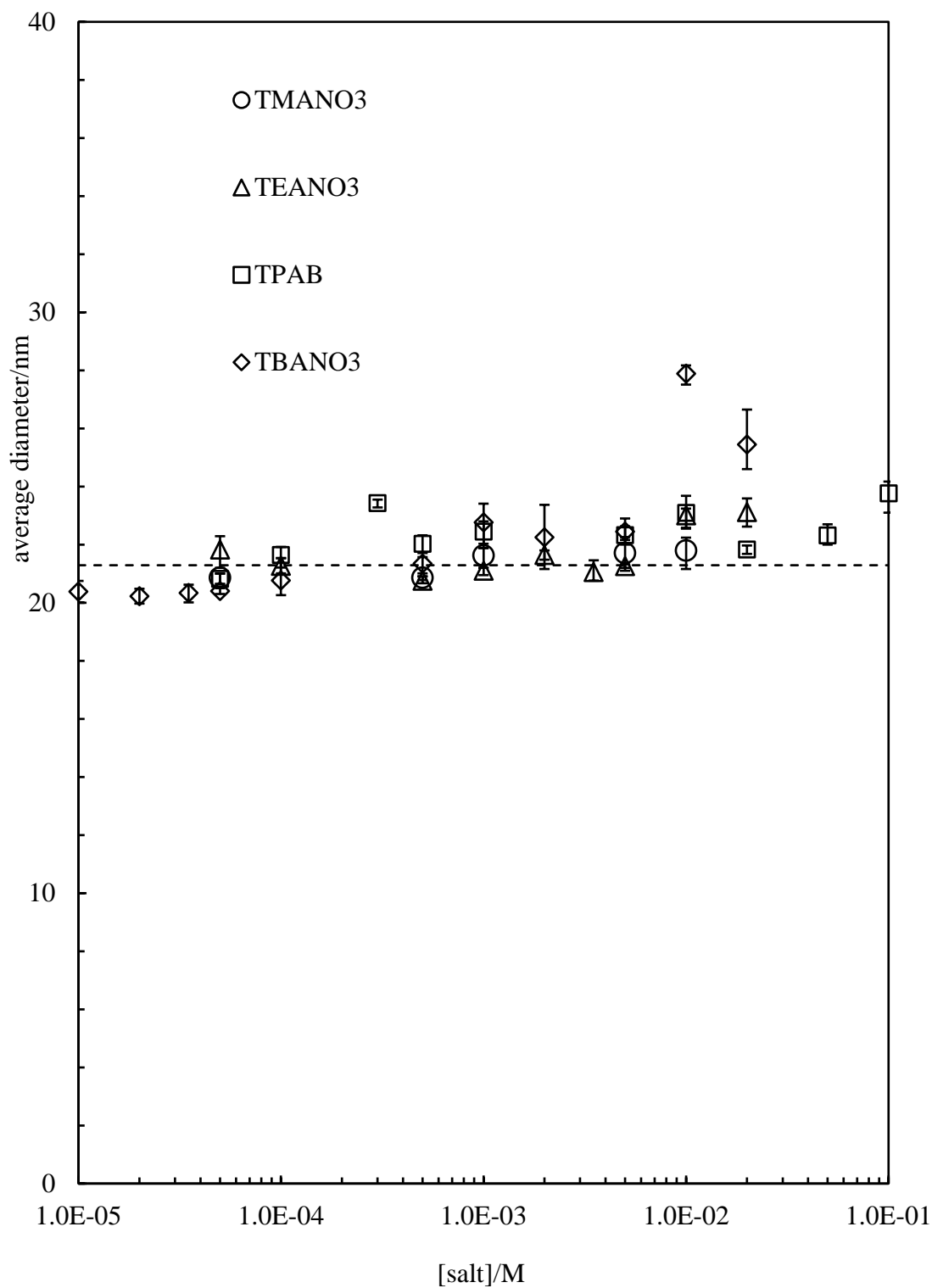
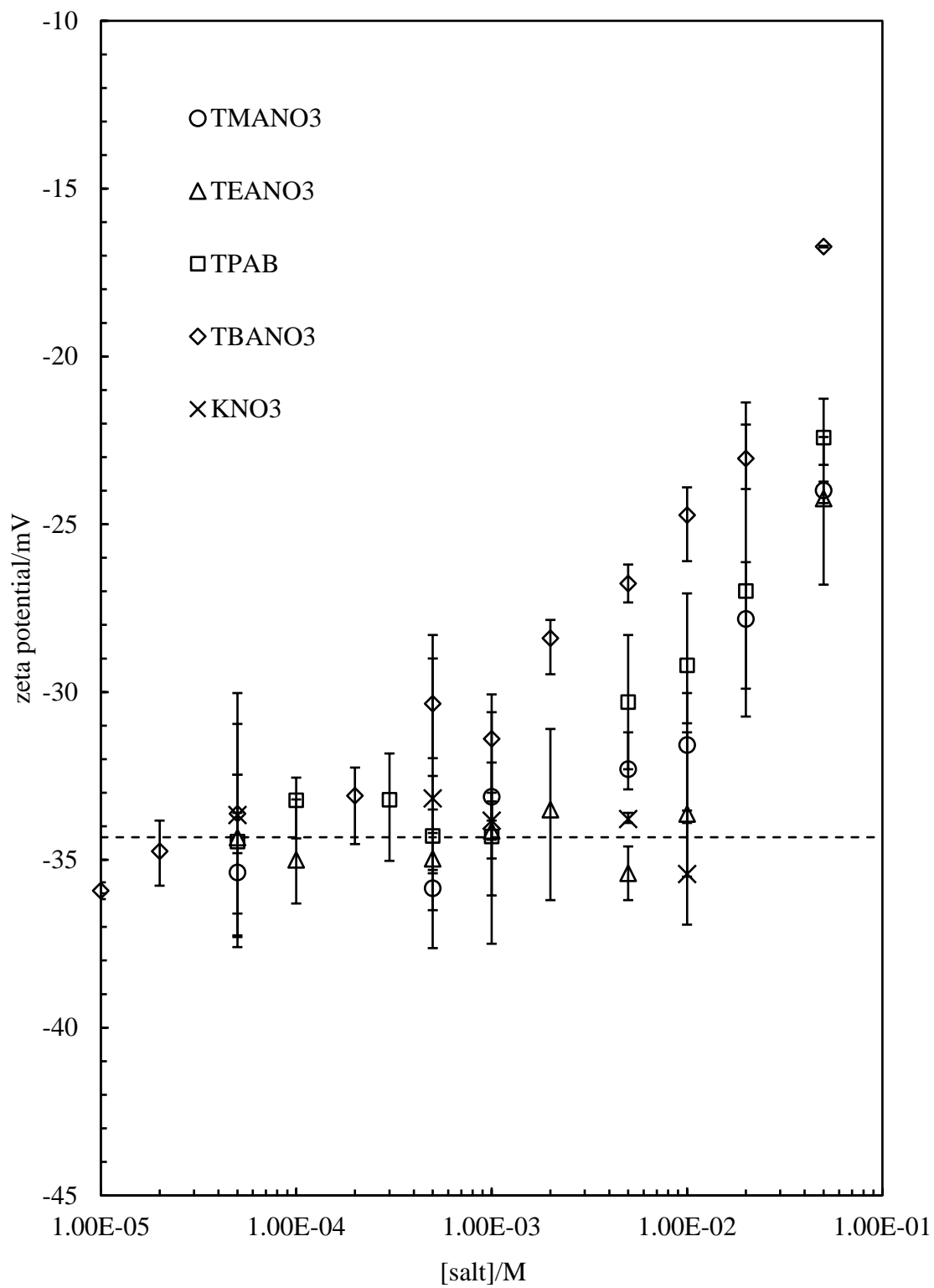


**Figure 3.3.** Zeta potential of Ludox HS-30 silica particles at different salt concentrations for 0.1 wt.% dispersions at pH 10. Dashed line indicates the zeta potential in pure water.



### 3.3 Emulsions stabilised by silica nanoparticles

#### 3.3.1 Effect of salt concentration at a fixed particle concentration

Prior to investigating emulsions stabilised by a mixture of silica particles and R<sub>4</sub>NX salts, emulsions containing either salt alone or silica particles alone were prepared. As shown in Figure 3.4, none of the four R<sub>4</sub>NX salts result in a stable emulsion at the concentrations studied, indicating that although some of these salts are reported surface-active<sup>16</sup> they are not effective emulsifiers. As expected, with hydrophilic silica particles alone, complete phase separation occurs immediately after homogenization at particle concentrations up to 5 wt.%. Since silica particles at high pH are highly negatively charged as is the octane-water interface due to preferential adsorption of hydroxyl ions,<sup>19</sup> electrostatic repulsion prevents their adsorption to the oil-water interface.

Figure 3.5 shows the appearance of oil-in-water (o/w) emulsions stabilised by 2 wt.% Ludox HS-30 silica nanoparticles in the presence of R<sub>4</sub>NX salts at pH 10 two weeks after preparation. For the shortest chain in the salt (TMANO<sub>3</sub>), no emulsification is possible up to 10<sup>-1</sup> M. In contrast, for TEANO<sub>3</sub> o/w emulsions begin to be stabilised to some extent at 3.5×10<sup>-3</sup> M, with the volume of residual emulsion increasing with salt concentration. This is a clear indication of the synergy between particles and salt in enhancing particle adsorption to the interface. By increasing the R chain length further (TPAB and TBANO<sub>3</sub>), the salt concentration required to initiate emulsion stabilization decreases (to 3×10<sup>-4</sup> M and 5×10<sup>-5</sup> M respectively). This is believed to be linked directly to the increased adsorption of R<sub>4</sub>N<sup>+</sup> ions to silica particle surfaces in water reported earlier<sup>8</sup> and correlates with the effect of salt on their zeta potential (Figure 3.3).

To quantify the stability of the emulsions to creaming and coalescence, the fractions of water ( $f_w$ ) and oil ( $f_o$ ) extracted below and above the stable emulsion layer respectively after 2 weeks are plotted in Figure 3.6, in which  $f = V_t/V_0$  where  $V_t$  is the volume of water or oil extracted by time  $t$  and  $V_0$  is their initial volume before homogenization. Apart from TMANO<sub>3</sub> for which  $f_o$  is equal to unity (completely unstable) at all salt concentrations, the stability to coalescence ( $f_o$ ) increases

progressively with salt concentration and with an increase in the chain length of the R group. It reaches a value of zero above  $5 \times 10^{-3}$  M and these emulsions remain completely stable for at least 1 year. In contrast,  $f_w$  decreases from unity to a constant value between 0.55 and 0.60, indicating that emulsions are partially unstable to creaming even at high salt concentration. The optical microscopy images of stable emulsions measured 2 weeks after preparation is shown in Figure 3.7. Spherical droplets were observed on each image. The median drop diameter of emulsions was measured by light diffraction after the determine of refractive index of R<sub>4</sub>NX salt solutions at studied concentrations and the result equals to that of water (1.333). Figure 3.8 shows the median drop diameter as a function of salt concentration. It remains approximately constant at 34  $\mu\text{m}$  for TEANO<sub>3</sub>-containing emulsions but decreases from 120  $\mu\text{m}$  at low salt concentrations where significant coalescence occurs to a constant value of *ca.* 40  $\mu\text{m}$  at  $5 \times 10^{-4}$  M for TPAB and TBANO<sub>3</sub> as salt. These results illustrate that addition of organic electrolyte is very effective in promoting hydrophilic particles to adsorb at the oil-water interface and enable stable emulsions to form.

Binks and Lumsdon<sup>5</sup> investigated the effect of TEAB on an o/w emulsion stabilised by Aerosil 200 silica particles. They found that at pH 6, the emulsions are stable to coalescence at all salt concentrations. The size of the droplets shows a remarkable minimum against salt concentration. Whereas all emulsions prepared at pH 10 underwent complete phase separation in 5 min. This is quite different from the results in this chapter, considering the salt they use is of high similarity with TBANO<sub>3</sub>. The reason might lie in the silica particles. Ludox HS-30 silica particles are prepared from precipitation at high pH, silanol groups present on the surface can ionise at high pH. Whereas Aerosil 200 are fumed silica, surface silanol groups do exist but some of them are linked to adjacent groups *via* Si-O-Si bonds, thus are not free to ionise. This difference might affect particles' sensitivity upon electrolyte induced flocculation in aqueous dispersions and influence their behaviours in emulsions.<sup>5</sup>

**Figure 3.4.** Appearance of octane-water emulsions (1:1 by volume) containing (a) TMANO<sub>3</sub>, (b) TEANO<sub>3</sub>, (c) TPAB and (d) TBANO<sub>3</sub> at different concentrations (given) at pH 10 taken 24 h after preparation. (e) Appearance of octane-water emulsions (1:1 by volume) stabilised by Ludox HS-30 silica nanoparticles in pure water at pH 10 taken 24 h after preparation.

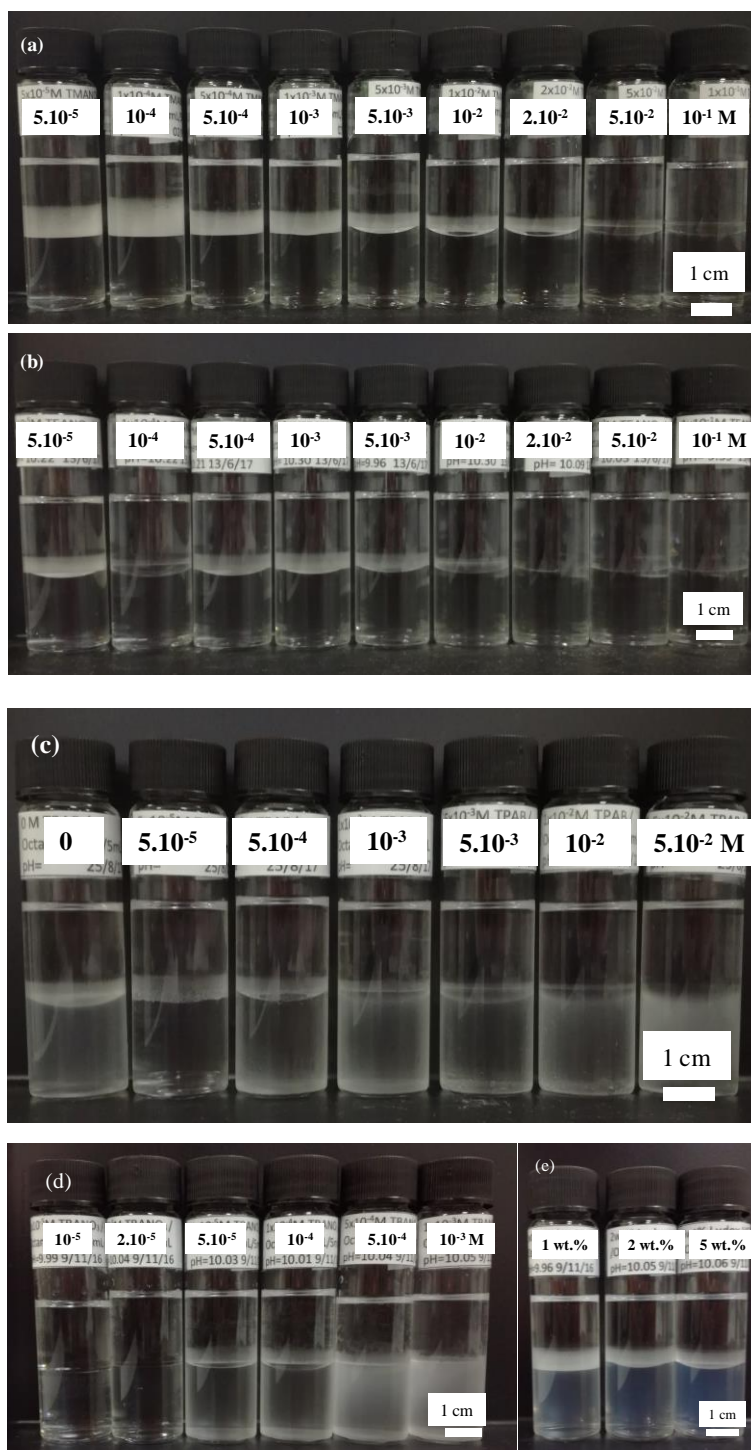


**Figure 3.5.** Appearance of octane-in-water emulsions (1:1 by volume) after two weeks stabilised by 2 wt.% Ludox HS-30 silica nanoparticles at different salt concentrations (given) at pH 10. (a) TMANO<sub>3</sub>, (b) TEANO<sub>3</sub>, (c) TPAB and (d) TBANO<sub>3</sub>.

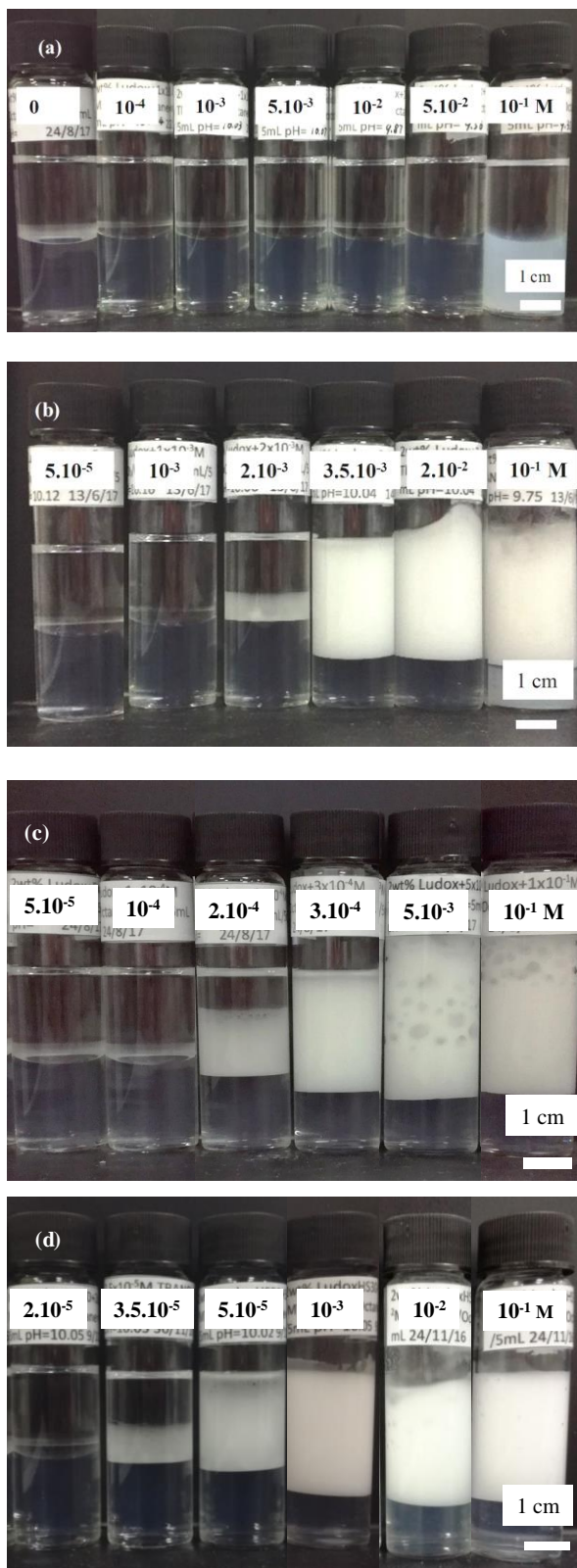


**Figure 3.6.** Stability to (a) coalescence ( $f_o$ ) and (b) creaming ( $f_w$ ) after two weeks of octane-in-water emulsions stabilised by 2 wt.% Ludox HS-30 silica nanoparticles at different salt concentrations at pH 10.

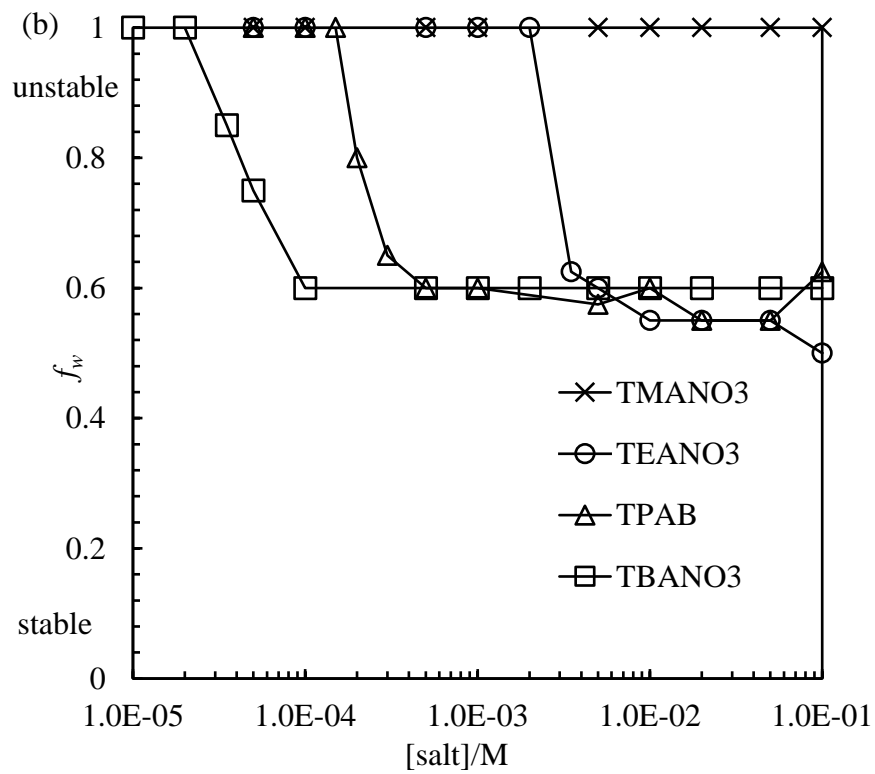
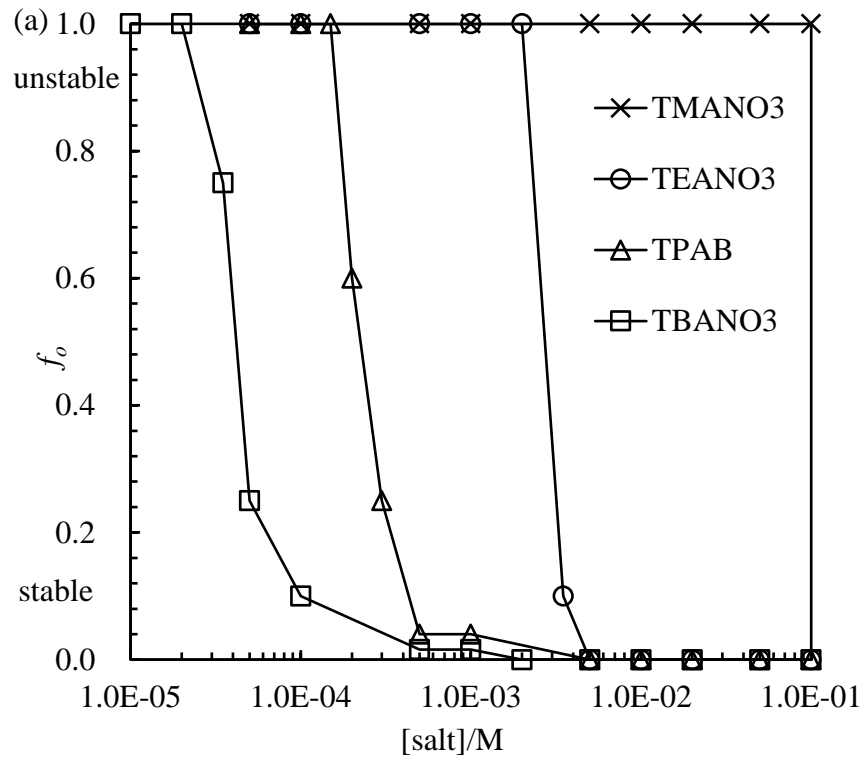


**Figure 3.7.** Optical microscopy of selected o/w emulsions stabilised by 2 wt.% Ludox HS-30 silica particles in the presence of (a) TEANO<sub>3</sub>, (b) TPAB and (c) TBANO<sub>3</sub> at pH ~10. Measured two weeks after preparation. Scale bar = 200 μm.

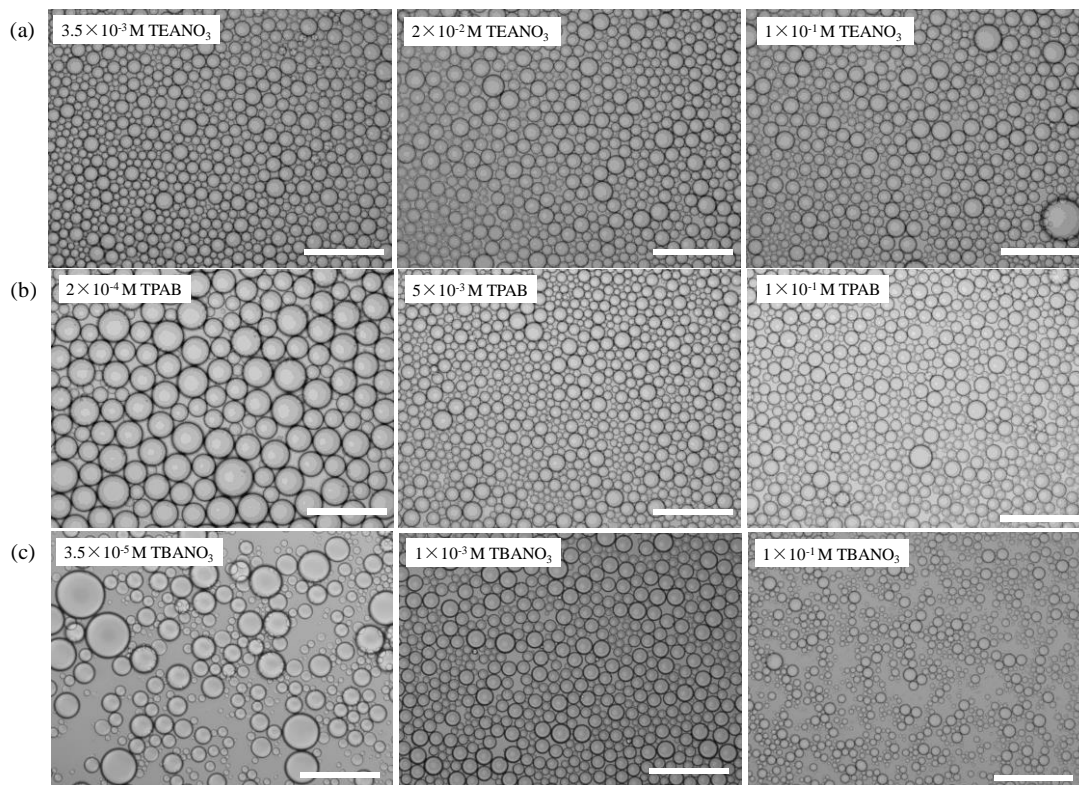
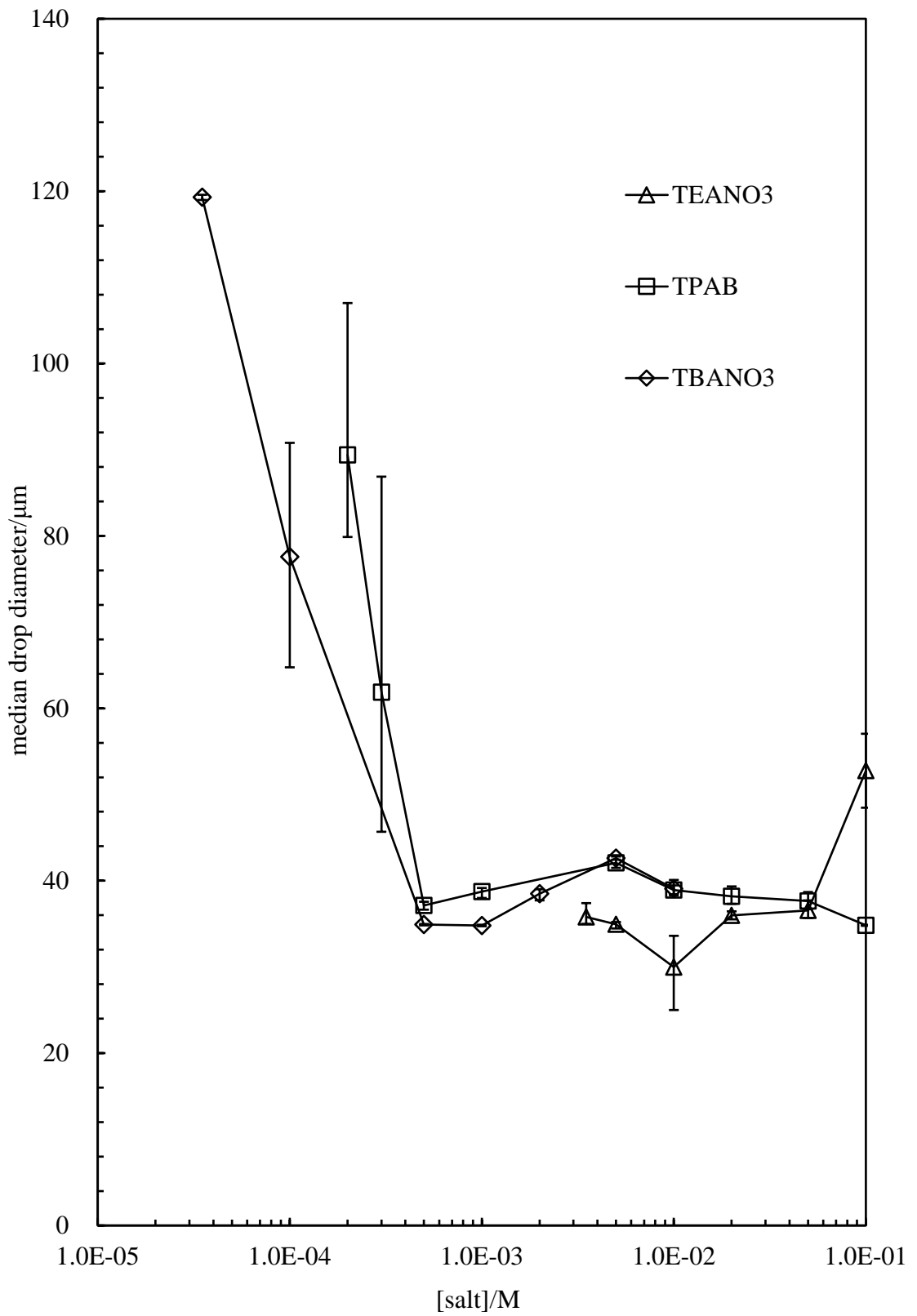


**Figure 3.8.** Variation in median drop diameter after two weeks of octane-in-water emulsions stabilised by 2 wt.% Ludox HS-30 silica particles *versus* salt concentration.



In order to assess the effect of salt on the potential modification of the particle wettability, the contact angle  $\theta_{o,w}$  of a water drop (pH 10) under octane on a hydrophilic glass substrate as a mimic for the surface of Ludox HS-30 nanoparticles was measured. Figure 3.9 contains plots of the contact angle  $\theta_{o,w}$  measured through water as a function of salt concentration for the four  $R_4NX$  salts. It is worth to note that the measurement of three-phase contact angle of glass slide surfaces is not exactly equivalent to the situation of silica particles adsorbing at the oil-water interface. In the former case, glass slides were immersed in the oil before loading water droplets on it, the organic salt only assess part of the glass surface (within the profile of water drops). While in the latter case, silica particles were dispersed in the solution of organic salts before adsorbing onto the oil-water interface. To overcome this, one can hang the glass slides in the salt solutions, then release oil drops in the solutions. The buoyancy will drive the oil drops to contact with the glass slide, hence, the contact angle can be measured. For  $TMANO_3$ , water more or less wets the surface (very hydrophilic,  $< 5^\circ$ ) and  $\theta_{o,w}$  is not affected by salt addition, consistent with particles remaining highly hydrophilic and unable to stabilise emulsions. By contrast,  $\theta_{o,w}$  increases to around  $25^\circ$  for  $TEANO_3$  implying a more hydrophobic surface. For TPAB and  $TBANO_3$  slight maxima of  $40^\circ$  and  $48^\circ$  are observed respectively, and the hydrophobicity at most salt concentrations increases progressively with R chain length. This is in good agreement with literature where contact angles of aqueous tetrapentylammonium bromide in air on a mica surface were around  $40-50^\circ$ .<sup>21</sup> Similar contact angle maxima have been reported in silica particle/cationic surfactant mixtures as a function of surfactant concentration, *e.g.* hexadecyltrimethylammonium bromide ( $C_{16}TAB$ ).<sup>15, 22</sup> Bilayer adsorption of  $C_{16}TA^+$  cations on the particle surface is widely accepted as an explanation of this phenomenon. That is, at low concentrations, by electrostatic attraction,  $C_{16}TA^+$  cations absorb on the negatively charged silica surface and form a monolayer, with the hydrophobic alkyl chains exposed in solution, resulting in increase of contact angle. After the formation of a monolayer  $C_{16}TA^+$  cations, further adsorption can occur *via* chain-chain interaction in alkyl chains forming a bilayer, now with hydrophilic  $-N(CH_3)_3^+$  groups toward the solution and results in decrease of contact angle.<sup>15</sup> In systems with TPAB and  $TBANO_3$  here, a similar bilayer might form although it is claimed that only monolayer adsorption occurs on mica immersed in  $R_4NBr$  solutions.<sup>21</sup> However, for  $R_4NX$  salts such as  $TMANO_3$ , the formation of

bilayer is unlikely because  $\text{TMA}^+$  is not amphiphilic as solutions of tetramethylammonium bromide is found to have higher surface tensions than water.<sup>7</sup>

Apart from the electrostatic attraction effect, different hypotheses have been proposed to explain the charge properties and coagulation behaviour of silica particles in  $\text{R}_4\text{MX}$  salt solutions at neutral pH.<sup>6</sup> The site binding model<sup>7,21</sup> states that at low salt concentrations,  $\text{R}_4\text{N}^+$  ions adsorb onto neutral  $\text{SiOH}$  groups without displacing protons, which should reduce the potential and cause coagulation. As salt concentration increases, salt cations then adsorb directly onto charged  $\text{SiO}^-$  sites in competition with protons. Because of the size of these ions, one  $\text{R}_4\text{N}^+$  ion may replace more than one proton. This exchange may increase the double-layer potential and net charge and hence lead to colloid stability.<sup>20</sup> However, this description is not applicable here as experiments were conducted at pH 10 where all surface sites are charged and no coagulation was evidenced. van der Donk *et al.*<sup>8</sup> put forward a stimulated adsorption model where salt cations adsorbed at siloxane bridges. This worked well for the adsorption of  $\text{TMA}^+$  ions on silica particles but not for  $\text{TEA}^+$  and  $\text{TPA}^+$  ions due to the overlap of the hydrophobically hydrated regions between adsorbed ions on adjacent sites. It is hard to compare the findings here easily with either of these models, but the possibility exists that partial bilayer formation can occur for the two longest salts at high concentration. Based on the discussion above, the schematic of possible mechanism of  $\text{R}_4\text{NX}$  salts adsorption onto silica particles enabling them to stabilise emulsions is shown in Figure 3.10.

Due to the similarity in behaviour noted above between the longer  $\text{R}_4\text{NX}$  salts and cationic surfactant, it is interesting to question at which chain length such a salt behaves like a surfactant in the stabilization of a Pickering emulsion. Hence, parallel experiments have been conducted with mixtures of silica particles and either dodecyltrimethylammonium bromide ( $\text{C}_{12}\text{TAB}$ ) or  $\text{C}_{16}\text{TAB}$ , which possess the same number of carbon atoms in the hydrophobic chain as  $\text{TPAB}$  and  $\text{TBANO}_3$  respectively. As shown in Figure 3.12,  $1 \times 10^{-4}$  M of  $\text{C}_{12}\text{TAB}$  readily stabilises coalescence-stable o/w emulsions with 2 wt.% of silica particles, compared with  $4 \times 10^{-3}$  M of  $\text{TPAB}$  being required. The creaming stability of emulsions increases with surfactant concentration, peaking at  $5 \times 10^{-3}$  M where flocculation of particles in water is maximum (see Figure 3.11). Since the critical micellization concentration (CMC) of  $\text{C}_{12}\text{TAB}$  is  $15.4 \times 10^{-3}$  M

at 25 °C,<sup>23</sup> the observed behaviour is solely due to surfactant monomer adsorption. In the case of C<sub>16</sub>TAB (CMC = 0.95 mM<sup>23</sup>), a small volume of stable Pickering emulsion forms at 2×10<sup>-5</sup> M, very close to that seen in TBANO<sub>3</sub> systems (3.5×10<sup>-5</sup> M). It is concluded that, regarding the ability to stabilise an emulsion with silica particles, TBANO<sub>3</sub> behaves like C<sub>16</sub>TAB, whereas TPAB behaves poorer than a surfactant with the same number of carbon atoms. The reason probably lies in the surface activity difference between electrolytes and surfactants. Evidence exists that R<sub>4</sub>NX salts have a lower surface activity than single or double-chained cationic surfactants with the same number of carbon atoms due to their symmetrical structure.<sup>18</sup> Indeed, it has been reported that the surface tension of water shows a decrease of ~10 mN m<sup>-1</sup> in the presence of 1 mM TPAB, whereas the corresponding value with 1 mM of TBAB is ~25 mN m<sup>-1</sup>.<sup>18</sup> By contrast, at the CMC of the surfactants, solutions with C<sub>12</sub>TAB and C<sub>16</sub>TAB show a very close value of surface tension decrease (~ 35 mN m<sup>-1</sup>)<sup>24</sup>. Hence, the surface activity of TPAB is much lower than that of C<sub>12</sub>TAB, whereas TBANO<sub>3</sub> is close to C<sub>16</sub>TAB in the term of surface activity.

**Figure 3.9.** Variation of the advancing contact angle measured through water of a water drop (pH 10) on a hydrophilic glass slide under octane with R<sub>4</sub>NX salt concentration. Contact angle for pure water is < 5°.

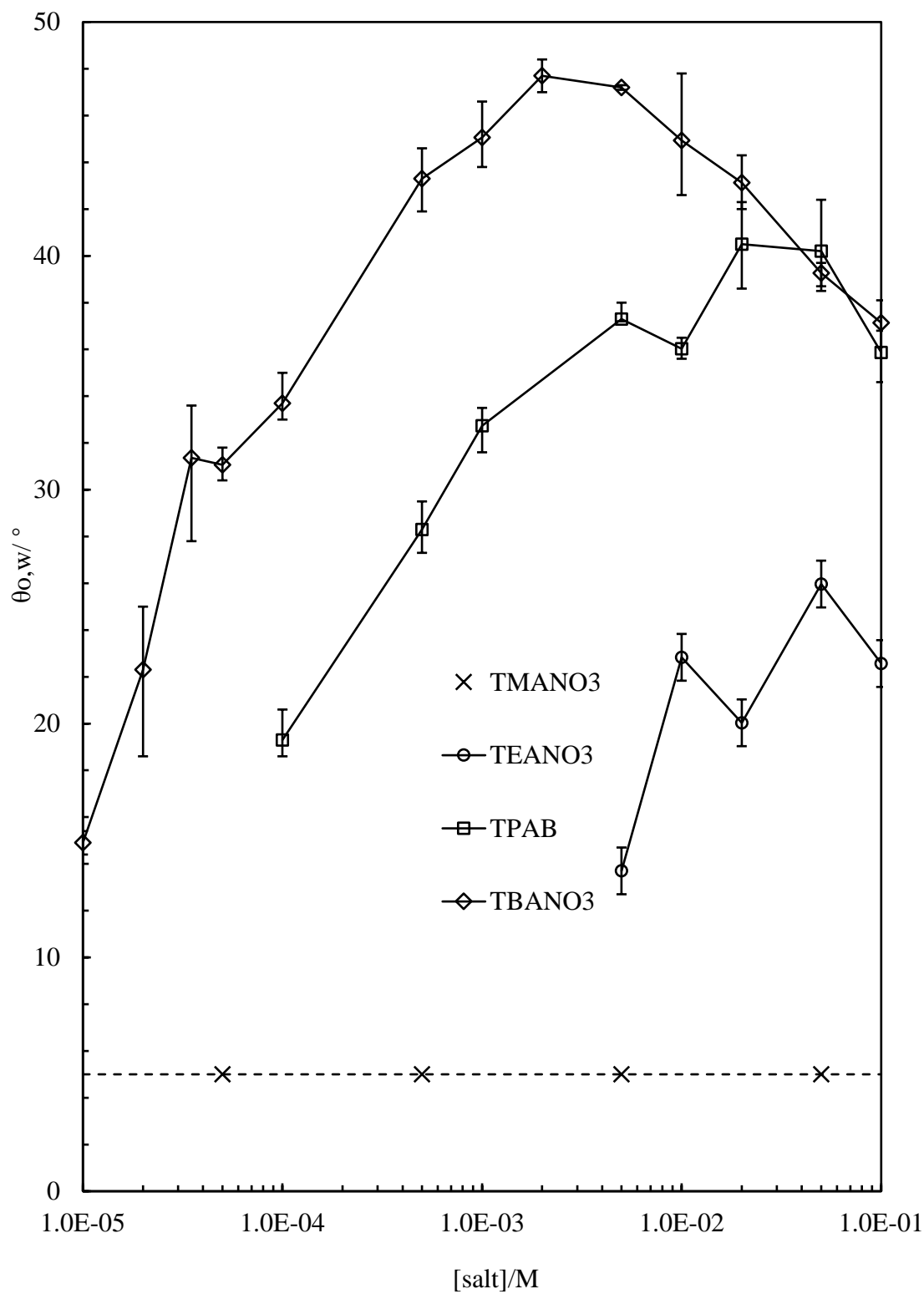


**Figure 3.10.** Schematic of (a) possible arrangement of  $R_4N^+$  cations on the surface of silica particle; (b)  $R_4N^+$  cations enable particles to adsorb onto oil-water interfaces.

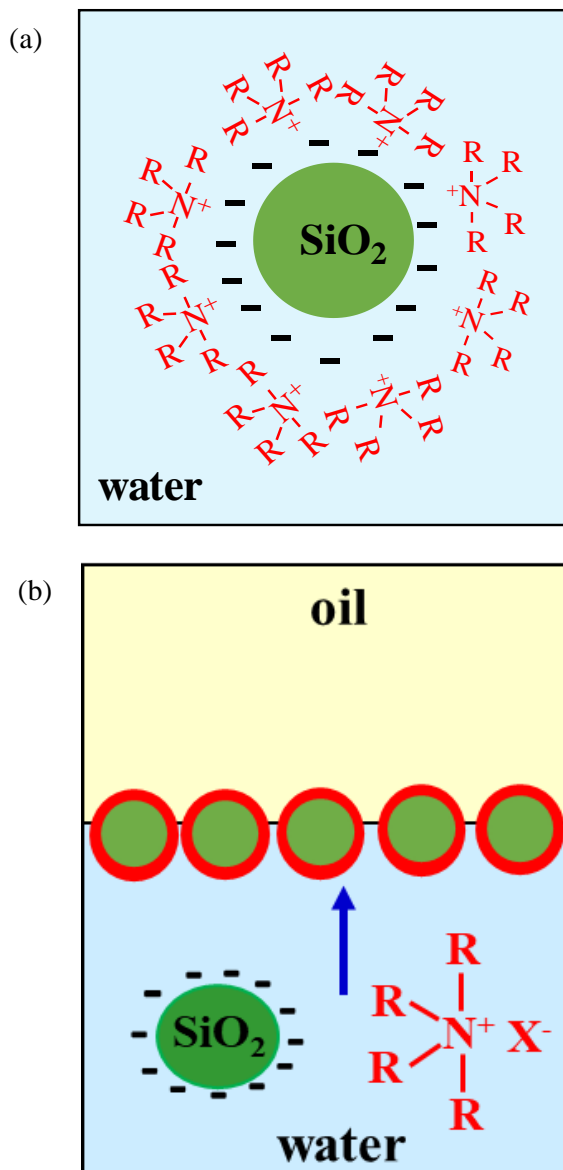


**Figure 3.11.** Appearance of 2 wt.% Ludox HS-30 silica dispersions at pH 10 in the presence of (a)  $C_{12}$ TAB and (b)  $C_{16}$ TAB at different concentrations (given, notice sediment from  $1 \times 10^{-4}$  M in latter) taken immediately after preparation.

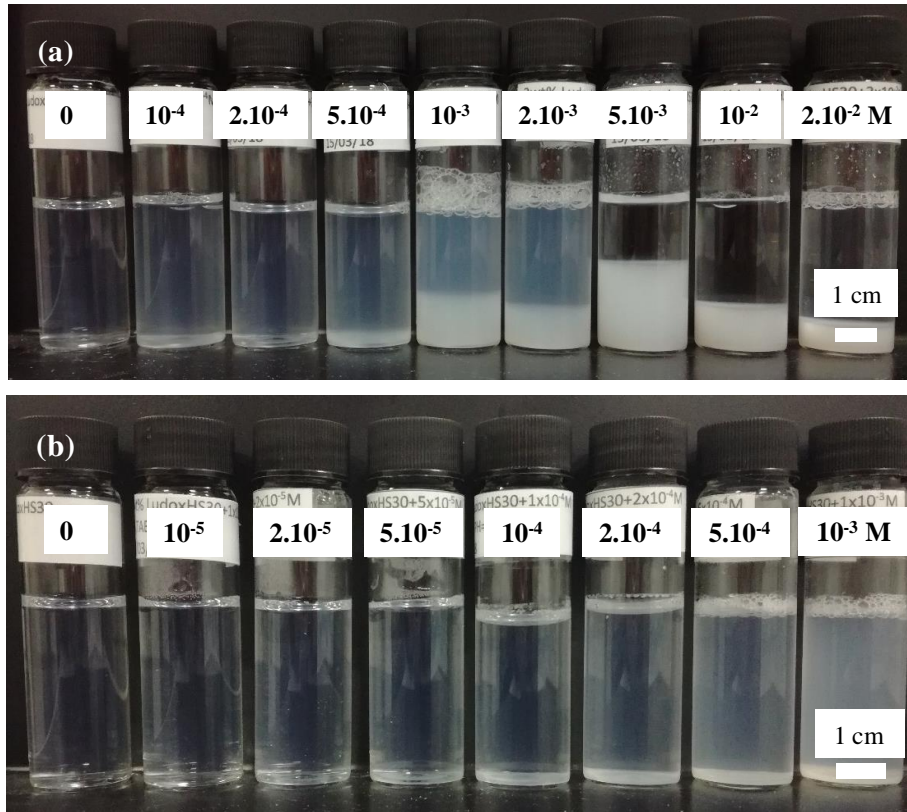
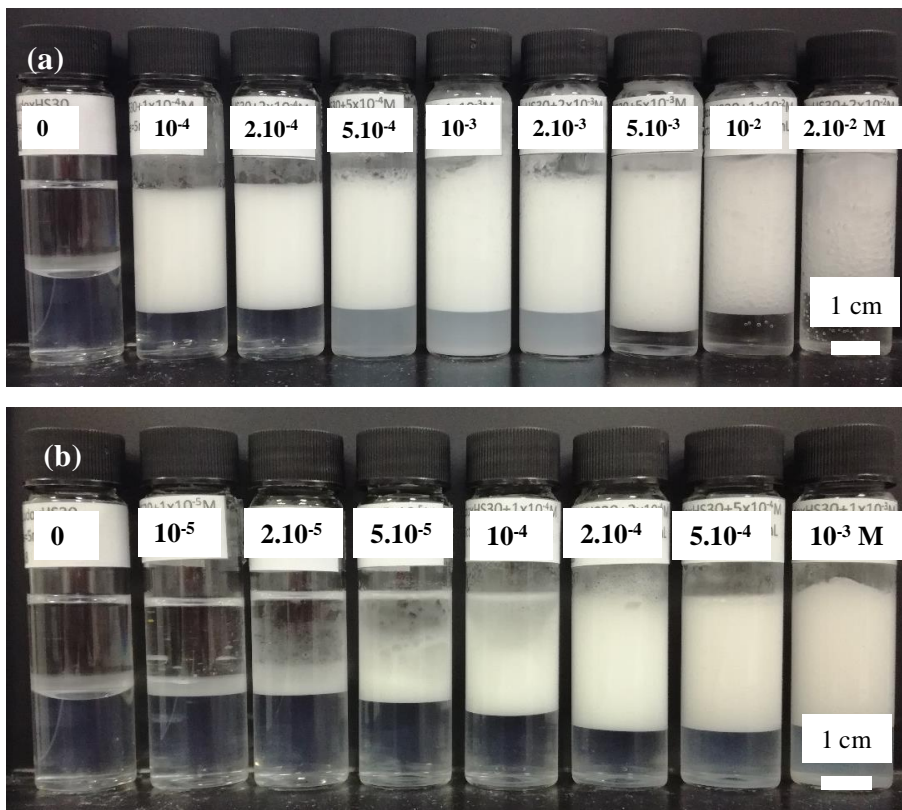


**Figure 3.12.** Appearance of octane-in-water emulsions (1:1 by volume) stabilised by 2 wt.% Ludox HS-30 silica nanoparticles at pH 10 in the presence of (a)  $C_{12}$ TAB and (b)  $C_{16}$ TAB at different concentrations (given) taken one week after preparation.



### 3.3.2 Effect of particle concentration at a fixed salt concentration

Particle concentration is an important factor affecting the properties of Pickering emulsion. In this section, emulsions were prepared at fixed salt concentration but varied particle concentrations. Figure 3.13 shows the appearance of emulsions prepared at different particle concentrations with  $5 \times 10^{-3}$  M of  $R_4NX$  salt with ethyl, propyl or butyl chains. This salt concentration was chosen as it is that for which emulsions are completely stable to coalescence at 2 wt.% particles. All emulsions exhibit creaming. Their stability to coalescence increases progressively with particle concentration as expected. Plots of  $f_o$  and  $f_w$  after 2 weeks for emulsions are given against particle concentration in Figure 3.14. In emulsions with  $TEANO_3$ , minimum in  $f_o$  and  $f_w$  are observed. Whereas in emulsions containing TPAB and  $TBANO_3$ ,  $f_w$  and  $f_o$  continuously decrease with salt concentrations. Spherical droplets were observed under optical microscopy (Figure 3.15) and the average droplet diameters are shown in Figure 3.16. While the droplet diameter containing  $TEANO_3$  remains constant, that with TPAB or  $TBANO_3$  continuously decrease from 150  $\mu m$  and 110  $\mu m$ , respectively, to 30  $\mu m$ . As has been extensively reported, increase of particle concentration may improve the emulsion stability as well as reduce droplet size, which is in agreement with the observations here. As particle concentration increases, more particles are possible to be trapped at the oil-water interfaces, providing a steric barrier preventing coalescence of drops from the initial homogenization stage, thus give emulsions with smaller droplets and higher stability, which is consistent with the limited coalescence phenomenon.<sup>25</sup> For  $TEANO_3$  however, it worth to note that coalescence sets in above 2 wt.% particles until complete phase separation ensues at 5 wt.%. As an explanation, since a higher salt concentration is required for  $TEANO_3$  to produce a stable emulsion *cf.* the higher homologues, at increasing particle concentration the adsorbed amount of salt cation on particle surfaces decreases at fixed salt concentration. Particles are not rendered sufficiently hydrophobic as a result and coalescence is inevitable.

**Figure 3.13.** Appearance of octane-in-water emulsions (1:1 by volume) after two weeks stabilised by Ludox HS-30 silica particles of different concentration (given) in the presence of  $5 \times 10^{-3}$  M salt at pH 10: (a)  $\text{TEANO}_3$ , (b) TPAB and (c)  $\text{TBANO}_3$ .

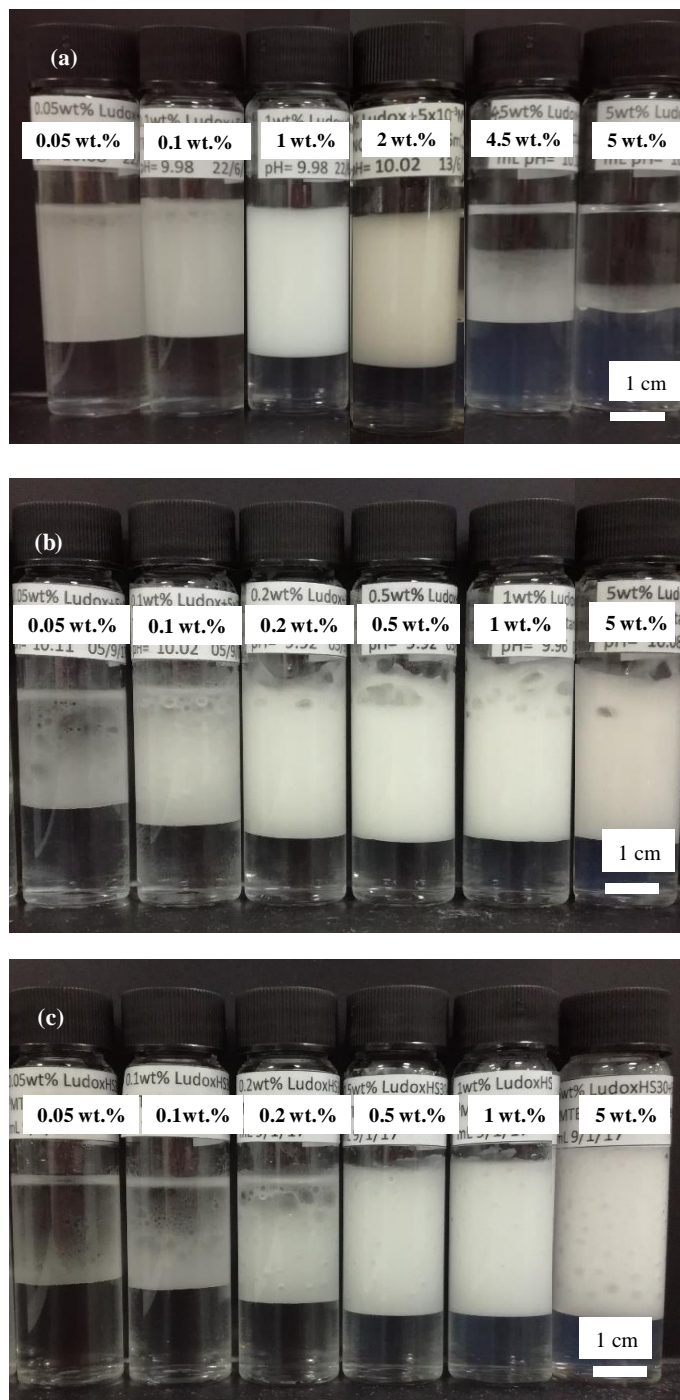


**Figure 3.14.** Stability to (a) coalescence ( $f_o$ ) and (b) creaming ( $f_w$ ) after two weeks of octane-in-water emulsions stabilised by Ludox HS-30 silica particles of different concentration in the presence of  $5 \times 10^{-3}$  M salt at pH 10.

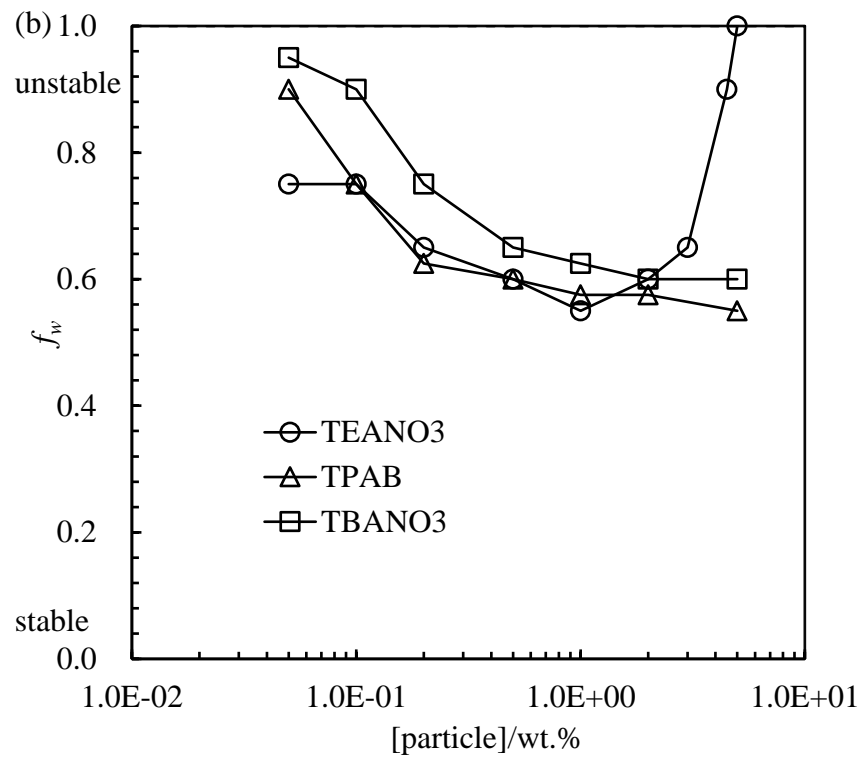
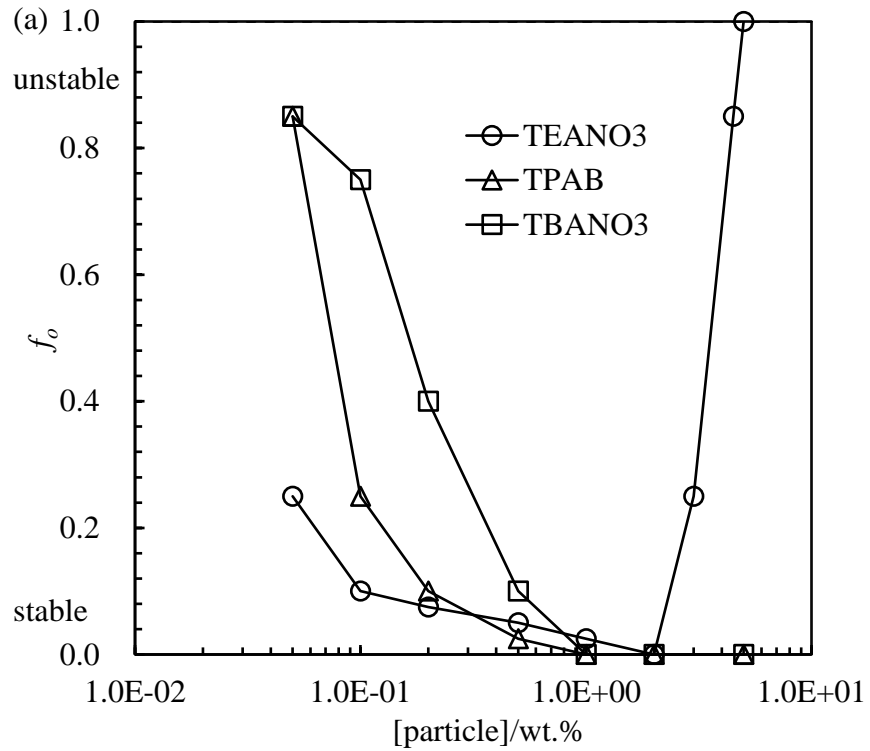


**Figure 3.15.** Optical microscopy of selected o/w emulsions stabilised by Ludox HS-30 silica particles at varied concentrations in the presence of  $5 \times 10^{-3}$  M (a) TEANO<sub>3</sub>, (b) TPAB and (c) TBANO<sub>3</sub> at pH ~10. Measured two weeks after preparation. Scale bar = 200  $\mu$ m.

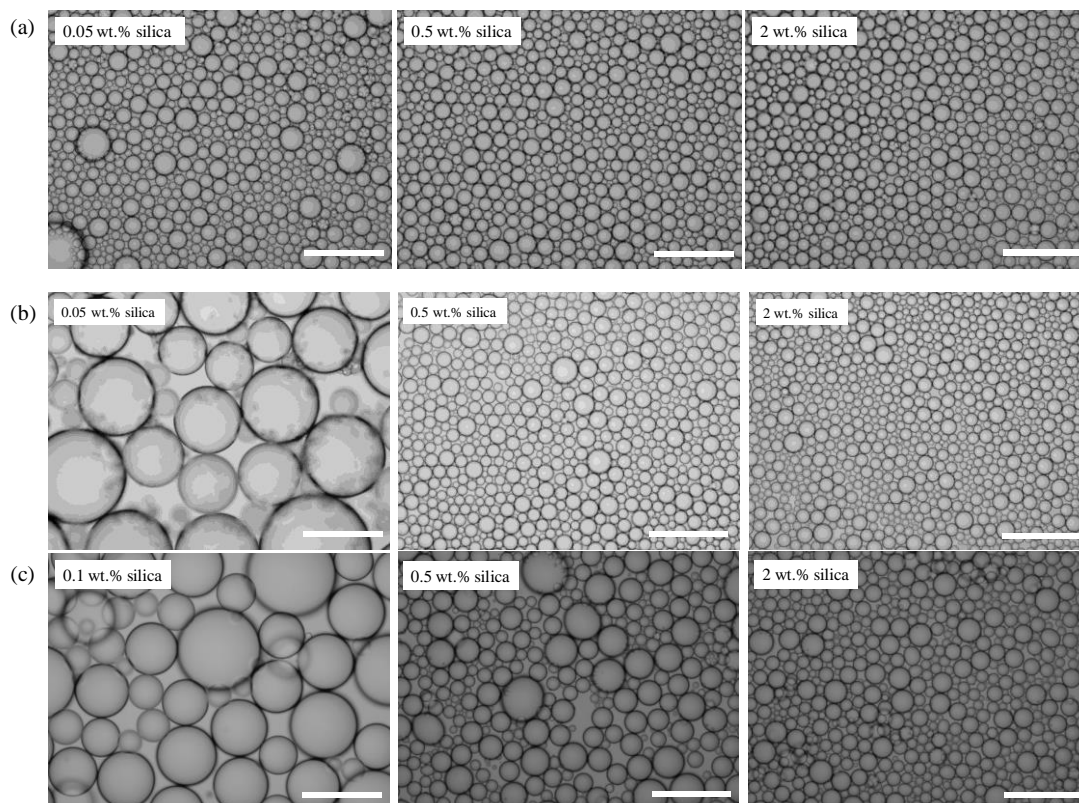
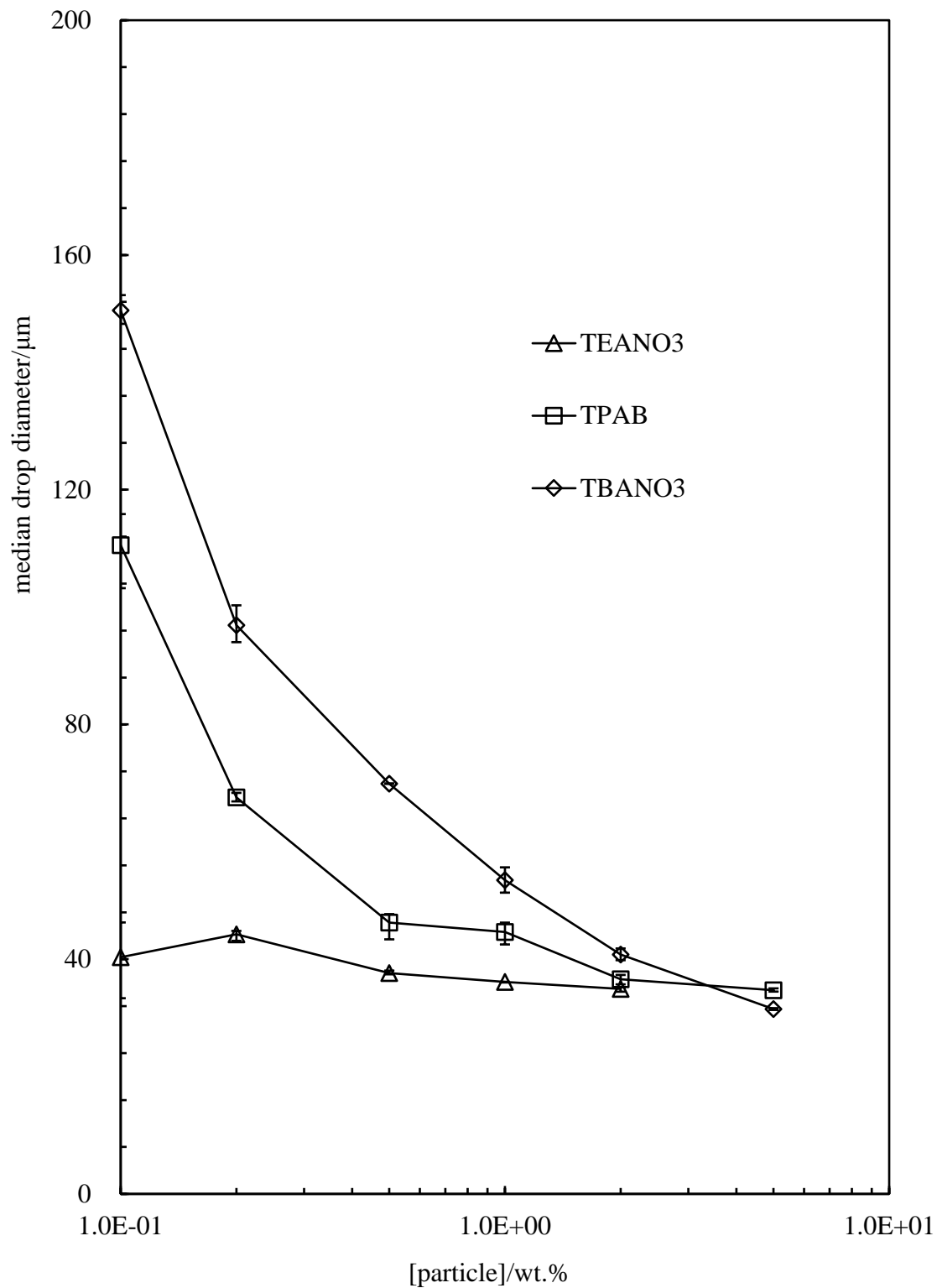


**Figure 3.16.** Variation of the median drop diameter after two weeks of octane-in-water emulsions stabilised by Ludox HS-30 silica particles at different concentrations in the presence of  $5 \times 10^{-3}$  M salt at pH 10.



### 3.4 Emulsions stabilised by micron-sized silica particles

In order to explore whether the adsorption of  $R_4NX$  salt on silica nanoparticles enabling emulsion stabilisation applies to larger particles and to be able to visualise particles on emulsion droplet interfaces, emulsions were prepared using 2 wt.% of monodisperse silica particles of around 2  $\mu\text{m}$  in diameter in systems containing  $TBANO_3$  at pH 10. The appearance of the o/w emulsions after 2 weeks can be seen in Figure 3.17 (a). From  $1 \times 10^{-4}$  M salt, emulsions become increasingly stable to coalescence even though they exhibit creaming. In Figure 3.17 (b) it can be seen that  $f_w$  remains constant at around 0.8, while  $f_o$  decreases dramatically to around 0.05 with salt concentration. Although a strict comparison with the nanoparticle-stabilised emulsions can only be made by choosing concentrations equating to the same number of particles, nonetheless it is clear that  $TBANO_3$  also activates large, charged silica particles to adsorb at the oil-water interface and stabilise an emulsion.

The arrangement of large silica particles on the surface of oil drops in emulsions was determined by optical microscopy. Micrographs at selected salt concentrations are given in Figure 3.18 where adsorbed particles are clearly visible. For droplets in the absence of salt or at low salt concentration ( $1 \times 10^{-4}$  M), particles are not close-packed with voids between them resulting in low coalescence stability of emulsions. Increasing the salt concentration to between  $5 \times 10^{-4}$  M and  $5 \times 10^{-3}$  M leads to an increase in the surface density of particles and a reduction in the inter-particle spacing (Figure 3.19), serving to order particles into a hexagonal arrangement. The average inter-particle distance is  $1.86 \pm 0.10$   $\mu\text{m}$ , very close to the particle diameter (1.83  $\mu\text{m}$ ) meaning that particles are virtually touching. Similar ordering has been seen before for polystyrene particles around silicone oil droplets in water.<sup>26</sup> It is likely that adsorption of  $TBA^+$  ions to silica particle surfaces leads to a reduction in electrostatic repulsion between adsorbed particles enabling them to close pack. However, the packing of particles becomes disordered at higher salt concentration ( $\geq 10^{-2}$  M). At  $5 \times 10^{-2}$  M, multilayer aggregation occurs and large inter-particle separation is observed (Figure 3.19). It is difficult to explain this but note that it may link to the measurable decrease in the three-phase contact angle shown in Figure 3.9 at higher salt concentrations. One possibility is that particles aggregate readily in the aqueous dispersion and adsorb onto oil-water interfaces as aggregates during homogenization,

which results in multilayer of particles around droplet surface.

The influence of particle concentration on emulsions with micron-sized particles has also been investigated at a fixed salt concentration of  $5 \times 10^{-3}$  M. The appearance of emulsions is shown in Figure 3.20 (a) where a minimum concentration of 1.5 wt.% of particles is needed. As illustrated on the optical microscopy images in Figure 3.20 (b), the packing of interfacial particles is loose and some coalescence occurs. At 2 wt.% particles, the emulsion is stable to coalescence and particles become close packed. Horozov and Binks<sup>27</sup> showed that partially hydrophobic silica particles ( $\theta_{o,w} = 65^\circ$ ) stabilised an o/w emulsion in which drops were covered by a dense particle monolayer. In contrast, highly hydrophobic silica particles ( $\theta_{o,w} = 152^\circ$ ) stabilised a water-in-oil emulsion in which particles were extremely repulsive and only covered a fraction of the interface. In comparison, in the silica + TBANO<sub>3</sub> system in this chapter, relatively dense particle monolayers are observed consistent with contact angles below  $90^\circ$  and o/w emulsions are preferred, in agreement with the earlier findings.

**Figure 3.17.** (a) Appearance of octane-in-water emulsions after two weeks stabilised by 2 wt.% silica particles ( $d = 1.83 \mu\text{m}$ ) at different  $\text{TBANO}_3$  concentrations (given) at pH 10. (b) Corresponding stability to creaming ( $f_w$ ) and coalescence ( $f_o$ ) of emulsions.

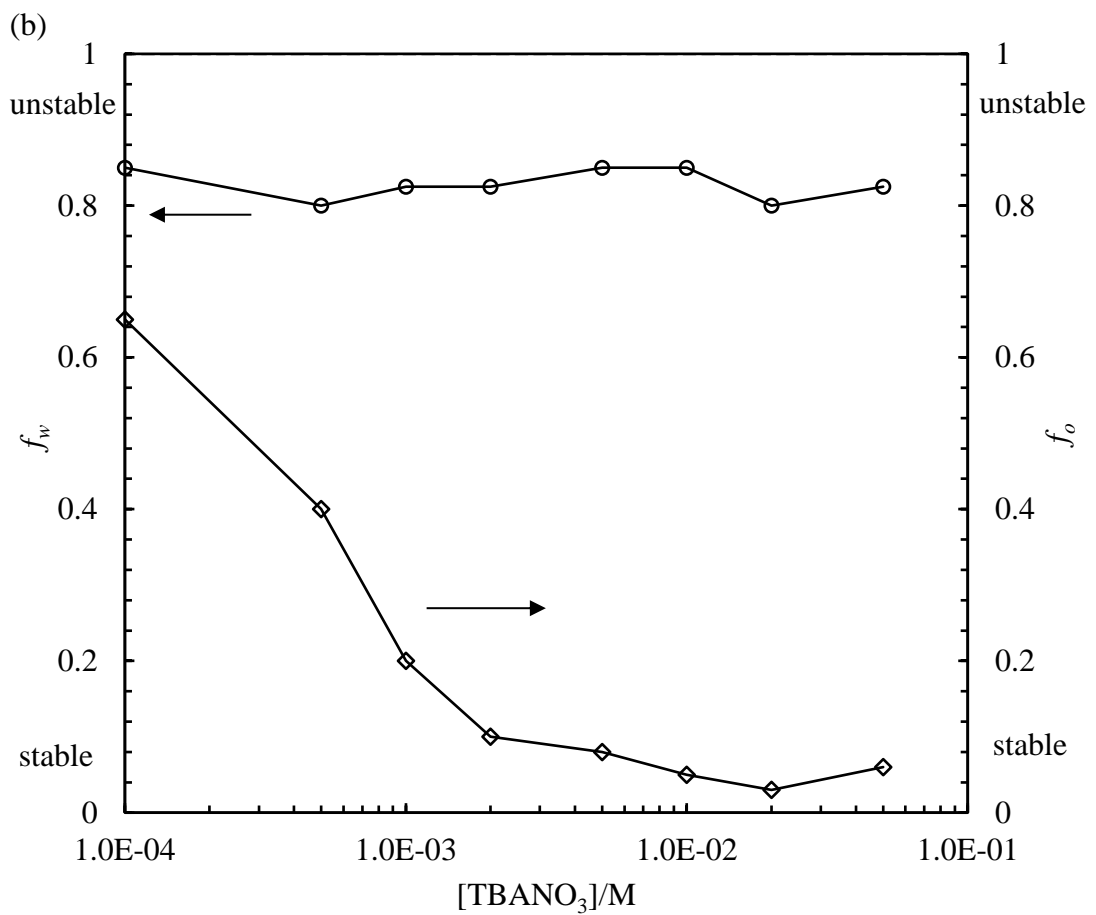
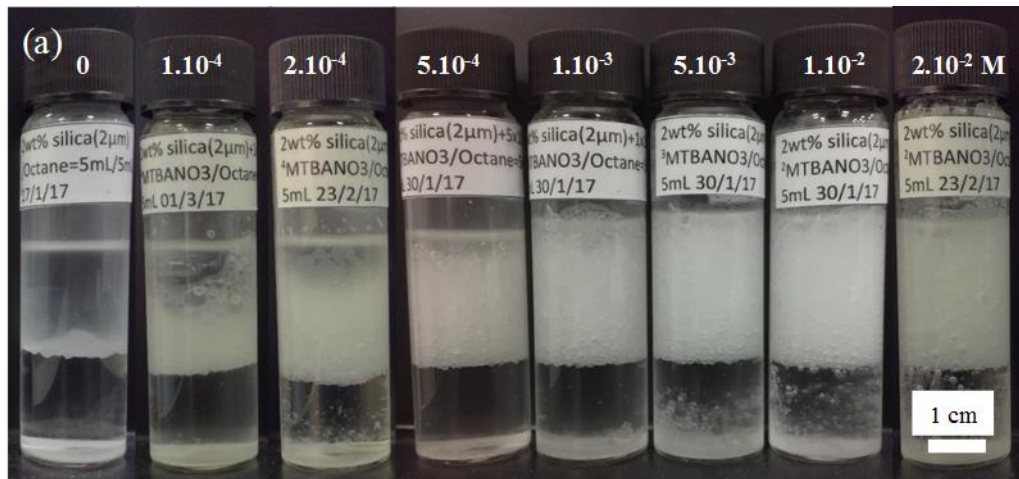


**Figure 3.18.** Selected optical micrographs of the surface of oil emulsion droplets in water stabilised by 2 wt.% silica particles ( $d = 1.83 \mu\text{m}$ ) at different  $[\text{TBANO}_3]$  (given) at pH 10 immediately after preparation. Scale bars =  $50 \mu\text{m}$ . Insets are enlarged portions of the droplet surface within the red frame; scale bars =  $5 \mu\text{m}$ . Hexagonal packing of particles is visible at intermediate salt concentration.

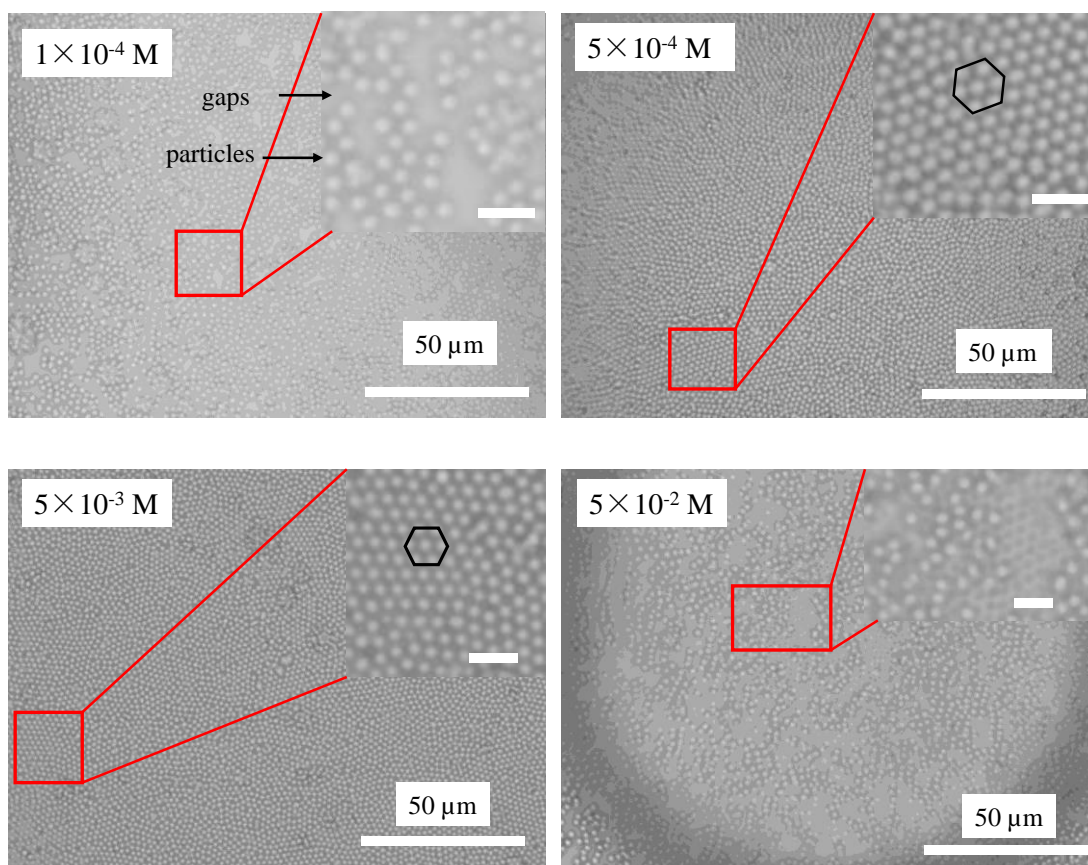


**Figure 3.19.** Variation of average inter-particle distance against [TBANO<sub>3</sub>] at pH 10 for silica particles (d = 1.83 μm) on the surface of octane-in-water emulsions stabilised by 2 wt.% particles.

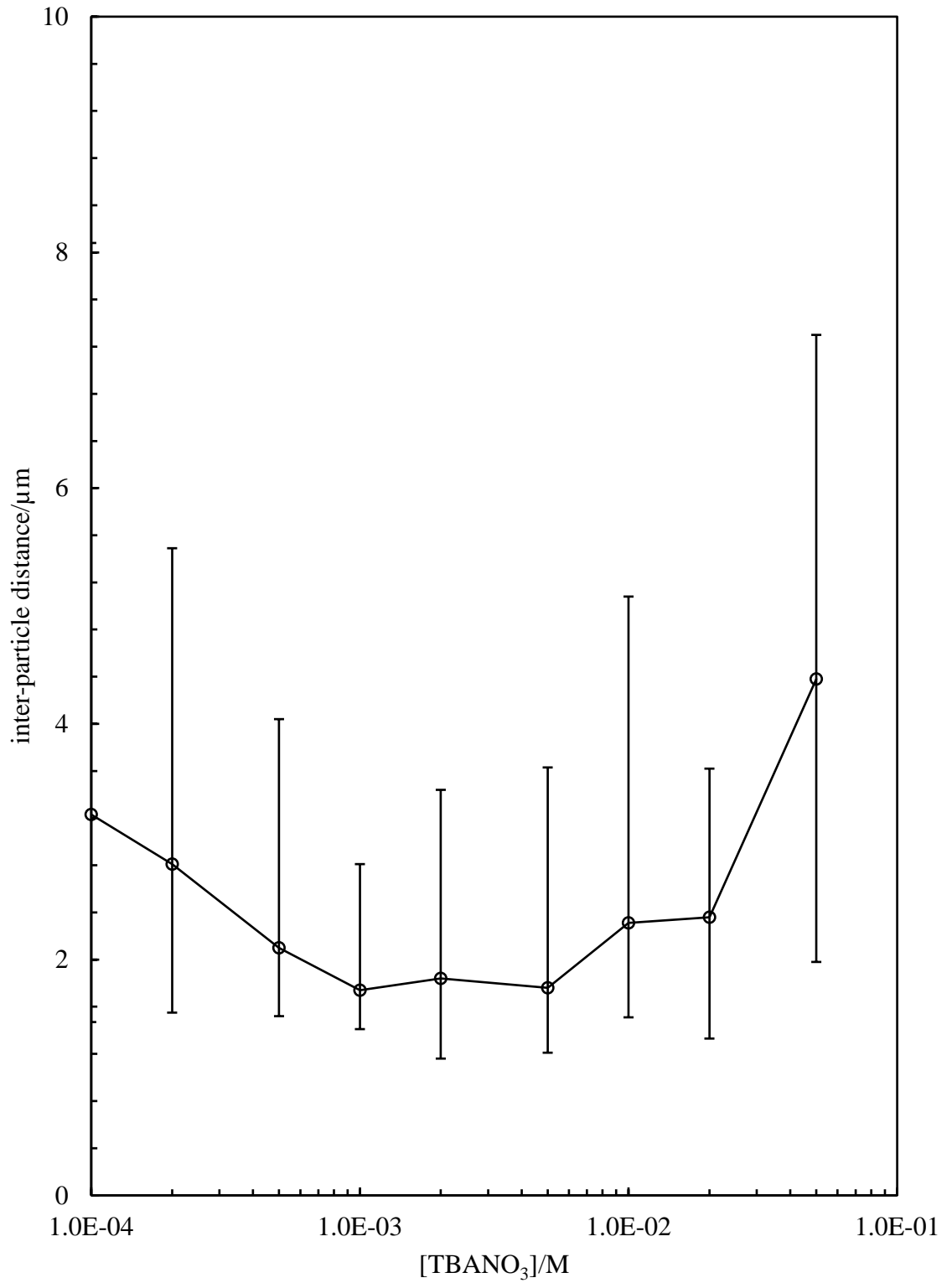
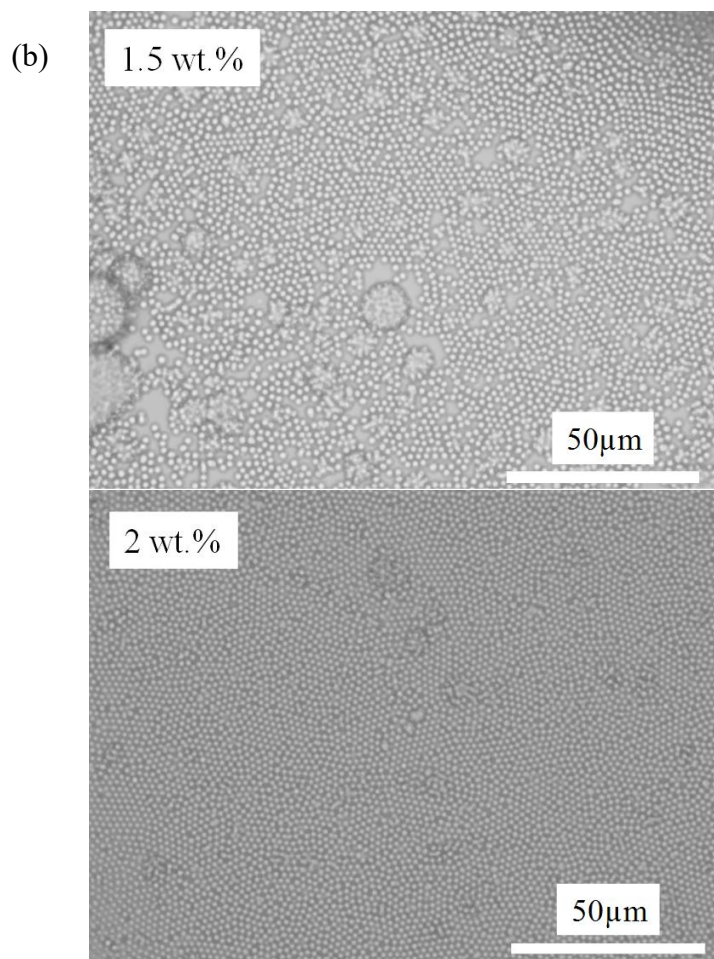
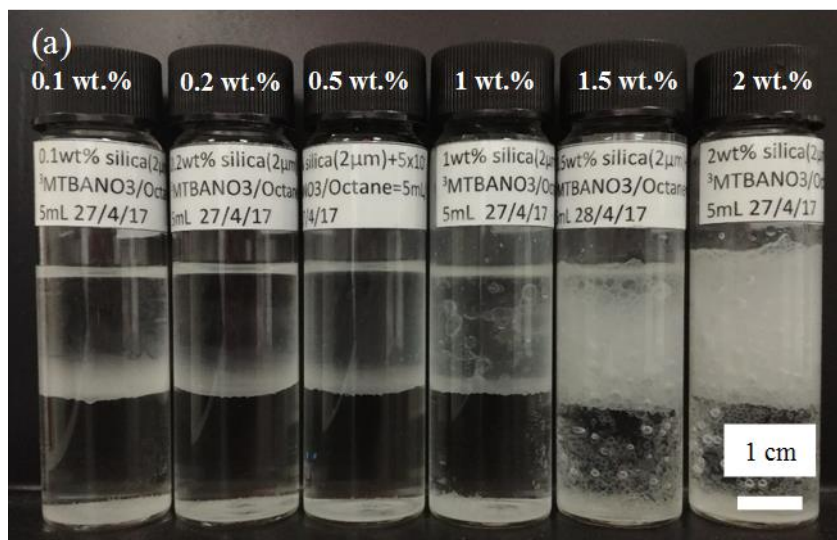


**Figure 3.20.** (a) Appearance of octane-in-water emulsions stabilised by different concentrations of silica particles ( $d = 1.83 \mu\text{m}$ ) in the presence of  $5 \times 10^{-3} \text{ M TBANO}_3$  at pH 10 taken two weeks after preparation. (b) Micrographs of the surface of oil emulsion droplets in (a) immediately after preparation.



### 3.5 Micron-sized silica particles at planar oil-water interfaces

The packing of particles around emulsion drops may not be perfect since the curvature of the interface can lead to disclinations. Studies exist in which particles have been spread at a planar liquid interface to simplify imaging and interpretation.<sup>28-32</sup> In the case of micron-sized silica particles silanised *ex situ*, a disorder to order transition was observed at the octane-water interface upon increasing the particle hydrophobicity.<sup>28</sup> Relatively hydrophilic particles formed disordered monolayers containing aggregated particles whereas very hydrophobic particles formed well-ordered monolayers with inter-particle distances larger than several particle diameters, consistent with Coulombic repulsion through the oil phase as a result of the presence of charges at the particle-oil surface. The effect of adding salt on hydrophilic particle monolayers was not investigated however. For comparison, investigation has been done on monolayers of large silica particles at the planar octane-water interface at pH 10 on addition of TBANO<sub>3</sub> to complement the emulsion studies. Selected images at different salt concentrations are given in Figure 3.21. Without salt, only a fraction of the spread particles remained at the interface with the rest sedimenting into the water phase as particles are extremely hydrophilic. Discrete particles as well as small aggregates were randomly adsorbed, with particle patches separated by particle-free domains. On addition of 10<sup>-4</sup> M TBANO<sub>3</sub>, the fraction of particles adsorbed increased tremendously and they formed a loose monolayer throughout. At 10<sup>-3</sup> M salt, the entire interface is covered by neighboring crystalline patches of particles each of which contains hexagonally close packed particles. When TBANO<sub>3</sub> further increased to 10 mM, disordered packing is observed again.

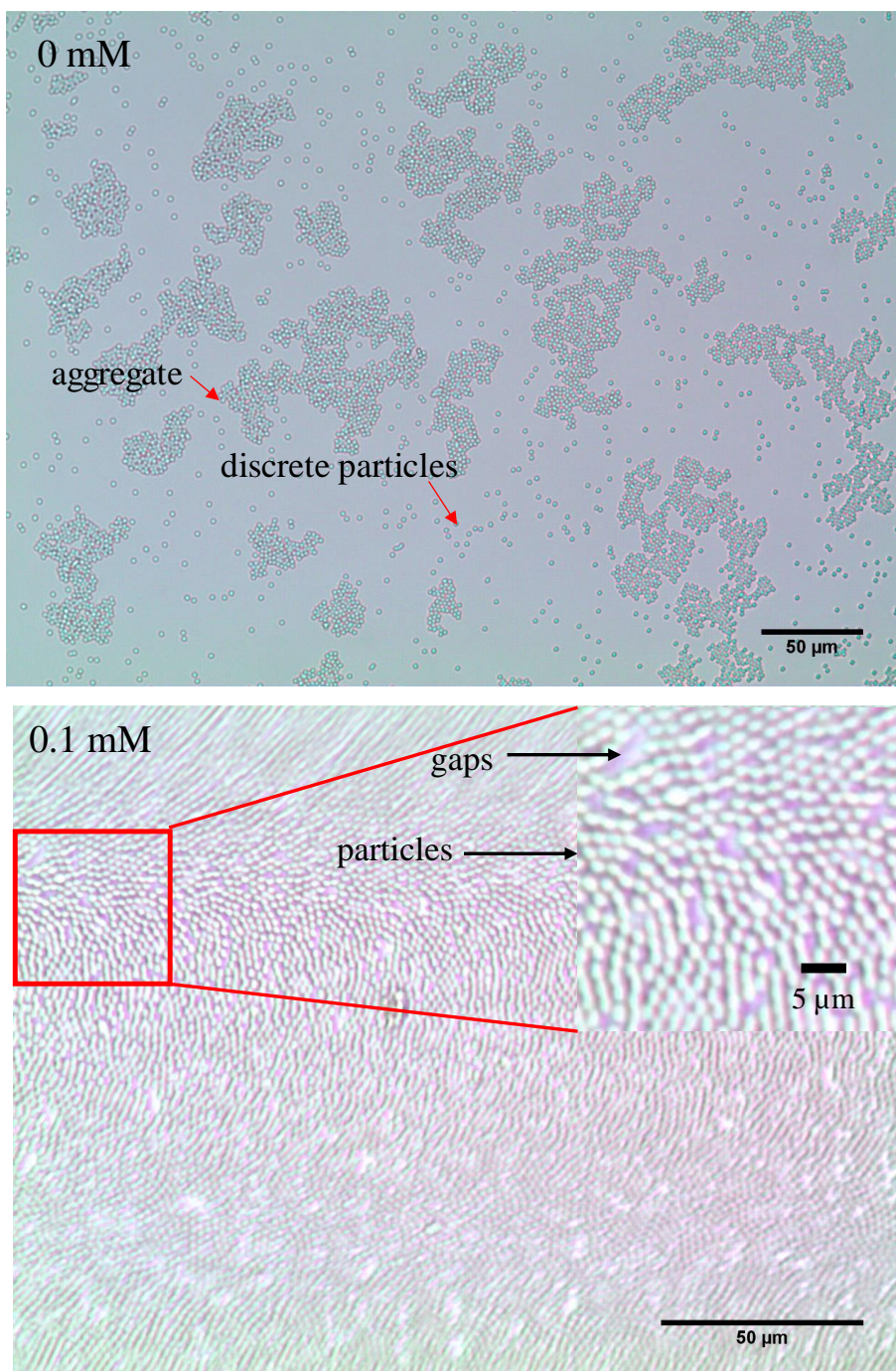
One may notice that, although the packing structures of particle monolayers at planar oil-water interface can be visually identified, the images are not as clear as those with particles at emulsion droplet surfaces (Figure 3.18). It is reasonable considering the different methods involved in taking the images. For the images of particles at emulsion droplet surface, the emulsion droplets are settled in the well of a dimple glass slide with a cover slide on top of the well. Under this circumstance, particles at droplet surfaces do not move, so it is possible to focus at high magnification. In contrast, images of particles at planar oil-water interface are taken directly at the fluid interface with a long-focus objective. Particles at the fluid interface experiencing a clear

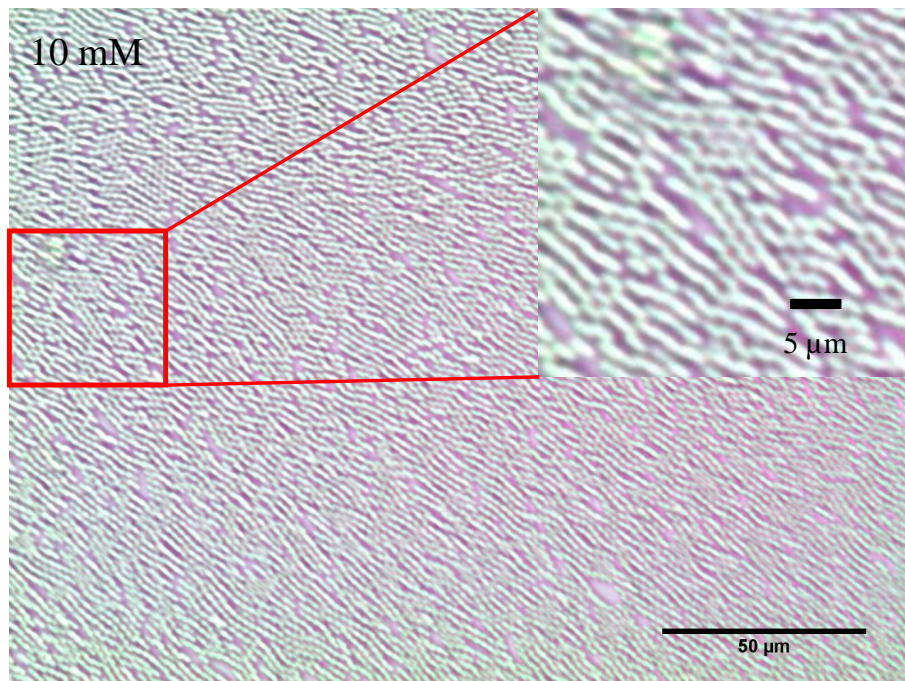
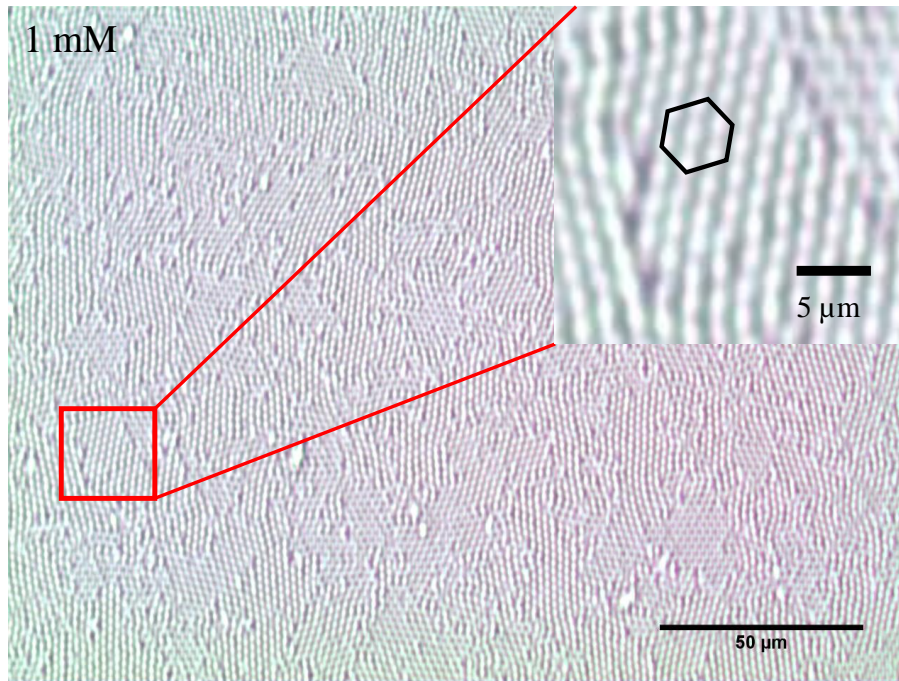
directional motion which is probably driven by a Marangoni flow arising from the surface tension imbalance between oil and water phase.<sup>33</sup> Convective flow might also contribute to the directional flow.<sup>34</sup> Consequently, it is difficult to snap particles and fuzzy images were obtained in some samples.

Figure 3.22 represents the inter-particle distance of neighboring particles, as can be seen, the dependence of the inter-particle separation on salt concentration follows the same trend as that observed on emulsion drop interfaces (Figure 3.19).

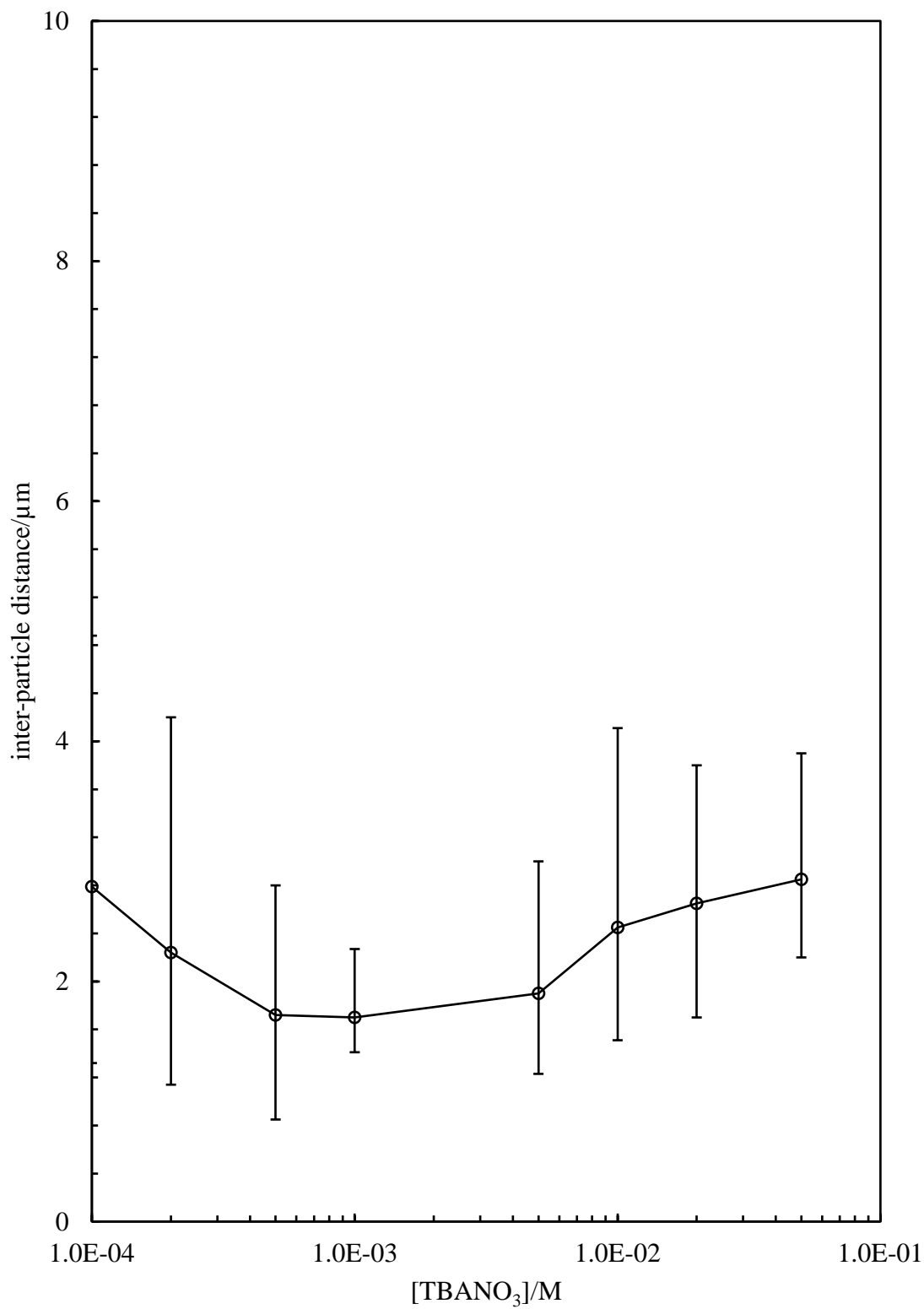
Silica particles are negatively charged at high pH, a high net energy barrier prevents the adsorption of particles to the interface. Thus, most particles subsided directly to water when injected at the interface. With the addition of a sufficient amount of  $\text{TBANO}_3$  in aqueous phase, the particle surface charge was screened, and the net energy barrier decreases considerably hence the particles readily adsorb to the oil-water interface.<sup>35</sup>

**Figure 3.21.** Selected micrographs showing silica particles spread at the planar octane-water interface by injecting 180  $\mu\text{L}$  of spreading solvent containing 1 wt.% silica particles ( $d = 1.83 \mu\text{m}$ ). Aqueous phase is either pure water or  $\text{TBANO}_3$  solution of different concentrations (given) at pH 10. The pH of the spreading solvent is 10 and all images were taken immediately after spreading. The insets are enlarged portions within the red frames.





**Figure 3.22.** Variation of average inter-particle distance against [TBANO<sub>3</sub>] at pH 10 for silica particles ( $d = 1.83 \mu\text{m}$ ) spread at the planar octane-water interface. The inter-particle distance is the separation between particle centres.



### 3.6 Conclusions

This chapter has investigated the properties of silica particles in aqueous dispersions as well as at oil-water interfaces in the presence of symmetrical tetraalkylammonium salt,  $R_4NX$ . Ludox HS-30 silica particles are highly charged and discrete in aqueous dispersions. Addition of  $R_4NX$  salts decreases the zeta potential of particles, with an increase of R chain length showing more significant ability in decreasing the zeta potential. This is attributed to specific absorption of  $R_4N^+$  ions on silica particle surfaces, which reduces the surface charge and increases the hydrophobicity of particle. However, unlike indifferent salts, the presence of these  $R_4NX$  salts do not coagulate particles.

The increase of particle hydrophobicity is reflected on the stabilization of emulsions by silica particles.  $TMANO_3$  does not promote emulsification of Ludox-HS 30 silica particles at any concentrations studied, while  $TEANO_3$ , TPAB and  $TBANO_3$  favour the stabilization of octane-in-water emulsions at certain concentrations. The stability of emulsions to both creaming and coalescence increase with increasing salt concentration as well as a growth of R chain length. In addition,  $TBANO_3$  behaves like a cationic surfactant with the same number of carbon atoms in the hydrophobic chains, *i.e.*,  $C_{16}TAB$ , in the ability of enhancing stabilization of emulsions.

The effect of particle concentration on the stability of emulsions has also been studied. The stability of emulsions to both creaming and coalescence increase with increasing particle concentrations. The emulsion droplet size follows the limited coalescence phenomenon: increase of particle concentration results in decrease of droplet size until plateaus. However, it is intriguing that high concentrations of silica particles in the presence of  $5 \times 10^{-3}$  M of  $TEANO_3$  cannot stabilize emulsions, which was attributed to limited salt adsorption on particles. At a fixed salt concentration and high particle concentrations, the amount of  $TEA^+$  ions adsorbing at particle surfaces is limited, which make the particles not hydrophobic enough to adsorb at oil-water interfaces.

The enhanced stability of emulsion by adding  $TBANO_3$  into Ludox HS-30 silica particles also applies to micron-sized silica particles. For the emulsion stabilised at a fixed particle concentration but varied  $TBANO_3$  concentration, their stability to

coalescence gradually increase with salt concentration, while the creaming stability did not change. The packing of the particles at the droplet surface changed from random loose packing to hexagonally closed packing then to multilayer aggregation as TBANO<sub>3</sub> concentration increases. For the emulsion stabilised at a fixed salt concentration but varied particle concentrations, emulsions can only be stabilised at particle concentrations higher than 1.5 wt.%. No significant difference was observed on the droplet size between the emulsion stabilised by 1.5 wt.% and 2 wt.% of particles. But the packing behaviour is of remarkable difference, the particles randomly adsorb at the droplet surface for the emulsion with 1.5 wt.% particle, whereas for the sample with 2 wt.% of particles, the particles form regions of hexagonal packing. When spread at planar oil-water interfaces, most particles subside directly into water when pure water is rendered as the aqueous phase, whereas in the presence of TBANO<sub>3</sub>, particles adsorb at the interface forming loose packing to close hexagonal package and back to a loose packing as [TBANO<sub>3</sub>] increases.

### 3.7 References

1. Okazaki, K.; Kawaguchi, M. Influence of monovalent electrolytes on rheological properties of gelled colloidal silica suspensions. *J. Dispersion Sci. Technol.* **2008**, *29*, 77-82.
2. Fuma, T.; Kawaguchi, M. Rheological responses of Pickering emulsions prepared using colloidal hydrophilic silica particles in the presence of NaCl. *Colloids Surf. A* **2015**, *465*, 168-174.
3. Frith, W.J.; Pichot, R.; Kirkland, M. and Wolf, B. Formation, stability, and rheology of particle stabilized emulsions: Influence of multivalent cations. *Ind. Eng. Chem. Res.* **2008**, *47*, 6434-6444.
4. Whitby, C.P.; Fischer, F.E.; Fornasiero, D. and Ralston, J. Shear-induced coalescence of oil-in-water Pickering emulsions. *J. Colloid Interface Sci.* **2011**, *361*, 170-177.
5. Binks, B.P. and Lumsdon, S.O. Stability of oil-in-water emulsions stabilised by silica particles. *Phys. Chem. Chem. Phys.* **1999**, *1*, 3007-3016.
6. Rubio, J. and Goldfarb, J. Stability of colloidal silica in the presence of quaternary ammonium salts. *J. Colloid Interface Sci.* **1971**, *36*, 289-291.

7. Rutland, M.; Pashley, R. The charging properties of monodisperse colloidal silica in symmetrical quaternary ammonium ion solutions. *J. Colloid Interface Sci.* **1989**, *130*, 448-456.
8. Van der Donck, J.; Vaessen, G.; Stein, H. Adsorption of short-chain tetraalkylammonium bromide on silica. *Langmuir* **1993**, *9*, 3553-3557.
9. Konrad, M.P.; Doherty, A.P.; Bell, S.E. Stable and uniform SERS signals from self-assembled two-dimensional interfacial arrays of optically coupled Ag nanoparticles. *Anal. Chem.* **2013**, *85*, 6783-6789.
10. Xu, Y.K.; Konrad, M.P.; Lee, W.W.Y.; Ye, Z.W. and Bell, S.E.J. A Method for Promoting Assembly of Metallic and Nonmetallic Nanoparticles into Interfacial Monolayer Films. *Nano Lett.* **2016**, *16*, 5255-5260.
11. Wang, M.; Zhang, Z. and He, J. A SERS Study on the Assembly Behavior of Gold Nanoparticles at the Oil/Water Interface. *Langmuir* **2015**, *31*, 12911-12919.
12. Zhou, Z.; Wu, P. and Ma, C. Hydrophobic interaction and stability of colloidal silica. *Colloids Surf.* **1990**, *50*, 177-188.
13. Koopal, L.K.; Goloub, T.; de Keizer, A. and Sidorova, M.P. The effect of cationic surfactants on wetting, colloid stability and flotation of silica. *Colloids Surf. A* **1999**, *151*, 15-25.
14. Goloub, T.P.; Koopal, L.K.; Bijsterbosch, B.H. and Sidorova, M.P. Adsorption of cationic surfactants on silica. Surface charge effects. *Langmuir* **1996**, *12*, 3188-3194.
15. Binks, B.P.; Rodrigues, J.A. and Frith, W.J. Synergistic interaction in emulsions stabilized by a mixture of silica nanoparticles and cationic surfactant. *Langmuir* **2007**, *23*, 3626-3636.
16. Tamaki, K. The surface activity of tetra-n-alkylammonium halides in aqueous solutions. The effect of hydrophobic hydration. *Bull. Chem. Soc. Jpn.* **1974**, *47*, 2764-2767.
17. Tamaki, K. The surface activity of tetrabutylammonium halides in the aqueous solutions. *Bull. Chem. Soc. Jpn.* **1967**, *40*, 38-41.
18. Dopierala, K. and Prochaska, K. The effect of molecular structure on the surface properties of selected quaternary ammonium salts. *J. Colloid Interface Sci.* **2008**, *321*, 220-226.

19. Kirby, B.J. and Hasselbrink, E.F. Zeta potential of microfluidic substrates: 1. Theory, experimental techniques, and effects on separations. *Electrophoresis* **2004**, *25*, 187-202.
20. Oh, M-H.; So, J-H.; Lee, J-D.; Yang, S-M. Preparation of silica dispersion and its phase stability in the presence of salts. *Korean J. Chem. Eng.*, **1999**, *16*, 532-537.
21. Claesson, P.; Horn, R.; Pashley, R. Measurement of surface forces between mica sheets immersed in aqueous quaternary ammonium ion solutions. *J. Colloid Interface Sci.* **1984**, *100*, 250-263.
22. Wei, X.; Zhang, W.; Lai, L.; Mei, P.; Wu, L.; Wang, Y. Different cationic surfactants-modified silica nanoparticles for Pickering emulsions. *J. Mol. Liq.* **2019**, *291*, 111341.
23. Evans, D.F.; Allen, M.; Ninham, B.; Fouda, A. Critical micelle concentrations for alkyltrimethylammonium bromides in water from 25 to 160 °C. *J. Solution Chem.* **1984**, *13*, 87-101.
24. Mędrzycka, K., and Zwierzykowski, W. Adsorption of alkyltrimethylammonium bromides at the various interfaces. *J. Colloid Interface Sci.*, **2000**, *230*, 67-72.
25. Arditty, S.; Whitby, C.P.; Binks, B.P.; Schmitt, V.; Leal-Calderon, F. Some general features of limited coalescence in solid-stabilized emulsions. *Eur. Phys. J. E* **2003**, *11*, 273-281.
26. Tarimala, S.; Dai, L.L. Structure of microparticles in solid-stabilized emulsions. *Langmuir* **2004**, *20*, 3492-3494.
27. Horozov, T.S.; Binks, B.P. Particle-Stabilized Emulsions: A Bilayer or a Bridging Monolayer? *Angew. Chem. Int. Ed.* **2006**, *45*, 773-776.
28. Horozov, T.S.; Aveyard, R.; Clint, J.H. and Binks, B.P. Order-disorder transition in monolayers of modified monodisperse silica particles at the octane-water interface. *Langmuir* **2003**, *19*, 2822-2829.
29. Aveyard, R.; Clint, J.H.; Nees, D. and Paunov, V.N. Compression and structure of monolayers of charged latex particles at air/water and octane/water interfaces. *Langmuir* **2000**, *16*, 1969-1979.
30. Aveyard, R.; Binks, B.; Clint, J.; Fletcher, P.; Horozov, T.; Neumann, B.; Paunov, V.; Annesley, J.; Botchway, S. and Nees, D. Measurement of long-

- range repulsive forces between charged particles at an oil-water interface. *Phys. Rev. Lett.* **2002**, *88*, 246102.
31. Horozov, T.S.; Aveyard, R.; Binks, B.P.; Clint, J.H. Structure and stability of silica particle monolayers at horizontal and vertical octane-water interfaces. *Langmuir* **2005**, *21*, 7405-7412.
  32. Reynaert, S.; Moldenaers, P.; Vermant, J. Control over colloidal aggregation in monolayers of latex particles at the oil-water interface. *Langmuir* **2006**, *22*, 4936-4945.
  33. Pimienta V. and Antoine C. Self-propulsion on liquid surfaces. *Curr. Opin. Colloid Interface Sci.* **2014**, *19*, 290-299.
  34. Nepomnyashchy A.; Legros J.C. and Simanovskii I. *Interfacial convection in multilayer systems*. Springer, New York, **2012**, ch. 2, pp. 41-151.
  35. Dugyala, V.R.; Muthukuru, J.S.; Mani, E. and Basavaraj, M.G. Role of electrostatic interactions in the adsorption kinetics of nanoparticles at fluid-fluid interfaces. *Phys. Chem. Chem. Phys.* **2016**, *18*, 5499-5508.

## CHAPTER 4

### PICKERING EMULSIONS OF PARTIALLY HYDROPHOBIC POLYSTYRENE LATEX PARTICLES

#### 4.1 Introduction

Surfactant-free monodisperse polystyrene (PS) particles have long been considered as suitable model systems to study the fundamental properties of colloidal particles. These particles are spherical, monodisperse and usually have clean surfaces. They are stabilized by the electrical repulsion force introduced by the charge groups on the surface which are covalently linked to the polymer molecules.<sup>1</sup> According to the theory of Derjaguin, Landau, Verwey, and Overbeek (DLVO)<sup>2,3</sup>, the presence of electrolytes in the aqueous phase will screen the surface charge and lead to aggregation of particles. However, as mentioned in section 1.3.2, in the systems with polystyrene latex particles, interesting charge reversal of particles induced by organic electrolytes has been reported.<sup>4-12</sup> Non-DLVO forces (*e.g.* structural forces or hydrophobic interaction forces) between electrolytes and colloidal particles have been widely involved in explaining the mechanism of charge reversal.<sup>7,10,11,13</sup> When organic counterions accumulate near the colloid surface, the hydrophobic groups adsorb onto the hydrophobic latex surface due to the hydrophobic effect. In addition to organic electrolytes, some inorganic salts have also been reported to induce charge reversal of PS particles. Theoretical simulations predict that charge inversion is possible to be induced by monovalent ions in the case of big ions due to steric effects.<sup>7,8</sup> For example, monovalent ions ( $\text{ClO}_4^-$  and  $\text{SCN}^-$ ) were reported to induce charge inversion of cationic amidine PS latex particles.<sup>8</sup> Ion-specific effects were widely suggested to account for the charge reversal induced by inorganic ions.<sup>14-17</sup>

With the charge reversal properties of PS particles in suspensions, it should be interesting to investigate their behaviour at oil-water interfaces. In the systems with inorganic particles such as silica, the variation in surface charge has dramatic influence on their surface properties. Addition of cationic surfactants induces charge reversal of silica particles, which results in phase inversion of emulsions they stabilised.<sup>18,19</sup> While polystyrene latex particles have been extensively investigated on the inter-

particle interactions in aqueous dispersions or their monolayers at planar fluid-fluid interfaces,<sup>20-23</sup> it is surprising that these particles have found a relatively narrow use as emulsifiers. Limited studies on emulsions stabilized by charge stabilised PS particles have been reported,<sup>24-30</sup> let alone the effect of charge reversal of particles on the properties of emulsions they stabilized. The prediction of emulsions stabilised by PS particles undergoing charge reversal is as following: oil-in-water emulsions would be preferred at low [salt], where particles are highly charged; water-in-oil emulsions at intermediate [salt] as a result of charge neutralization of particles and oil-in-water emulsions again at high [salt] after charge reversal.

This chapter investigated emulsions stabilized by PS latex particles with three different surface groups (sulfate, amidine and carboxyl). In the system with negatively charged sulfate latex particles, tetrapentylammonium bromide (TPeAB) was added as the electrolyte. Charge reversal of particles was observed. The effect of charge reversal on the properties of emulsions with dodecane stabilized by sulfate latex particles were studied. The hydrophobicity of particles in the presence of electrolytes was evaluated by measuring the three-phase contact angles of micron-sized particles at oil-water interfaces using the Gel Trapping Technique (GTT). In the system with carboxyl latex particles, no charge reversal was induced by TPeAB at pH 11 where particles were fully ionized. W/O emulsions were obtained at all TPeAB concentrations when dodecane was used as the oil phase. In order to find out whether the preferential stabilization of w/o emulsions occurs specifically with dodecane or universally with non-polar oils, heptane was used as the oil phase instead of dodecane. In addition, polydimethylsiloxane (PDMS) of slightly higher polarity than that of alkanes was used. Emulsions inverting from w/o to o/w was observed. It seems that a slight increase in the oil polarity results in remarkable influence on the properties of emulsions. However, this requires further confirmation, e.g., increasing the oil polarity to a larger extent to see what happens. The adsorption of TPeA<sup>+</sup> ions onto negatively charged particle surface were attributed to the hydrophobic attraction between polystyrene surface and alkyl chains of TPeA<sup>+</sup> ions. To prove this, we tried to adjust the pH of the aqueous phase to 3, where carboxyl latex particles lose their surface charge. Addition of TPeAB leads to positive charge of particles. The properties of emulsions with dodecane stabilized by these particles were investigated. In the system with positively charged amidine latex particles, sodium thiocyanate (NaSCN) was added to induce

charge reversal of particles. The influence of the electrolyte concentration on the properties of emulsions they stabilized have been studied.

In 1913, Bancroft wrote that ‘hydrophile colloids tend to make water the dispersing phase while hydrophobic colloids make water the disperse phase’.<sup>31</sup> This is the so-called Bancroft rule, which helps predict the emulsion type during the mixing of oil and water. This rule works quite well in predicting the type of macro-emulsions stabilized by surfactants, that is, surfactants with higher solubility in water will give o/w emulsions while those more soluble in oil will result in w/o emulsions. However, controversy exists when we try to render the Bancroft rule to describe w/o emulsions stabilized by polystyrene particles. If we determine whether the emulsion follow the Bancroft rule or not depending on the phase in which particles are initially dispersed, these w/o emulsions should be regarded as breaking the Bancroft rule as particles are initially dispersed in water. However, if our decision is based on the hydrophobicity of particles, w/o emulsions indeed follow the Bancroft since polystyrene particles are hydrophobic. Therefore, the empirical Bancroft rule is not suitable for predicting the type of Pickering emulsions.

## **4.2 Systems with sulfate latex particles**

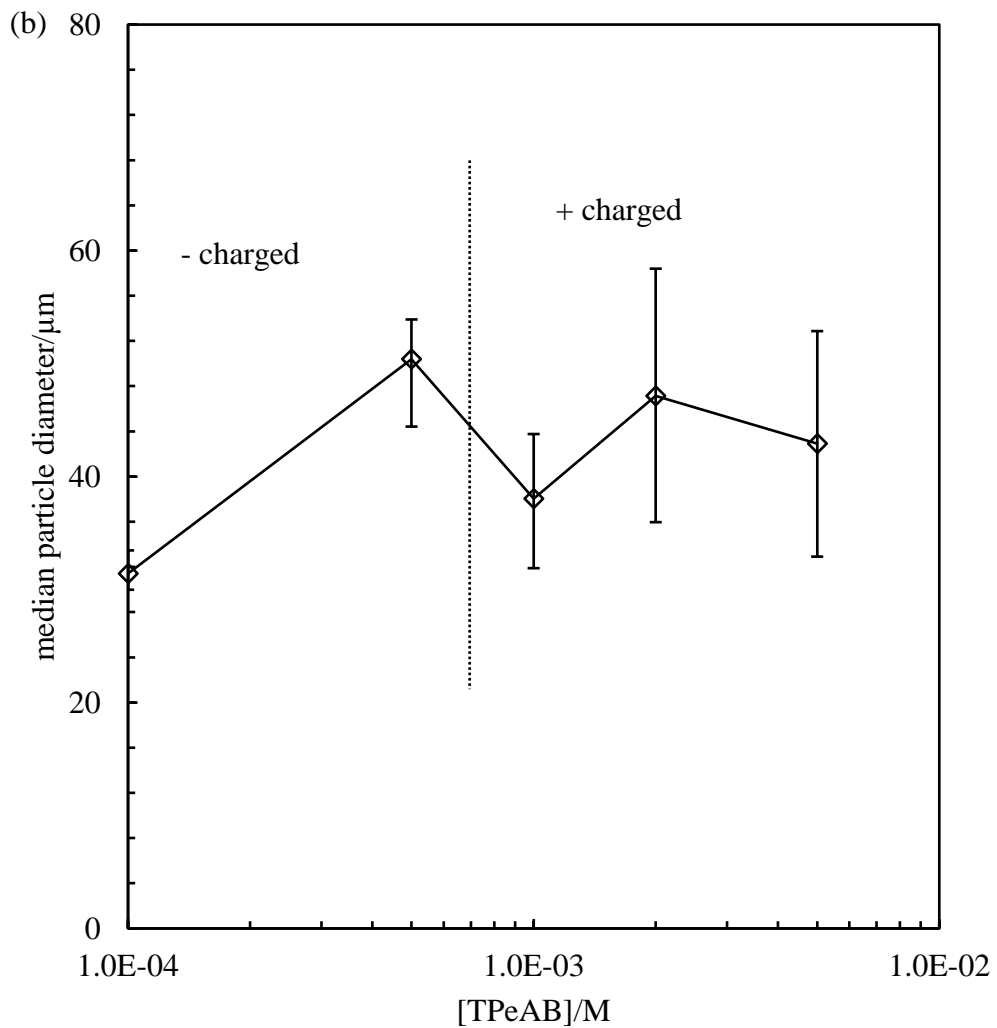
### *4.2.1 Aqueous dispersion of sulfate latex particles*

Prior to investigating the properties of emulsions stabilised by sulfate latex particles, the properties of aqueous particle dispersions were studied. The pH of the dispersions was maintained at 4 to avoid the dissolving effects of CO<sub>2</sub> as the pH of CO<sub>2</sub>-saturated water at room temperature under atmospheric pressure is 3 to 4.<sup>32,33</sup> The particles are negatively charged with surface groups fully ionized regardless of pH. Figure 4.1 (a) shows the appearance of 2 wt.% particle dispersions at varied TPeAB concentrations. Particles are initially discrete in water, but when  $1 \times 10^{-4}$  M of TPeAB is added, they aggregate and large particle flocs are visually observed. The particle size was measured by light diffraction using the Mastersizer 2000. Figure 4.1 (b) represents the median particle diameter as a function of [TPeAB]. The average diameter of sulfate PS latex particles in pure water is 0.15  $\mu\text{m}$  (not shown), a log normal distribution corresponding to a single particle population centred between 0.1  $\mu\text{m}$  and 0.2  $\mu\text{m}$  was observed (Figure 4.2). Addition of  $1 \times 10^{-4}$  M of TPeAB

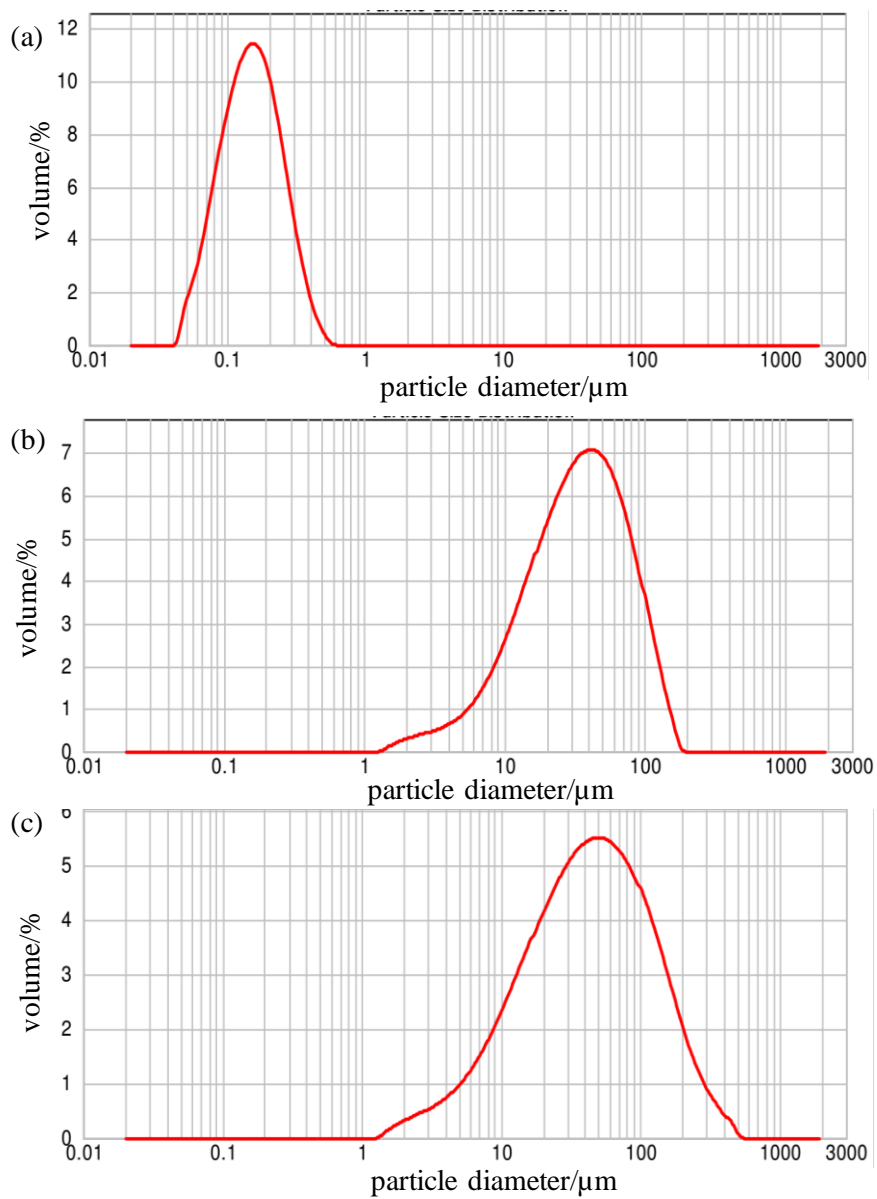
immediately causes the formation of large aggregates, an average particle diameter of 31  $\mu\text{m}$  was obtained with wide distribution ranging from 1  $\mu\text{m}$  to 200  $\mu\text{m}$ .

Figure 4.3 shows the zeta potential of 0.0008 wt.% sulfate PS latex particles in KCl and TPeAB solutions. As can be seen, the zeta potential of particles in water is -40 mV, the absolute values increase with increasing KCl concentration, reaching a maximum then decreasing continuously. Such maxima has been widely observed before, and the hairy layer model and the ion-adsorption model have been proposed to explain this phenomenon.<sup>1,34,35</sup> By contrast, a trace amount of TPeAB ( $5 \times 10^{-5}$  M) significantly decreases the zeta potential to -22 mV, increase of [TPeAB] results in continuous decrease of the absolute value until charge reversal occurs between  $5 \times 10^{-4}$  M and  $1 \times 10^{-3}$  M, after which particles become increasingly positively charged. According to the DLVO theory, addition of electrolytes screens the surface charge, suppressing the double-layer repulsion and causing aggregation in colloids.<sup>25</sup> Particles tend to aggregate faster near the the isoelectric point (IEP) and become stable away from this point.<sup>9,12</sup> However, in the present system, large flocs of particles were observed after the IEP, even at the highest salt concentration. It is suggested that the interaction between polystyrene particles and specific organic electrolytes is beyond the DLVO framework, and non-DLVO hydrophobic effect is involved. Hydrophobic groups on the counterions strongly interact with the colloids and induce charge reversal,<sup>7</sup> which should also account for the aggregation of particles at high salt concentrations. Similar phenomenon has been observed in systems with tetraphenylarsonium ions and sulfonated latex particles.<sup>4,7</sup> One might notice that, unlike the results in the KCl, the zeta potential of particles in TPeAB does not show the maximum. This may also lie in the strong adsorption of TPeA<sup>+</sup> cations on the negatively charged particle surfaces. The corresponding strongly diminished repulsion between the surface groups causes the hairy layer to shrink. While the influence of shear plane movement caused by charge screening is minor, as a result, the maximum in zeta potential is eliminated.<sup>4</sup>

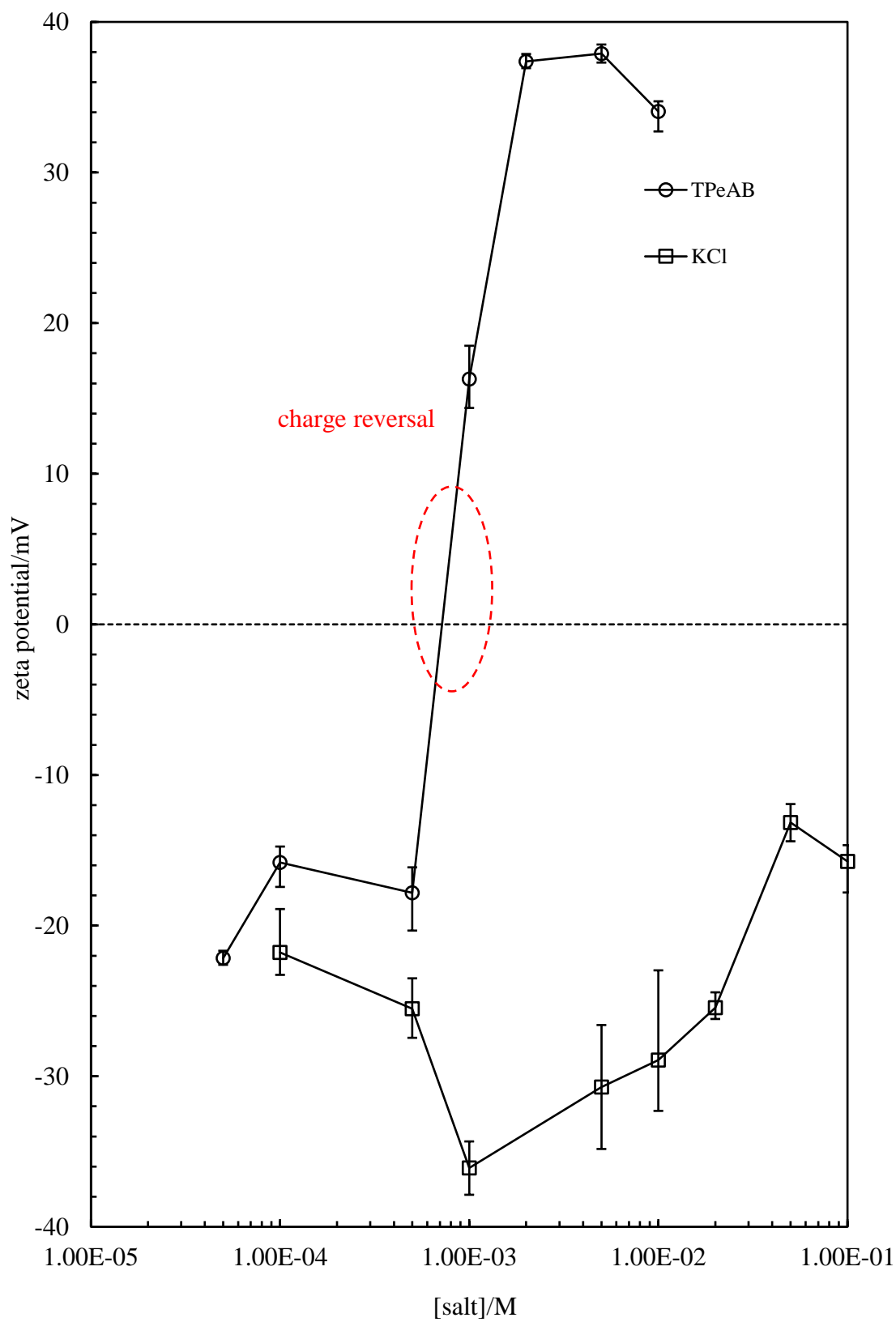
**Figure 4.1.** (a) Appearance of 2 wt.% sulfate PS latex particle ( $d = 0.2 \mu\text{m}$ ) dispersions in the presence of TPeAB at pH 4, taken immediately after preparation. (b) Average diameter of particles in (a). The average diameter of particles without salt is  $0.15 \mu\text{m}$  (not shown).



**Figure 4.2.** Size distribution of sulfate latex particles (quoted  $d = 0.2 \mu\text{m}$ ) in the presence of (a) 0 M, (b)  $1 \times 10^{-4}$  M and (c)  $1 \times 10^{-3}$  M TPeAB at pH 4.



**Figure 4.3.** Zeta potential of 0.0008 wt.% sulfate PS latex particles ( $d = 0.2 \mu\text{m}$ ) in the presence of TPeAB or KCl at different concentrations at pH 4.

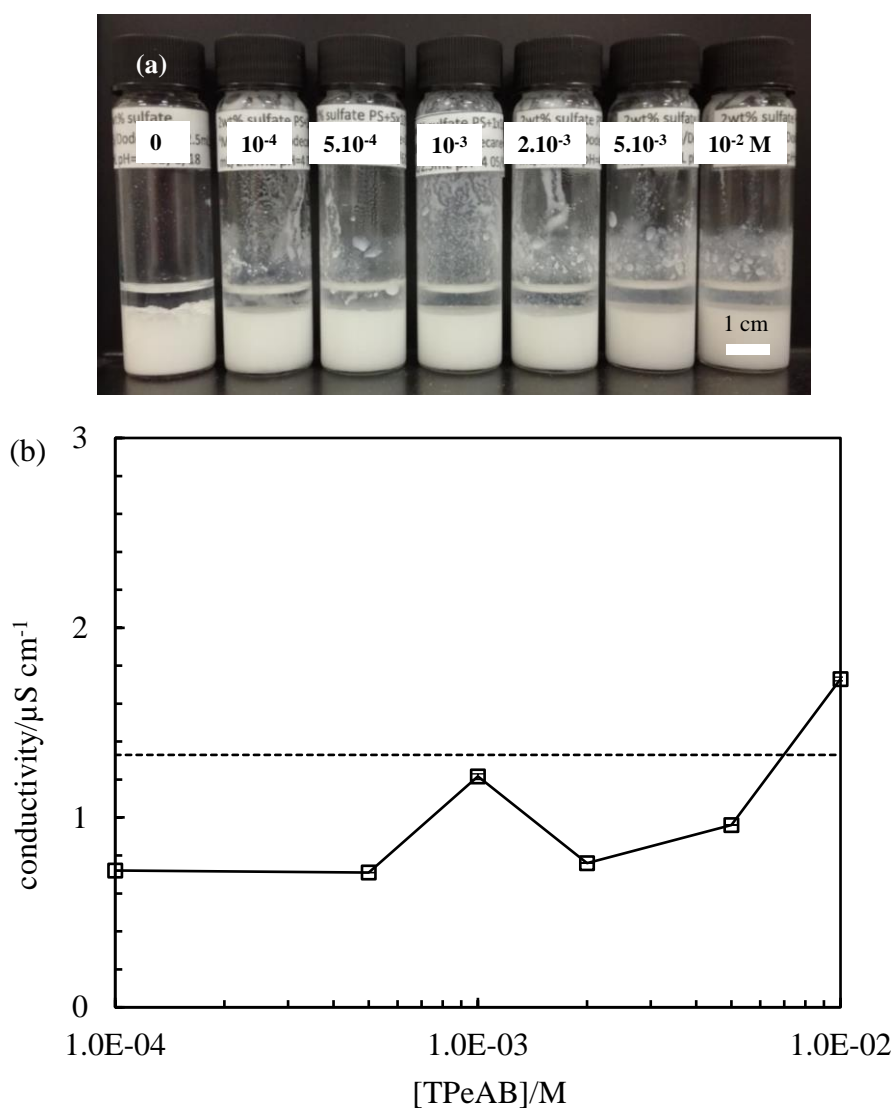


#### 4.2.2 Emulsions with dodecane as the oil phase

Batches of emulsions were prepared by homogenizing 2.5 mL of 2 wt.% sulfate latex particle dispersion in the presence of TPeAB at pH 4 with 2.5 mL dodecane. The appearance of emulsions is shown in Figure 4.4 (a) and the emulsion type is determined as water-in-oil (w/o) from the drop test. The conductivities of emulsions were measured immediately after homogenization and the results are represented in Figure 4.4 (b). The conductivities of the emulsions are very low, indicating that the emulsions are all w/o. This system exhibits two intriguing properties. Firstly, the particles are partially hydrophobic, but they are initially dispersed in water due to the presence of ionizable sulfate surface groups. The polystyrene portion give the particles hydrophobic character whereas sulfate groups contribute to the hydrophilic character of particles. It seems that there is a competition between the particle surface and surface groups in determining the emulsion type. For sulfate latex particles, the hydrophobic polystyrene portion on the particle apparently dominates the emulsion type as w/o emulsions are stabilized regardless of the sign of surface charge or the concentration of electrolyte added. This is reasonable as  $\text{SO}_4^-$  groups only occupy ~ 5% of the particle surface while 95% of it is ions-free polystyrene surface. Similar w/o emulsions have been prepared by Golemanov *et al.*<sup>25</sup> with sulfate polystyrene latex particles in the presence of NaCl. Secondly, unlike normal emulsions where emulsifiers are dispersed in the continuous phase, in the emulsions stabilised by sulfate PS latex particles, the emulsifier (latex particles) is contained in the disperse phase. Golemanov *et al.*<sup>25</sup> suggested these emulsions are anti-Bancroft type because the stabilizers (particles) are in the disperse phase while the empirical Bancroft rule<sup>31</sup> defines emulsifiers (surfactants) dissolving in the continuous phase. Conventional emulsions breaking the Bancroft rule are usually unstable to coalescence. When the emulsifier (*e.g.* surfactant) is dissolved in the drop phase, the adsorption of surfactant molecules on the oil-water interface is retarded due to limited supply of surfactant from the drop interior. As a result, the film between two colliding drops drains much faster than it does in the case when the surfactant is in the continuous phase. This effect speeds up coalescence of droplets and leads to destabilization of emulsions. However, in the case of Pickering emulsions, the adsorption of particles at the oil-water interface form a dense layer (shell-like), which provide steric stabilization to coalescence.<sup>25</sup> According to the empirical Bancroft rule, hydrophile colloids tend to make water the

dispersing phase while hydrophobic colloids make water the disperse phase.<sup>31</sup> If we apply the Bancroft rule to particle-stabilised emulsions, it can also be expressed as hydrophilic particles stabilise o/w emulsions while hydrophobic particles stabilise w/o emulsions. Therefore, w/o emulsions stabilised by sulfate latex particles are believed following the Bancroft rule. Further emulsions prepared in this chapter following the Bancroft rule or not are determined according to the contact angle of particles at oil-water interfaces.

**Figure 4.4.** (a) Appearance of water-in-dodecane emulsions ( $\phi_w = 0.5$ ) stabilized by 2 wt.% of 0.2  $\mu\text{m}$  sulfate PS latex particles in varied concentrations (given) of TPeAB at pH 4, taken one week after preparation. (b) Conductivity of emulsions in (a), measured immediately after homogenization. Dashed line shows the conductivity of the emulsion without salt.



Optical microscopy of selected emulsions is shown in Figure 4.5, spherical droplets can be clearly seen from the images. Figure 4.6 is a plot of the average droplet diameter calculated from the image. Without salt, droplets with an average diameter of 320  $\mu\text{m}$  are obtained, indicating that sulfate latex particles alone are able to stabilise emulsions, but the droplets are very large. When TPeAB is added, a dramatic decrease in the droplet size is observed,  $1 \times 10^{-4}$  M of salt results in droplets of 55  $\mu\text{m}$  in diameter. A minimum of diameter is observed at  $1 \times 10^{-3}$  M by increasing the concentration of TPeAB. The increase of droplet size at high salt concentration might be due to charge reversal of particles, where particles are increasingly positively charged. Particles adsorbed at the oil-water interface tend to repel each other and the packing of particles on droplet surface is loose, which results in coalescence of neighbouring droplets. We recall that average particle flocs size higher than 40  $\mu\text{m}$  are determined in the aqueous suspensions with TPeAB. It has been widely reported that larger particles stabilise larger droplets.<sup>24</sup> Thus, if particle flocs adsorbing on the droplet surface are intact, larger droplets are expected. However, in the produced emulsions, the emulsion droplets with [TPeAB] are much smaller than that without salt. One possibility is that the presence of TPeAB decreases the oil-water interfacial tension, which curves the interface into smaller water droplets. This is reasonable because TPeAB is proved to decrease the air-water surface tension to  $\sim 50$  mN/m at around 1 mM.<sup>36,37</sup> Another possibility is that the high-speed shearing during the homogenization disrupts the particle flocs.<sup>25</sup> Indeed, in section 5.2.3.2, single particles as well as small clusters of several particles on the droplet surface were detected by cryogenic scanning electron microscopy.

**Figure 4.5.** Optical microscopy images of water-in-dodecane emulsions (1:1 by volume) stabilized by 2 wt.% sulfate PS latex particles ( $d = 0.2 \mu\text{m}$ ) in the presence TPeAB at pH 4, taken two days after preparation.

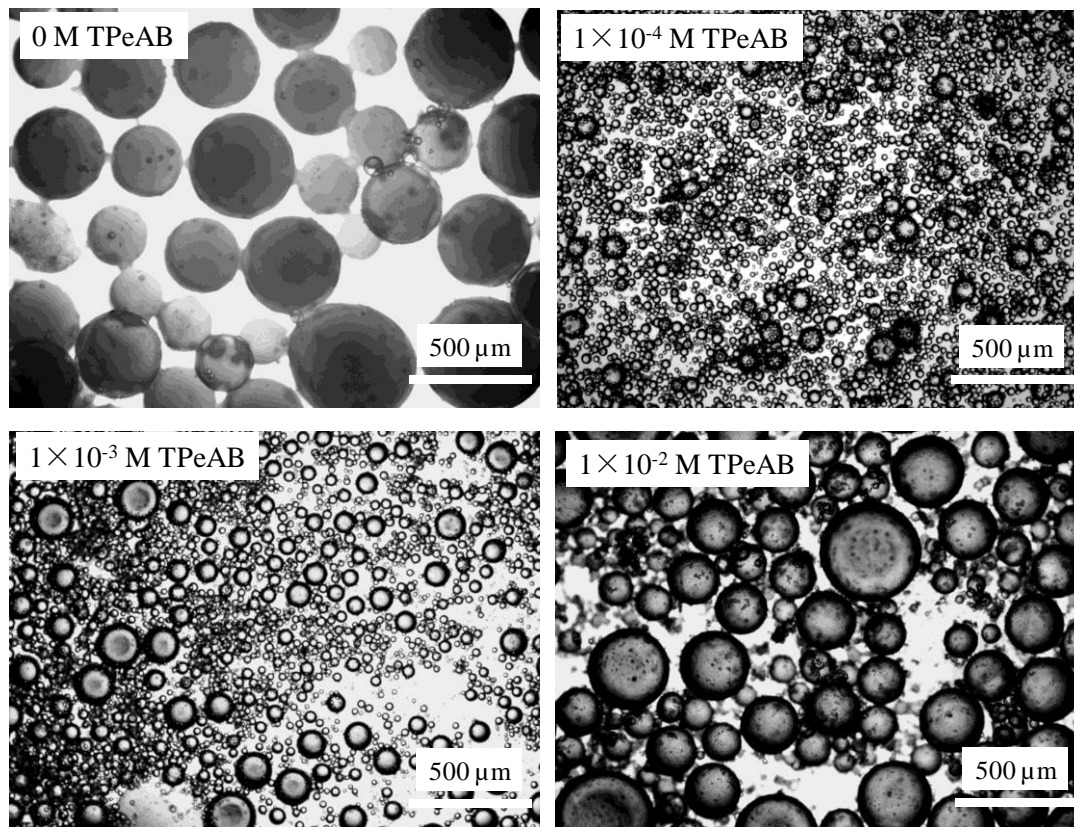
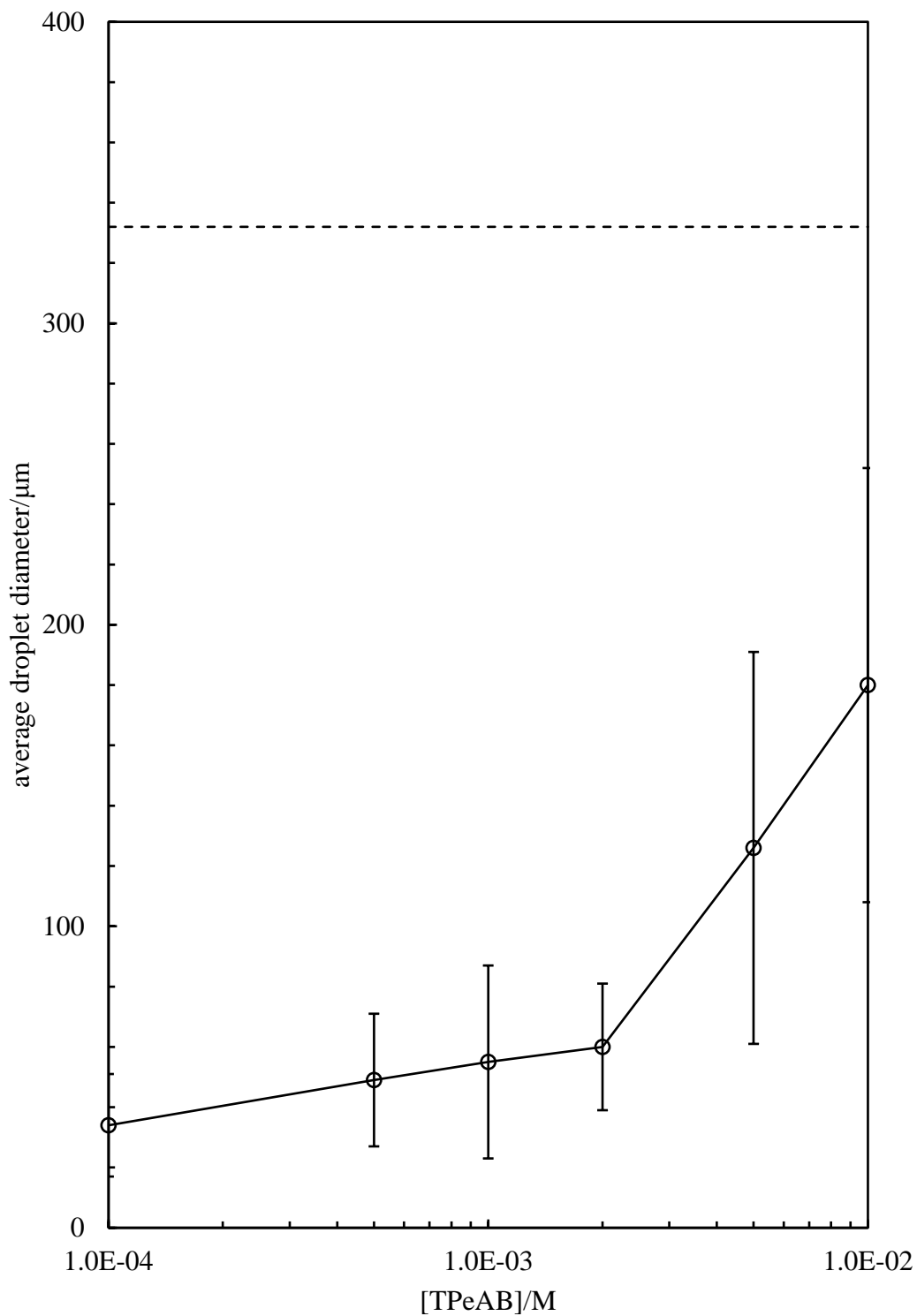


**Figure 4.6.** Average droplet diameter of water-in-dodecane emulsions stabilised by 2 wt.% sulfate PS latex particles ( $d = 0.2 \mu\text{m}$ ) *versus* [TPeAB] at pH 4, calculated from optical microscopy images. Dashed line represents the average droplet diameter of the emulsion without TPeAB.



In order to understand the properties of emulsions stabilized by sulfate latex particles, it is necessary to determine the hydrophobicity of particles in TPeAB solutions. The three-phase contact angle ( $\theta$ ) of sulfate latex particles at the dodecane-water interface was measured by GTT. In order to be detected by SEM, micron-sized particles ( $d = 2 \mu\text{m}$ ) were used. It's assumed that large and small particles have a similar hydrophobicity as the surface charge density of particles has been selected as close to each other as possible, that is,  $-25 \text{ mC/m}^2$  for  $2 \mu\text{m}$  particles and  $-6 \text{ mC/m}^2$  for  $0.2 \mu\text{m}$  particles. Figure 4.7 shows SEM images of sulfate latex particles gel-trapped and micro-cast with Sylgard PDMS. The visible part of particle surfaces on the Sylgard PDMS has been immersed in the aqueous phase while the particle surface immersed by the Sylgard PDMS has been originally in the oil phase. The  $\theta$  is calculated by using Equation 2.6 or 2.7 after measuring the contact line diameter of the individual particles from the SEM images,  $d_c$ , and fitting a circular profile on the particles to determine their equatorial diameter,  $D$ . The result is plotted in Figure 4.8 as a function of [TPeAB]. The  $\theta$  of particles at the dodecane-water (without salt) interface is  $101 \pm 5^\circ$ , slightly lower than reported  $120 \pm 12^\circ$  of sulfate latex particles ( $d = 1.6 \mu\text{m}$ ) at the octane-water interface.<sup>38</sup> Addition of TPeAB results in a distinct increase of  $\theta$ , while a slight decrease is observed as the salt concentration increases, although all of them are above  $115^\circ$ . A schematic of possible arrangement of TPeA<sup>+</sup> ions on the surface of sulfate latex particles is shown in Figure 4.9. At low salt concentrations, TPeA<sup>+</sup> ions absorb onto negatively charged sites on the particle surface by electrostatic attraction, with the hydrophobic chains exposed to water, which increase the hydrophobicity of particles. When charge neutralization is achieved, hydrophobic interaction between TPeA<sup>+</sup> ions and polystyrene surface dominates, with the polar parts of ions exposed to water, resulting in decrease of particle hydrophobicity. The hydrophobic attraction is so strong that it even happens when particles are positively charged. The contact angle results indicate that w/o emulsions should be preferentially stabilized, which is consistent with the findings in Figure 4.4.

**Figure 4.7.** Scanning electron microscopy images of monolayers of monodispersed sulfate latex particles ( $d = 2 \mu\text{m}$ ) on the surface of Sylgard PDMS obtained by the gel trapping technique (GTT) at the dodecane-water interface. The observation angle  $\delta = 80^\circ$ . Scale bar = 500 nm. The visible part of particle surfaces on the Sylgard PDMS has been immersed in water while the particle surface immersed in the Sylgard PDMS has been originally in oil. The particle contact line diameter,  $d_c$ , can be measured directly from the SEM images, the particle equatorial diameter,  $D$ , is obtained by extrapolation after fitting the particle profile with a circle (as illustrated on the SEM images).

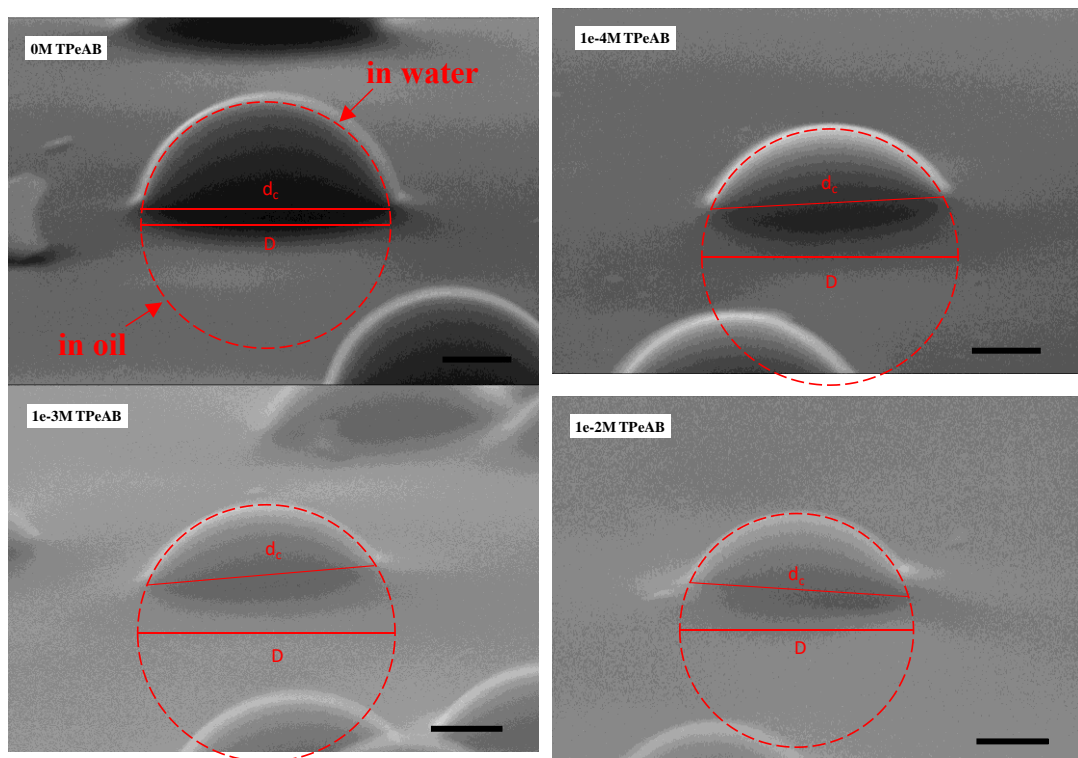


**Figure 4.8.** Three-phase contact angle ( $\theta$ ) of sulfate latex particles ( $d = 2 \mu\text{m}$ ) at the dodecane-water interface against [TPeAB] at pH 4. Horizontal dashed line indicates the contact angle of particles at the dodecane-water interface without salt.

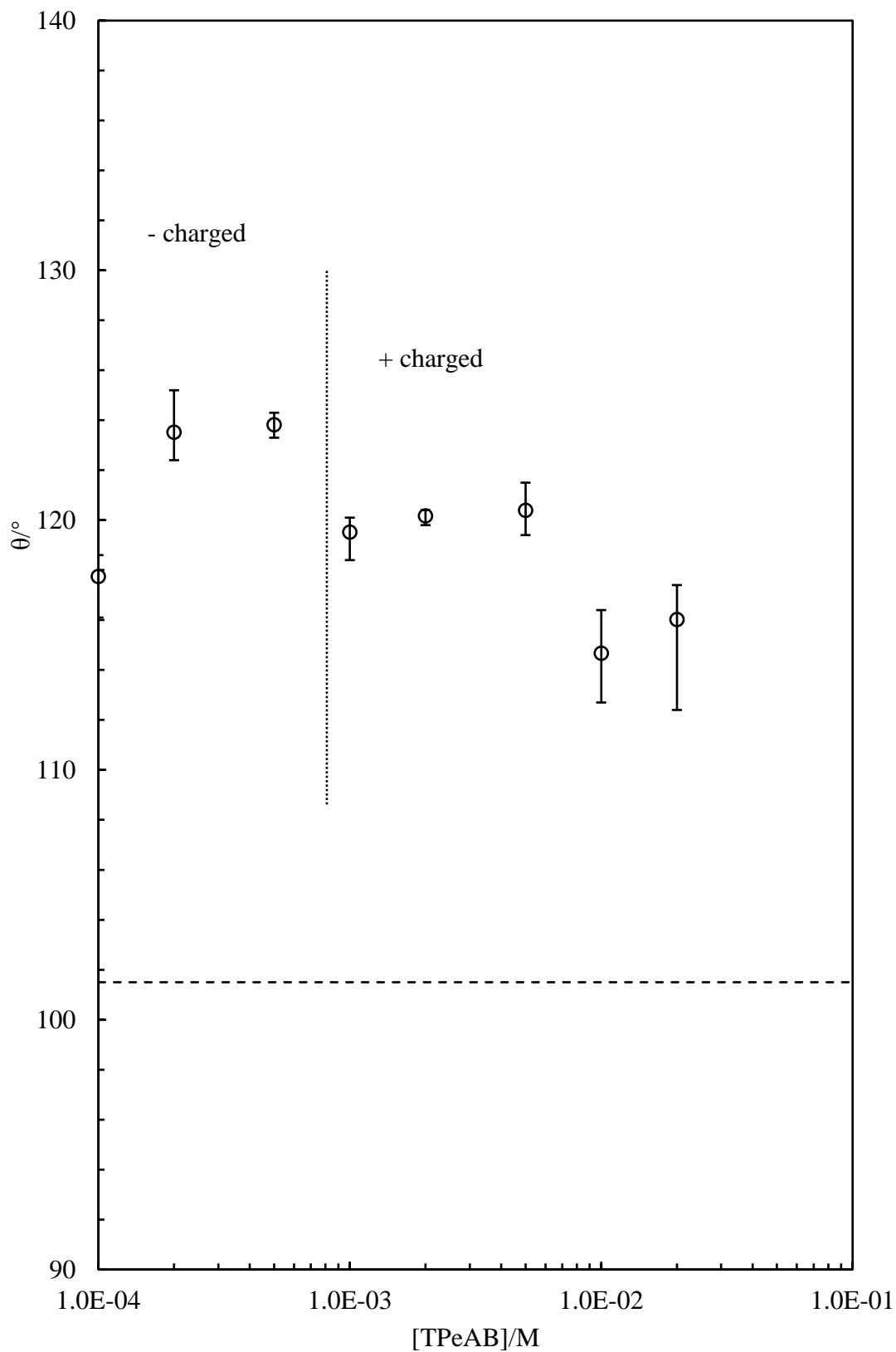
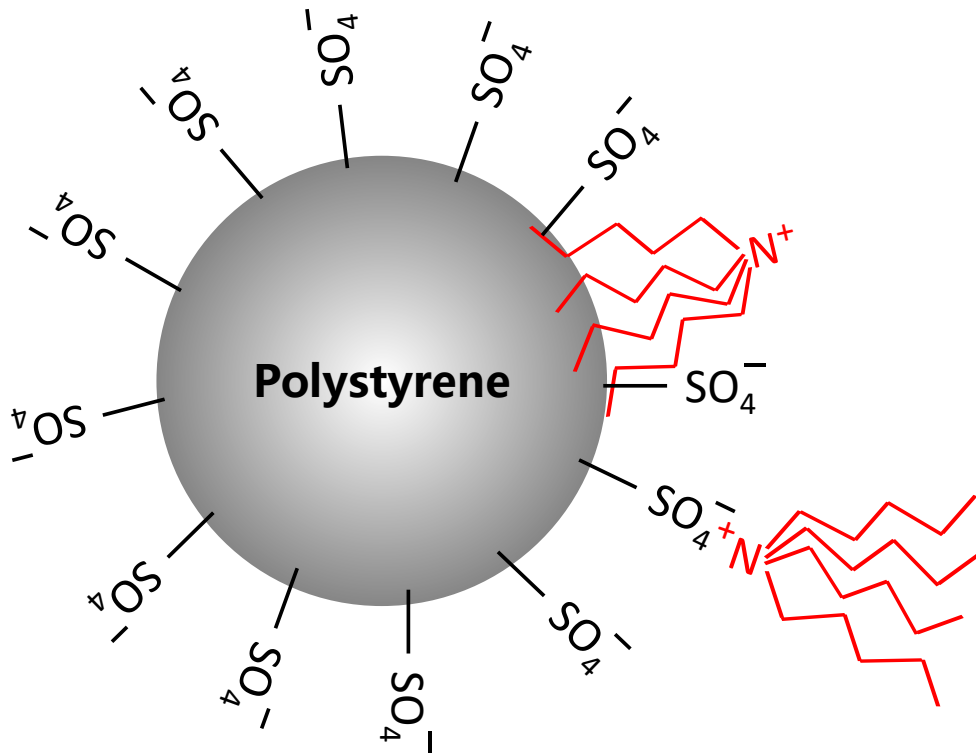


**Figure 4.9.** Schematic of possible adsorption of TPeA<sup>+</sup> ions onto sulfate latex particles.



### 4.3 Systems with carboxyl latex particles

#### 4.3.1 Aqueous dispersion of carboxyl latex particles at pH 11

The surface charge density of sulfate latex particles used in the system above is relatively low ( $-6 \text{ mC/m}^2$ ), which probably results in polystyrene surface domination on the type of emulsions they stabilized. Hence, carboxyl latex particles of higher surface charge density ( $-103 \text{ mC/m}^2$ ) when fully ionized were used in this section. The pKa of carboxyl groups on the surface of polystyrene latex particle is 4.9 and the zeta potential of carboxyl latex particles keeps relatively constant at  $\text{pH} > 9$ .<sup>10,39</sup> Therefore, carboxyl latex dispersions were prepared at pH 11 to assure full deprotonation of carboxyl groups. The appearance of particle dispersions in the presence of TPeAB is shown in Figure 4.10 (a). The zeta potential of 0.0004 wt.% carboxyl latex particles was measured in KCl and TPeAB solutions at pH 11 and is shown in Figure 4.10 (b). Particles are discrete in water and at low salt concentrations. Large aggregates can be observed under optical microscope at  $5 \times 10^{-3} \text{ M}$  and above (see Figure 4.11), much larger than that of sulfate latex particles since surface the charge density of the latter is much lower. The zeta potential in water is about  $-52 \text{ mV}$ , the absolute value increases with KCl concentration. Addition of TPeAB gradually decreases the magnitude of the zeta potential but no charge reversal is observed within the salt concentrations studied. The adsorption of  $\text{TPeA}^+$  ions onto the surface of carboxyl latex should involve a combination of electrostatic attraction between  $\text{COO}^-$  groups and  $\text{TPeA}^+$  cations and hydrophobic attraction between polystyrene surface and alkyl chains of  $\text{TPeA}^+$  ions. It might be that the concentration of  $\text{TPeA}^+$  ions is not high enough to neutralise the surface charge on carboxyl latex particles, charge reversal should be expected at higher concentrations of TPeAB.

**Figure 4.10.** (a) Appearance of 2 wt.% carboxyl PS latex particle ( $d = 0.2 \mu\text{m}$ ) dispersions in varied concentrations (given) of TPeAB at pH 11, taken immediately after preparation. (b) Zeta potential of 0.0004 wt.% carboxyl PS latex particles in KCl or TPeAB solutions at pH 11.

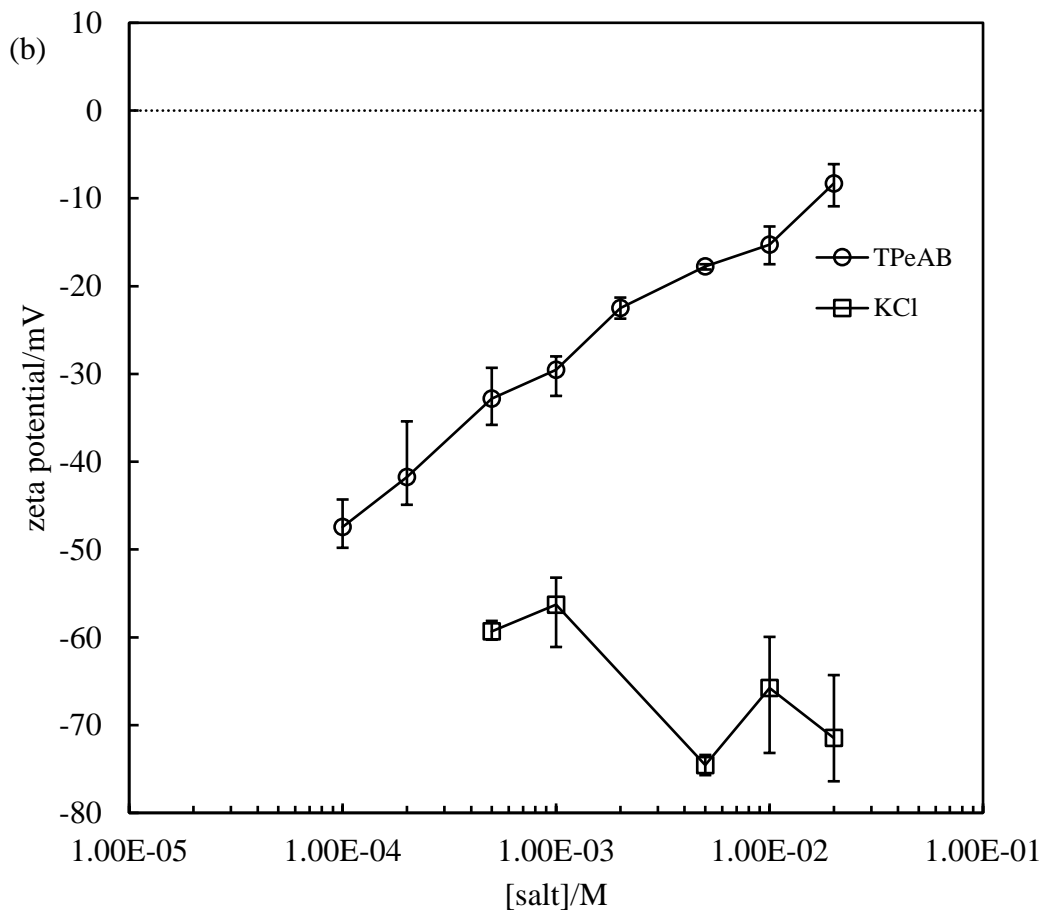
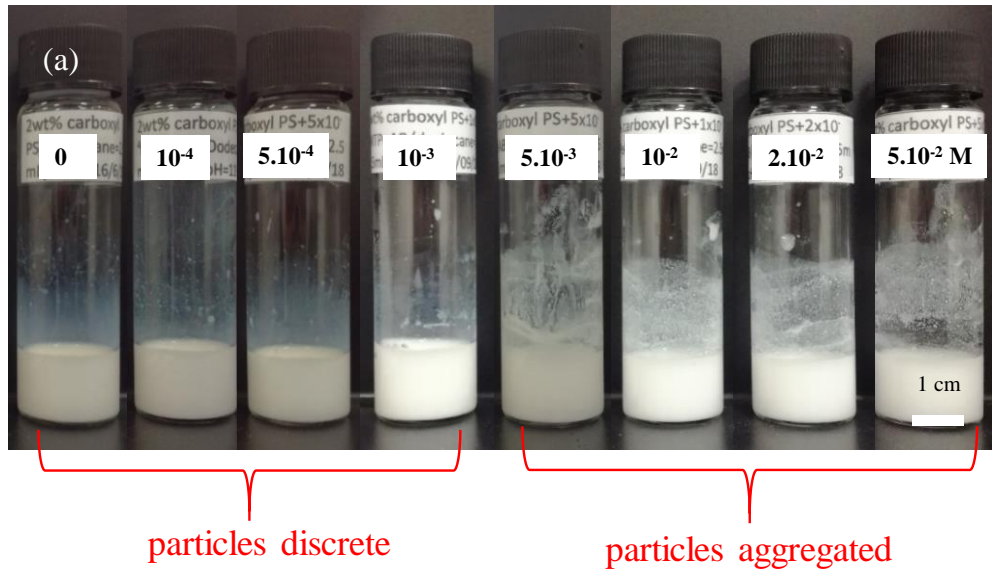
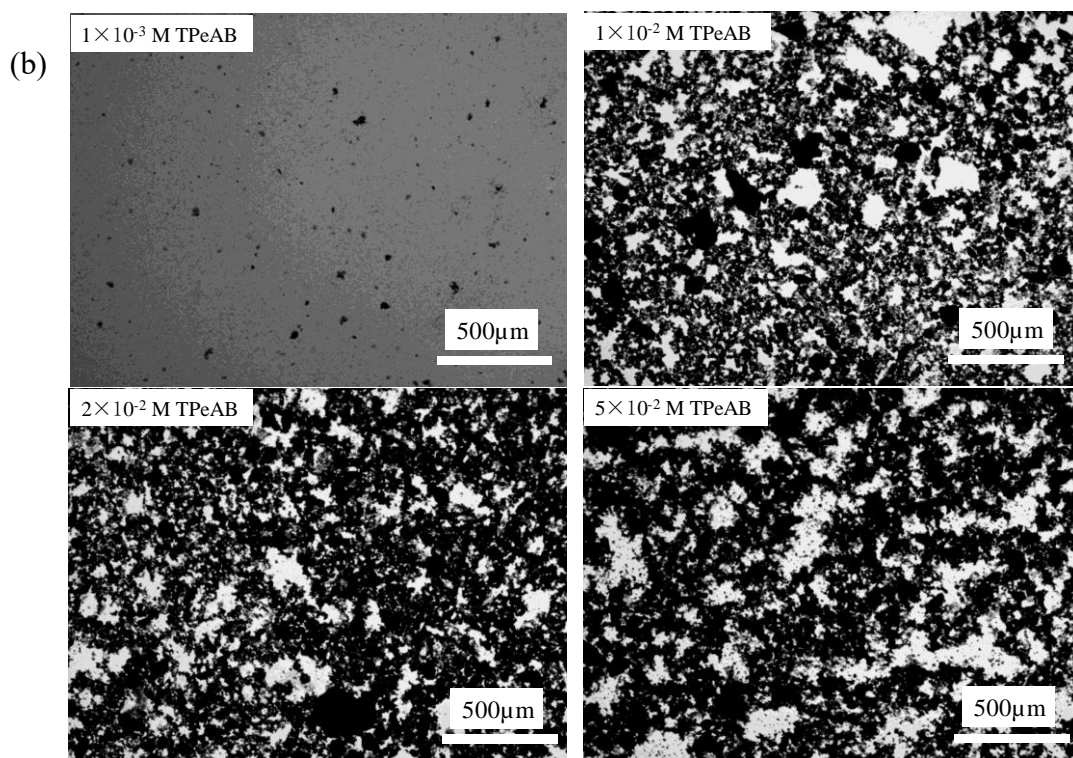
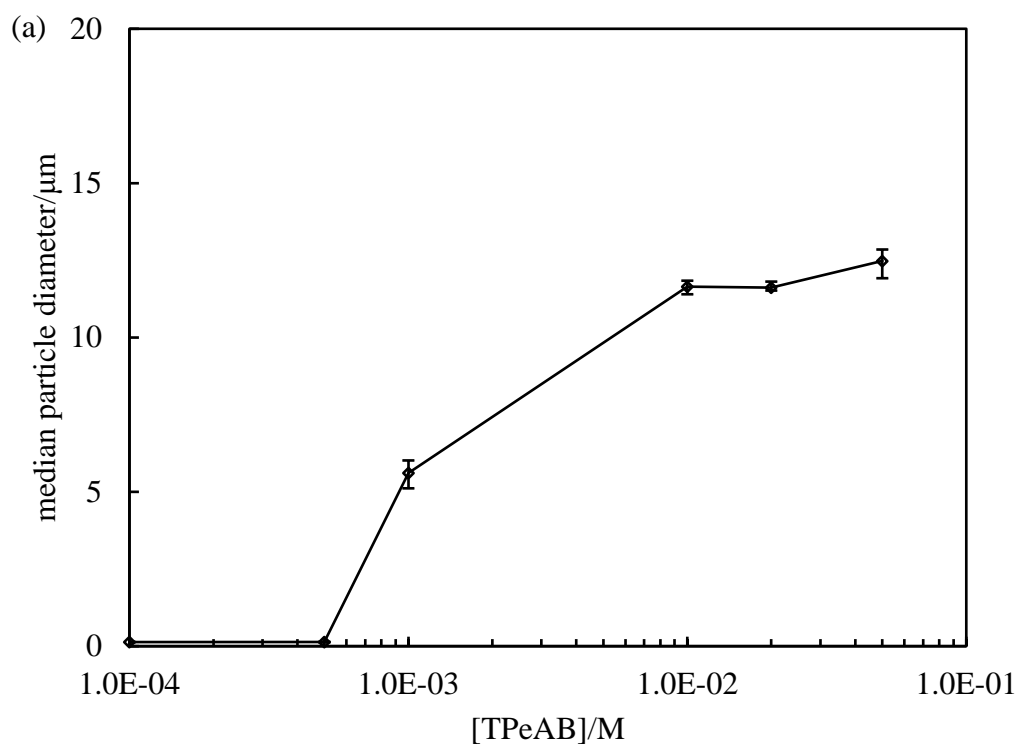


**Figure 4.11.** (a) Average diameter of carboxyl PS latex particles (quoted  $d = 0.2 \mu\text{m}$ ) at different [TPeAB] at pH 11. (b) Optical microscopy images of 2 wt.% carboxyl PS latex particles ( $d = 0.2 \mu\text{m}$ ) in the presence of TPeAB at pH 11.



### 4.3.2 Emulsions with dodecane at pH 11

A series of emulsions were prepared by homogenizing 2.5 mL of 2 wt. % carboxyl PS latex dispersion at pH 11 with 2.5 mL dodecane and the appearance is shown in Figure 12 (a). Again, all w/o emulsions were obtained, the results of conductivity measurement are represented in Figure 4.12 (b). In the emulsion without salt, most of the oil is extracted immediately after homogenization and large droplets are visually observed in the oil phase. By contrast, for emulsions with TPeAB, the height of oil extracted decreases with [salt]. To quantify the stability of the emulsions to creaming and coalescence, the fractions of water ( $f_w$ ) and oil ( $f_o$ ) resolved below and above the stable emulsion layer respectively after one week are plotted in Figure 4.13. As can be seen,  $f_w$  keeps at zero indicating emulsions are completely stable to coalescence except the one at the highest salt concentration. By contrast,  $f_o$  decreases with salt concentration, which means increasing stability to sedimentation.

Optical micrography images of selected emulsions are shown in Figure 4.14 (a) and Figure 4.14 (b) shows the average diameter of droplets, which decreases rapidly with salt concentration until a plateau at 20  $\mu\text{m}$ . For emulsions without TPeAB, there are several small spherical water droplets along with large non-spherical droplets. The emulsion droplets easily coalesce when subjected to shear as some droplets are destroyed during the transfer from the vessel to a glass slide. In comparison, for emulsions with TPeAB, much smaller droplets are observed under the microscope, the droplet size decreases gradually with [TPeAB]. One may notice that there are some relatively larger black droplets co-existing with translucent smaller droplets on the microscopy images. In some food emulsions stabilized by octinyl succinic anhydride starch, similar black droplets were observed and they were confirmed as w/o/w droplets.<sup>40</sup> However, the black droplets here are unlikely double emulsions as no tinny droplets were observed inside the black droplets even at higher magnifications, as illustrated in the insert of the image with  $1 \times 10^{-4}$  M TPeAB in Figure 4.14. The appearance of black and translucent droplets is possibly due to contrast difference, considering the presence of polystyrene latex particles inside the water droplets. In addition, if we adjust the strength of the light, these black droplets can also be translucent. Figure 4.15 represents the  $\theta$  of particles ( $d = 3.5 \mu\text{m}$ ) at the dodecane-water interface against [TPeAB] measured by GTT. The value without salt is  $\sim 115^\circ$ ,

increase of salt concentration results in gradually decrease of  $\theta$ . However,  $\theta$  is lower than that of sulfate latex particles at dodecane-water interfaces at the corresponding TPeAB concentrations, although all of them are still above  $90^\circ$ , which is consistent with w/o emulsions obtained. Lower  $\theta$  of carboxyl latex particles at dodecane-water interfaces is likely due to their higher surface charge density. The w/o emulsions stabilized by carboxyl latex particles follow the Bancroft rule as they are hydrophobic at all salt concentrations.

**Figure 4.12.** (a) Appearance of water-in-dodecane emulsions (1:1 by volume) stabilized by 2 wt.% carboxyl PS latex particles ( $d = 0.2 \mu\text{m}$ ) in varied concentrations (given) of TPeAB at pH 11, taken one week after preparation. (b) Conductivity of emulsions in (a) measured immediately after homogenization.

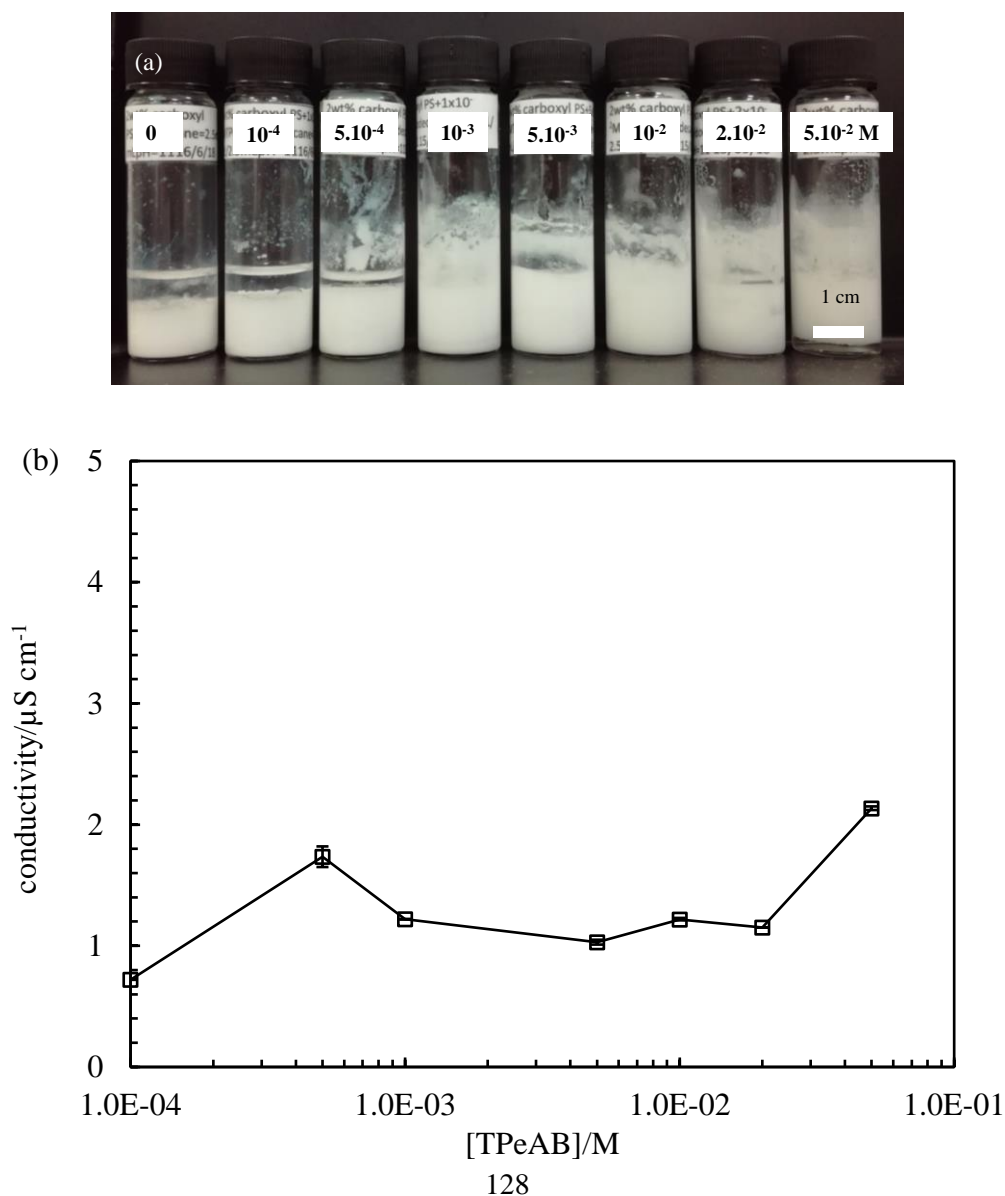


**Figure 4.13.** The stability to sedimentation ( $f_o$ ) and coalescence ( $f_w$ ) of water-in-dodecane emulsions (1:1 by volume) stabilized by 2 wt.% carboxyl PS latex particles ( $d = 0.2 \mu\text{m}$ ) in varied concentrations (given) of TPeAB at pH 11, measured one week after preparation. Dashed line indicates  $f_o$  of emulsion stabilized by 2 wt.% carboxyl PS latex particles alone (no salt).

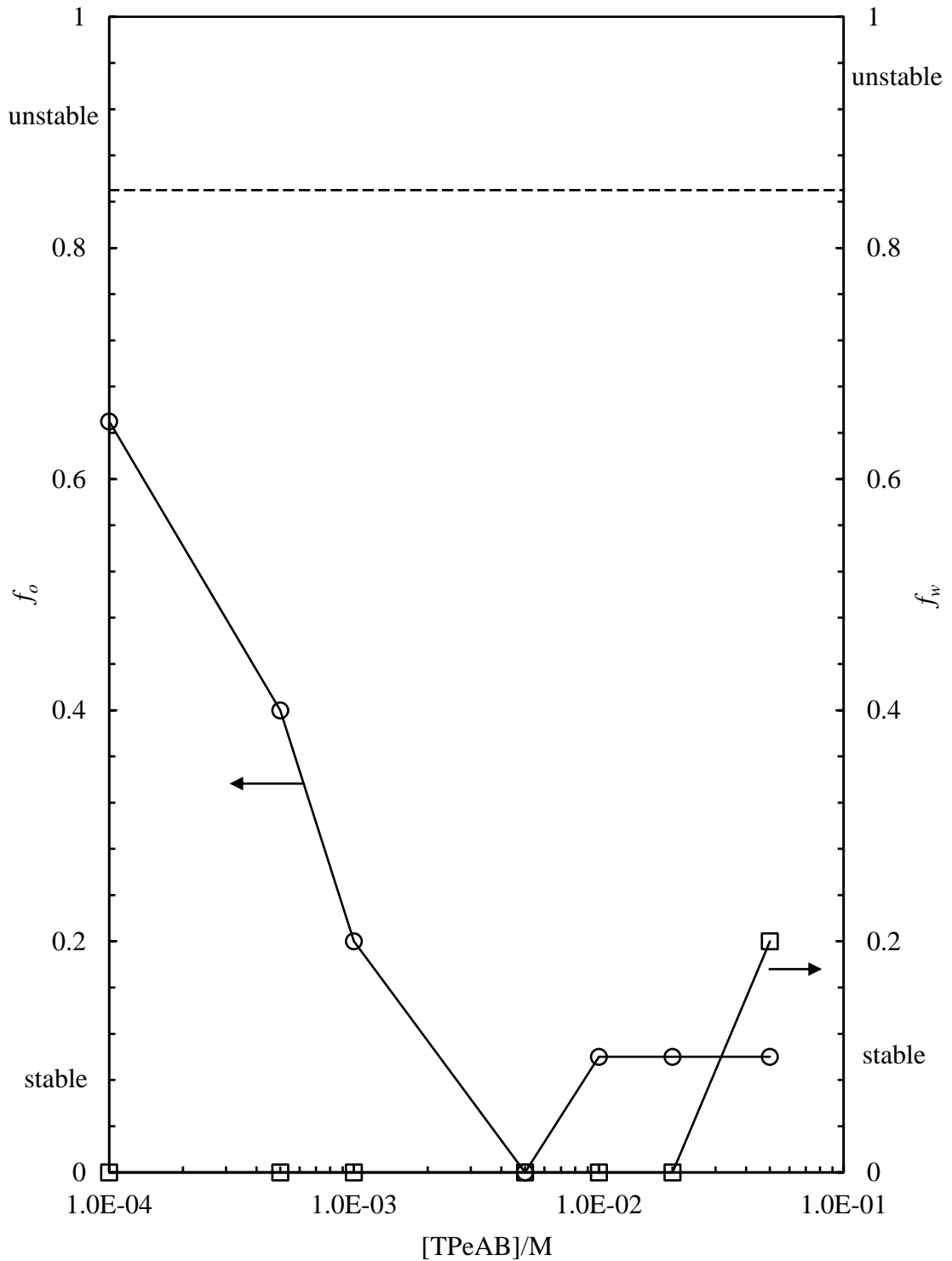


**Figure 4.14.** (a) Optical microscopy images of selected water-in-dodecane emulsions (1:1 by volume) stabilized by 2 wt.% carboxyl PS latex particles in the presence of TPeAB at pH 11, taken two days after preparation. The insert in the image of  $1 \times 10^{-4}$  M TPeAB is a magnified droplet. (b) Average droplet diameter of water-in-dodecane emulsions in (a), dashed line represents the emulsion without salt.

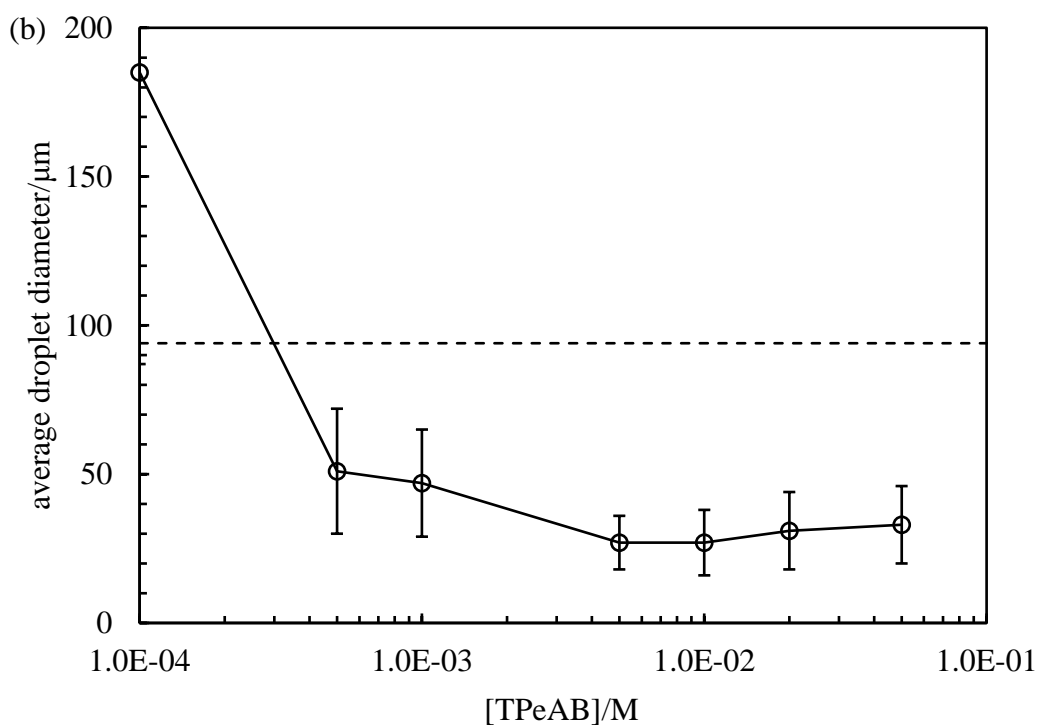
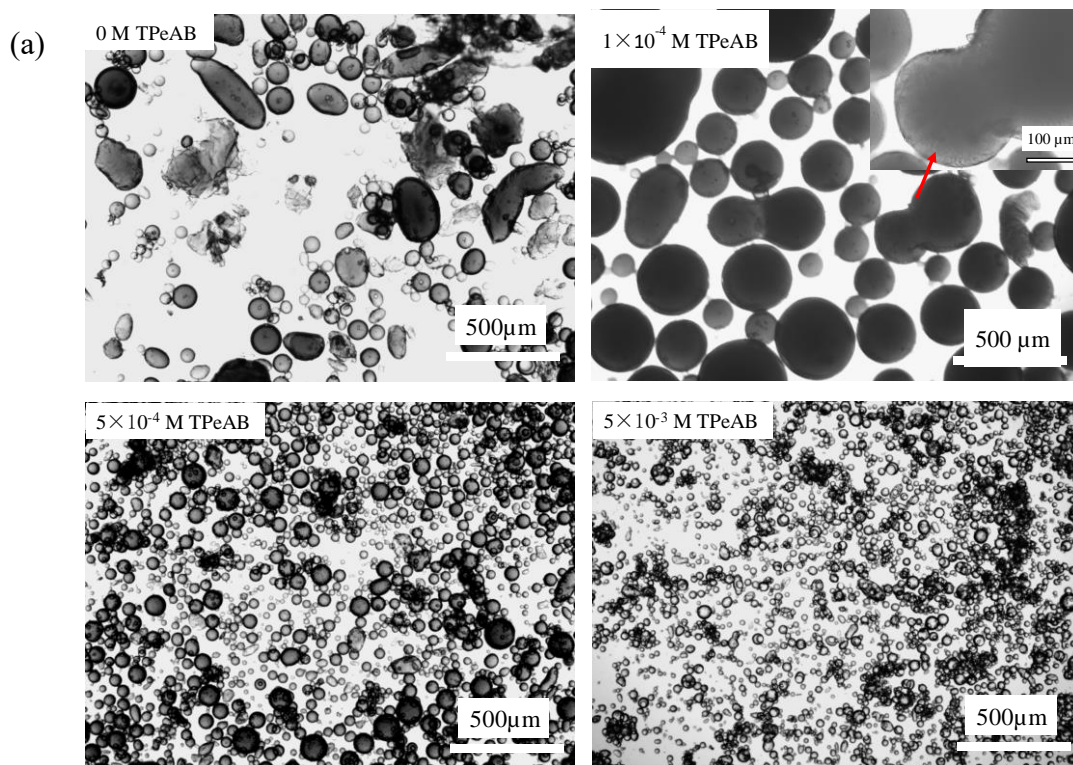
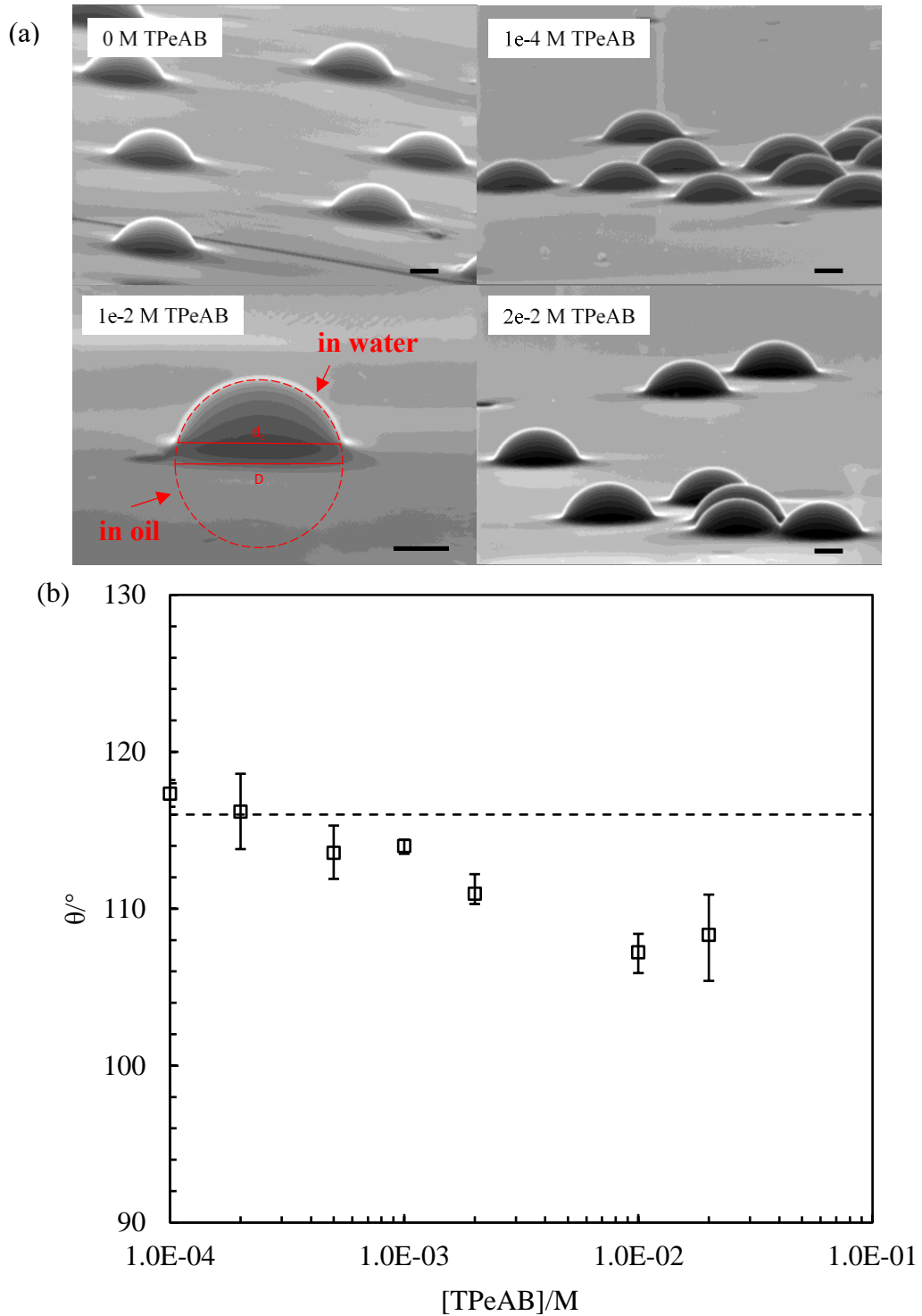


**Figure 4.15.** (a) SEM of monodispersed carboxyl latex particles ( $d = 3.5 \mu\text{m}$ ) on the surface of PDMS obtained by the GTT at dodecane-water interface. The observation angle  $\delta = 80^\circ$ . Scale bar =  $1 \mu\text{m}$ . (b) Three-phase contact angles ( $\theta$ ) of carboxyl latex particles ( $d = 3.5 \mu\text{m}$ ) at the dodecane-water interface against [TPeAB]. The dashed line indicates the contact angle of particles at the dodecane-water interface without salt.



### 4.3.3 Aqueous dispersion of carboxyl latex particles at pH 3

Carboxyl latex particles are pH-dependent, they are negatively charged at high pHs but will lose their surface charge in acidic environments. It is therefore interesting to study the properties of particles and their behaviours at oil-water interfaces when losing their surface charges. At  $\text{pH} \leq \text{pK}_a - 2$ , the carboxyl groups are said to be fully protonated.<sup>41</sup> Thus, in this section, the pH of the particle dispersions was adjusted to 3. Figure 4.16 (a) is the appearance of 2 wt.% carboxyl PS latex particle dispersions in TPeAB solutions. The particles flocculate and large particle aggregates were observed in all samples. Figure 4.16 (b) is the plot of particle size against salt concentration. The diameter of particle aggregates is  $\sim 20 \mu\text{m}$  regardless of salt concentration, nearly a hundred times higher than the original particles ( $d = 0.2 \mu\text{m}$ ). The particles received from the manufacturer are discrete at neutral pH, particle surfaces are partially ionized, which provides charge stability of particles. At pH 3, the carboxyl groups on the particle surface are fully protonated and lose their charges, which lead to flocculation of particles. Figure 4.17 represents the zeta potential of 0.0004 wt.% carboxyl PS latex particles in TPeAB solutions at pH 3. The zeta potential of carboxyl latex in pure water at this pH is about +9 mV, the absolute value of zeta potential increases continuously with salt concentrations. This is reasonable as the accumulation of  $\text{TPeA}^+$  cations on the surface of particles increase the positive charge of particle surfaces. It hints that addition of salt leads to the flocculation of particles even when they are highly positively charged, which reflects the strong hydrophobic attraction between particle surfaces and alkyl chains on  $\text{TPeA}^+$  ions.

**Figure 4.16.** (a) Appearance of 2 wt.% carboxyl PS latex particle ( $d = 0.2 \mu\text{m}$ ) dispersions in varied concentrations (given) of TPeAB at pH 3. (b) Average diameter of carboxyl PS latex particles (quoted  $d = 0.2 \mu\text{m}$ ) against [TPeAB] at pH 3.

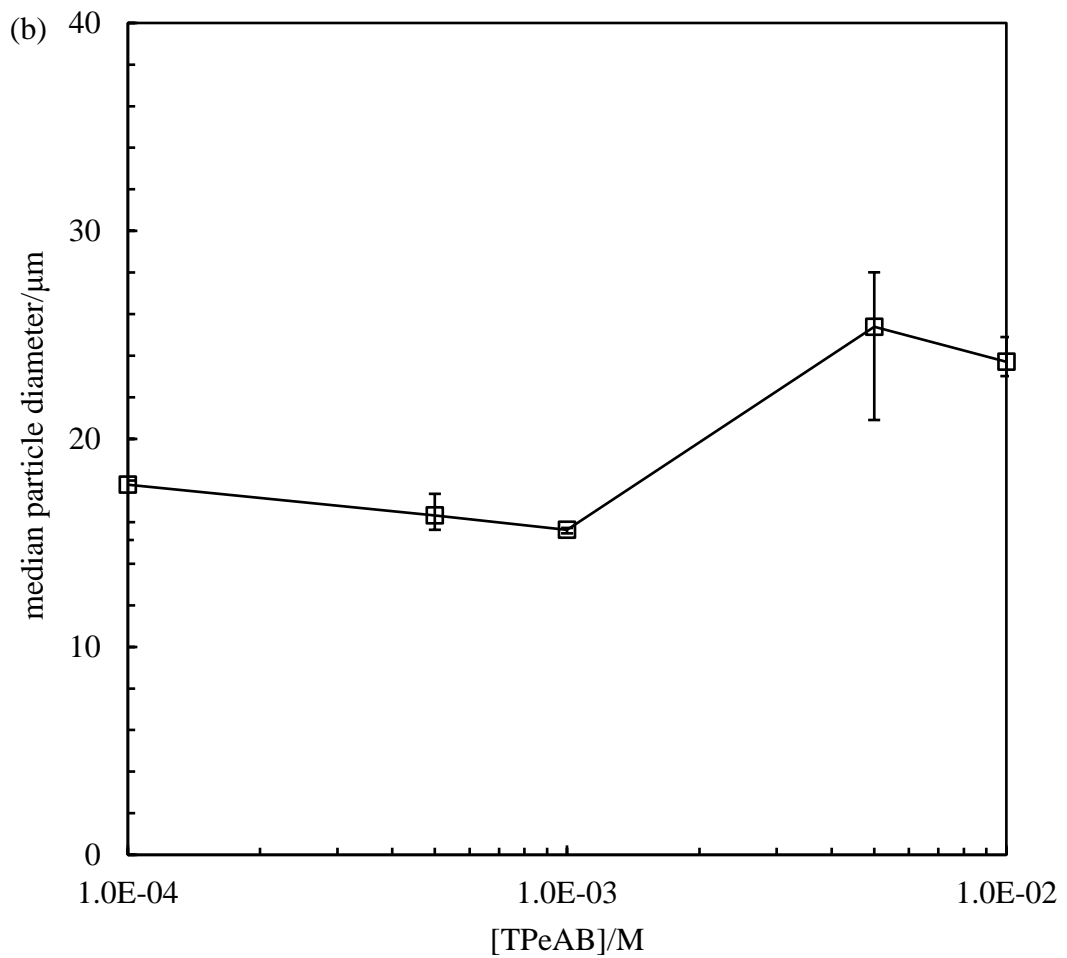
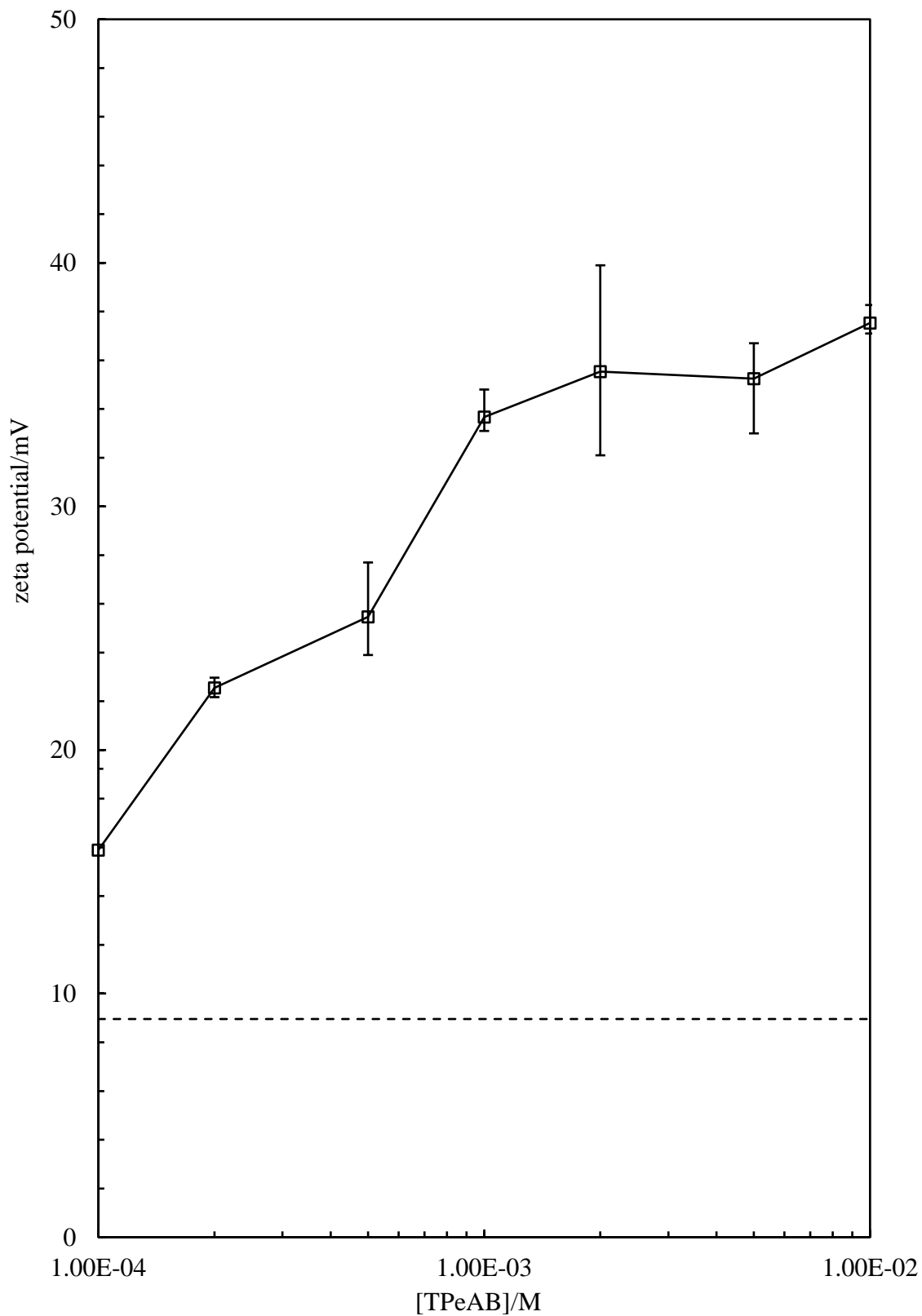


**Figure 4.17.** Zeta potential of 0.0004 wt.% carboxyl PS latex particles ( $d = 0.2 \mu\text{m}$ ) against [TPeAB] at pH 3. The dashed line indicates the zeta potential of carboxyl PS latex particles in water (without salt).



#### 4.3.4 Emulsions with dodecane at pH 3

Batches of emulsions were prepared by homogenizing 2 wt.% carboxyl PS latex particle dispersion at pH 3 with dodecane at an oil: water ratio of 1:1. The appearance of emulsions is shown in Figure 4.18 (a). From the drop test the emulsions are all determined as w/o regardless of salt concentration. The conductivities of the emulsions are all about  $2 \mu\text{S cm}^{-1}$ , as illustrated in Figure 4.18 (b), consistent with w/o emulsions. In all samples, oil was extracted from the emulsions, the addition of salt induces no difference on the amount of oil extracted from the emulsions. These results indicate that the emulsions are partially stable to sedimentation, and the presence of TPeAB induces little influence on the stability of emulsions to sedimentation. On the other hand, no water is observed released from the emulsions, which means these emulsions are stable to coalescence. Figure 4.19 plots  $f_o$  and  $f_w$  of the emulsions against [TPeAB] at long time. The  $f_o$  of the emulsion without salt is 0.3 and the  $f_o$  of emulsions with TPeAB remains constant. The  $f_w$  of all emulsions keeps at zero. Optical microscopy images of each emulsion are shown in Figure 4.20 (a). Spherical droplets are observed on all images. The average droplet size of the emulsions without salt is about  $40 \mu\text{m}$ . The addition of salt induces little influence on the droplet size of emulsions, as illustrated in Figure 4.20 (b).

**Figure 4.18.** (a) Appearance of water-in-dodecane emulsions (1:1 by volume) stabilized by 2 wt.% carboxyl PS latex particles ( $d = 0.2 \mu\text{m}$ ) in varied concentrations (given) of TPeAB at pH 3, taken two weeks after preparation. (b) Conductivity of dodecane-in-water emulsions in (a), measured immediately after homogenization. The dashed line indicates the conductivity of the emulsion without salt.

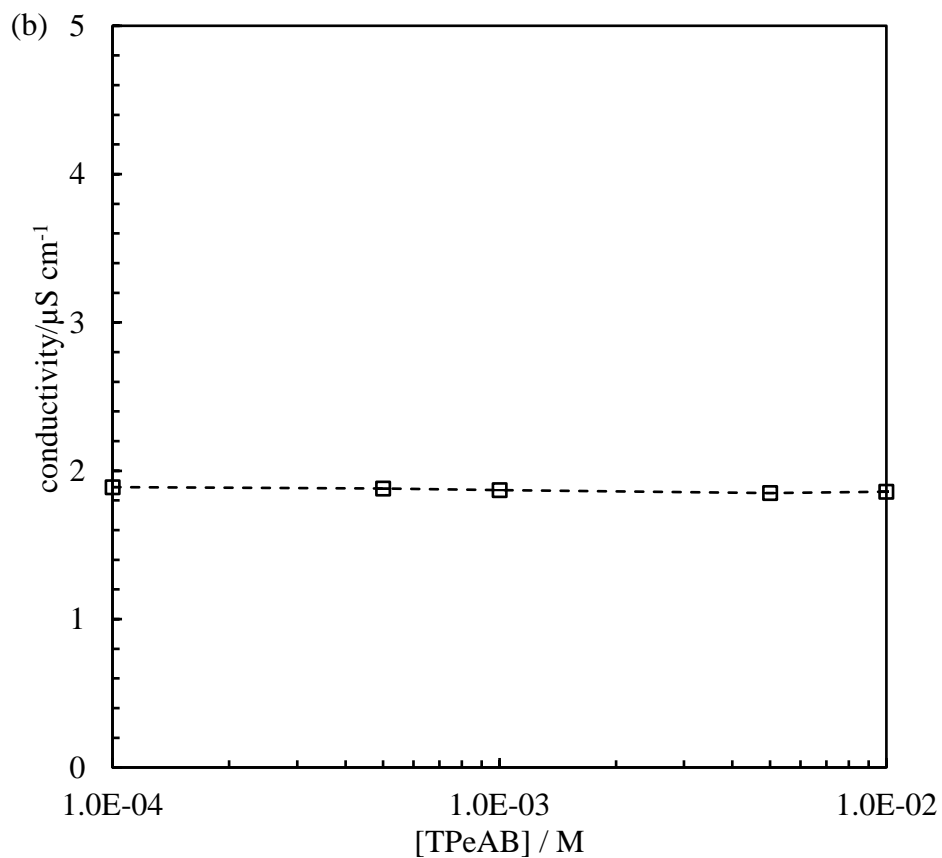
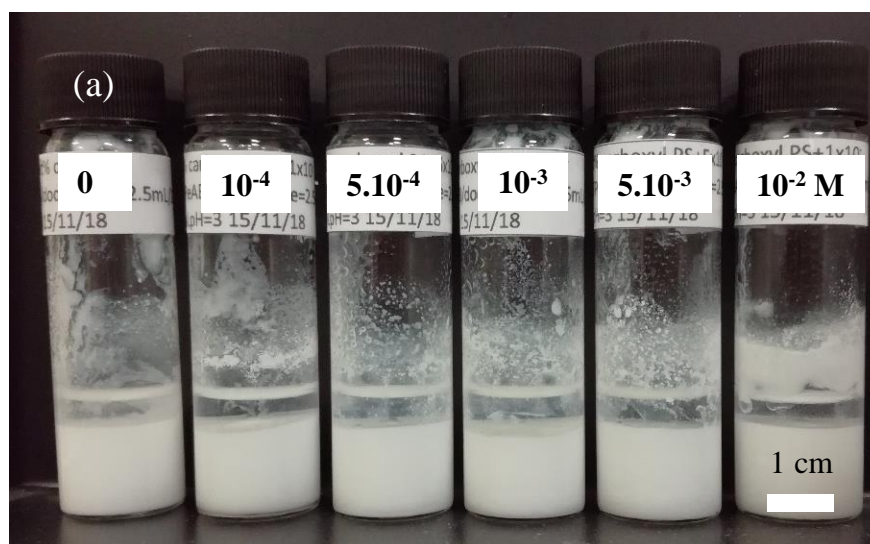


**Figure 4.19.** The  $f_o$  and  $f_w$  of water-in-dodecane emulsions (1:1 by volume) stabilized by 2 wt.% carboxyl PS latex particles ( $d = 0.2 \mu\text{m}$ ) against [TPeAB] at pH 3, measured 1 week after preparation. Dashed line indicates the  $f_o$  of the emulsion without salt.

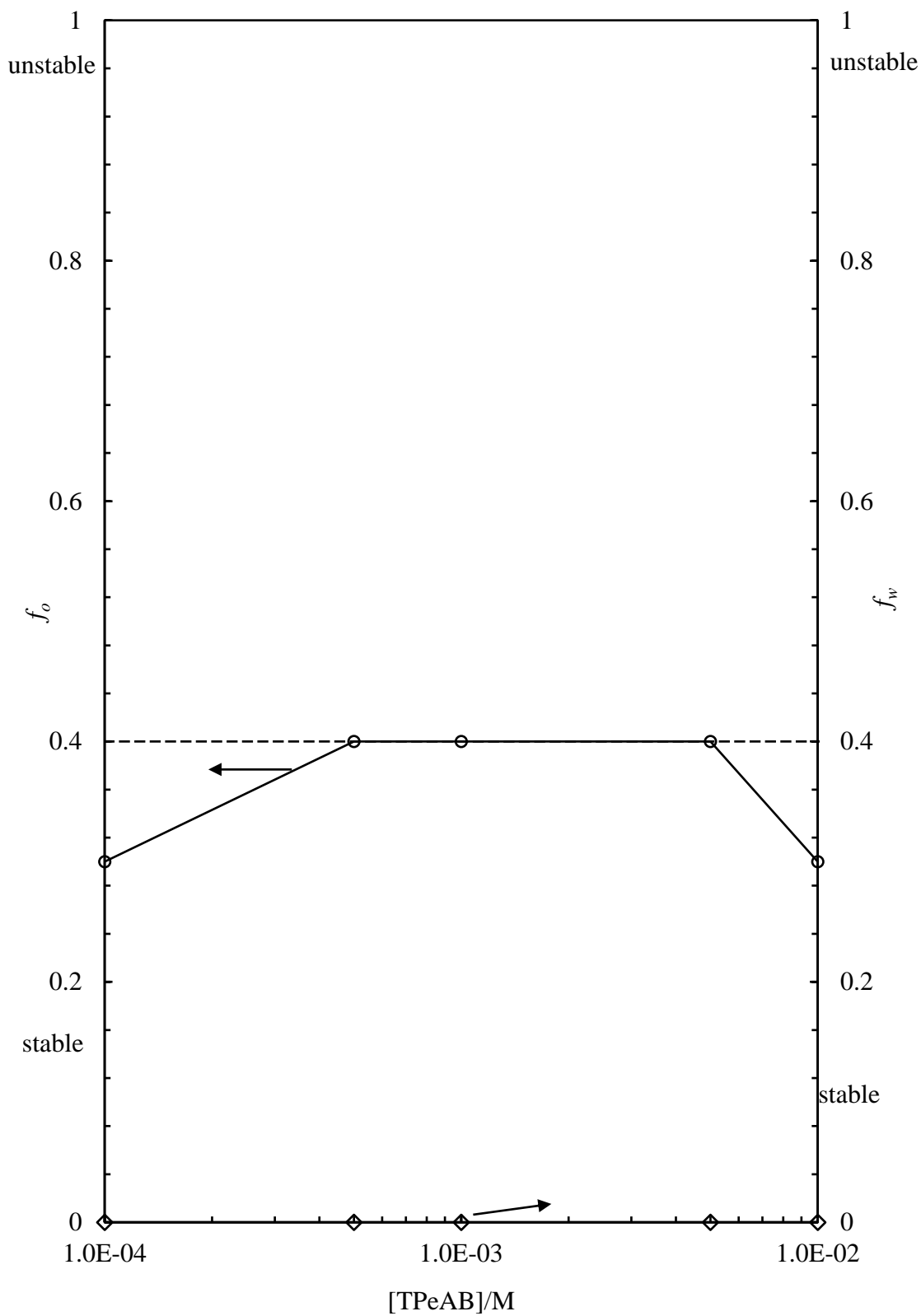
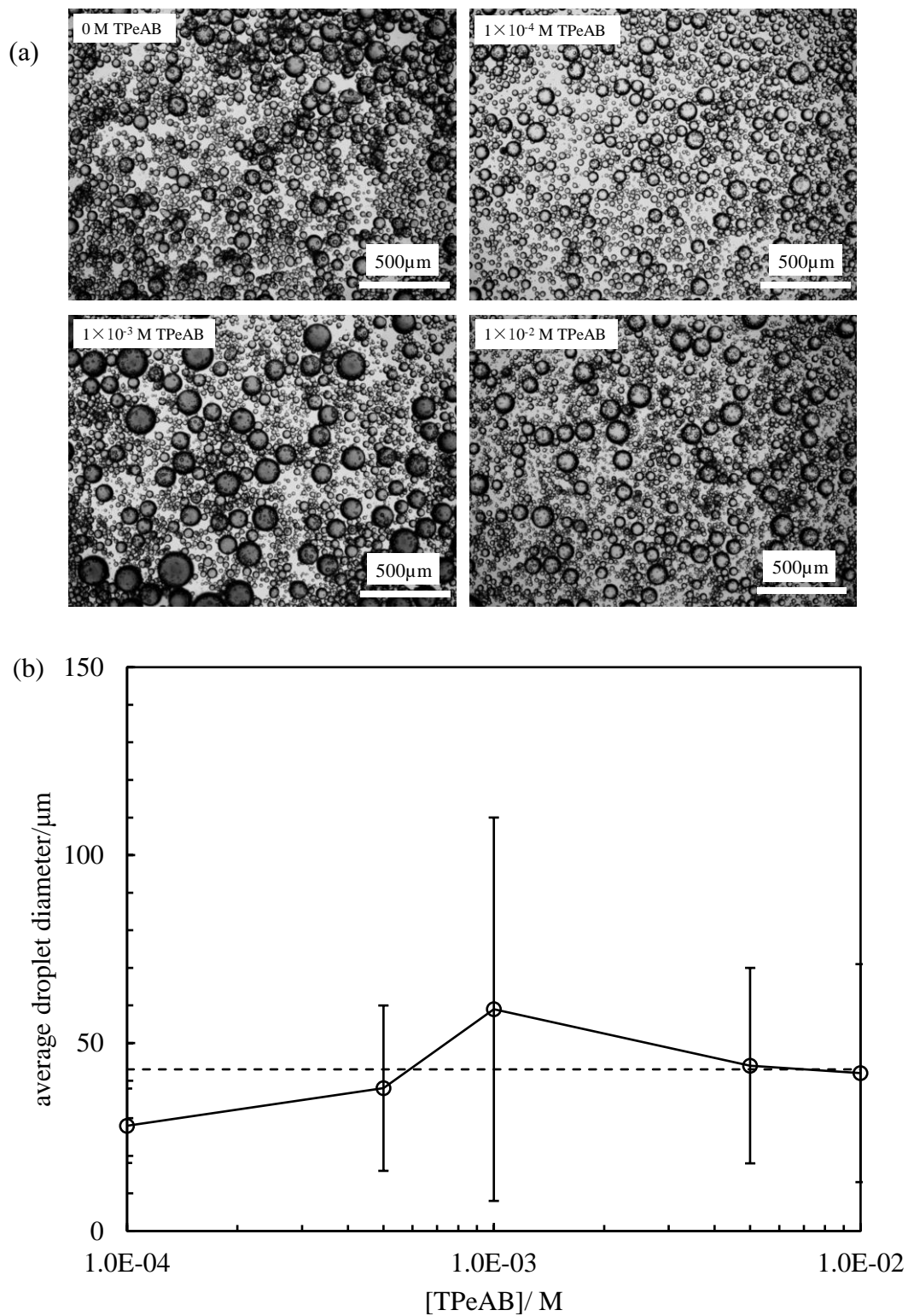


**Figure 4.20.** Optical microscopy images of water-in-dodecane emulsions (1:1 by volume) stabilized by 2 wt.% carboxyl PS latex particles ( $d = 0.2 \mu\text{m}$ ) in TPeAB at pH 3, taken 24 hours after preparation. (b) Average droplet diameter of emulsions calculated from the optical microscopy images.



#### 4.3.5 Emulsions with heptane at pH 11

Batches of emulsions were prepared by homogenizing 2 wt. % carboxyl PS latex dispersion at pH 11 and heptane at a water: oil ratio of 1:1. The appearance of the emulsions is shown in Figure 4.21 (a). Emulsions are all determined as w/o from the drop test, in agreement with the conductivity results in Figure 4.21 (b). A layer of clear oil was observed on the top of each emulsion, which results from the sedimentation of emulsions. Increase of salt concentration results in increasing stability to sedimentation,  $f_o$  of emulsions decreases rapidly with increasing salt concentrations until it plateaus at 0.3 (Figure 4.22). Large droplets were observed under optical microscope, non-spherical droplets were also observed in the emulsion with  $1 \times 10^{-4}$  M TPeAB (Figure 4.23). The contact angle of 3.5  $\mu\text{m}$  particles at heptane-water interfaces is plotted in Figure 4.24. The  $\theta$  of particle at heptane-water (without salt) interface is  $128 \pm 2^\circ$ , which gradually decreases to  $111^\circ$  with the increase of salt concentration, slightly higher than the  $\theta$  of same particles at dodecane-water interfaces at corresponding salt concentrations. The w/o emulsions in this system follow the Bancroft rule.

**Figure 4.21.** (a) Appearance of water-in-heptane emulsions (1:1 by volume) stabilized by 2 wt. % carboxyl PS latex particles ( $d = 0.2 \mu\text{m}$ ) in varied concentrations (given) of TPeAB at pH 11, taken one week after preparation. (b) Conductivity of water-in-heptane emulsions in (a) against [TPeAB].

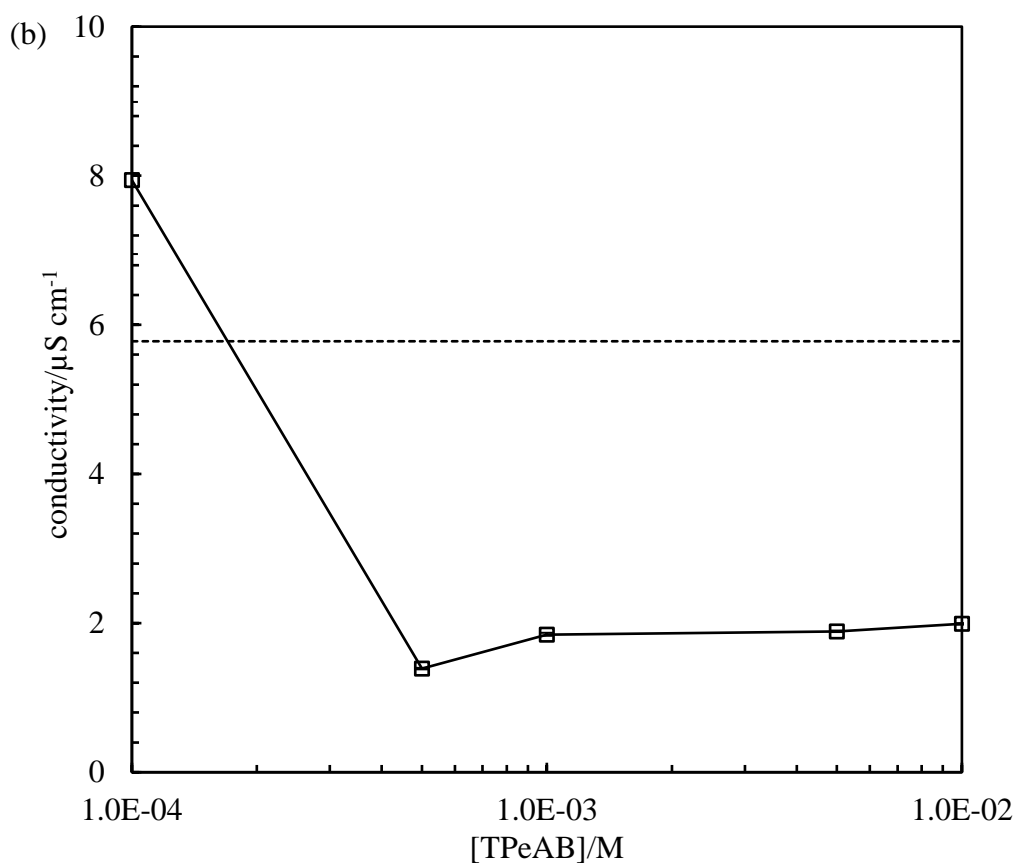


**Figure 4.22.** The  $f_o$  and  $f_w$  of water-in-heptane emulsions (1:1 by volume) stabilized by 2 wt. % carboxyl PS latex particles ( $d = 0.2 \mu\text{m}$ ) as a function of [TPeAB] at pH 11, measured one week after preparation. Dashed line indicates the  $f_o$  of emulsions without salt,  $f_w$  keeps at zero at all salt concentrations.

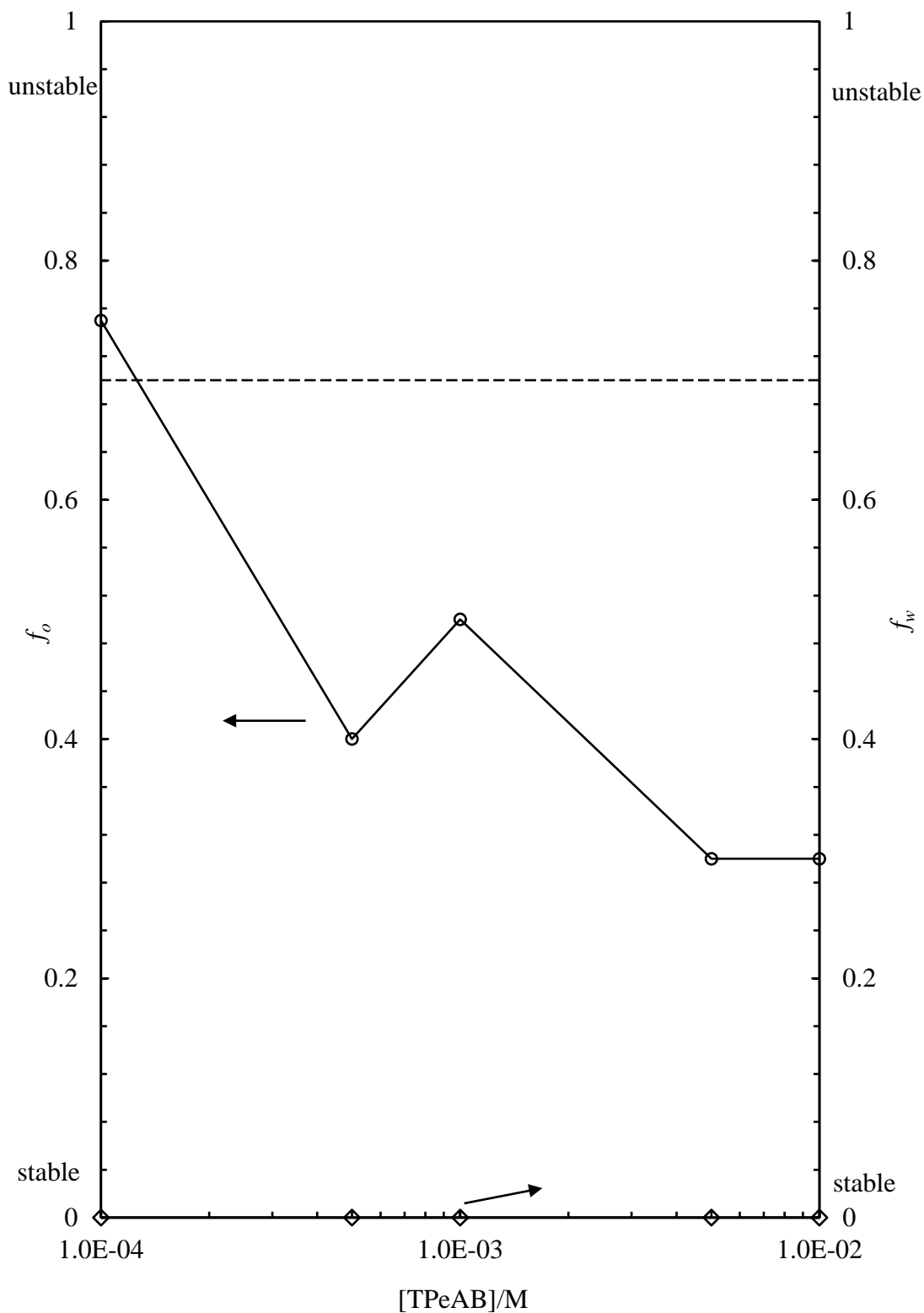


**Figure 4.23.** Optical micrographs of water-in-heptane emulsions (1:1 by volume) stabilized by 2 wt. % carboxyl PS latex particles ( $d = 0.2 \mu\text{m}$ ) as a function of [TPeAB] at pH 11, taken 24 hours after preparation.

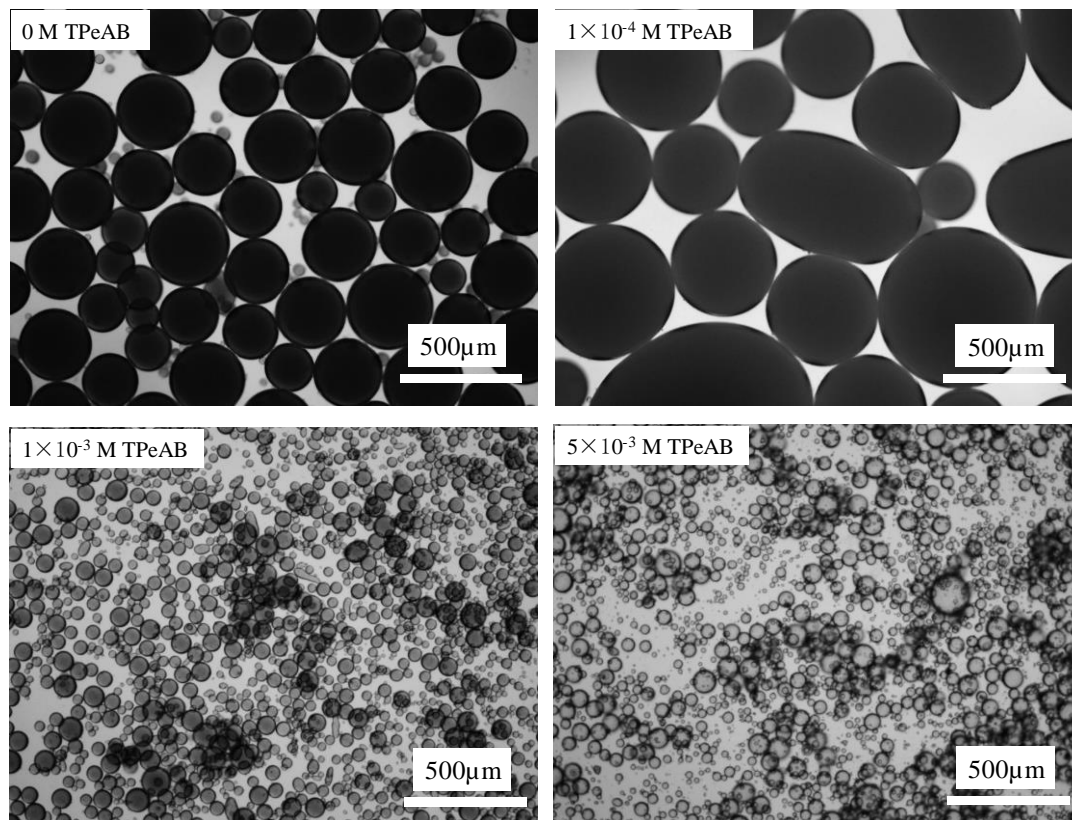
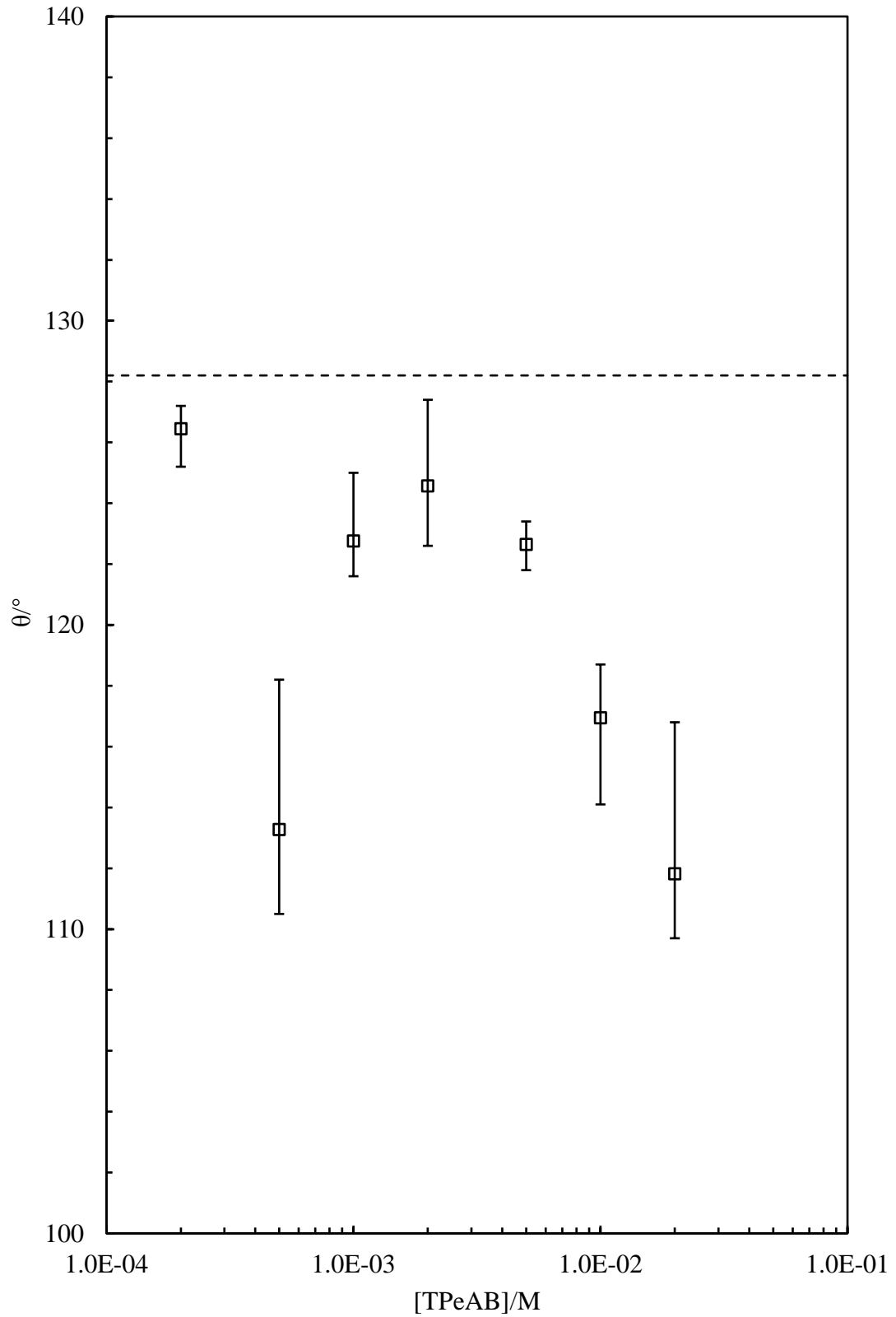


**Figure 4.24.** Three-phase contact angles ( $\theta$ ) of carboxyl latex particles ( $d = 3.5 \mu\text{m}$ ) at the heptane-water interface against [TPeAB] at pH 11. Dashed line indicates the  $\theta$  of particles at the heptane-water interface without salt.



#### 4.3.6 Emulsions with 1 cS PDMS at pH 11

The contact angle results of carboxyl latex particles at dodecane-water interfaces indicate that we are able to decrease the hydrophobicity of polystyrene particles by adding an organic electrolyte. However, the magnitude of contact angle change was not significant enough to tune the particle surface from hydrophobic ( $\theta > 90^\circ$ ) to hydrophilic ( $\theta < 90^\circ$ ). To further decrease the three-phase contact angle of carboxyl latex particles, polydimethylsiloxane (PDMS, 1cS) with slightly higher polarity ( $\epsilon = 2.3-2.8$ ) than that of dodecane ( $\epsilon = 2.0$ ) was used as the oil phase. The appearance of the emulsions and corresponding optical microscopy images of selected samples are shown in Figure 4.25 (a). The result of conductivity measurement is represented in Figure 4.25 (b). In the samples with  $\text{TPeAB} \leq 5 \times 10^{-4}$  M, the conductivities of emulsions are very low ( $< 6 \mu\text{S cm}^{-1}$ ), w/o emulsions are determined. Phase inversion occurs at higher salt concentrations where much higher conductivities ( $> 80 \mu\text{S cm}^{-1}$ ) are determined. Emulsions are all stable to coalescence, w/o emulsions at low salt concentrations are partially unstable to sedimentation and o/w emulsions at high [TPeAB] are partially unstable to creaming (Figure 4.26). In addition, at the highest salt concentration ( $1 \times 10^{-2}$  M), the resolved water is clear, indicating that the particles initially in the aqueous phase transfer to the emulsion phase after homogenization. As can be seen from the droplet diameter plot (Figure 4.27), the droplets of w/o emulsions are large and spherical whereas much smaller droplets are obtained in o/w emulsions.

The contact angle of particles at PDMS (1cS)-water interfaces is represented in Figure 4.28. As can be seen, the  $\theta$  of particles at  $\text{TPeAB} \leq 5 \times 10^{-4}$  M are far above  $90^\circ$ , consistent with w/o emulsions obtained. By contrast, at  $1 \times 10^{-3}$  M TPeAB,  $\theta$  is approximately  $87^\circ$ , and an o/w emulsion is now preferred. Higher concentrations of salt result in slight increase of  $\theta$  ( $\geq 90^\circ$ ) and o/w emulsions. Hence, emulsions at low salts concentrations ( $\leq 5 \times 10^{-4}$  M) follow the Bancroft rule but break it at high concentrations. The adsorption of  $\text{TPeA}^+$  ions on the particle surface not only screens the surface charge but also changes the wettability of particles. It is likely that the adsorption of  $\text{TPeA}^+$  ions on the particle surface by hydrophobic interaction increases the hydrophilicity of particle surfaces. Similar phase inversion of emulsions has been reported by Binks and Rodrigues on emulsions stabilized by ionizable carboxyl-coated polystyrene nanoparticles upon increasing the pH value.<sup>28</sup>

**Figure 4.25.** Appearance and selected optical microscopy images of PDMS (1 cS)-water emulsions stabilized by carboxyl latex particles ( $d = 0.2 \mu\text{m}$ ) in varied concentrations (given) of TPeAB at pH 11. (b) Conductivity and type of PDMS-water emulsions in (a).

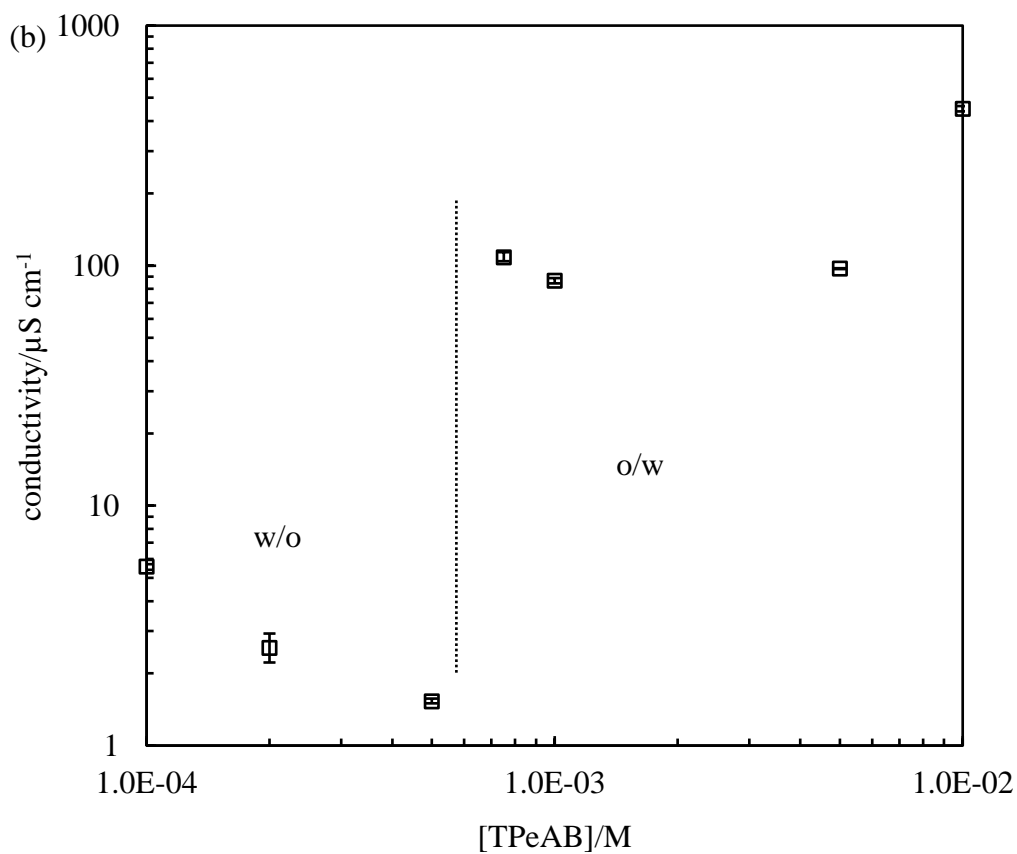
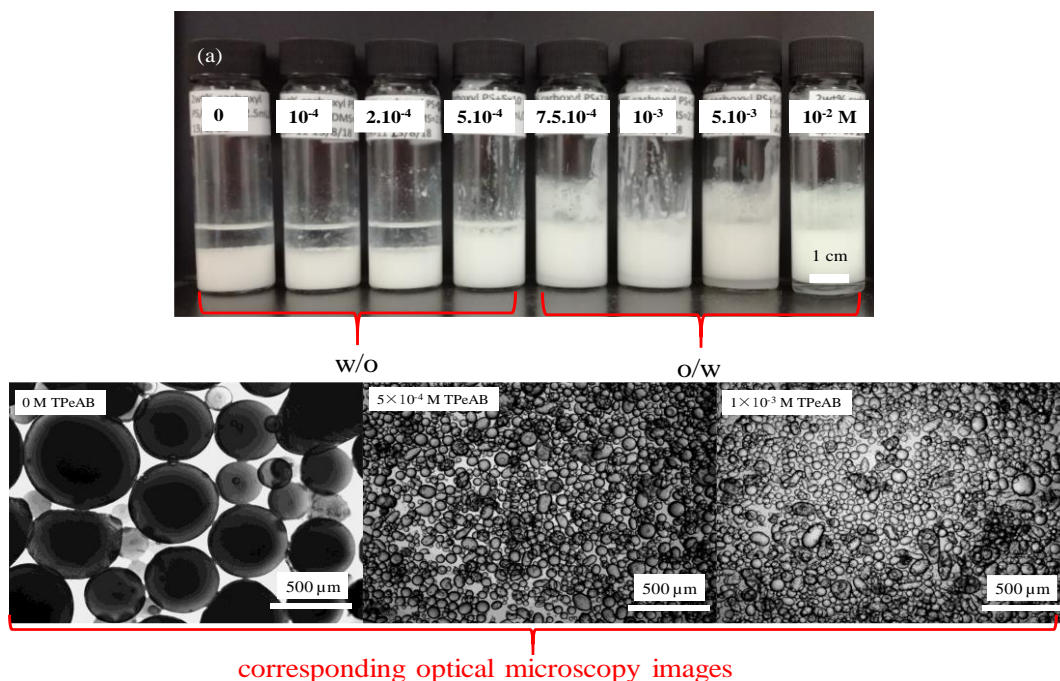


**Figure 4.26.** The  $f_o$  (left hand ordinate, circles) and  $f_w$  (right hand ordinate, squares) of PDMS (1 cS)-water emulsions (1:1 by volume) stabilized by 2 wt.% carboxyl PS latex particles ( $d = 0.2 \mu\text{m}$ ) against [TPeAB] at pH 11, measured one week after preparation. Horizontal dashed line indicates the  $f_o$  of emulsion prepared by carboxyl PS latex particles alone (no salt).

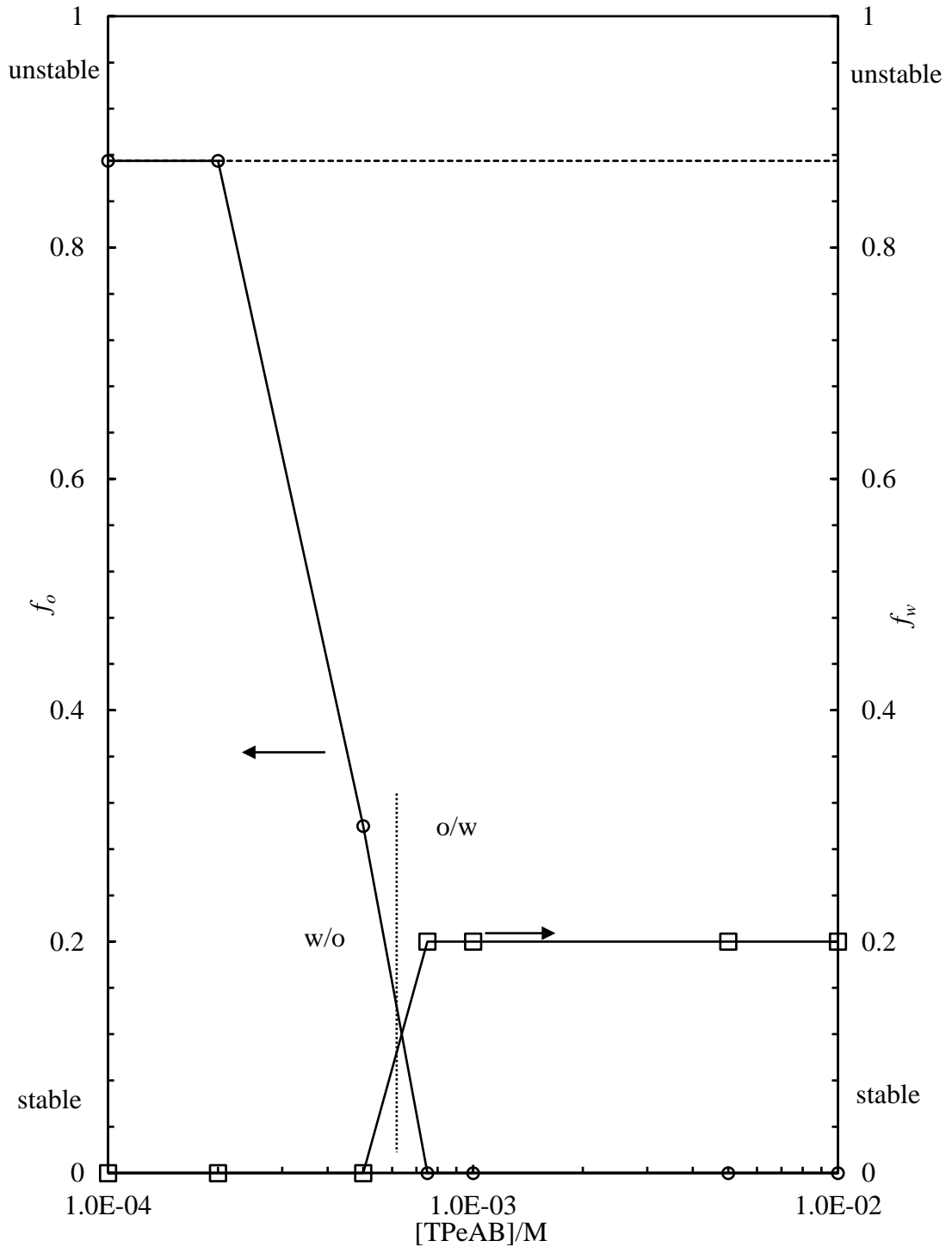


**Figure 4.27.** Average droplet diameter of PDMS (1 cS)-water emulsions (1:1 by volume) stabilized by 2 wt.% carboxyl PS latex particles ( $d = 0.2 \mu\text{m}$ ) against [TPeAB] at pH 11, calculated from the optical microscopy of emulsion droplets using Image J.

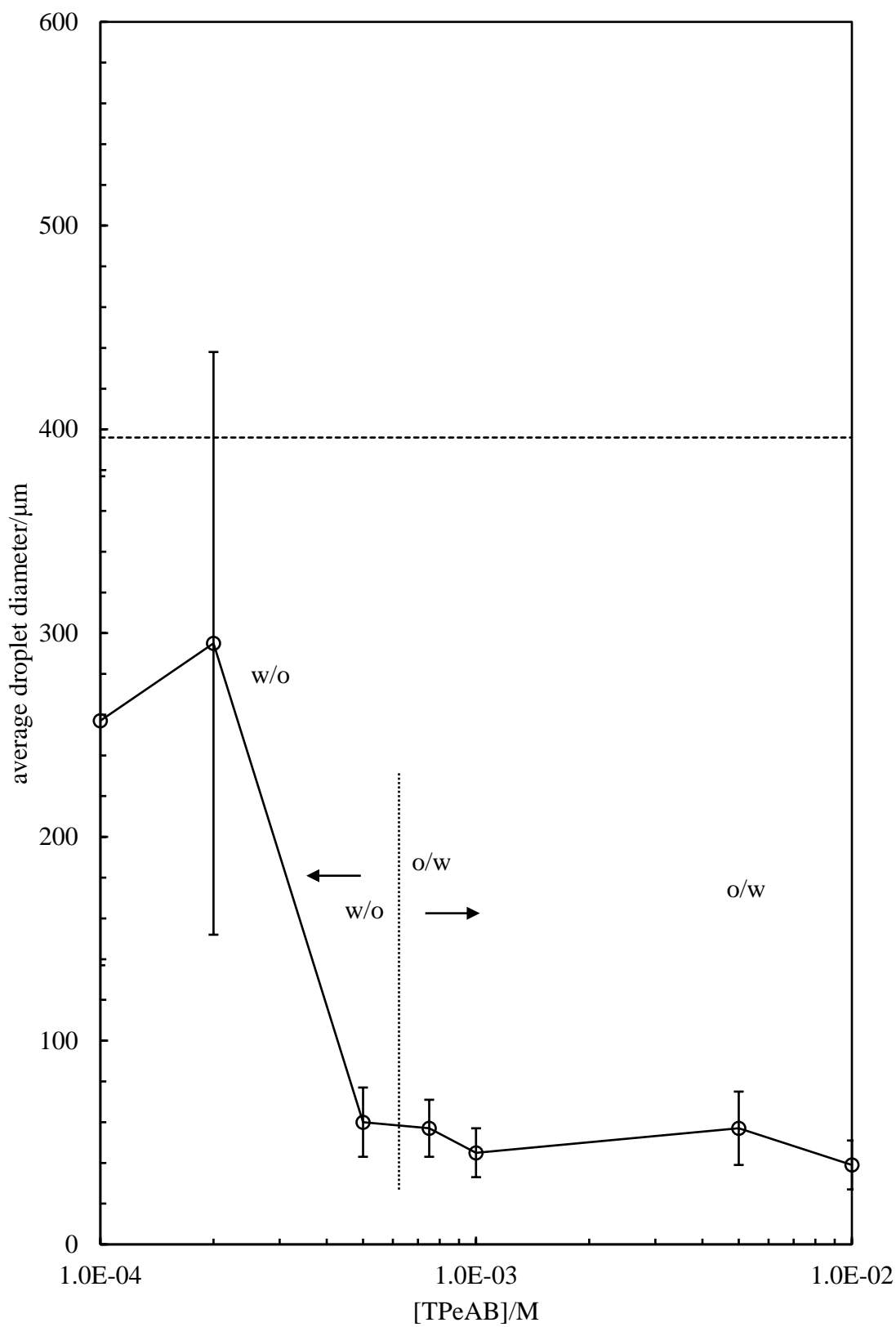
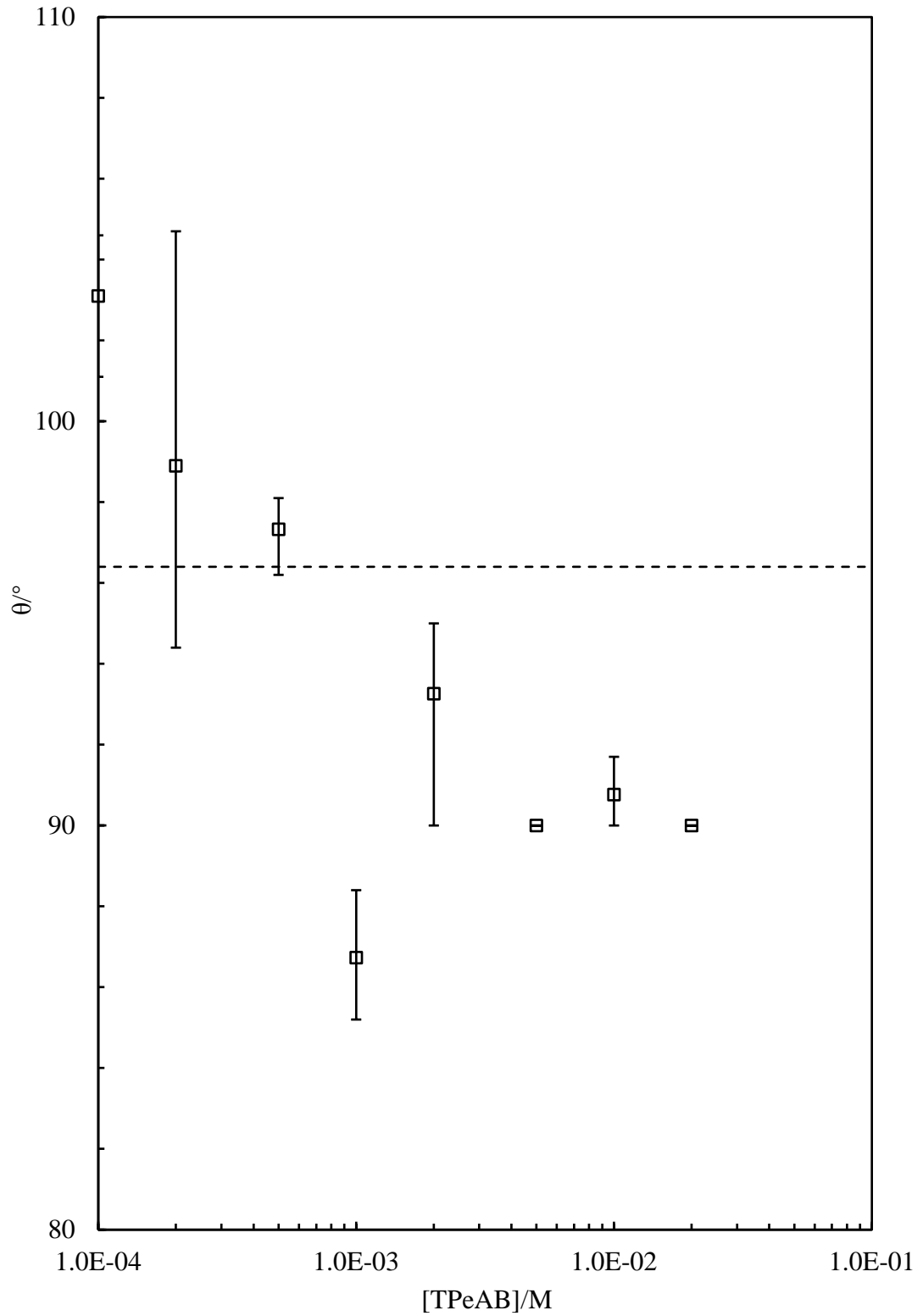


**Figure 4.28.** Three-phase contact angles ( $\theta$ ) of carboxyl latex particles ( $d = 3.5 \mu\text{m}$ ) at the PDMS (1cS)-water interface against [TPeAB]. Dashed line indicates the  $\theta$  of particles at the PDMS (1cS)-water interface without salt.



#### 4.3.7 Emulsions with 50 cS PDMS at pH 11

Batches of emulsions were prepared by homogenizing 2.5 mL of 2 wt. % carboxyl PS latex dispersion at pH 11 with 2.5 mL 50 cS PDMS. The appearance of the emulsions is shown in Figure 4.29 (a) and the conductivity of emulsions is plotted in Figure 4.29 (b). In the samples with TPeAB  $\leq 4 \times 10^{-4}$  M, the conductivities are relatively high, it seems that water is the continuous phase. If this is true, the conductivity of emulsions should increase with increasing salt concentrations, however, an opposite trend is obtained. In addition, in the drop test, emulsion droplets float on the surface of water, accompanied by particles dispersing into water. A small sample was taken from the white layer of the emulsion without TPeAB and observed under the optical microscope. The images are shown in Figure 4.30. As can be seen, un-emulsified aqueous particle dispersion as well as water droplets dispersing in oil were observed. Thus, it can be concluded that w/o emulsions are formed at low salt concentrations, which are unstable to coalescence and sedimentation. The volume of emulsion increases with salt concentration and in the sample containing  $5 \times 10^{-4}$  M of TPeAB, the emulsion is stable to coalescence. High conductivities were observed in samples with higher concentrations of salt. Emulsions are dispersed in water in the drop test, indicating that now water is the continuous phase. Emulsions are stable to coalescence but partially unstable to creaming. The water layer in the emulsion with  $5 \times 10^{-3}$  M TPeAB is clear, meaning that particles initially in the aqueous phase all transfer to the emulsion phase after homogenization. In addition, at the highest salt concentration ( $5 \times 10^{-2}$  M), emulsions are stable to both creaming and coalescence. Optical microscopy of emulsions is shown in Figure 4.31 and the average droplet diameter is represented in Figure 4.32. At low salt concentrations ( $\leq 4 \times 10^{-4}$  M), several spherical water droplets were observed. In the sample with  $5 \times 10^{-4}$  M of TPeAB, spherical as well as non-spherical droplets were observed. Multiple emulsion droplets were observed at higher salt concentrations. As these emulsions are dispersed in water, they were determined as water-in-oil-in-water (w/o/w) type. Hence, emulsions invert from w/o to w/o/w at TPeAB concentrations between  $5 \times 10^{-4}$  and  $1 \times 10^{-3}$  M, close to that of emulsions with PDMS (1 cS). The average diameter of oil globules is about 100  $\mu\text{m}$  (see Figure 4.32). One may notice that a distinct increase in the droplet size occurs upon phase inversion of emulsions. This is consistent with literature, where dramatic changes in the emulsion drop diameter has been reported on phase

inversion.<sup>42</sup> In addition, the highest concentration of salt results in simple o/w emulsions.

**Figure 4.29.** (a) Appearance of water-PDMS (50 cS) emulsions (1:1 by volume) stabilized by 2 wt.% carboxyl PS latex particles ( $d = 0.2 \mu\text{m}$ ) in varied concentrations (given) of TPeAB at pH 11, taken 1 week after preparation. (b) Conductivity and type of emulsions in (a). Horizontal dashed line represents the conductivity of the emulsion stabilised by carboxyl PS latex particles alone (no salt).

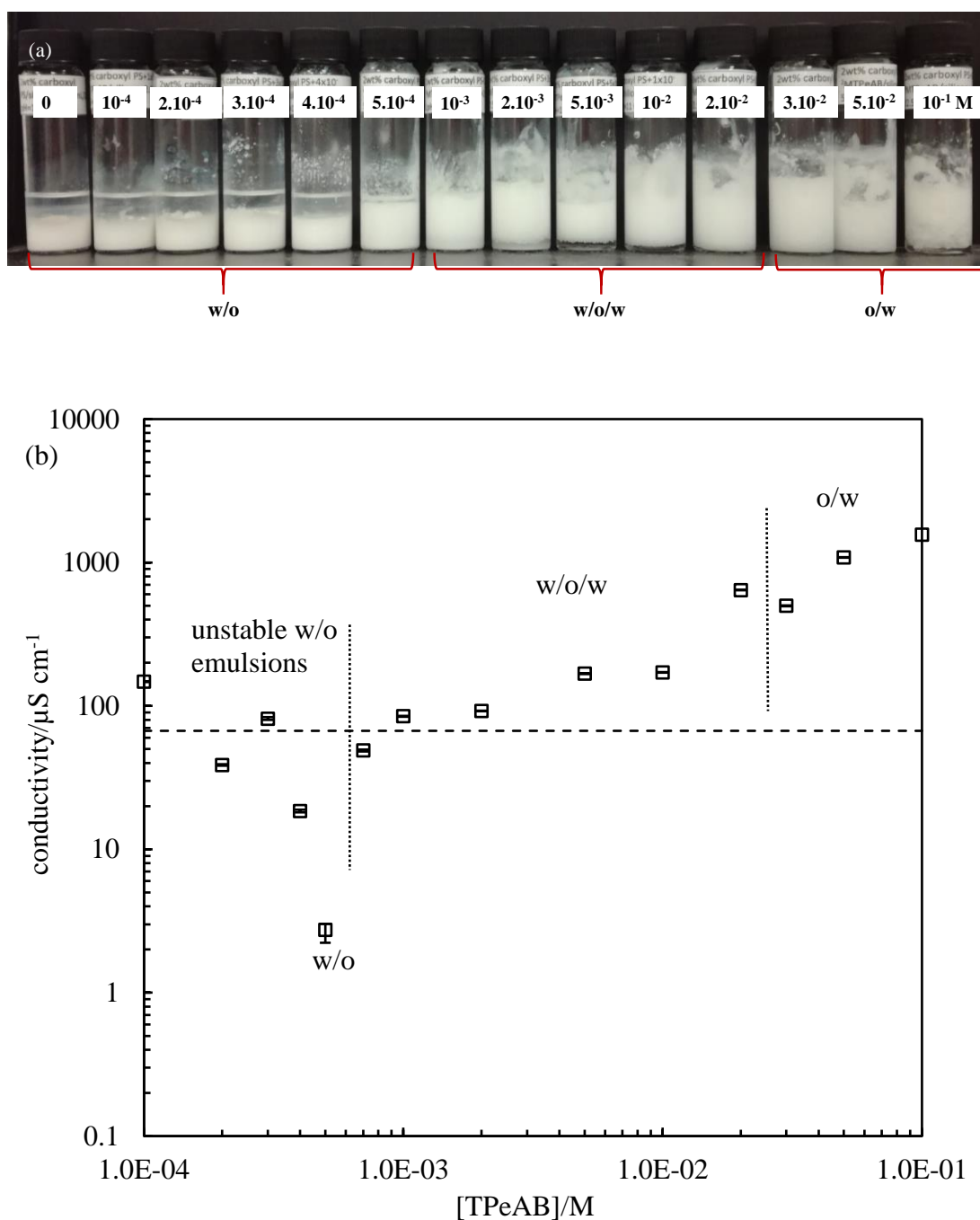


**Figure 4.30.** (a) Photo of a small sample of water-PDMS (50 cS) emulsion (1:1 by volume) stabilized by 2 wt.% carboxyl PS latex particles at pH 11, taken 24 hours after preparation. (b) Optical microscopy image of the droplet free area in (a). (c) Optical microscopy image of water droplets in (a).

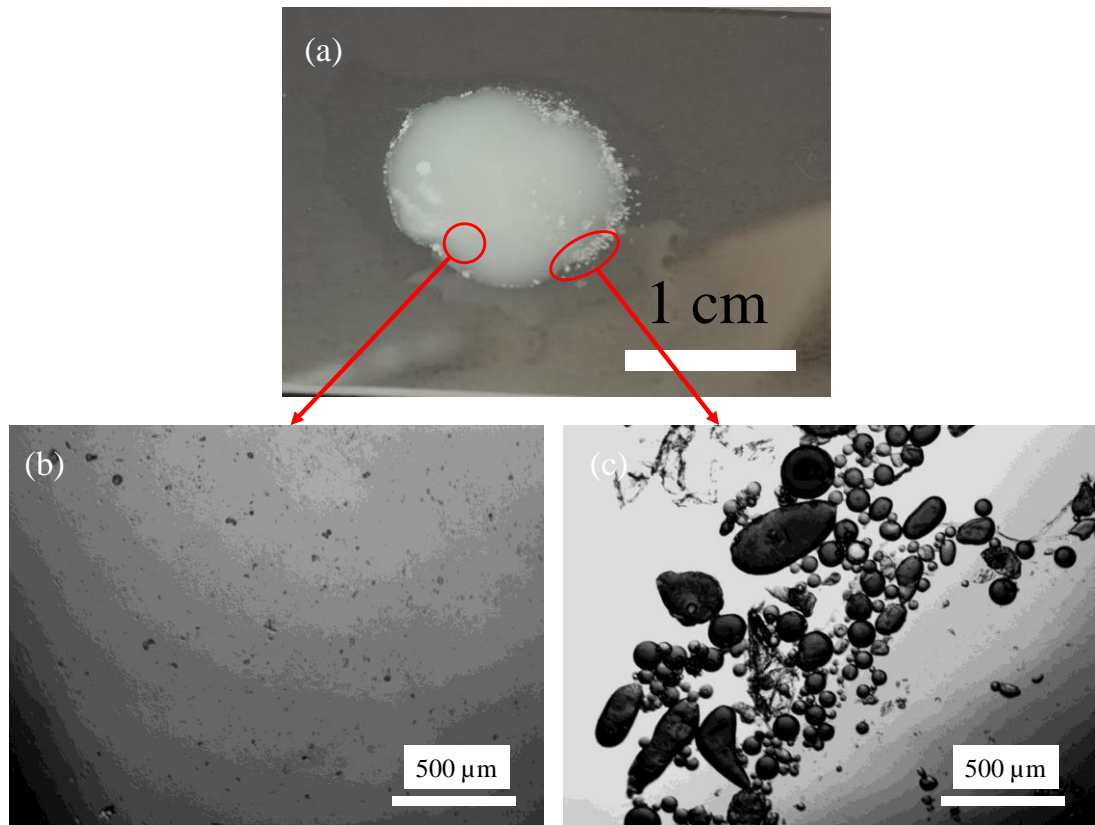


**Figure 4.31.** Optical microscopy images of water-PDMS (50 cS) emulsions (1:1 by volume) stabilized by 2 wt.% carboxyl PS latex particles ( $d = 0.2 \mu\text{m}$ ) in the presence of TPeAB at pH 11, taken 24 hours after preparation.

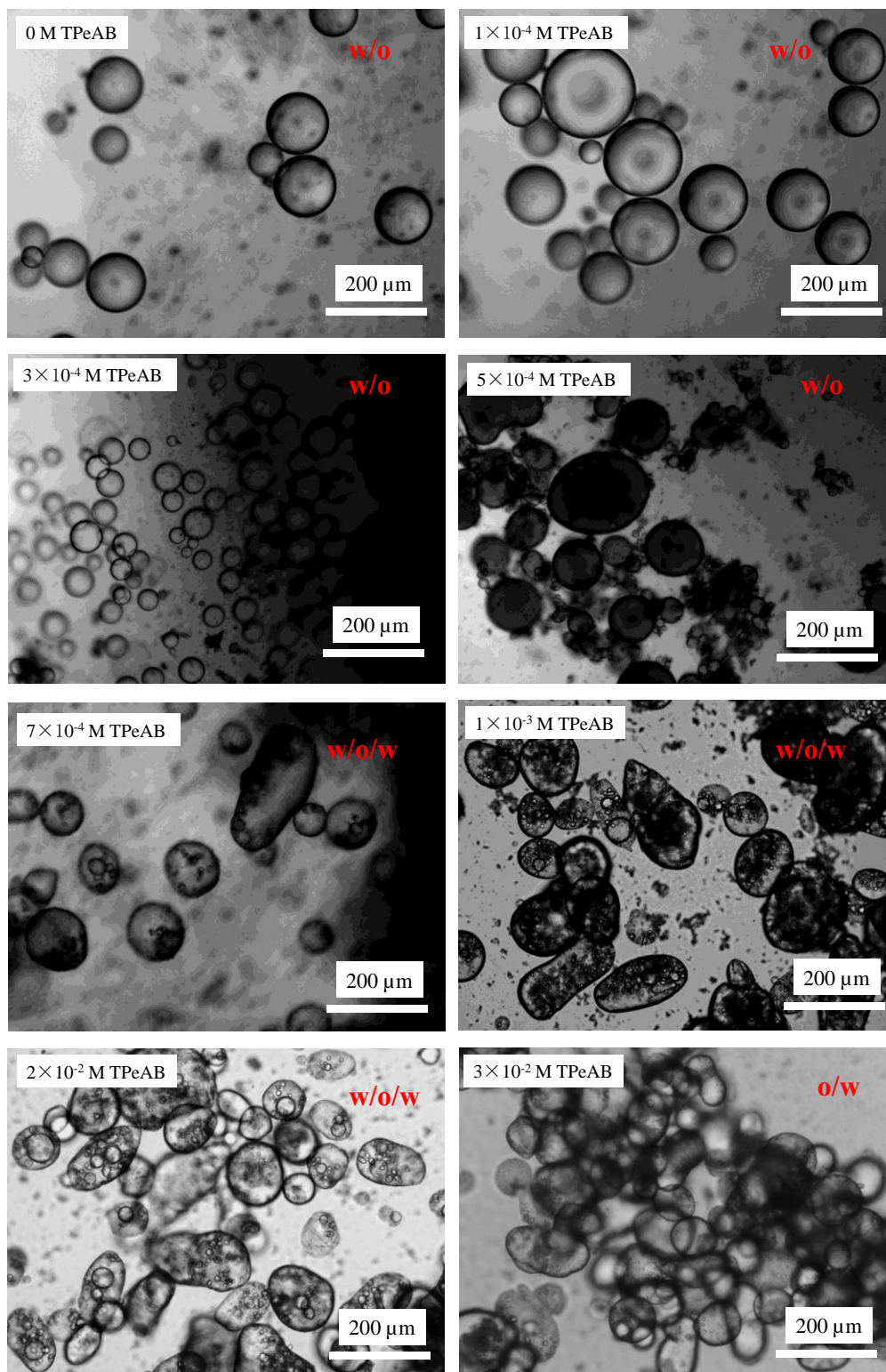
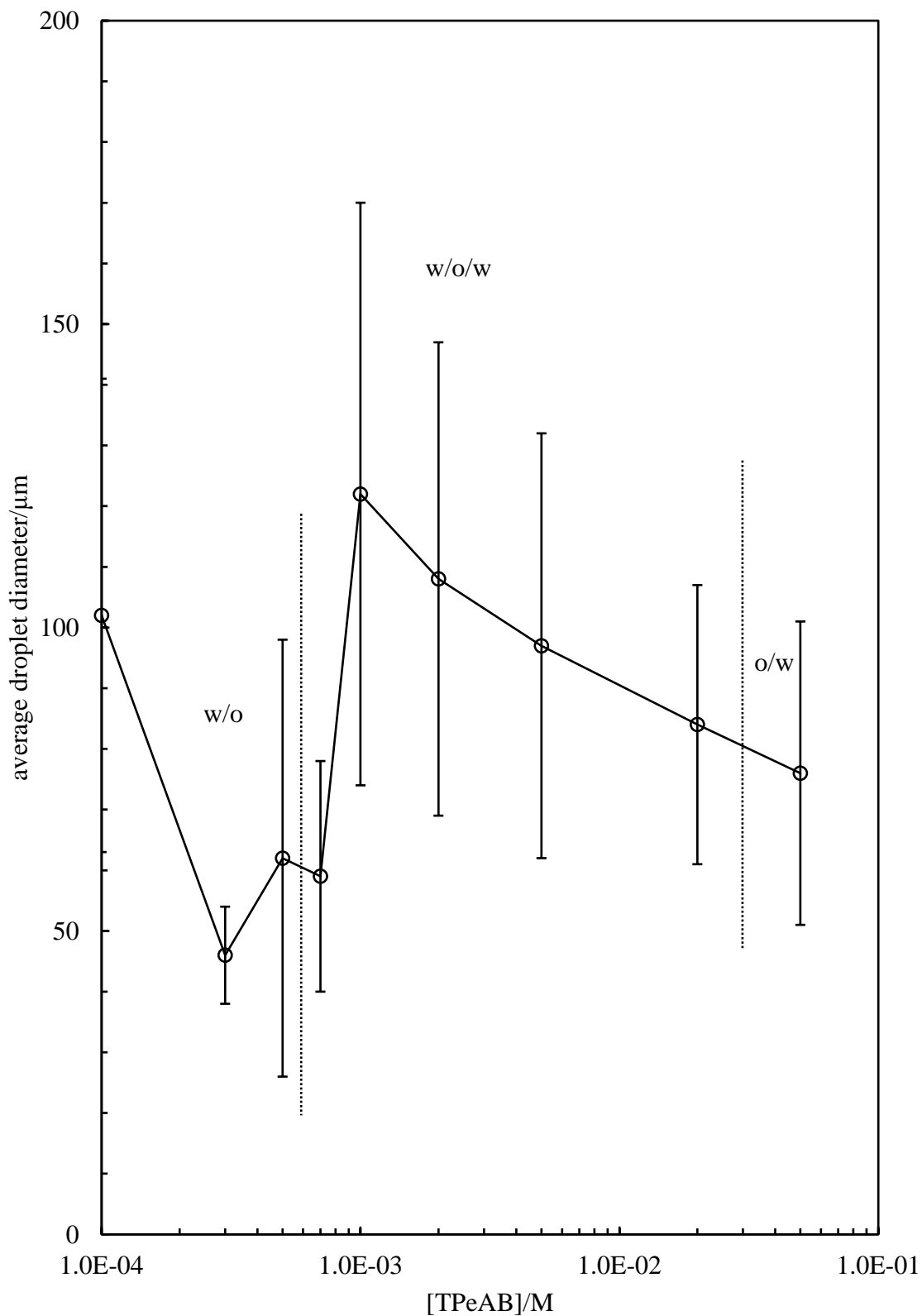
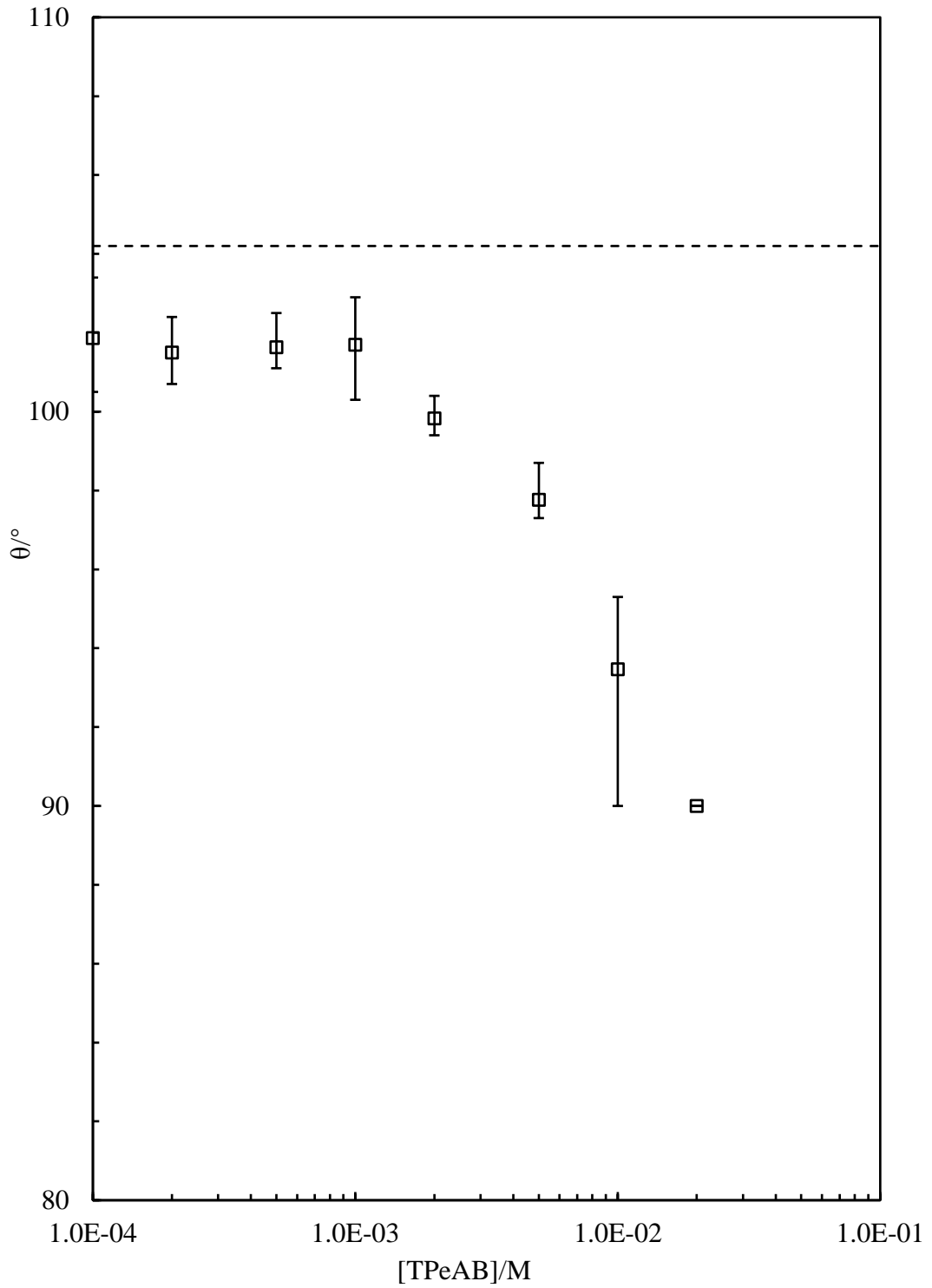


**Figure 4.32.** Average droplet diameter and type of water-PDMS (50 cS) emulsions (1:1 by volume) stabilized by 2 wt.% carboxyl PS latex particles ( $d = 0.2 \mu\text{m}$ ) against [TPeAB] at pH 11, calculated from the microscopy images of emulsion droplets using Image J.



The formation of multiple emulsions typically requires two different surfactants or two types of solid particles (with different hydrophobicities) to stabilize the oil-water interfaces of opposite curvature. There have been limited reports on multiple emulsion stabilized by a single type of solid particles.<sup>43,44</sup> Binks and Whitby reported multiple w/o/w emulsions stabilized by hydrophobic silica particles and PDMS oil at  $\phi_o = 0.5$  and  $0.6$ .<sup>43</sup> In this system, the formation of multiple emulsions was attributed to the high viscosity of PDMS oil, which is a mixture of silicone oils of different viscosity. The adsorption of PDMS onto silica surfaces vary the wettability of particles. Similar findings have been reported on systems with silica particles and triglyceride oil.<sup>44</sup> Emulsion formation can be seen simplistically as consisting of two processes: fragmentation of the bulk liquids and the resulting large drops and the possible coalescence of such drops. Multiple emulsion formation occurs as a result of the coalescence of drops enclosing the continuous phase into drops of the dispersed phase. In the system with carboxyl latex particles and PDMS (50 cS), as the viscosity is high, the coalescence seems to dominate during the homogenization. By contrast, in the case of PDMS (1 cS), which is of lower viscosity, fragmentation dominates during emulsion formation. The contact angle of 3.5  $\mu\text{m}$  carboxyl latex particles at PDMS (50 cS)-water interfaces is plotted against TPeAB at pH 11 in Figure 4.33. The  $\theta$  of particle at PDMS (50 cS)-water (without salt) interface is  $\sim 104^\circ$ . The increase of salt concentration results in a continuous decrease of  $\theta$  until  $90^\circ$ , nearly the same as that of particles at low viscosity. It indicates that the polarities of PDMS of 1 cS and 50 cS are very close to each other. The w/o emulsions formed at low salt concentrations ( $\leq 5 \times 10^{-4}$  M) follow the Bancroft rule. However, water-continuous emulsions at higher salt concentrations are anti-Bancroft type as contact angles of particles are still above  $90^\circ$ .

**Figure 4.33.** Three-phase contact angles ( $\theta$ ) of carboxyl latex particles ( $d = 3.5 \mu\text{m}$ ) at the PDMS (50 cS)-water interface against [TPeAB]. Dashed line indicates the contact angle of particles at the PDMS (50 cS)-water interface without salt.



## 4.4 Systems with amidine latex particles

### 4.4.1 Aqueous dispersion of amidine latex particles

Batches of amidine ( $\text{C}(\text{NH})\text{NH}_2$ ) PS latex dispersions in sodium thiocyanate (NaSCN) solutions were prepared at pH 4, particles are positively charged due to the ionization of amidine groups. Figure 4.34 (a) shows the appearance of particle dispersions, in which particles are discrete until  $5 \times 10^{-2}$  M of NaSCN was added. The average particle diameter is represented in Figure 4.35 (a). Large particle aggregates were observed under optical microscope, as shown in Figure 4.35 (b). The zeta potential of 0.0004 wt.% amidine PS latex particles in water is +45 mV (Figure 4.34 (b)), whereas a maximum was observed in KCl, consistent with the standard electrokinetic model proposed by O'Brien and White.<sup>45-47</sup> Addition of  $1 \times 10^{-5}$  M NaSCN dramatically decreases the zeta potential to +30 mV, increase of salt concentration keeps it at a constant value before a sharp decrease occurs after  $3 \times 10^{-4}$  M. Charge reversal was observed between  $5 \times 10^{-4}$  M and  $1 \times 10^{-3}$  M of NaSCN. Similar charge reversal of PS latex particles with amine groups on the surface induced by  $\text{SCN}^-$  ions has been reported before.<sup>8,17</sup> Ion-specific effects was widely accepted as the explanation for this phenomenon. Kosmotropic ions such as  $\text{Cl}^-$  can hardly induce charge reversal because they are highly hydrated and do not adsorb at particle surfaces, whereas chaotropic  $\text{SCN}^-$  ions are poorly hydrated and can interact strongly with the hydrophobic amidine PS particle surfaces and even induce charge reversal.<sup>13</sup> In a recent report, Calero and Faraudo<sup>8</sup> argued that the hydrophobic effect is the driving force for charge reversal of particles induced by monovalent ions, as they found that charge reversal occurs on the condition that both counterions and particle surface are poorly hydrated, which also consistent with our results. It is worth to note that amidine particles do not aggregate until  $5 \times 10^{-2}$  M of NaSCN, far above the IEP of the particles. This should also due to specific adsorption of  $\text{SCN}^-$  ions. Short range repulsive force derives from particles surrounded by  $\text{SCN}^-$  ions and hinders the aggregation of particles. Reversible aggregation of amidine latex particles in NaSCN solutions has been observed, where clusters with 2.45 particles on average were detected in 0.6 M NaSCN.<sup>48</sup>

**Figure 4.34.** (a) Appearance of 2 wt.% amidine PS latex particle ( $d = 0.2 \mu\text{m}$ ) dispersions in varied concentrations of NaSCN at pH 4, taken immediately after preparation. (b) Zeta potential of 0.0004 wt.% amidine PS latex particles in NaSCN or KCl at pH 4.

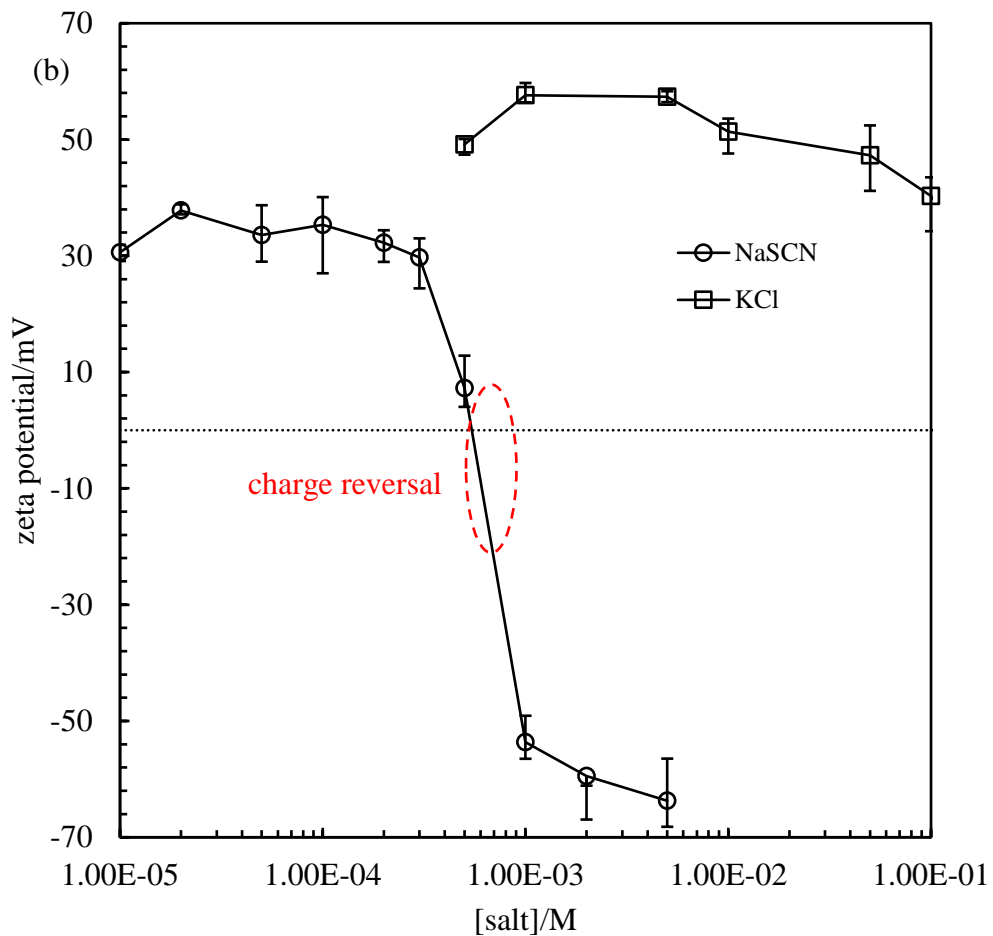
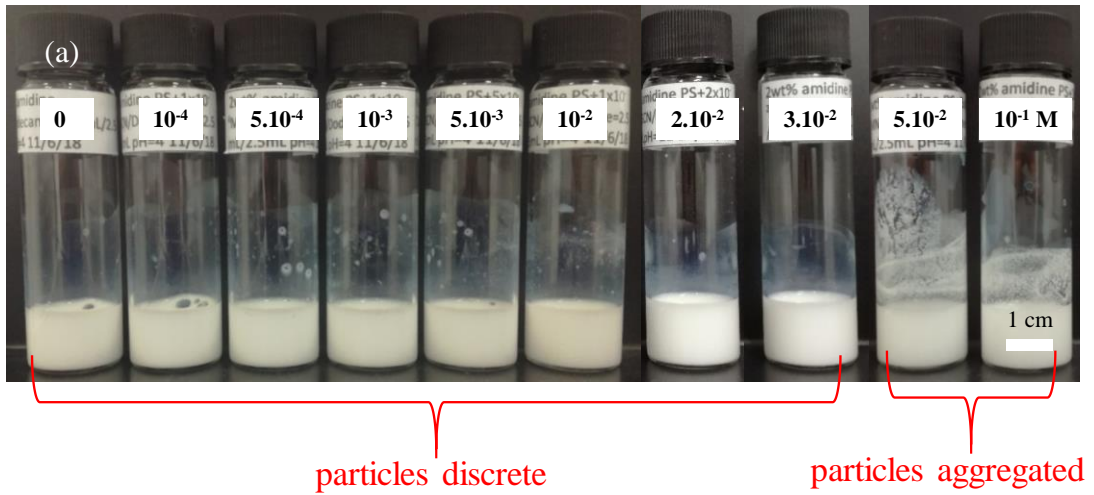
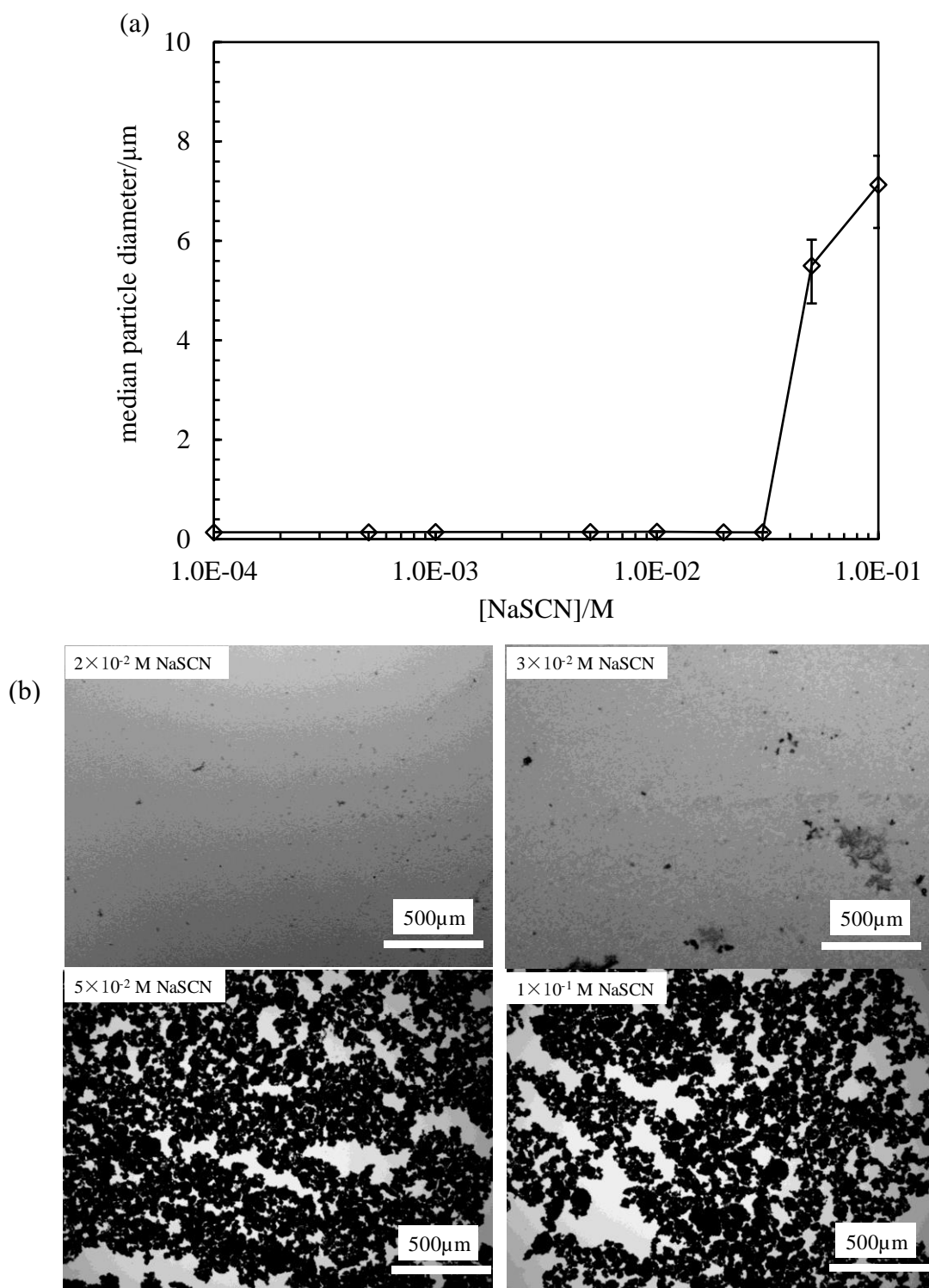


**Figure 4.35.** (a) Average diameter of amidine PS latex particles (quoted  $d = 0.2 \mu\text{m}$ ) against  $[\text{NaSCN}]$  at pH 4. (b) Selected optical microscopy images of amidine PS latex particles in NaSCN solutions.



#### 4.4.2 Emulsions with dodecane as the oil phase

The appearance of emulsions stabilised by 2 wt.% amidine latex particles is shown in Figure 4.36 (a) and all w/o emulsions were determined from conductivity measurement (Figure 4.36 (b)). Polystyrene particles with grafted copolymer molecules containing amine groups were reported to stabilise o/w emulsions as the particles were rendered more hydrophilic.<sup>49</sup> Apparently, amidine latex particles here are not hydrophilic enough, may be due to lower density of amidine groups on particle surfaces. The emulsions are stable to coalescence but partially unstable to sedimentation,  $f_o$  of the emulsions decreases with salt concentration, meaning that stability of emulsions to sedimentation increases with increasing NaSCN concentrations (see Figure 4.37). It appears that charge screen or hydrophobic interactions promotes the adsorption of particles onto oil-water interfaces and enhances the stability of emulsions. However, charge reversal or the aggregation of particles hardly induces any special effect in the stability of emulsions. Figure 4.38 shows the optical microscopy images of emulsions and the plot of the average droplet diameter. Very large spherical droplets were observed in the emulsion without salt, addition of NaSCN decreases the droplet size. Non-spherical droplets were observed along with spherical droplets.

**Figure 4.36.** (a) Appearance of water-in-dodecane emulsions (1:1 by volume) stabilized by 2 wt.% amidine PS latex particles ( $d = 0.2 \mu\text{m}$ ) in varied concentrations of NaSCN at pH 4, taken one week after preparation. (b) Conductivity of emulsions in (a), measured immediately after homogenization. Dashed line represents the conductivity of an emulsion stabilized by amidine latex particles alone (no salt).

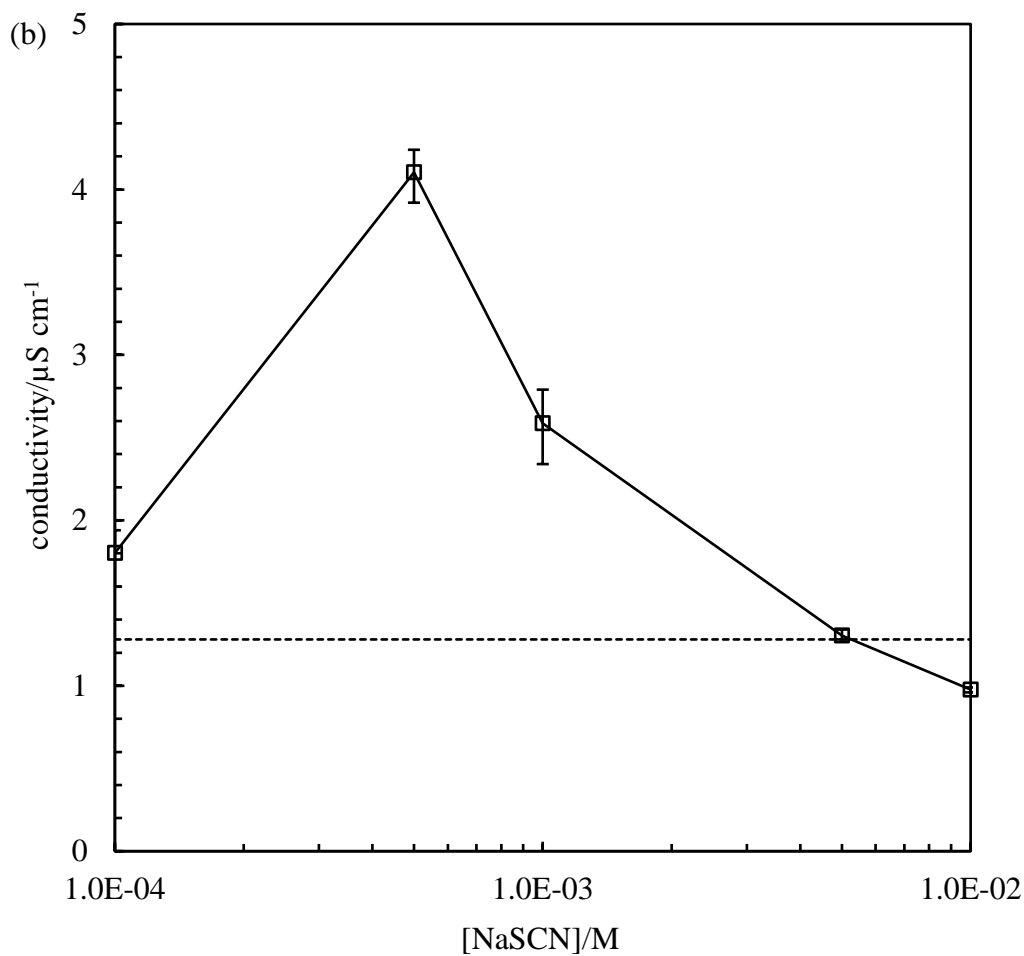
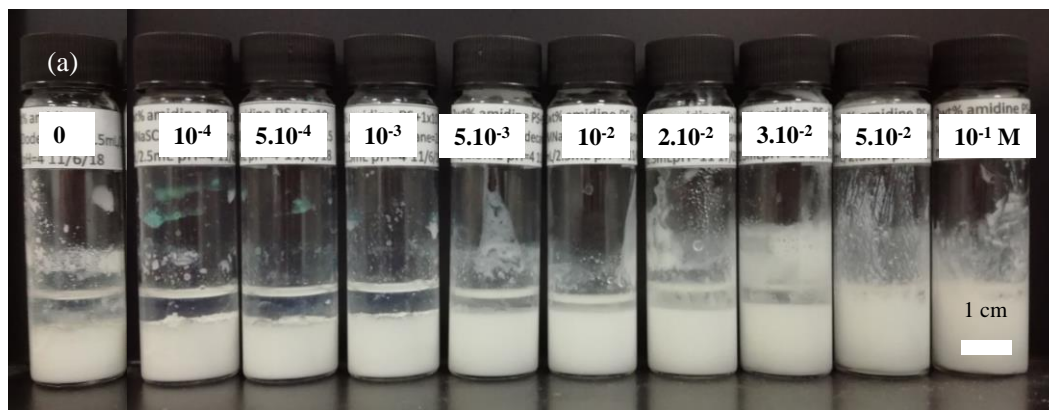


**Figure 4.37.** The stability to sedimentation ( $f_o$ ) and coalescence ( $f_w$ ) of water-in-dodecane emulsions (1:1 by volume) stabilized by 2 wt.% amidine PS latex particles ( $d = 0.2 \mu\text{m}$ ) against [NaSCN] at pH 4, measured one week after preparation. Dashed line indicates  $f_o$  of emulsion prepared by amidine PS latex particles alone (no salt),  $f_w$  of emulsions keeps at zero at all concentrations.

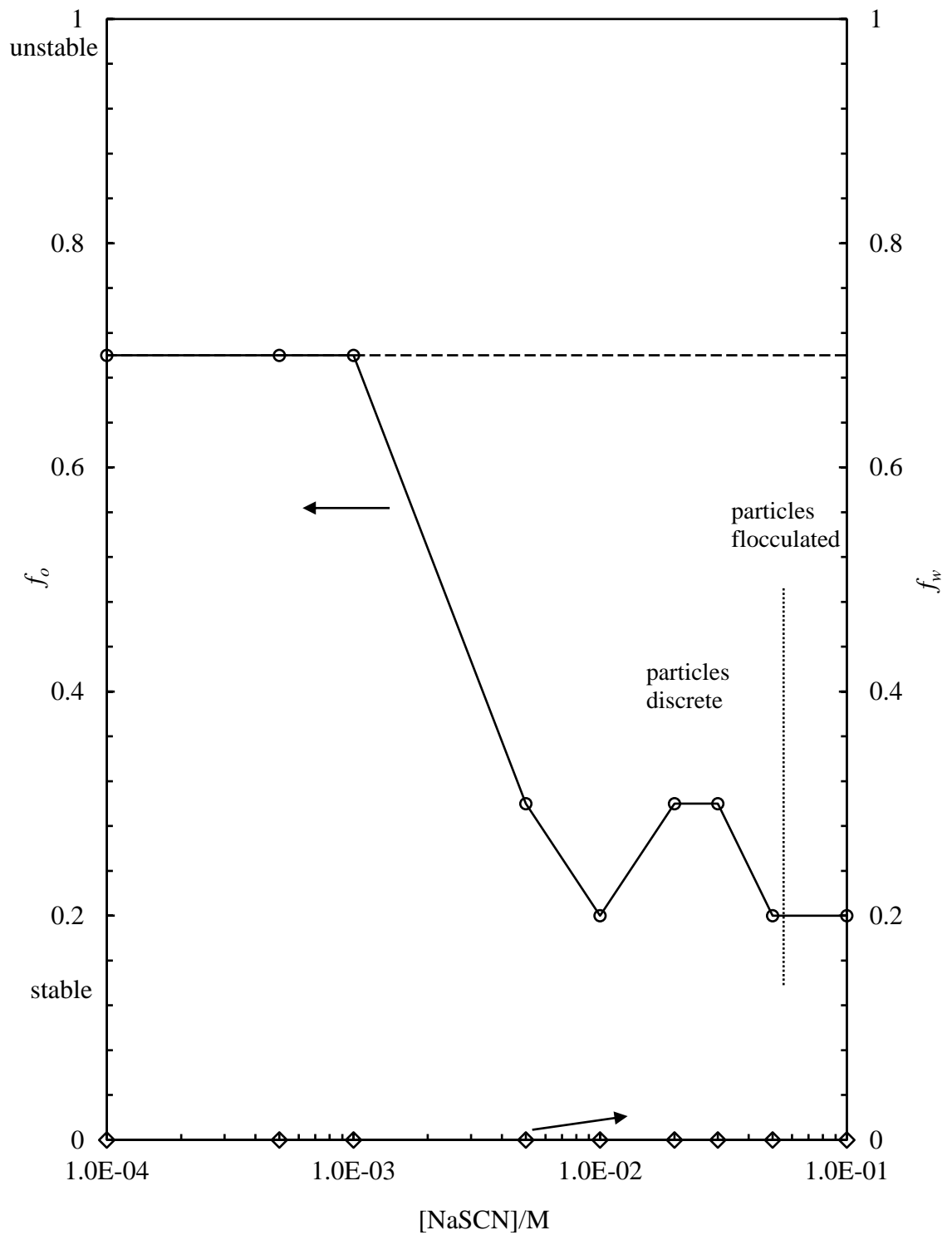


**Figure 4.38.** (a) Selected optical microscopy images of water-in-dodecane emulsions (1:1 by volume) stabilized by 2 wt.% amidine PS latex particles ( $d = 0.2 \mu\text{m}$ ) in NaSCN at pH 4, taken 24 hours after preparation. (b) Average droplet diameter of emulsions.

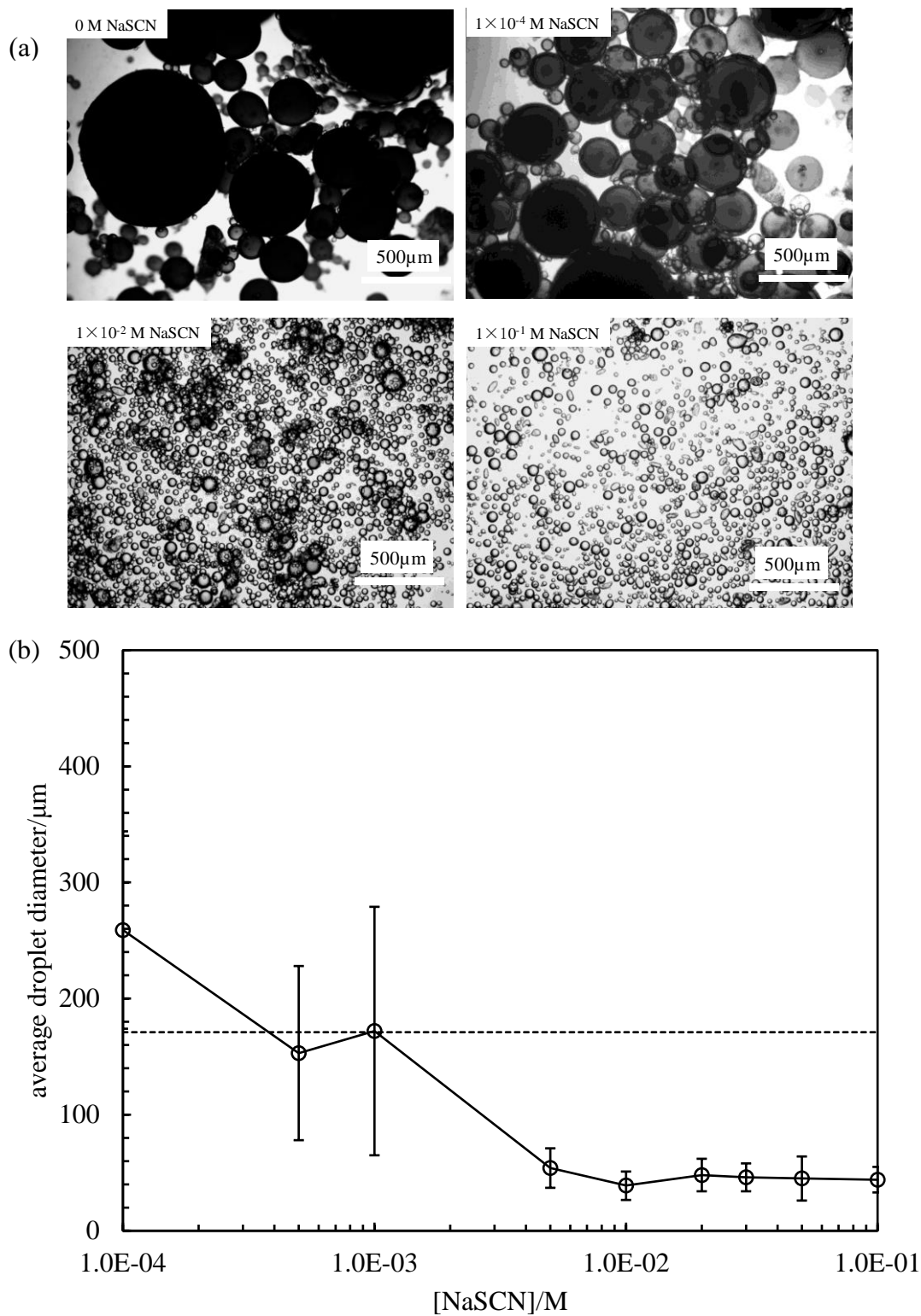
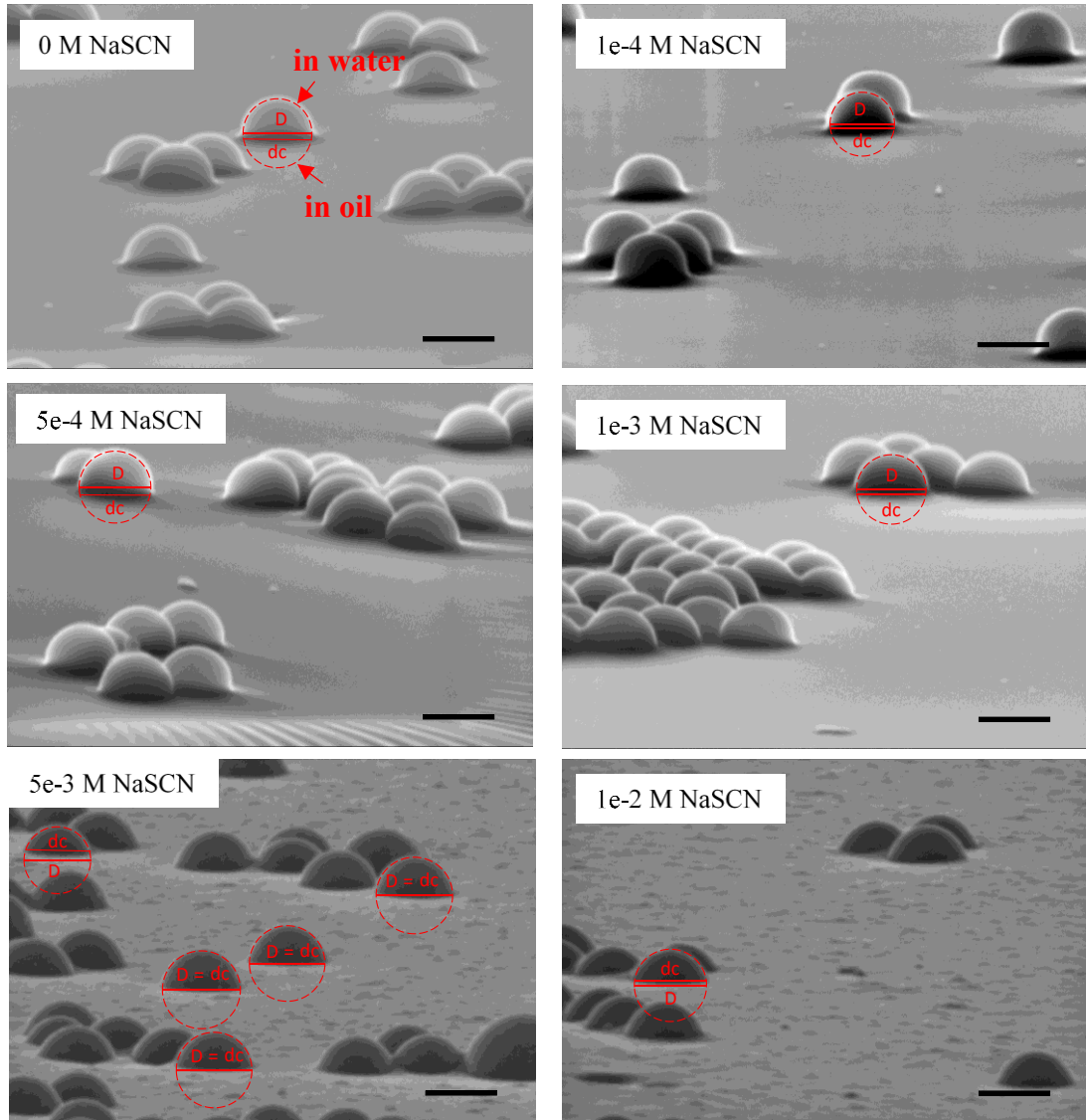
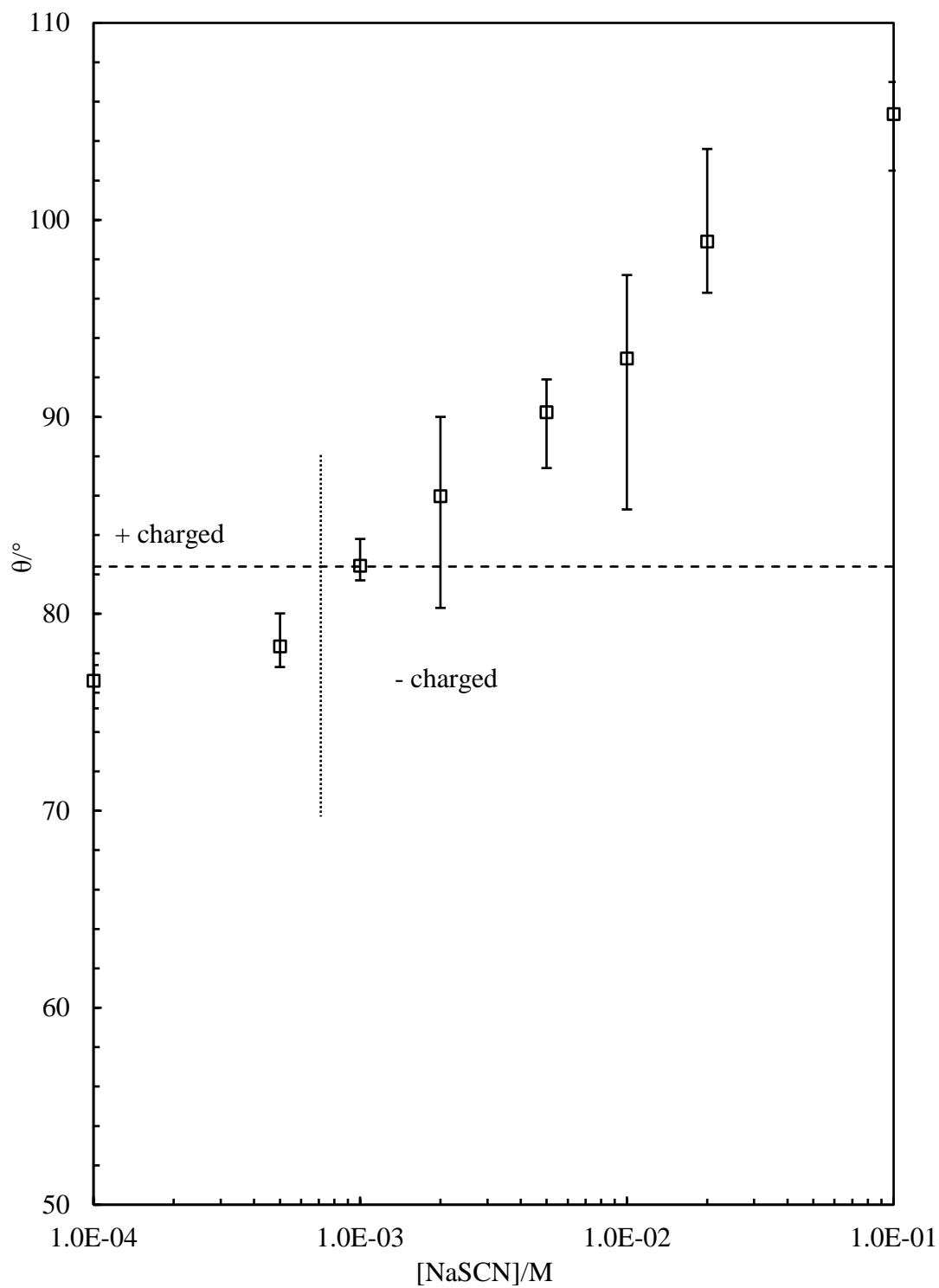


Figure 4.39 shows SEM micrographs of 1  $\mu\text{m}$  amidine latex particles gel-trapped and micro-cast with Sylgard PDMS at the dodecane-water interface at pH 4. The calculated three-phase contact angle is plotted in Figure 4.40. A value of  $82^\circ$  is obtained for the particles without salt, while a slight decrease is obtained upon addition of  $1 \times 10^{-4}$  M NaSCN. Subsequent increase of salt concentration results in a gradual increase of  $\theta$  to  $105^\circ$ . It is reasonable that due to ion specificity,  $\text{SCN}^-$  ions accumulation on amidine latex particles breaks the water structure around particles,<sup>15</sup> which results in the decrease of  $\theta$ . Increase of  $\text{SCN}^-$  concentration increases the  $\theta$  because poorly hydrated ions replace the water molecules around particles. A schematic of possible arrangement of  $\text{SCN}^-$  ions on the surface of amidine latex particles is shown in Figure 4.41. The contact angle results indicate that the particles should preferentially stabilize o/w emulsions at low salt concentrations ( $< 5 \times 10^{-3}$  M) where contact angles are below  $90^\circ$  and w/o emulsions at higher salt concentrations. However, as shown above, w/o emulsions were obtained at all salt concentrations. Emulsions at low salt concentrations ( $< 5 \times 10^{-3}$  M) are anti-Bancroft type while at high salt concentrations follow the Bancroft rule. One reason these angles cannot be completely linked to emulsions is they refer to planar interfaces not curved ones. Also, slight differences in angle may exist between large (for contact angle measurements) and small (for emulsion stabilization) particles. In addition, when angles get close to  $90^\circ$ , the difference between the particle contact line diameter ( $d_c$ ) and the particle equatorial diameter ( $D$ ) is extremely small, while small numerical difference would result in dramatic difference when it converted to angle, which might result in larger errors of results.

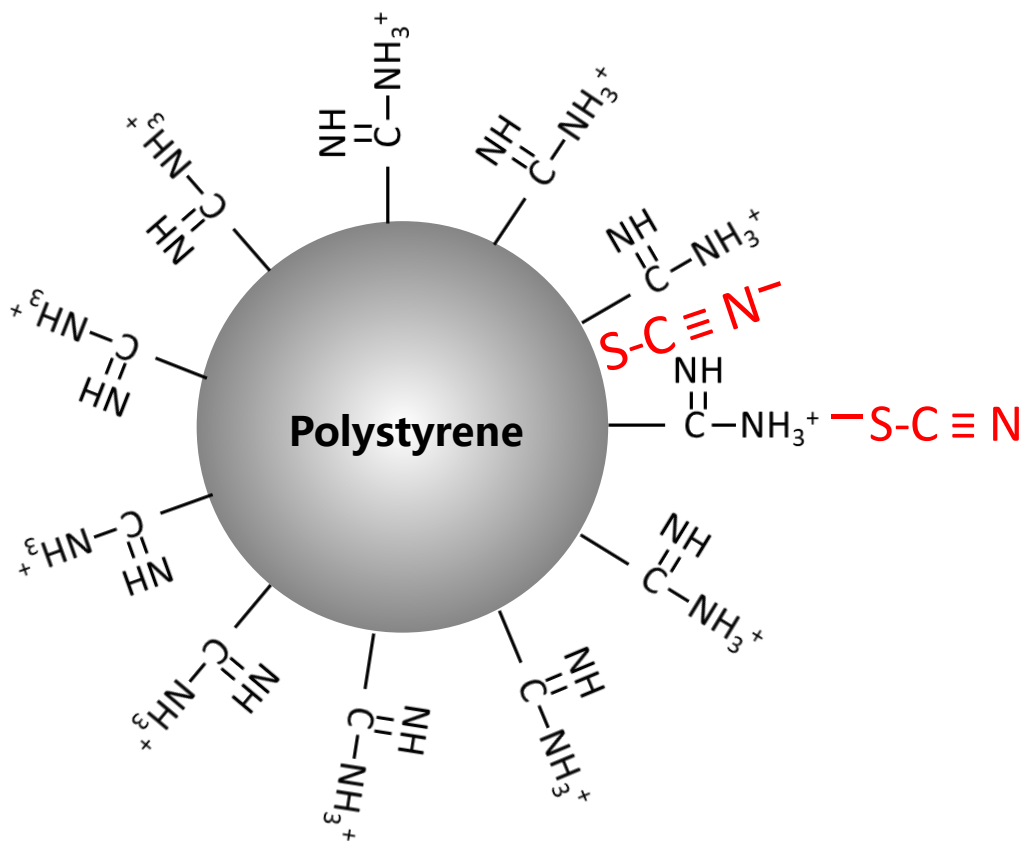
**Figure 4.39.** SEM of monolayers of monodispersed amidine latex particles ( $d = 1 \mu\text{m}$ ) on the surface of Sylgard PDMS obtained by GTT at the dodecane-water interface in the presence of NaSCN. The observation angle  $\delta = 80^\circ$ . Scale bar =  $1 \mu\text{m}$ .



**Figure 4.40.** Three-phase contact angles ( $\theta$ ) of monodispersed amidine latex particles ( $d = 1 \mu\text{m}$ ) at the dodecane-water interface in the presence of NaSCN, horizontal dashed line indicates the contact angle of particles at the dodecane-water interface without salt.



**Figure 4.41.** Schematic of possible adsorption of  $\text{SCN}^-$  ions onto amidine latex particle surface.



#### 4.5 Conclusions

Pickering emulsions stabilized by polystyrene latex particles with different surface groups (sulfate, amidine and carboxyl) in the presence of specific electrolytes have been investigated. The particles used are partially hydrophobic but initially dispersed in water due to their surface charges. The presence of TPeAB in aqueous dispersions of sulfate and carboxyl latex particles reduces the surface charge of particles even induces charge reversal of sulfate latex particles. However, the type of emulsion with non-polar oils such as dodecane and heptane stabilized by these particles is dominated by the hydrophobic polystyrene part on the particles. Consequently, w/o emulsions are preferentially stabilized by these particles. In contrast, surface charge seems to play a minor role in determining the emulsion type. The adsorption of  $\text{TPeA}^+$  ions slightly decreases the hydrophobicity of particles, which

increases the stability of emulsions to both coalescence and sedimentation. Whereas charge reversal induces little specific influence on the stability or type of emulsions.

An intriguing phenomenon on systems with carboxyl latex particles is that, when PDMS (1 cS or 50 cS) is used as the oil phases, emulsions invert from w/o to o/w as the salt concentration increases. In addition, w/o/w double emulsions are observed at moderate salt concentrations with 50 cS PDMS as the oil phase. The three-phase contact angle of particles at PDMS (1 cS)-water or PDMS (50 cS)-water interfaces at pH 11 consistently decreases from  $\sim 105^\circ$  to  $90^\circ$  with the increase of salt concentrations. It seems that a slight increase in the polarity of oil results in dramatic influence on the properties of emulsions stabilized by carboxyl latex particles. However, this requires further confirmation. For future experiments, even more polar oils are suggested for the preparation of emulsions.

For systems with amidine PS latex, addition of NaSCN between  $5 \times 10^{-4}$  M and  $1 \times 10^{-3}$  M in the aqueous dispersion leads to charge reversal of particles. However, the particles do not aggregate until  $5 \times 10^{-2}$  M of NaSCN. Adsorption of  $\text{SCN}^-$  ions onto amidine latex particles is possibly due to ion specific effect. Poorly hydrated  $\text{SCN}^-$  ions break the structure of water around particles and even increase the surface hydrophobicity of particles. Emulsions of dodecane stabilized by amidine PS particles are all w/o, although the contact angle of particles at dodecane-water interfaces is lower than  $90^\circ$  at low salt concentrations. Again, charge reversal of particles shows little influence on the properties of emulsions.

The Bancroft rule states that colloids dispersed in the aqueous phase preferentially stabilize o/w emulsions while those dispersed in the oil phase usually give w/o emulsions. This rule works well in predicting the type of macro-emulsions stabilized by surfactants. Surfactants soluble in water stabilize o/w emulsions and those soluble in oil result in w/o emulsions. If we straightly apply the Bancroft rule to Pickering emulsions, it implies that particles initially dispersed in water should give o/w emulsions. In this manner, the w/o emulsions stabilized by polystyrene particles in this chapter are anti-Bancroft type as these particles are initially dispersed in water. However, the Bancroft rule could also be interpreted according to the hydrophobicity of particles, *i.e.*, the preferential wettability of particle by the aqueous phase or the oil

phase. In this case, this rule should predict that hydrophilic particles stabilize o/w emulsions and hydrophobic particles stabilize w/o emulsions. As a result, the w/o emulsions stabilized by hydrophobic polystyrene particles are consistent with the Bancroft rule. Based on the discussion above, the Bancroft rule might be not suitable to describe Pickering emulsions.

#### 4.6 References

1. Midmore, B. and Hunter, R. The effect of electrolyte concentration and co-ion type on the  $\zeta$ -potential of polystyrene latices. *J. Colloid Interface Sci.* **1988**, *122*, 521-529.
2. Derjaguin, B. and Landau, L. Stability theory of strongly charged lyophobic sols and of the adhesion of strongly charged particles in electrolyte solutions. *Acta Phys. Chim.* **1941**, *14*, 633-662.
3. Verwey, E. and Overbeek, J.T.G. Theory of the stability of lyophobic colloids. Elsevier, Amsterdam, **1948**.
4. Van den Hoven, T.J. and Bijsterbosch, B. Streaming currents, streaming potentials and conductances of concentrated dispersions of negatively-charged, monodisperse polystyrene particles. Effect of adsorbed tetraalkylammonium ions. *Colloids Surf.* **1987**, *22*, 171-185.
5. Yu, W.; Bouyer, F. and Borkovec, M. Polystyrene sulfate latex particles in the presence of poly (vinylamine): absolute aggregation rate constants and charging behavior. *J. Colloid Interface Sci.* **2001**, *241*, 392-399.
6. Lin, W.; Galletto, P. and Borkovec, M. Charging and aggregation of latex particles by oppositely charged dendrimers. *Langmuir* **2004**, *20*, 7465-7473.
7. Martín-Molina, A.; Calero, C.; Faraudo, J.; Quesada-Pérez, M.; Travesset, A. and Hidalgo-Álvarez, R. The hydrophobic effect as a driving force for charge inversion in colloids. *Soft Matter* **2009**, *5*, 1350-1353.
8. Calero, C.; Faraudo, J. and Bastos-González, D. Interaction of monovalent ions with hydrophobic and hydrophilic colloids: Charge inversion and ionic specificity. *J. Am. Chem. Soc.* **2011**, *133*, 15025-15035.
9. Sadeghpour, A.; Szilágyi, I. and Borkovec, M. Charging and aggregation of positively charged colloidal latex particles in presence of multivalent polycarboxylate anions. *Z. Phys. Chem.* **2012**, *226*, 597-612.

10. Sugimoto, T.; Nishiya, M. and Kobayashi, M. Electrophoretic mobility of carboxyl latex particles: effects of hydrophobic monovalent counter-ions. *Colloid Polym. Sci.* **2017**, *295*, 2405-2411.
11. Smith, A.M.; Maroni, P. and Borkovec, M. Attractive non-DLVO forces induced by adsorption of monovalent organic ions. *Phys. Chem. Chem. Phys.* **2018**, *20*, 158-164.
12. Szilagyi, I.; Sadeghpour, A. and Borkovec, M. Destabilization of colloidal suspensions by multivalent ions and polyelectrolytes: From screening to overcharging. *Langmuir* **2012**, *28*, 6211-6215.
13. Schneider, C.; Hanisch, M.; Wedel, B.; Jusufi, A. and Ballauff, M. Experimental study of electrostatically stabilized colloidal particles: Colloidal stability and charge reversal. *J. Colloid Interface Sci.* **2011**, *358*, 62-67.
14. López-León, T.; Ortega-Vinuesa, J.L. and Bastos-González, D. Ion-specific aggregation of hydrophobic particles. *ChemPhysChem* **2012**, *13*, 2382-2391.
15. López-León, T.; Jódar-Reyes, A.B.; Bastos-González, D. and Ortega-Vinuesa, J.L. Hofmeister effects in the stability and electrophoretic mobility of polystyrene latex particles. *J. Phys. Chem. B* **2003**, *107*, 5696-5708.
16. Schwierz, N.; Horinek, D. and Netz, R.R. Anionic and cationic Hofmeister effects on hydrophobic and hydrophilic surfaces. *Langmuir* **2013**, *29*, 2602-2614.
17. Oncsik, T.; Trefalt, G.; Borkovec, M. and Szilagyi, I. Specific ion effects on particle aggregation induced by monovalent salts within the Hofmeister series. *Langmuir* **2015**, *31*, 3799-3807.
18. Binks, B.P. and Rodrigues, J.A. Double inversion of emulsions by using nanoparticles and a di-chain surfactant. *Angew. Chem. Int. Ed.* **2007**, *46*, 5389-5392.
19. Cui, Z.G.; Yang, L.L.; Cui, Y.Z. and Binks, B.P. Effects of surfactant structure on the phase inversion of emulsions stabilized by mixtures of silica nanoparticles and cationic surfactant. *Langmuir* **2010**, *26*, 4717-4724.
20. Onoda, G.Y. Direct observation of two-dimensional, dynamic clustering and ordering with colloids. *Phys. Rev. Lett.* **1985**, *55*, 226-229.
21. Ghezzi, F. and Earnshaw, J. Formation of meso-structures in colloidal monolayers. *J. Phys.: Condens. Matter* **1997**, *9*, L517-L523.

22. Aveyard, R.; Clint, J.H.; Nees, D. and Paunov, V.N. Compression and structure of monolayers of charged latex particles at air/water and octane/water interfaces. *Langmuir* **2000**, *16*, 1969-1979.
23. Al-Shehri, H.; Horozov, T.S. and Paunov, V.N. Adsorption of carboxylic modified latex particles at liquid interfaces studied by the gel trapping technique. *Soft Matter* **2014**, *10*, 6433-6441.
24. Binks, B. and Lumsdon, S. Pickering emulsions stabilized by monodisperse latex particles: effects of particle size. *Langmuir* **2001**, *17*, 4540-4547.
25. Golemanov, K.; Tcholakova, S.; Kralchevsky, P.; Ananthapadmanabhan, K. and Lips, A. Latex-particle-stabilized emulsions of anti-Bancroft type. *Langmuir* **2006**, *22*, 4968-4977.
26. Tarimala, S. and Dai, L.L. Structure of microparticles in solid-stabilized emulsions. *Langmuir* **2004**, *20*, 3492-3494.
27. Tarimala, S.; Ranabothu, S.R.; Vernetti, J.P. and Dai, L.L. Mobility and in situ aggregation of charged microparticles at oil-water interfaces. *Langmuir* **2004**, *20*, 5171-5173.
28. Binks, B.P. and Rodrigues, J.A. Inversion of emulsions stabilized solely by ionizable nanoparticles. *Angew. Chem. Int. Ed.* **2005**, *117*, 445-448.
29. Nallamilli, T.; Mani, E. and Basavaraj, M.G. A Model for the prediction of droplet size in Pickering emulsions stabilized by oppositely charged particles. *Langmuir* **2014**, *30*, 9336-9345.
30. Nallamilli, T.; Binks, B.P.; Mani, E. and Basavaraj, M.G. Stabilization of Pickering emulsions with oppositely charged latex particles: influence of various parameters and particle arrangement around droplets. *Langmuir* **2015**, *31*, 11200-11208.
31. Bancroft, W.D. The theory of emulsification, V. *J. Phys. Chem.* **1913**, *17*, 501-519.
32. Toews, K.L.; Shroll, R.M.; Wai, C.M. and Smart, N.G. pH-defining equilibrium between water and supercritical CO<sub>2</sub>. Influence on SFE of organics and metal chelates. *Anal. Chem.* **1995**, *67*, 4040-4043.
33. Peng, C.; Crawshaw, J.P.; Maitland, G.C.; Trusler, J.M. and Vega-Maza, D. The pH of CO<sub>2</sub>-saturated water at temperatures between 308 K and 423 K at pressures up to 15 MPa. *J. Supercrit. Fluids* **2013**, *82*, 129-137.

34. Elimelech, M. and O'Melia, C.R. Effect of electrolyte type on the electrophoretic mobility of polystyrene latex colloids. *Colloids Surf.* **1990**, *44*, 165-178.
35. Tuin, G.; Senders, J. and Stein, H. Electrophoretic properties of monodisperse polystyrene particles. *J. Colloid Interface Sci.* **1996**, *179*, 522-531.
36. Tamaki, K. The surface activity of tetra-n-alkylammonium halides in aqueous solutions. The effect of hydrophobic hydration. *Bull. Chem. Soc. Jpn.* **1974**, *47*, 2764-2767.
37. Dopierala, K. and Prochaska, K. The effect of molecular structure on the surface properties of selected quaternary ammonium salts. *J. Colloid Interface Sci.* **2008**, *321*, 220-226.
38. Maestro, A.; Bonales, L.; Ritacco, H.; Rubio, R. and Ortega, F. Effect of the spreading solvent on the three-phase contact angle of microparticles attached at fluid interfaces. *Phys. Chem. Chem. Phys.* **2010**, *12*, 14115-14120.
39. Behrens, S.H.; Christl, D.I.; Emmerzael, R.; Schurtenberger, P. and Borkovec, M. Charging and aggregation properties of carboxyl latex particles: Experiments versus DLVO theory. *Langmuir* **2000**, *16*, 2566-2575.
40. Kasprzak M., Wilde P., Hill S.E., Harding S.E., Ford R. and Wolf B. Non-chemically modified waxy rice starch stabilised w/o emulsions for salt reduction. *Food Funct.* **2019**, *10*, 4242-4255.
41. Po, H.N. and Senozan, N. The Henderson-Hasselbalch equation: its history and limitations. *J. Chem. Ed.* **2001**, *78*, 1499-1503.
42. Binks, B.P. and Lumsdon, S. Catastrophic phase inversion of water-in-oil emulsions stabilized by hydrophobic silica. *Langmuir* **2000**, *16*, 2539-2547.
43. Binks, B.P. and Whitby, C.P. Silica particle-stabilized emulsions of silicone oil and water: aspects of emulsification. *Langmuir* **2004**, *20*, 1130-1137.
44. Binks, B.P. and Rodrigues, J. Types of phase inversion of silica particle stabilized emulsions containing triglyceride oil. *Langmuir* **2003**, *19*, 4905-4912.
45. Alvarez, R.H.; De las Nieves, F. and Bijsterbosch, B. Electrokinetic studies on positively charged polystyrene latices. *Colloids Surf.* **1986**, *21*, 259-266.
46. Borkovec, M.; Behrens, S.H. and Semmler, M. Observation of the mobility maximum predicted by the standard electrokinetic model for highly charged amidine latex particles. *Langmuir* **2000**, *16*, 5209-5212.

47. O'Brien, R.W. and White, L.R. Electrophoretic mobility of a spherical colloidal particle. *J. Chem. Soc. Far. Trans. II* **1978**, 74, 1607-1626.
48. López-León, T.; López-López, J.M.; Odriozola, G.; Bastos-González, D. and Ortega-Vinuesa, J.L. Ion-induced reversibility in the aggregation of hydrophobic colloids. *Soft Matter* **2010**, 6, 1114-1116.
49. Amalvy, J.I.; Armes, S.P.; Binks, B.P.; Rodrigues, J.A. and Unali, G.F. Use of sterically-stabilised polystyrene latex particles as a pH-responsive particulate emulsifier to prepare surfactant-free oil-in-water emulsions. *Chem. Comm.* **2003**, 1826-1827.

## CHAPTER 5

### DESTABILISATION OF PICKERING EMULSIONS BY SOLID PARTICLES

#### 5.1 Introduction

Pickering emulsions are ultra-stable to coalescence due to the adsorption of solid particles at the droplet surfaces providing steric barrier for droplets.<sup>1</sup> However, in some industrial processes such as oil recovery and mineral processing, the destabilization of Pickering emulsions is required.<sup>2,3</sup> The outstanding stability of Pickering emulsions makes the destabilization process difficult. Stimulus-responsive particles have been designed to render emulsions they form stable or unstable on demand.<sup>4</sup> However, these emulsions are either sensitive to pH changes<sup>5</sup> or requiring specific stimulus such as external electric field<sup>6</sup> or magnetic field<sup>7</sup>. Recently, Whitby and Wanless<sup>8</sup> reviewed the strategies used for the destabilization of general Pickering emulsions, including altering particle wettability, competitive displacement of particles at fluid interfaces, flocculating drops and particles, transferring mass between the liquid phases, inducing coalescence of droplets by shear or compressive stress. In addition, Whitby *et al.*<sup>9</sup> investigated the destabilization of o/w emulsions prepared by mixtures of titania particles and silica particles in the aqueous phase. The titania particles are partially hydrophobic and stabilized o/w emulsions, whereas the hydrophilic silica particles behaved as destabilizers by being entrapped in the titania particle layer around droplets. High silica concentrations result in coalescence of emulsions as they hinder the formation of the titania particle layers. Griffith and Daigle<sup>10</sup> destabilized o/w Pickering emulsions using hydrophobic fumed silica particles. They found that highly hydrophobic particles destabilize o/w Pickering emulsions, whereas completely hydrophilic or slightly hydrophobic particles are unable to coalesce the model emulsion. Using solid particles to destabilize Pickering emulsions is interesting as it overcomes the limitations of using surfactants which requires high speed shearing<sup>11</sup> or solvents which requires large volume.<sup>12,13</sup> However, there is a lack of systematical studies on factors affecting the destabilization efficiency of Pickering emulsions. In Griffith and Daigle's report, the most hydrophobic particles used have a contact angle of 75° at the toluene-water interface.<sup>10</sup> Further investigations

of the hydrophobicity of added particles and other factors on the destabilization efficiency should be conducted. In addition, the mechanism of solid particles breaking Pickering emulsions remains a mystery.

This chapter systematically investigated the destabilization of Pickering emulsions by adding solid particles. Firstly, the destabilization of water-in-oil (w/o) emulsions is described. Monodispersed silica particles of sub-micron size, hydrophilic silica particles of 2  $\mu\text{m}$  in diameter and fumed silica particles were employed as the destabilizers. The effects of particle size and concentration as well as particle hydrophobicity were studied. In systems containing 2  $\mu\text{m}$  silica particles, the mechanism of particles destabilizing Pickering emulsions was deduced. Secondly, the destabilization of oil-in-water (o/w) emulsions stabilized by fumed silica particles was studied. Monodispersed silica particles with a diameter of 0.3  $\mu\text{m}$ , Zonyl MP 1100 particles, OTFE particles and fumed silica particles were used as the destabilizers. The effects of particle hydrophobicity and concentration on the destabilization efficiency were studied.

## **5.2 Destabilization of water-in-oil emulsions stabilized by polystyrene latex particles**

### *5.2.1 The effect of stirring on emulsions*

Prior to the destabilization of emulsions, a model water-in-dodecane emulsion was prepared by homogenizing 2 wt.% carboxyl latex particles ( $d = 0.2 \mu\text{m}$ ) with dodecane at  $\phi_w = 0.5$  and pH 3. The appearance of the emulsion is shown in Figure 5.1 (a) and (b). As has been studied in section 4.3.4, the emulsion is stable to coalescence but partially unstable to sedimentation, nearly 30% of initial oil was extracted from the emulsion after 24 hours of quiescence. Before adding destabilizers to the emulsion, the effect of stirring on the stability of the emulsion was studied. The emulsion was rendered to stir at 300 rpm, photos of the of the emulsion and optical microscopy images of emulsion droplets were taken regularly during the stirring. Figure 5.1 (c) shows the appearance of the emulsion after different periods of stirring time. As can be seen, the oil extracted from the emulsion keeps at 30% of the initially added volume and no free water is observed, which indicates that the emulsion is macroscopically stable against stirring. Optical microscopy images of emulsion droplets after different

stirring time are shown in Figure 5.2. Without stirring, spherical and small droplets are observed. However, one hour of stirring results in formation of large and deformed droplets. Increase in the stirring time gives more large droplets. This is consistent with shear-induced coalescence of o/w Pickering emulsions reported by Whitby *et al.*<sup>14</sup>, where droplets increase in size, but no free oil was extracted in the first shearing stage. The main interactions between the particles are long-range electrical repulsion and van der Waals attraction. Carboxyl latex particles at pH 3 are protonated losing their surface charges, hence, the repulsion between droplets they stabilize is low and attraction dominates the interaction. In addition, it was reported that emulsion drops covered with friable layers of aggregated particles are less stable than those covered by compact layers of discrete particles under stress.<sup>15</sup> As will be shown in section 5.2.3.2 on the cryo-scanning electron microscopy (Cryo-SEM) image of the model emulsion, droplets are loosely packed by particles. Particle-free areas between particle clusters were observed around droplets. Thus, shearing such emulsion will presumably enhance the rate of coalescence. Figure 5.3 is a plot of average droplet diameter against stirring time. As can be seen, the droplet diameter increases gradually with stirring time and plateaus at 200  $\mu\text{m}$  after 3.5 hours.

**Figure 5.1.** Appearance of a water-in-dodecane emulsion ( $\phi_w = 0.5$ ) stabilized by 2 wt.% carboxyl PS latex particles ( $d = 0.2 \mu\text{m}$ ) at pH 3, taken (a) immediately, (b) 24 hours after homogenization and (c) immediately after stirring at 300 rpm for different time.

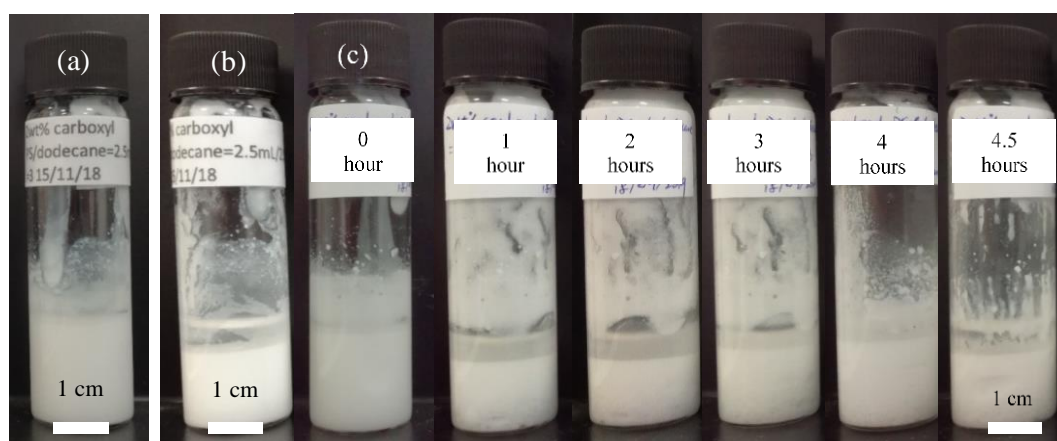


**Figure 5.2.** Selected optical microscopy of a water-in-dodecane emulsion ( $\phi_w = 0.5$ ) stabilized by 2 wt.% carboxyl PS latex particles ( $d = 0.2 \mu\text{m}$ ) at pH 3 after stirring at 300 rpm for different time (given). Taken immediately after stirring.

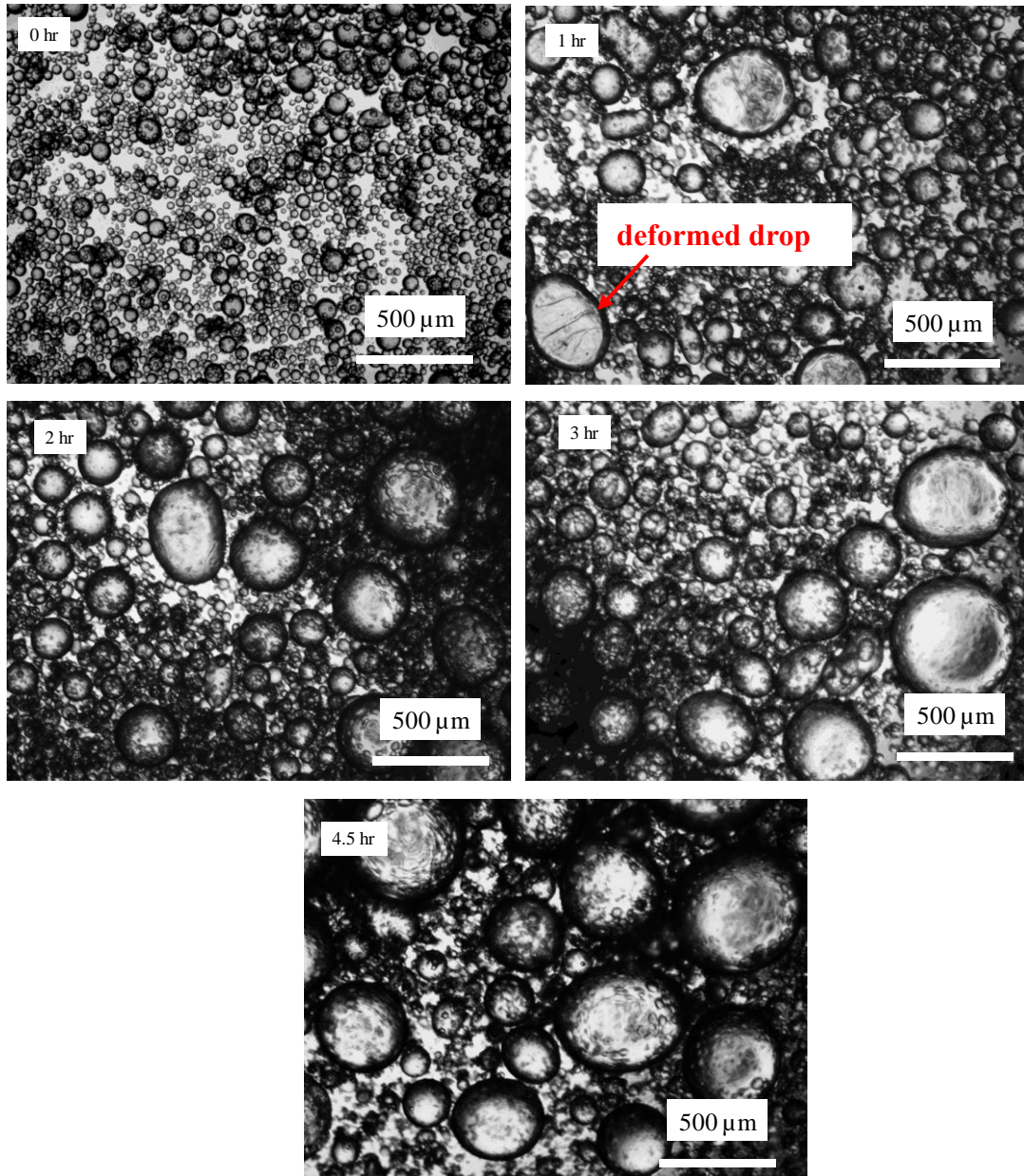
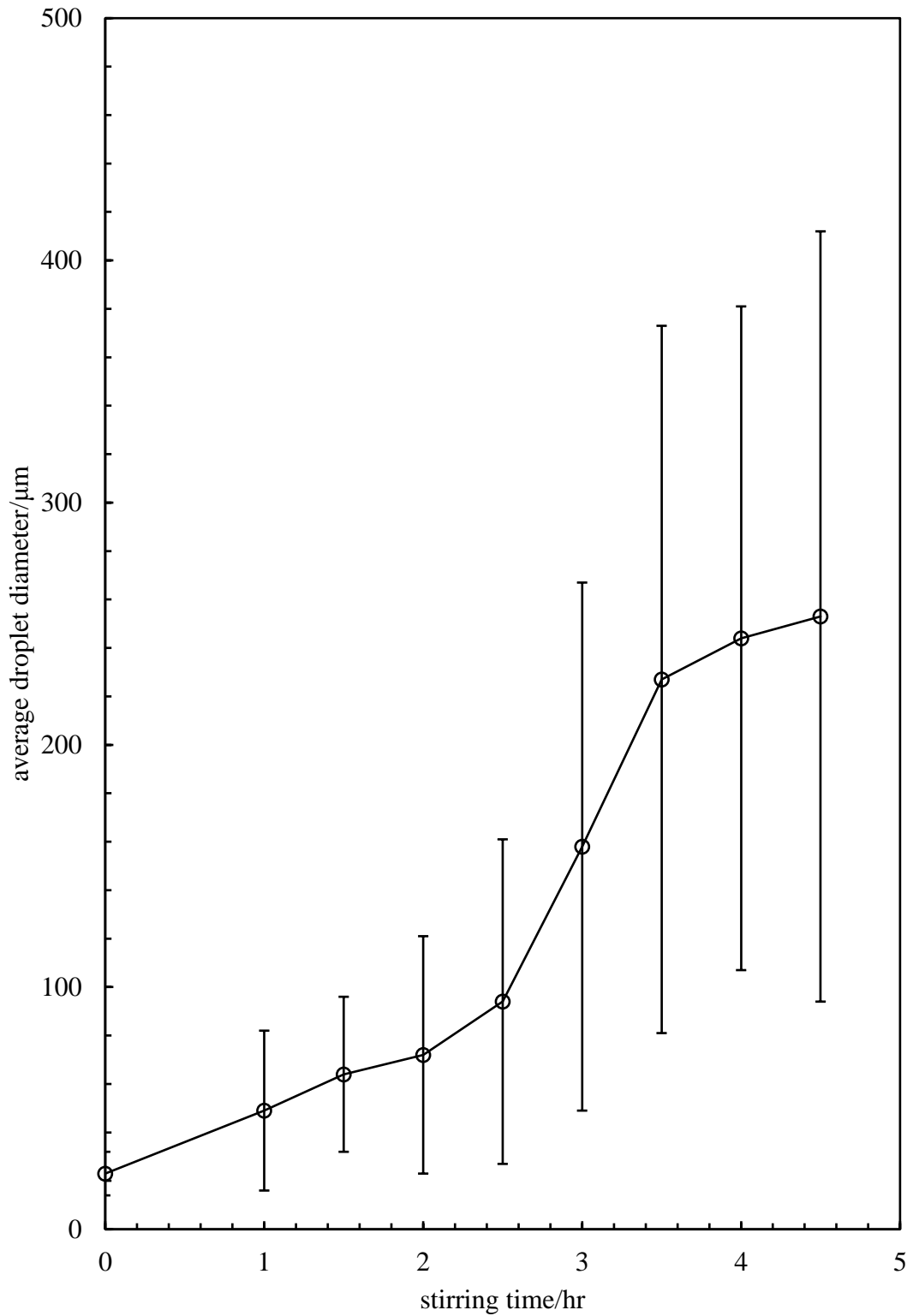


**Figure 5.3.** Average droplet diameter of a water-in-dodecane emulsion ( $\phi_w = 0.5$ ) stabilized by 2 wt.% carboxyl PS latex particles ( $d = 0.2 \mu\text{m}$ ) at pH 3 after stirring at 300 rpm for different time, measured from the optical microscopy of droplets using Image J and plotted against stirring time.



## 5.2.2 By adding sub-micron silica particles

### 5.2.2.1 Addition of hydrophilic silica particles of varied size

In this section, hydrophilic monodispersed silica particles of varied diameters were added at a fixed particle number to destabilize water-in-oil emulsions stabilized by 2 wt.% carboxyl PS latex particles ( $d = 0.2 \mu\text{m}$ ) at  $\phi_w = 0.5$  and pH 3. The particle number ( $\sim 4 \times 10^9$ ) was fixed at that equals to 0.001g of  $0.3 \mu\text{m}$  particles. The volume of model emulsion was fixed at 5 mL.

Figure 5.4 shows the appearance of the emulsions after adding monodispersed silica particles and stirring at 300 rpm for different time. As can be seen in Figure 5.4 (a), water starts to extract from the emulsions upon stirring. A thin layer of water at the bottom of each vessel was observed within 5 minutes. By contrast, 4.5 hours of stirring results in large volume of water, as shown in Figure 5.4 (b). The resolved water is turbid, and the turbidity increases with particle size, implying the presence of particles in water. The particles in the resolved water are possibly carboxyl latex particles or silica particles or both of them, which requires further confirmation. Figure 5.5 represents the stability of the emulsions to sedimentation ( $f_o$ ) and coalescence ( $f_w$ ) against stirring time. As can be seen, both  $f_o$  and  $f_w$  increase with increasing stirring time until reaching plateaus. However, the constant values at the plateaus are close to each other. Figure 5.6 plots the  $f_o$  and  $f_w$  of the emulsions against particle size after 4.5 hours of stirring. The  $f_o$  plot shows slight fluctuations but  $f_w$  almost keeps constant at 0.8 except the sample with  $0.3 \mu\text{m}$  silica particles, in which a maximum of 0.9 is obtained. These results indicate that particles of  $0.3 \mu\text{m}$  are quite effective in destabilising the w/o emulsions, nearly 90% of initial water is released after stirring, although complete phase separation of emulsions was not observed. Increase of particle size in the sub-micron range makes almost no difference on the destabilisation efficiency. Figure 5.7 shows the optical microscopy images of the emulsion droplets after stirring for 4.5 hours and Figure 5.8 represents the average droplet diameter. In the emulsion with  $0.3 \mu\text{m}$  silica, most of the emulsion droplets are broken and carboxyl PS latex particle aggregates along with remaining emulsion droplets were observed under the microscope. By contrast, in the emulsions containing larger silica particles, very large droplets were observed. The droplets aggregate and most of them are

deformed. The droplet size keeps relatively constant as the silica particle size increases. It was reported that addition of poor-quality solvent to emulsions stabilised by organoclay particles results in small aggregates of droplets, which self-assemble into random networks of deformed droplets.<sup>13</sup> There is high consistency between the results here and that in the literature. It is sensible since for fresh added silica particles, the continuous phase of the emulsion (dodecane) is a poor-quality solvent. Silica particles adsorb at oil-water interfaces and aggregate droplets. Subsequent coalescence of droplets results in detached carboxyl latex particles, as observed on the microscopy of emulsion destabilised by 0.3  $\mu\text{m}$  particles.

**Figure 5.4.** Appearance of water-in-dodecane emulsions ( $\phi_w = 0.5$ ) stabilized by 2 wt.% carboxyl PS latex particles ( $d = 0.2 \mu\text{m}$ ) at pH 3 after adding hydrophilic monodispersed silica particles at a fixed particle number and varied diameter (given), stirring at 300 rpm for (a) 5 min and (b) 4.5 hours. Photos were taken immediately after stirring.

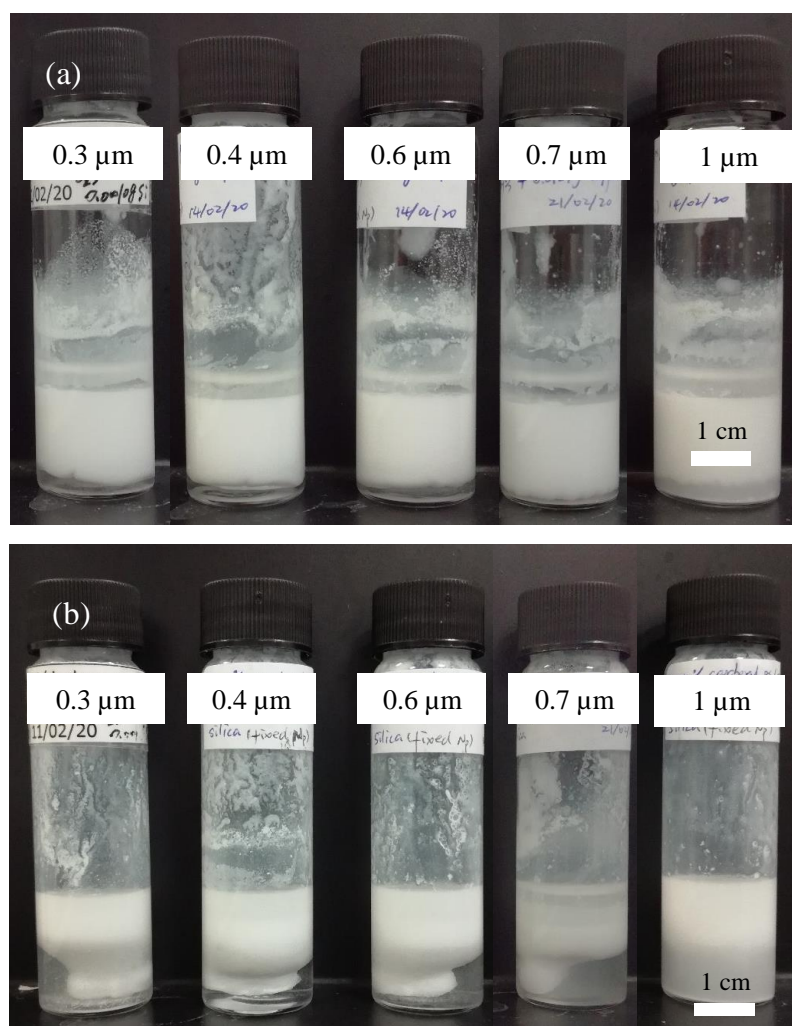


**Figure 5.5.** (a)  $f_o$  and (b)  $f_w$  of water-in-dodecane emulsions ( $\phi_w = 0.5$ ) stabilized by 2 wt.% carboxyl PS latex particles ( $d = 0.2 \mu\text{m}$ ) at pH 3 after adding hydrophilic monodispersed silica particles at a fixed particle number and varied diameters (given) and stirring at 300 rpm, plotted against stirring time.

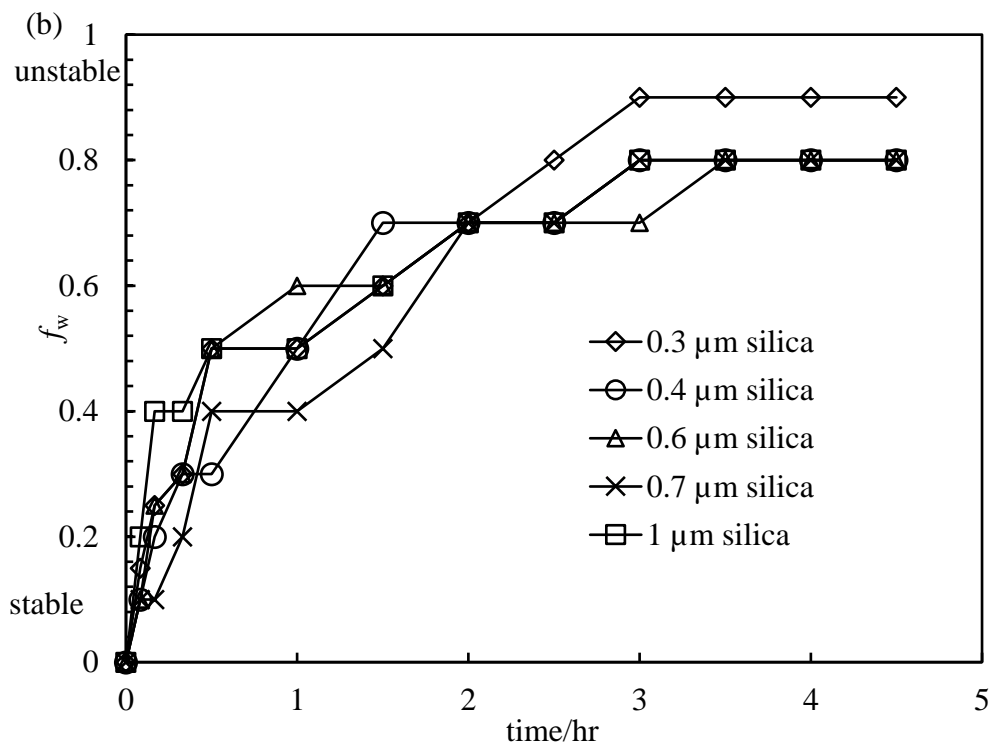
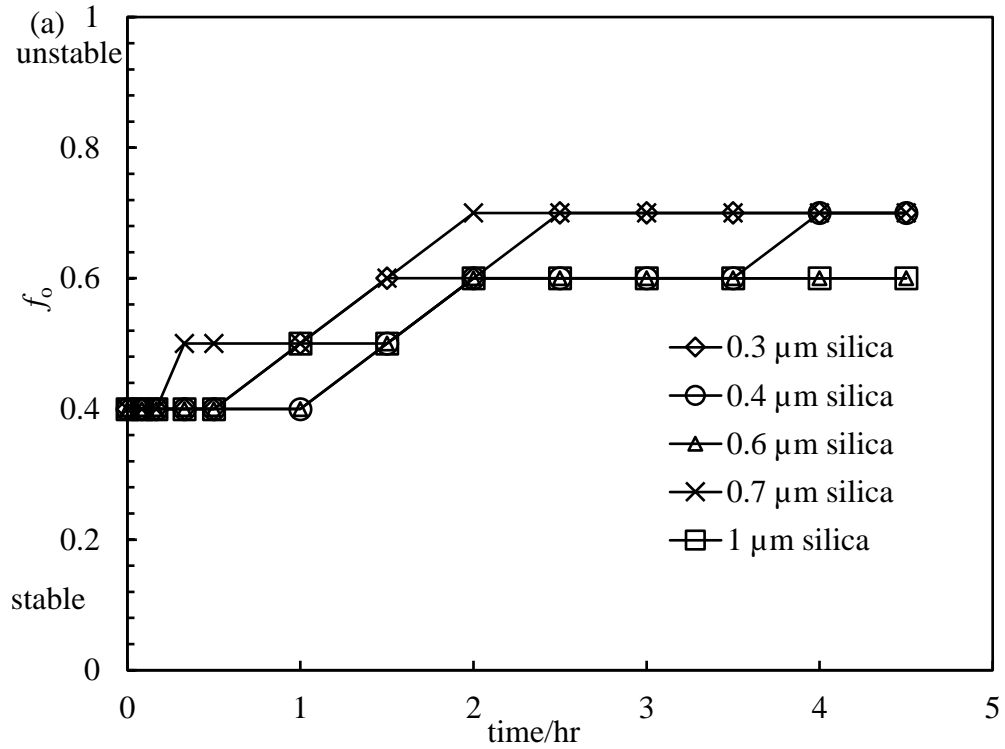


**Figure 5.6.** The  $f_o$  and  $f_w$  of water-in-dodecane emulsions ( $\phi_w = 0.5$ ) stabilized by 2 wt.% carboxyl PS latex particles ( $d = 0.2 \mu\text{m}$ ) at pH 3 after adding hydrophilic monodispersed silica particles at a fixed particle number and varied diameter (given) and stirring at 300 rpm for 4.5 hours.

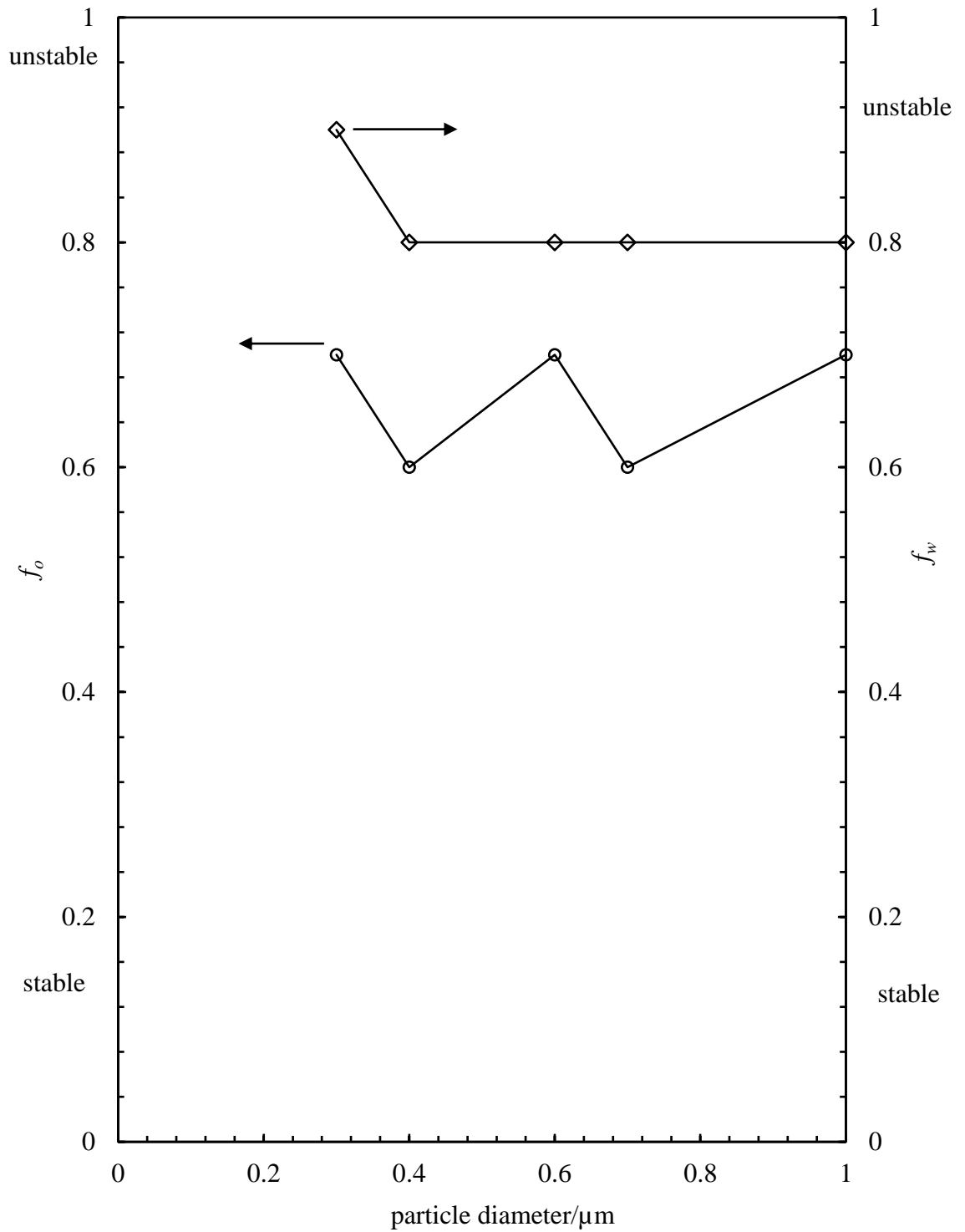


**Figure 5.7.** Optical microscopy of water-in-dodecane emulsions ( $\phi_w = 0.5$ ) stabilized by 2 wt.% carboxyl PS latex particles ( $d = 0.2 \mu\text{m}$ ) at pH 3 after adding hydrophilic monodispersed silica particles at a fixed particle number and varied diameter (given) and stirring at 300 rpm for 4.5 hours.

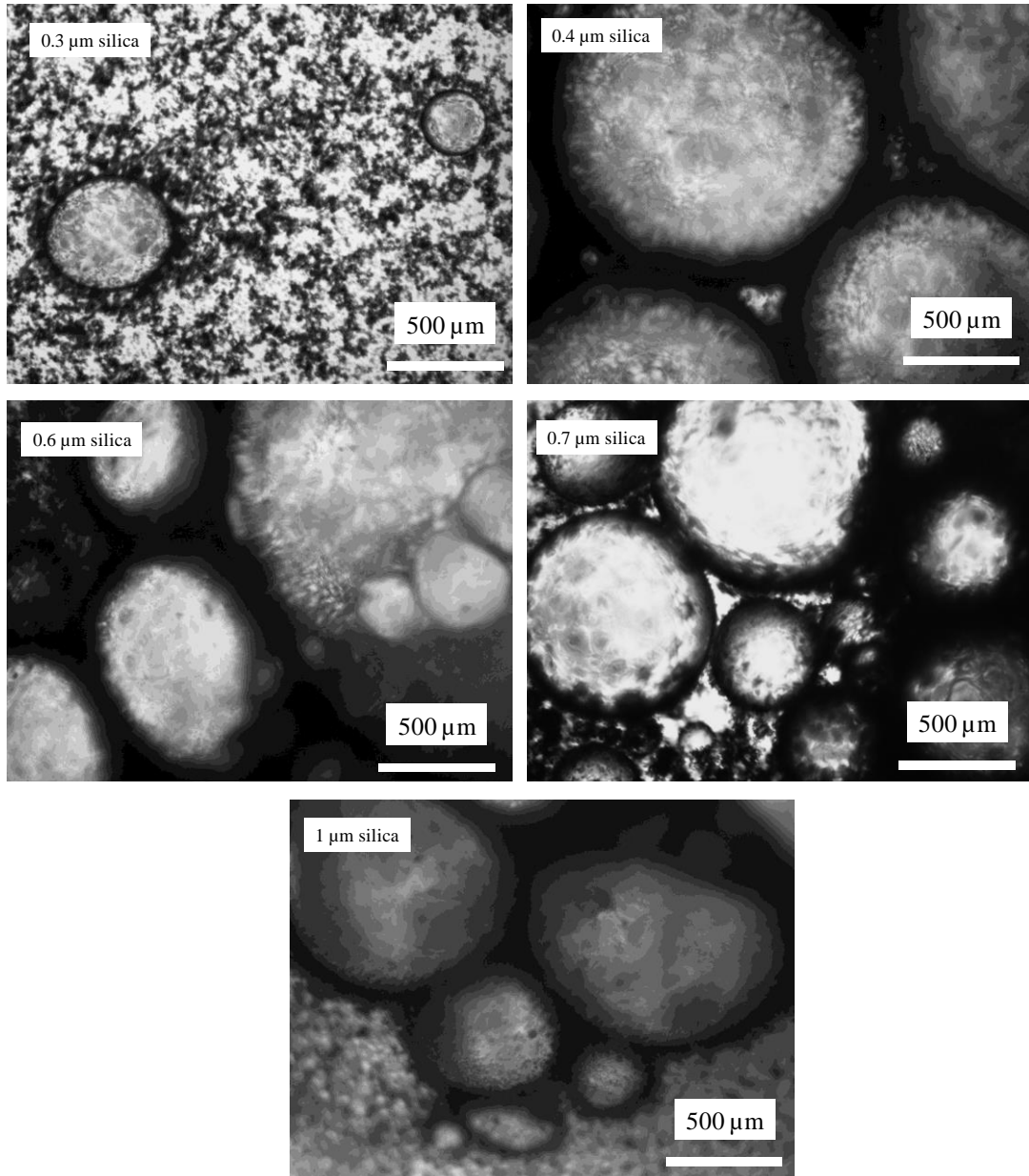
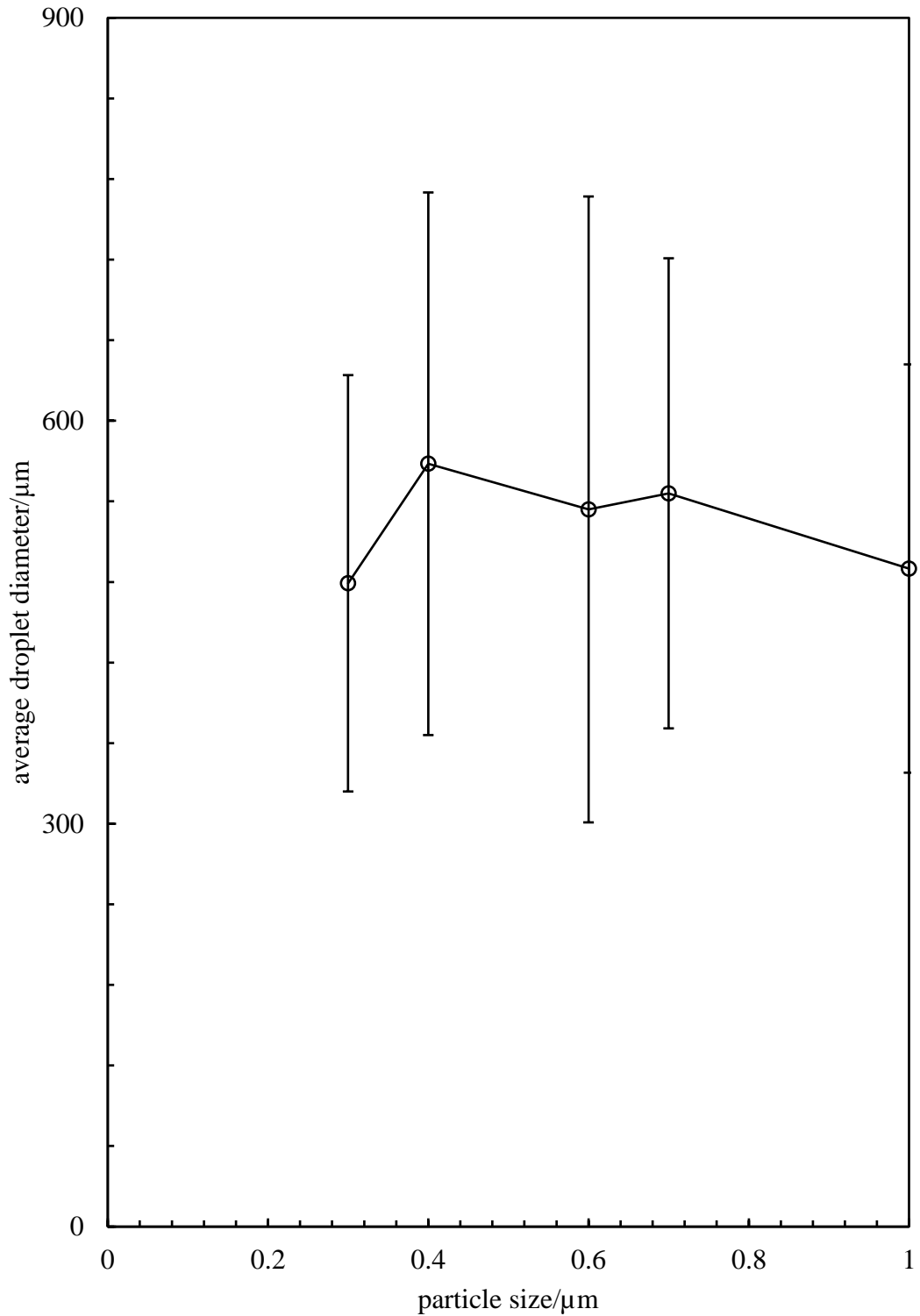


**Figure 5.8.** Average droplet diameter of water-in-dodecane emulsions ( $\phi_w = 0.5$ ) stabilized by 2 wt.% carboxyl PS latex particles ( $d = 0.2 \mu\text{m}$ ) at pH 3 after adding hydrophilic monodispersed silica particles at a fixed particle number and varied diameter and stirring at 300 rpm for 4.5 hours.



### 5.2.2.2 Addition of 0.3 $\mu\text{m}$ silica particles of varied concentration

The last section investigated the effect of particle size on the destabilization efficiency and found that 0.3  $\mu\text{m}$  silica particles are the most efficient in destabilising w/o emulsion compared with larger particles. It is worthwhile to investigate the effect of particle concentration on the destabilisation efficiency of the same emulsions. Therefore, in this section, hydrophilic monodispersed silica with a diameter of 0.3  $\mu\text{m}$  were added at different concentrations to destabilize water-in-oil emulsions stabilized by 2 wt.% carboxyl PS latex particles ( $d = 0.2 \mu\text{m}$ ) at  $\phi_w = 0.5$  and pH 3. Figure 5.9 shows the appearance of the emulsions after adding silica particles and stirring at 300 rpm for different time. Water is released from each emulsion immediately when the stirring starts. After 4.5 hours of stirring, large volume of water is released from the emulsions. In the samples with 0.3 wt.% and 0.5 wt.% silica particles, the height of resolved water layers is slightly lower than those with less particles. Figure 5.10 plots the  $f_o$  and  $f_w$  of emulsions against silica particle concentrations after the destabilisation procedure. In general, both  $f_o$  and  $f_w$  decrease slightly with silica particle concentration, indicating that higher silica particle concentration is less efficient in destabilizing the emulsion. Hydrophilic silica particles tend to form aggregates in dodecane due to the hydrophobic effect of the oil, which will be confirmed in Figure 5.21 (c) where aggregates of silica particles were observed. The aggregated particles are less efficient to be dispersed into the continuous phase between the droplets by gentle stirring because of their larger size compared with monodispersed particles. Increase of the particle concentration possibly promotes the formation of larger aggregates. As a result, lower destabilization efficiency was obtained. Figure 5.11 shows the optical microscopy images of the emulsion droplets after stirring. In the emulsion with 0.025 wt.% silica, most of the emulsion droplets are broken and carboxyl PS latex particle aggregates are observed under microscope. Larger droplets were observed in other samples while detached carboxyl latex particle aggregates were not observed in emulsions with silica particles at 0.2 wt.% and higher concentrations. The droplet diameter of remaining emulsions peaks at 0.1 wt.% silica particles (see Figure 5.12).

**Figure 5.9.** Appearance of water-in-dodecane emulsions ( $\phi_w = 0.5$ ) stabilized by 2 wt.% carboxyl PS latex particles ( $d = 0.2 \mu\text{m}$ ) at pH 3 after adding hydrophilic monodispersed silica particles ( $d = 0.3 \mu\text{m}$ ) at varied concentrations (given, relative to the mass of emulsion) and stirring at 300 rpm for (a) 5 min and (b) 4.5 hours. Photos were taken immediately after stirring.

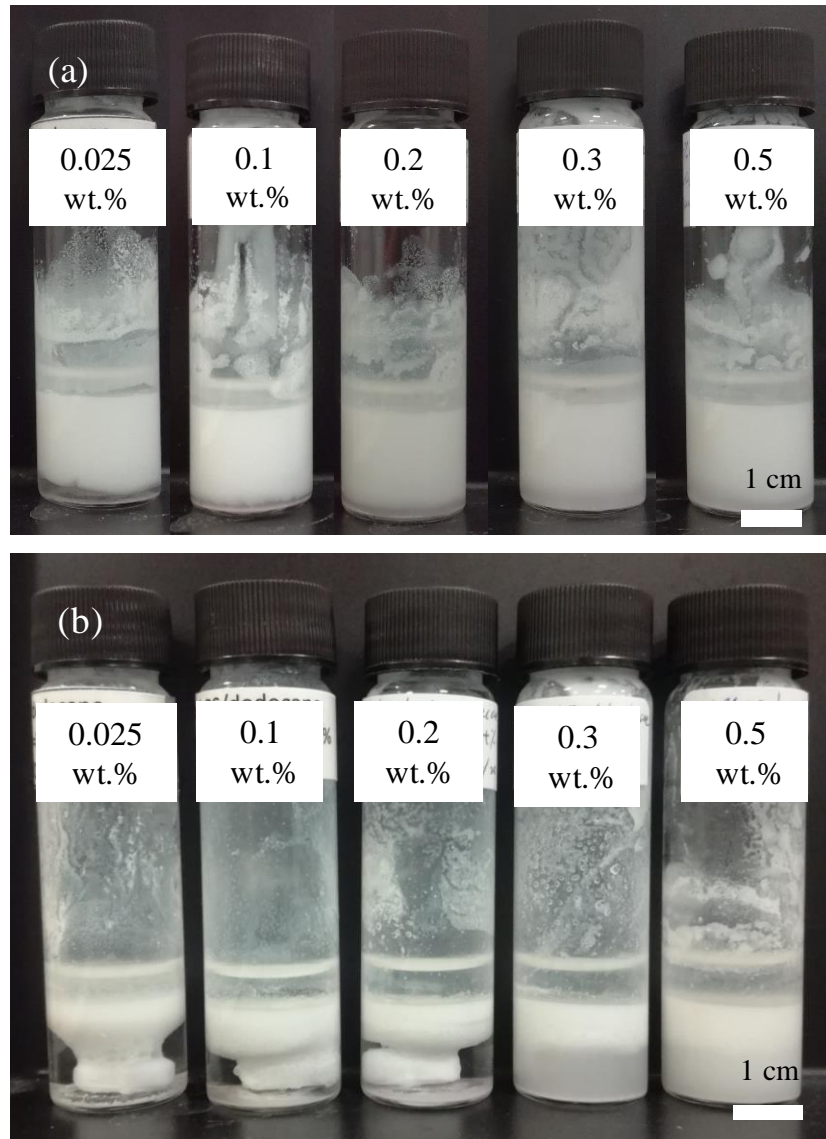


**Figure 5.10.** The  $f_o$  and  $f_w$  of water-in-dodecane emulsions ( $\phi_w = 0.5$ ) stabilized by 2 wt.% carboxyl PS latex particles ( $d = 0.2 \mu\text{m}$ ) at pH 3 after adding hydrophilic monodispersed silica particles ( $d = 0.3 \mu\text{m}$ ) at varied concentrations (given, relative to the mass of emulsion) and stirring at 300 rpm for 4.5 hours.

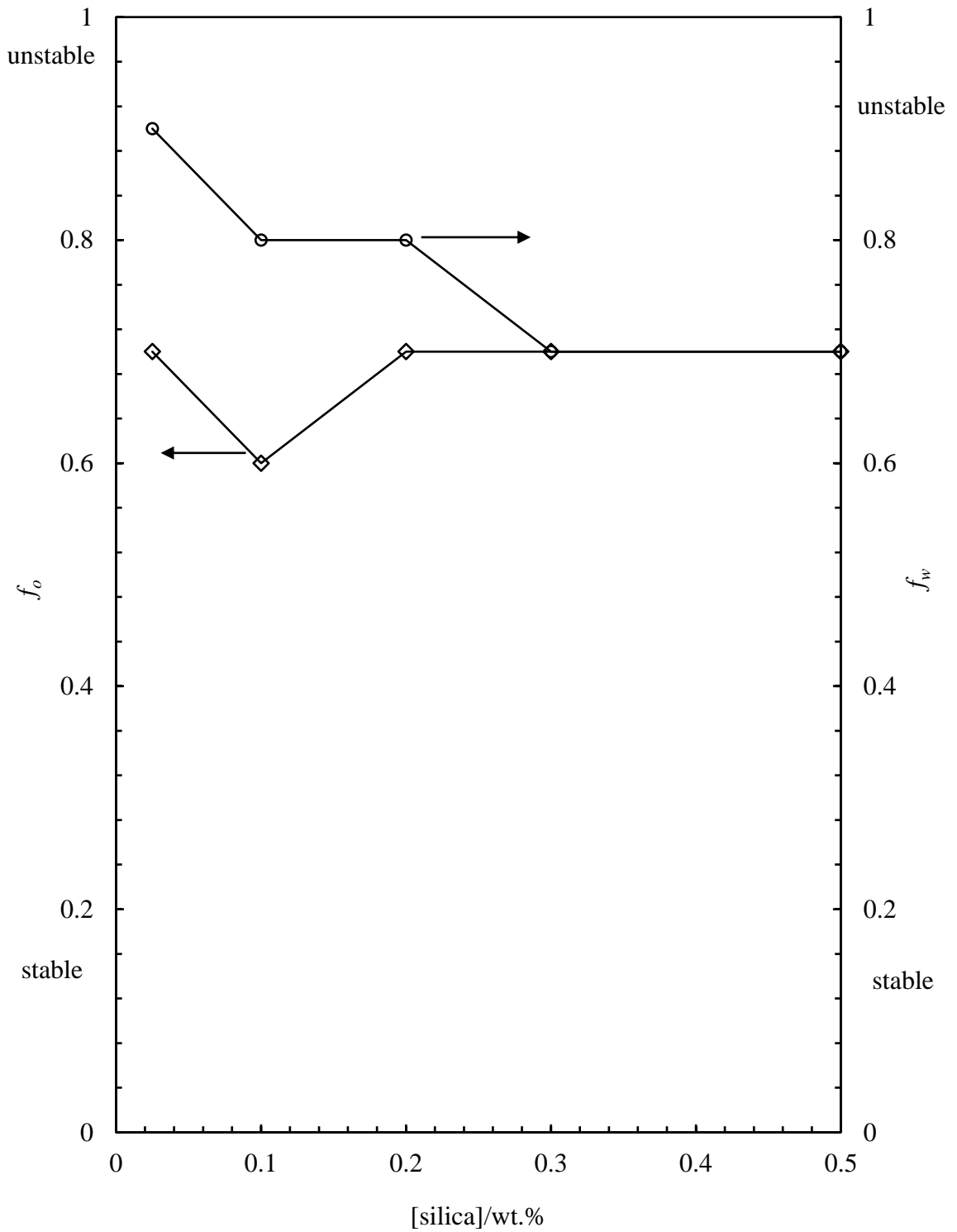


**Figure 5.11.** Optical microscopy images of water-in-dodecane emulsions ( $\phi_w = 0.5$ ) stabilized by 2 wt.% carboxyl PS latex particles ( $d = 0.2 \mu\text{m}$ ) at pH 3 after adding hydrophilic monodispersed silica particles ( $d = 0.3 \mu\text{m}$ ) at varied concentrations (given, relative to the mass of emulsion) and stirring at 300 rpm for 4.5 hours.

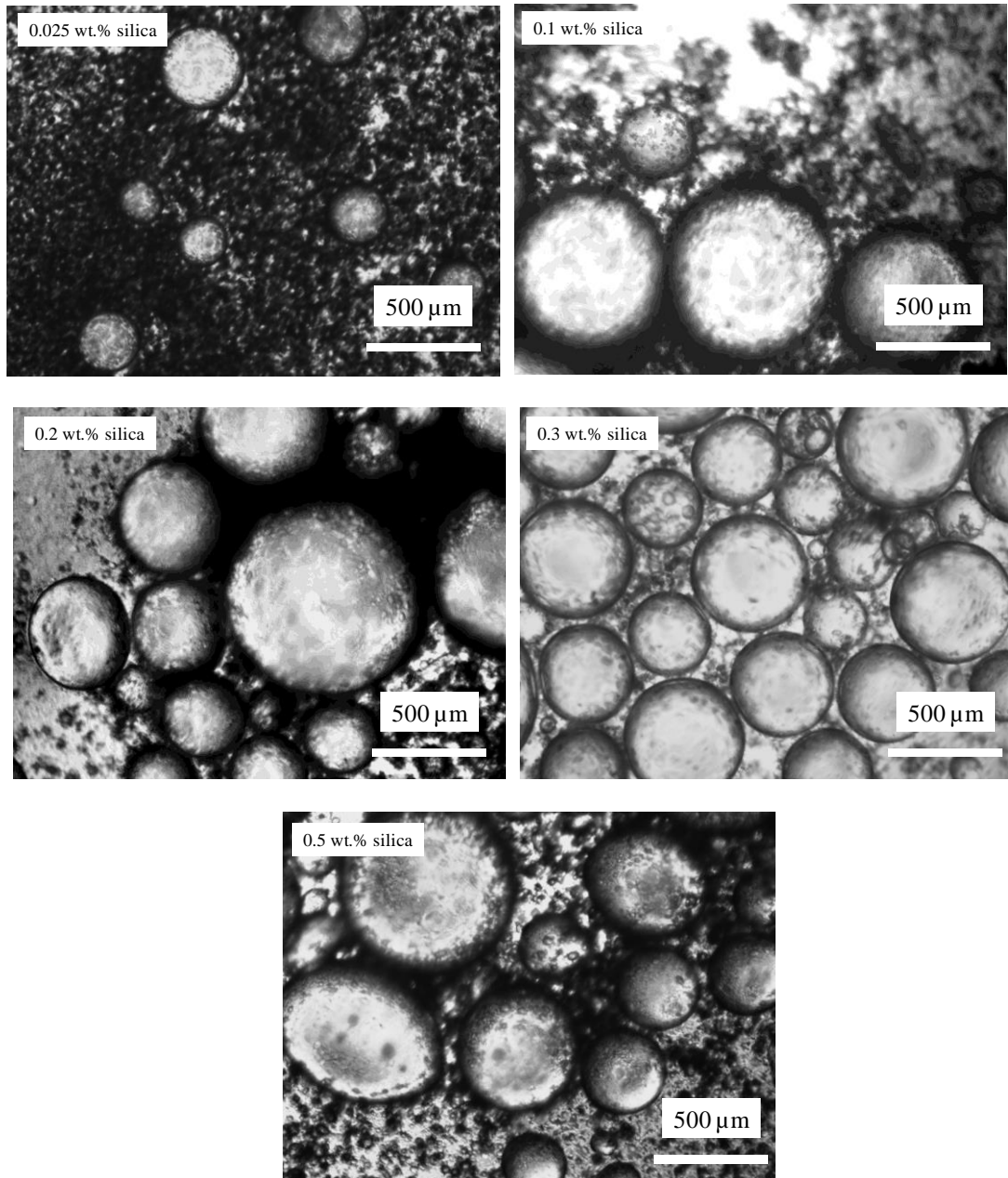
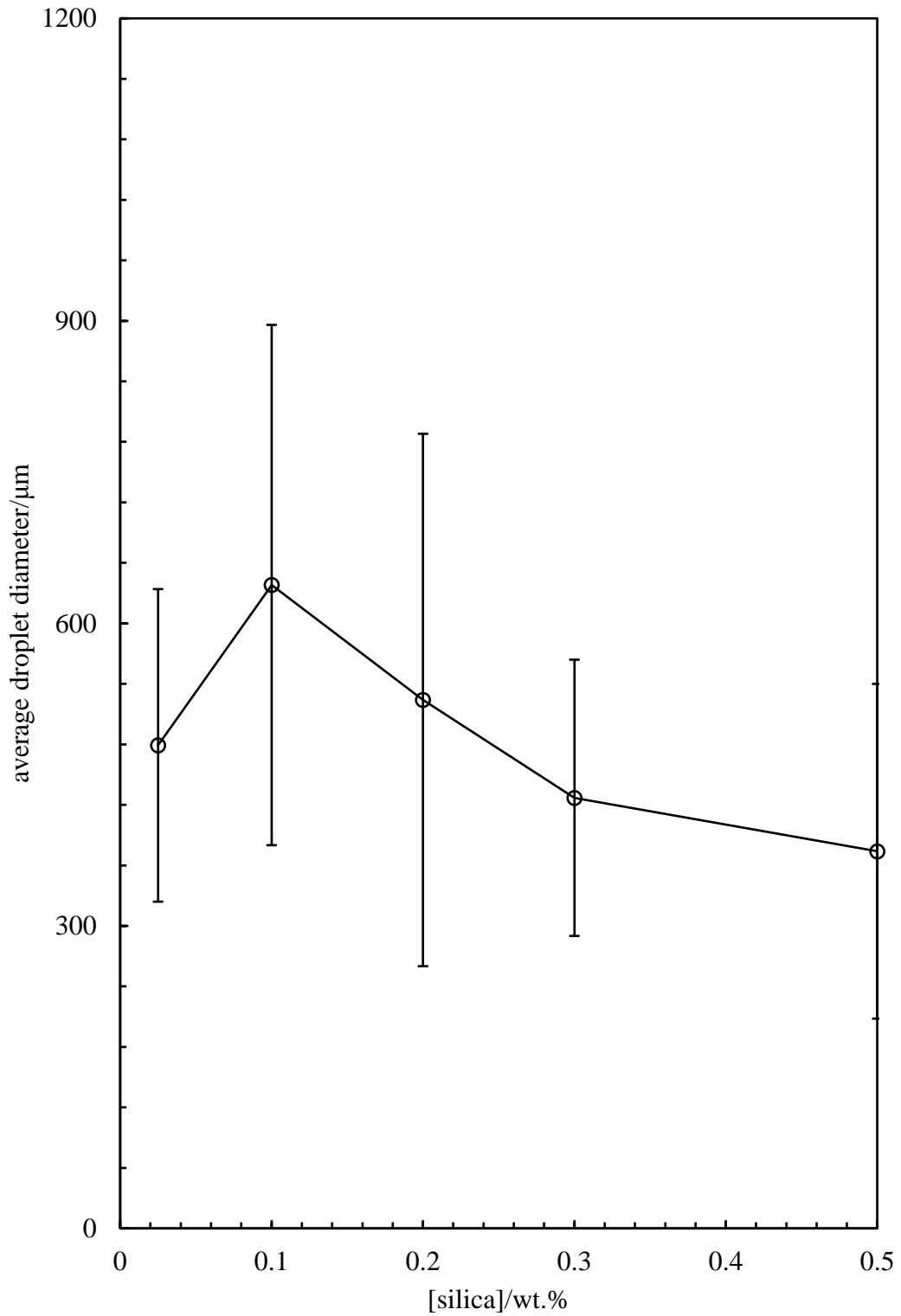


**Figure 5.12.** Average droplet diameter of water-in-dodecane emulsions ( $\phi_w = 0.5$ ) stabilized by 2 wt.% carboxyl PS latex particles ( $d = 0.2 \mu\text{m}$ ) at pH 3 after adding hydrophilic monodispersed silica particles ( $d = 0.3 \mu\text{m}$ ) at different concentrations (given, relative to the mass of emulsion) and stirring at 300 rpm for 4.5 hours.



### 5.2.2.3 Addition of 0.3 $\mu\text{m}$ silica particles of varied hydrophobicity

In this section, monodispersed silica particles with a diameter of 0.3  $\mu\text{m}$  were hydrophobized by different concentrations of dichlorodimethylsilane (DCDMS) and rendered to destabilize w/o emulsions stabilized by carboxyl latex particles at  $\phi_w = 0.5$ . The hydrophobisation of silica particles has been explained in section 2.2.5. Glass slides were hydrophobized simultaneously with the silica particles to evaluate the hydrophobicity of particles after reacting with DCDMS. Figure 5.13 represents the contact angle of hydrophobized glass slides at air-water and dodecane-water interfaces against DCDMS concentrations used for the hydrophobization. Both advancing and receding contact angles were determined. The advancing contact angles are higher than the receding ones at all DCDMS concentrations, which is well-known as contact angle hysteresis due to surface roughness and heterogeneity.<sup>16</sup> The advancing contact angle of glass slides at air-water interfaces ( $\theta_{a,w}$ ) increases gradually from  $\sim 60^\circ$  to  $105^\circ$  as DCDMS concentration increases. Similarly, that at the dodecane-water interface ( $\theta_{o,w}$ ) increases from  $\sim 85^\circ$  to  $\sim 140^\circ$ . Hence, particles vary from moderate hydrophilic to highly hydrophobic. The contact angle of particles at dodecane-water interface is termed as  $\theta_{o,w}$  as it was measured by immersing glass slides in the oil before placing a drop of water on it, consistent with silica particles contacting with the oil first when added as destabilisers.

Figure 5.14 shows the appearance of emulsions after adding 0.025 wt.% of 0.3  $\mu\text{m}$  silica particles with varied hydrophobicity and stirring at 300 rpm for 4.5 hours. Photos were taken immediately after stirring. In the presence of silica particles, water is released from emulsions upon stirring, and 4.5 hours of stirring results in large volume of water in each sample. Figure 5.15 represents the  $f_o$  and  $f_w$  of emulsions against DCDMS concentrations. As the DCDMS concentration increases,  $f_o$  keeps constant while  $f_w$  increases slightly before decreases. These results indicate that hydrophilic silica particles are relatively more efficient than hydrophobic ones in destabilizing w/o emulsions. However, the most efficient particles are completely hydrophilic and those hydrophobized by  $1 \times 10^{-3}$  M DCDMS. The mechanism of solid particles destabilizing Pickering emulsions will be deduced in section 5.2.3.3. It is reasonable that complete hydrophilic particles show the highest efficiency in the destabilization as they are wetted by the inner phase (water) of droplets. Once silica

particles adsorb onto the droplet surface, they tend to protrude the interface and enter the inner phase of the droplet, which results in coalescence of emulsion. However, for hydrophobic particles (hydrophobized by  $1 \times 10^{-3}$  M DCDMS), their behavior in the destabilization process is surprising since they are more wetted by the continuous phase (oil). Theoretically, these particles are expected to enhance the stability of the model w/o emulsions. The reason for hydrophobic monodispersed silica particles destabilizing w/o emulsions is unclear. One speculation is that these particles are more readily to adsorb onto oil-water interface considering their three-phase contact angle ( $115^\circ$ ). However, the contact angle is not high enough to bridge droplets in the manner of enhancing the emulsion stability. As a result, these particles behave as destabilizers. More particles adsorbing at the droplet surface break more droplets. Figure 5.16 shows the optical microscopy images and Figure 5.17 plots the average droplet diameter of the emulsions after stirring. The droplets are large and deformed. Droplet diameter peaks at  $1 \times 10^{-3}$  M DCDMS.

**Figure 5.13.** Advancing and receding contact angles of water drops on glass slides hydrophobized at different DCDMS concentrations measured in: (a) air and (b) dodecane by the Kruss DSA 10 instrument.

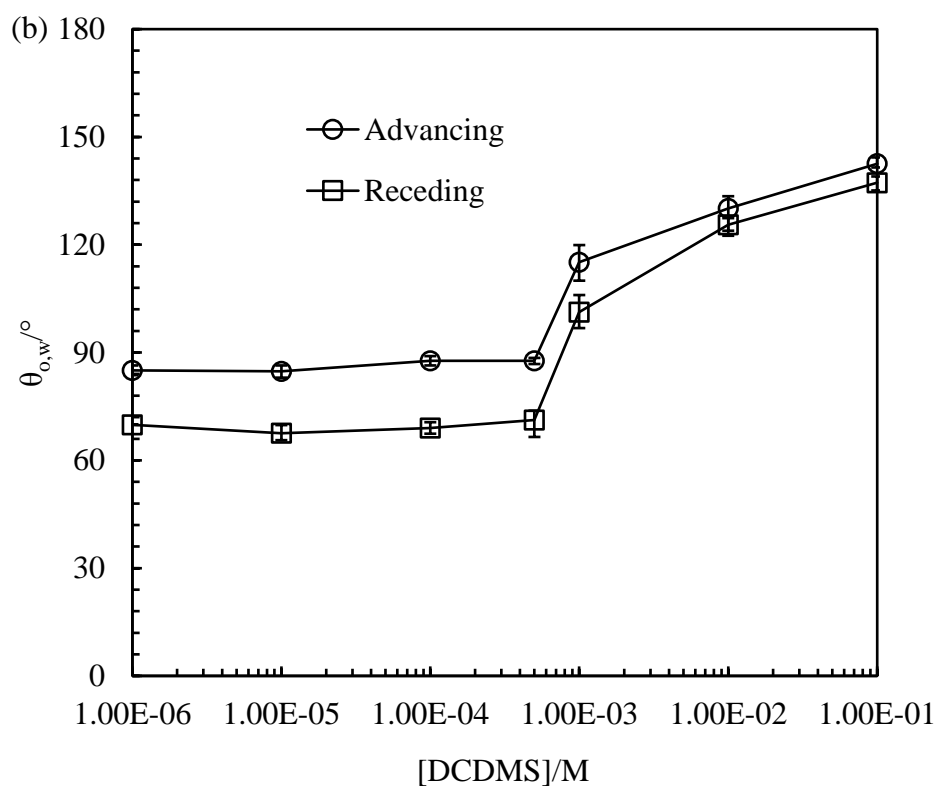
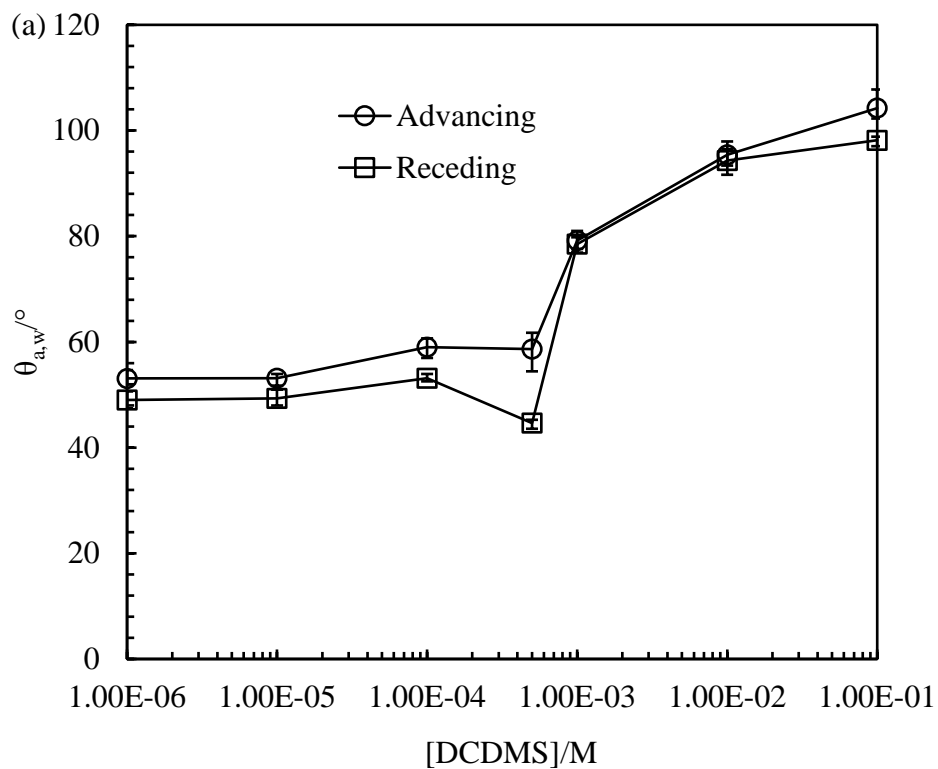


**Figure 5.14.** Appearance of water-in-dodecane emulsions ( $\phi_w = 0.5$ ) stabilized by 2 wt.% carboxyl PS latex particles ( $d = 0.2 \mu\text{m}$ ) at pH 3 after adding 0.025 wt.% (relative to the mass of emulsion) hydrophobized monodispersed silica particles ( $d = 0.3 \mu\text{m}$ ) and stirring at 300 rpm for (a) 5 min and (b) 4.5 hours. Silica particles were hydrophobized by different concentrations of DCDMS (given). Photos were taken immediately after stirring.

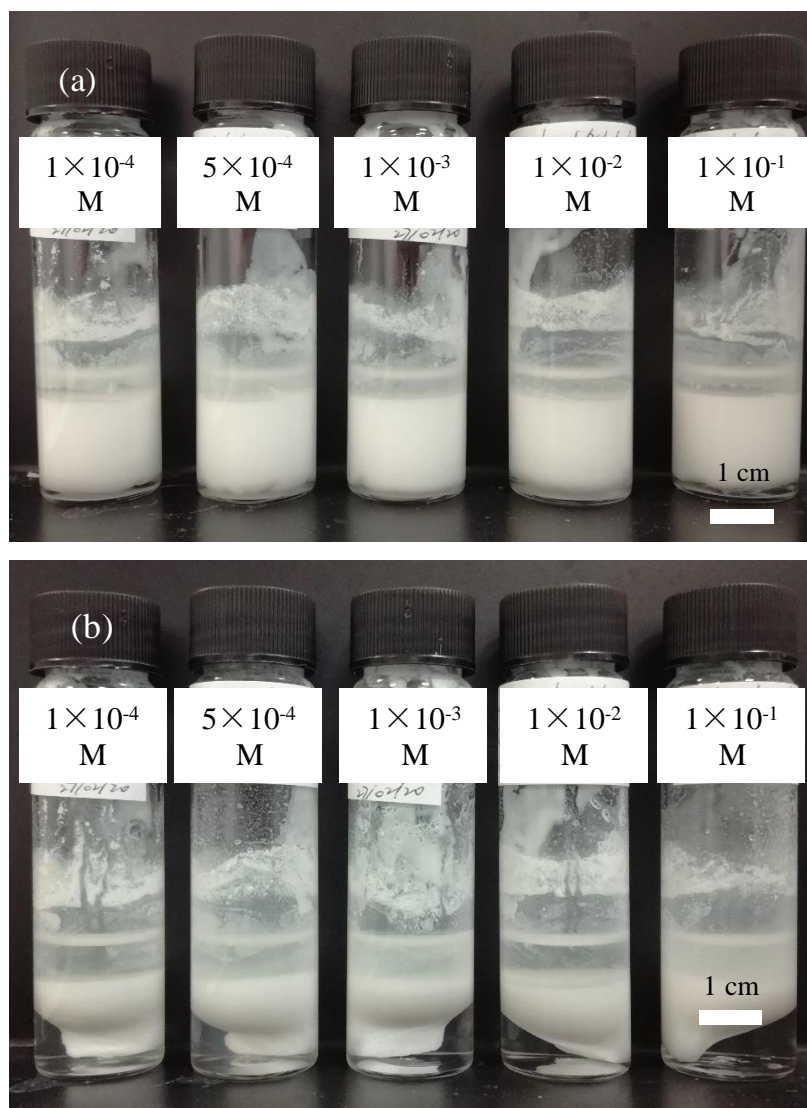


**Figure 5.15.** The  $f_o$  and  $f_w$  of water-in-dodecane emulsions ( $\phi_w = 0.5$ ) stabilized by 2 wt.% carboxyl PS latex particles ( $d = 0.2 \mu\text{m}$ ) at pH 3 after adding 0.025 wt.% (relative to the mass of emulsion) hydrophobized monodispersed silica particles ( $d = 0.3 \mu\text{m}$ ) and stirred at 300 rpm 4.5 hours. Silica particles were hydrophobized by DCDMS at different concentrations (given). Dashed line represents  $f_w$  of the emulsion destabilised by completely hydrophilic particles.

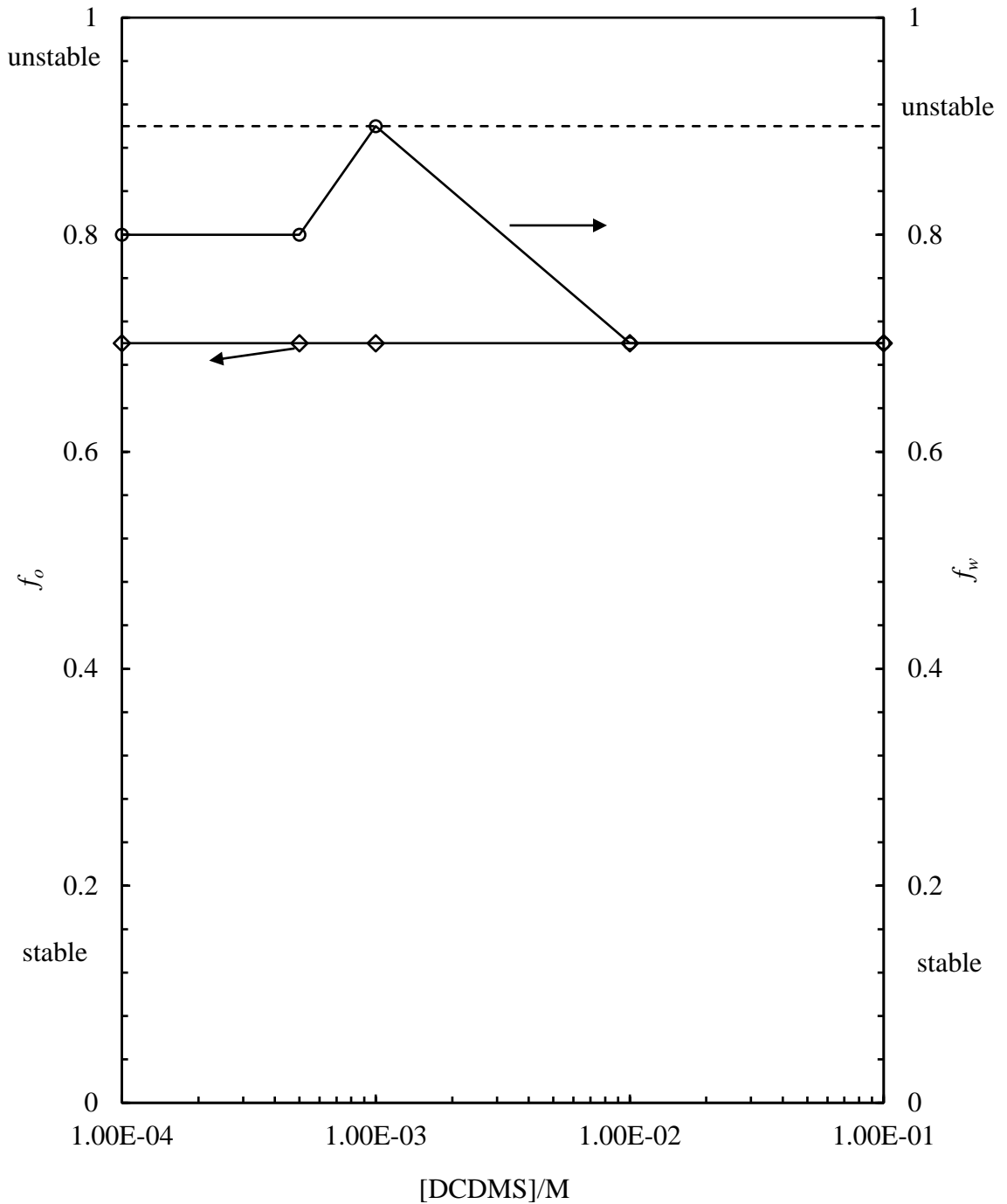


**Figure 5.16.** Optical microscopy of water-in-dodecane emulsions ( $\phi_w = 0.5$ ) stabilized by 2 wt.% carboxyl PS latex particles ( $d = 0.2 \mu\text{m}$ ) at pH 3 after adding 0.025 wt.% (relative to the mass of emulsion) hydrophobized monodispersed silica particles ( $d = 0.3 \mu\text{m}$ ) and stirring at 300 rpm 4.5 hours. Silica particles were hydrophobized by different concentration of DCDMS (given).

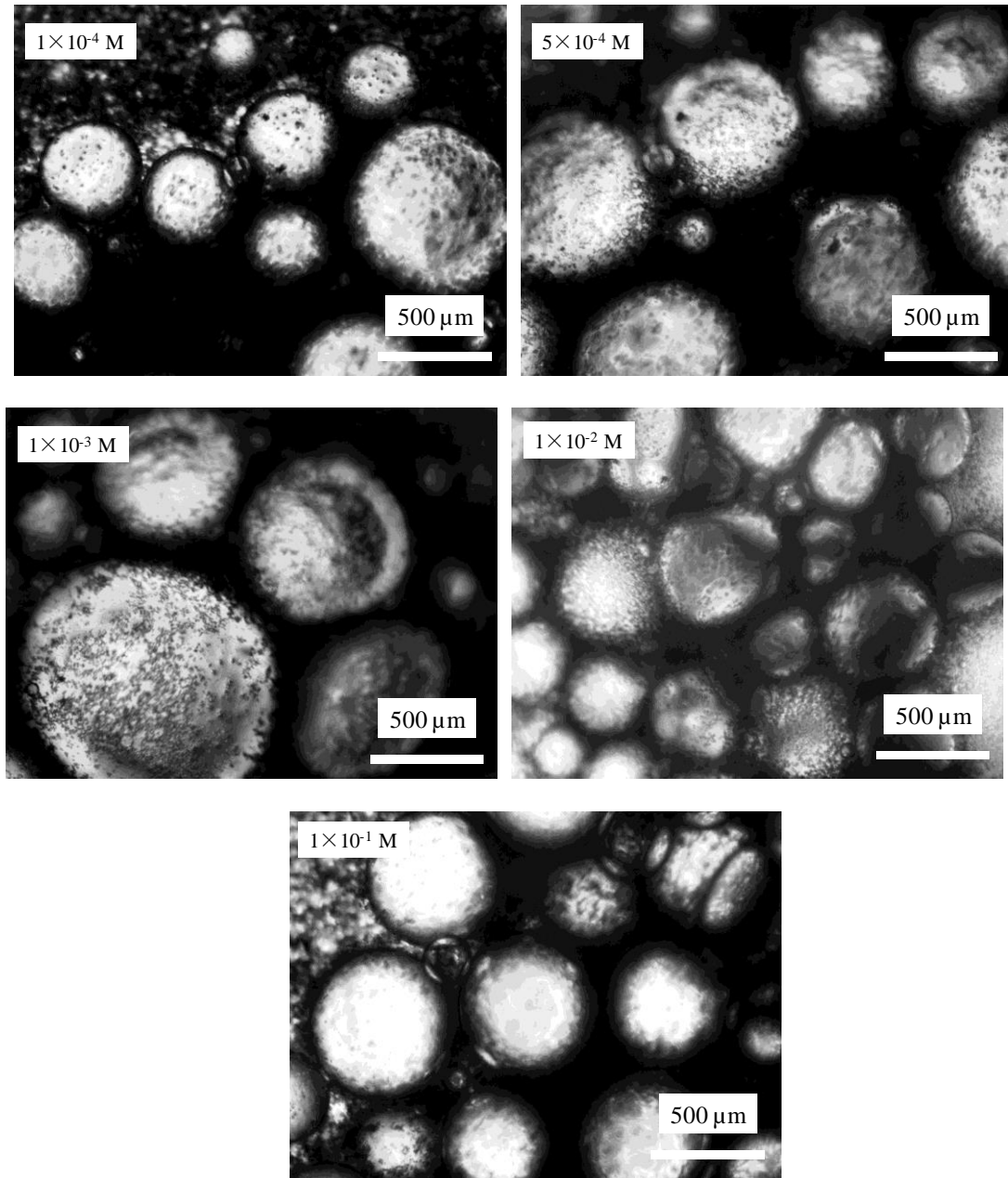
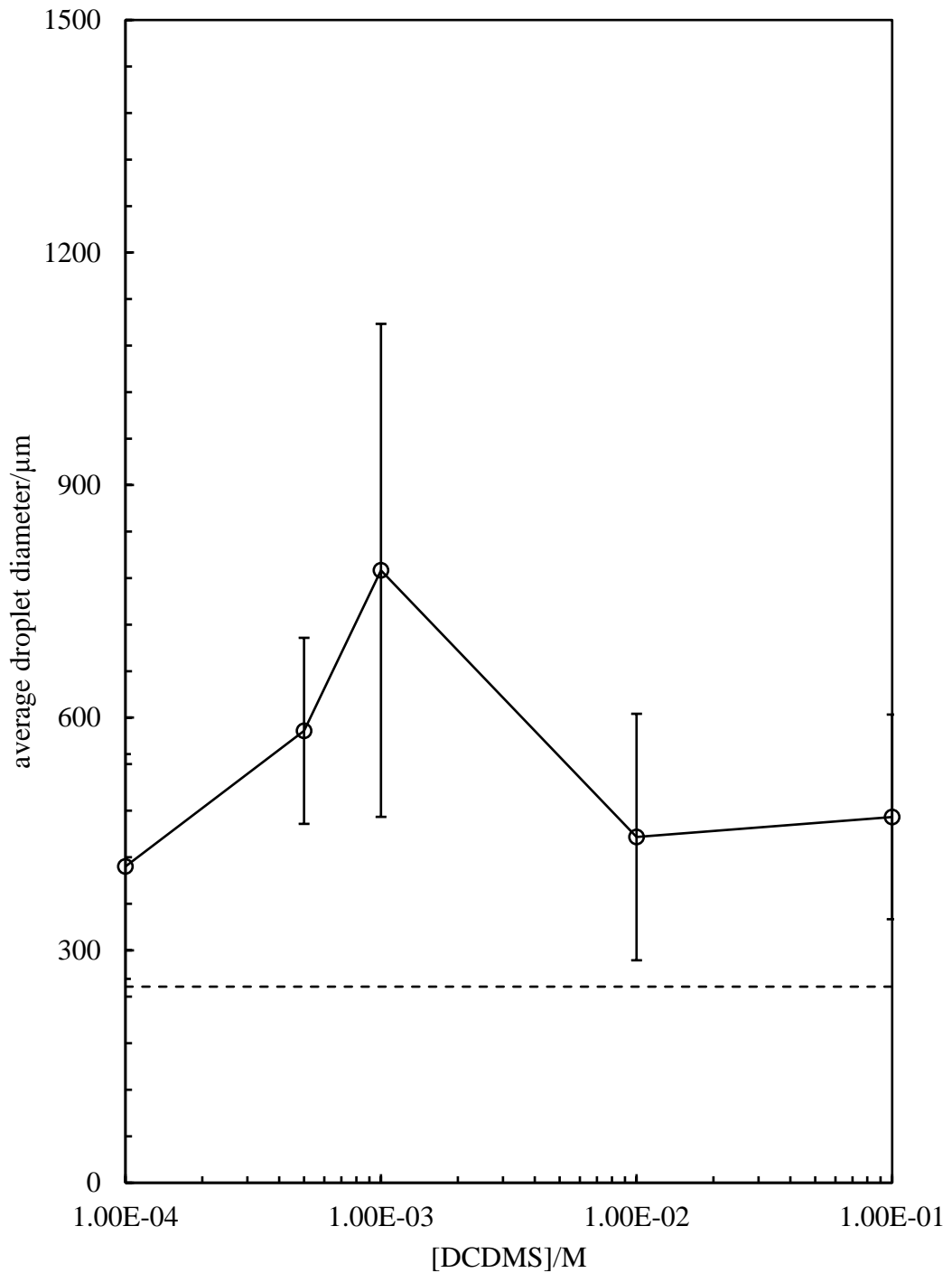


**Figure 5.17.** Average droplet diameter of water-in-dodecane emulsions ( $\phi_w = 0.5$ ) stabilized by 2 wt.% carboxyl PS latex particles ( $d = 0.2 \mu\text{m}$ ) at pH 3 after adding 0.025 wt.% (relative to the mass of emulsion) hydrophobized monodispersed silica particles ( $d = 0.3 \mu\text{m}$ ) and stirring at 300 rpm 4.5 hours. Silica particles were hydrophobized by different concentration of DCDMS (given). Dashed line represents the diameter of the emulsion droplet destabilised by completely hydrophilic particles.



### 5.2.3 By adding 2 $\mu\text{m}$ hydrophilic silica particles

#### 5.2.3.1 Destabilization at $\phi_w = 0.5$

In order to explore the mechanism of solid particles destabilising Pickering emulsions, hydrophilic monodispersed silica particles with a diameter of 2  $\mu\text{m}$  were used as the destabilisers. On one hand, these particles are 10 times of carboxyl latex particles in diameter, which makes it easy to observe the particles adsorbed at the droplet surfaces under the optical microscope. On the other hand, silica particles are apparently different from carboxyl PS latex particles in elemental components which makes it possible to trace the position of the silica particles using cryo-scanning electron microscopy (Cryo-SEM) with energy dispersive X-ray spectrometry (EDX). Figure 5.18 (a) shows the appearance of emulsions after adding hydrophilic monodispersed silica particles ( $d = 2 \mu\text{m}$ ) and stirring at 300 rpm for 4.5 hours. Emulsions containing low concentrations of silica particles show no macroscopic coalescence. By contrast, water is released from the emulsions at silica particle concentrations higher than 0.23 wt.%. Complete phase separation occurs in emulsions with 0.3 wt.% and 0.5 wt.% of particles, in which the volume of water released equals to the initial volume added for the preparation of emulsions. The white layers in the middle are likely particle flocs in the oil phases. Figure 5.18 (b) represents  $f_o$  and  $f_w$  of emulsions against silica particle concentrations after the destabilisation process. The height of oil layer for the samples containing 0.3 wt.% and 0.5 wt.% silica particles was measured by including the white layers above the resolved water. Both  $f_o$  and  $f_w$  increase with silica particle concentration until reach one, indicating that higher silica particle concentration is more efficient in destabilization. This seems disagree with the previous findings where higher concentrations of 0.3  $\mu\text{m}$  hydrophilic silica particles result in lower destabilisation efficiency. However, if expressed in particle number, 0.5 wt.% of 2  $\mu\text{m}$  particles is dramatically less than 0.025 wt.% of 0.3  $\mu\text{m}$  particles. It appears that a minimum number of particles is required for the destabilisation of emulsions. Figure 5.19 shows the optical microscopy images of the remaining emulsions. When 0.1 wt.% silica was added, large water droplets were observed. In the emulsions with silica particles  $\geq 0.3$  wt.%, droplets disappear whereas particle aggregates are observed instead. Figure 5.20 shows the average droplet diameter of remaining emulsions. The value for the initial emulsion (without destabilisers) after

stirring is about 200  $\mu\text{m}$ . Addition of 0.1 wt.% silica particles induces little difference, while addition of 0.2 wt.% silica particles results in a significant increase in droplet diameter. Further increase of particle concentration continuously increases the droplet size until those with more than 0.3 wt.% silica, where no droplets were observed.

**Figure 5.18.** (a) Appearance of water-in-dodecane emulsions ( $\phi_w = 0.5$ ) stabilized by 2 wt.% carboxyl PS latex particles ( $d = 0.2 \mu\text{m}$ ) at pH 3 after adding hydrophilic monodispersed silica particles ( $d = 2 \mu\text{m}$ ) at different concentrations (given) and stirring at 300 rpm. Images were taken immediately after 4.5 hours of stirring. (b)  $f_o$  and  $f_w$  of emulsions in (a).

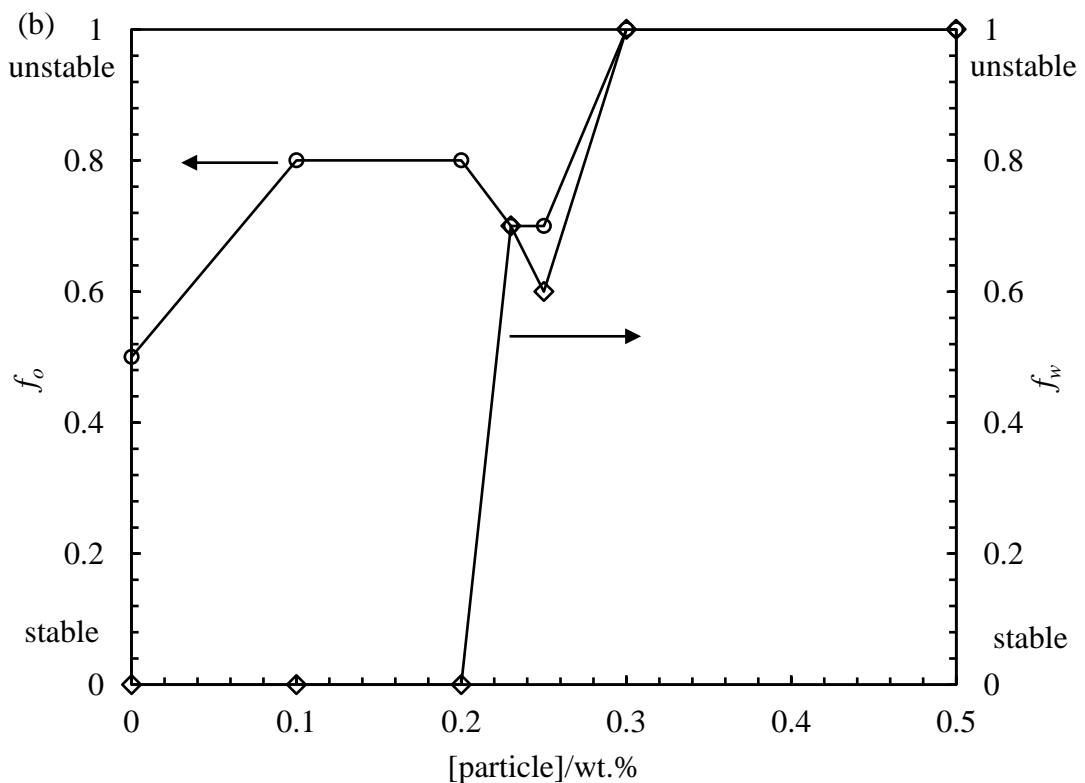


**Figure 5.19.** Optical microscopy images of water-in-dodecane emulsions ( $\phi_w = 0.5$ ) stabilized by 2 wt.% carboxyl PS latex particles ( $d = 0.2 \mu\text{m}$ ) at pH 3 after adding hydrophilic monodispersed silica particles ( $d = 2 \mu\text{m}$ ) at different concentrations (given) and stirring at 300 rpm for 4.5 hours. Taken immediately after stirring. Scale bar = 500  $\mu\text{m}$ .

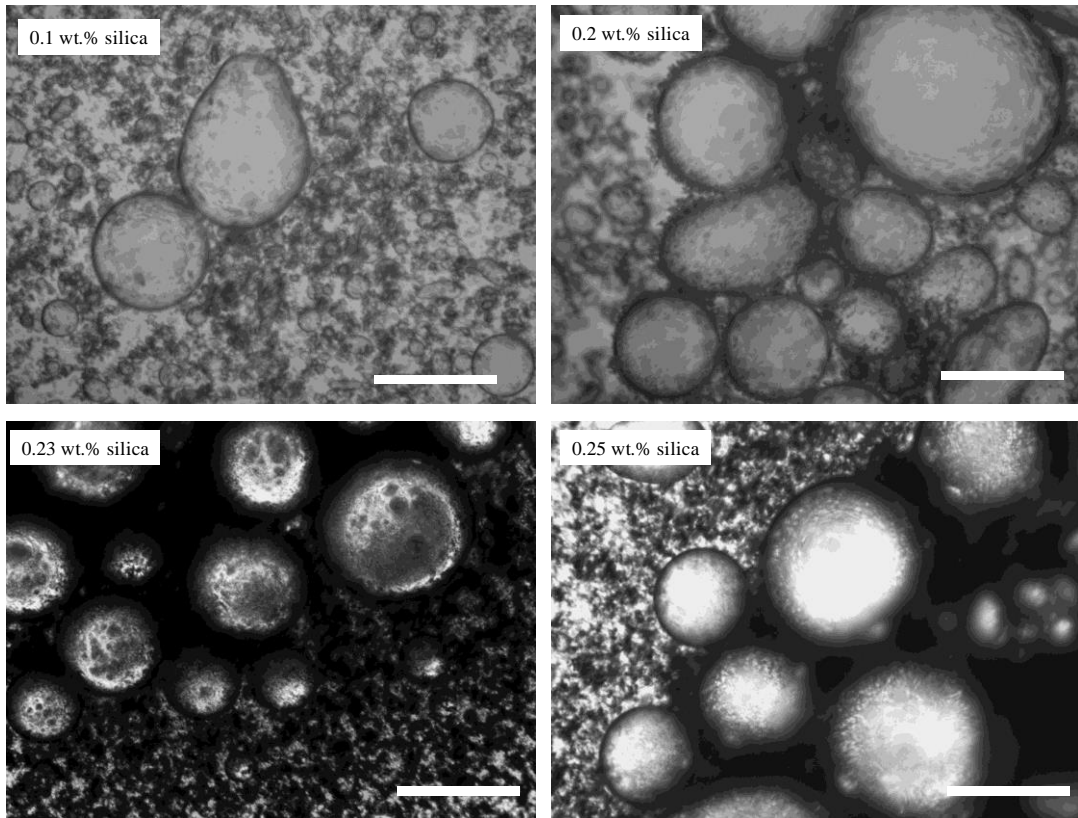
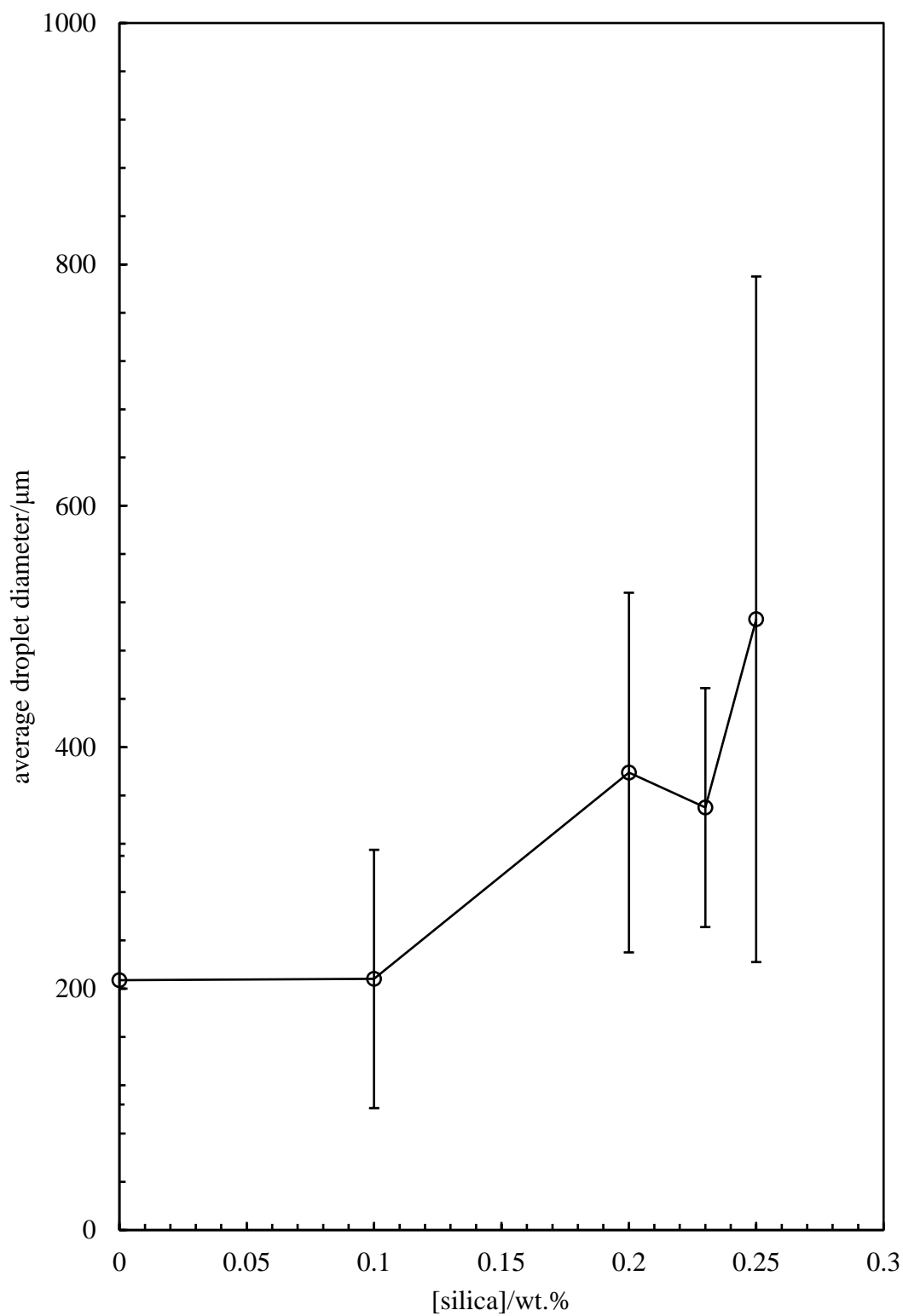


**Figure 5.20.** Average droplet diameter of water-in-dodecane emulsions ( $\phi_w = 0.5$ ) stabilized by 2 wt.% carboxyl PS latex particles ( $d = 0.2 \mu\text{m}$ ) at pH 3 after adding hydrophilic monodispersed silica particles ( $d = 2 \mu\text{m}$ ) at different concentrations and stirring at 300 rpm for 4.5 hours.



To explore the position of each type of particles after the destabilization, optical microscopy images of each phase were taken. As controls, the optical microscopy images of carboxyl latex particles and monodispersed silica particles in water at pH 3 were taken together with monodispersed silica particles in dodecane, as shown in Figure 5.21 (a), (b) and (c), respectively. Large aggregates of carboxyl latex particles were observed in the aqueous dispersion, whereas silica particles were discrete in water, and small aggregates co-existing with single particles were observed in dodecane. Figure 5.22 shows the samples in the oil layers after destabilisation of the emulsions. In the emulsion without and with 0.1 wt.% silica particles, particle aggregates attaching at droplets were observed. The appearance of the aggregates resembles the carboxyl latex aggregates in the aqueous dispersion. In emulsions with moderate concentrations of silica particles, free carboxyl latex aggregates along with several emulsion droplets were observed. By contrast, in the samples containing higher concentrations of silica particles, only carboxyl latex particle aggregates were observed. Figure 5.23 shows the optical microscopy of resolved aqueous phase after stirring. Discrete particles were observed on all images, which look the same as silica particles in the aqueous dispersion. In addition, the number of particles on each image increases with added silica particle concentrations. This indicates that silica particles travel from the oil phase to the aqueous phase after breaking of emulsion droplets. This is reasonable as silica particles are highly hydrophilic and tend to be wetted by water. By contrast, the carboxyl particle aggregates which initially dispersed in aqueous phases end up in oil phase, indicating these particles travel from the aqueous phase to the oil phase during stirring.

**Figure 5.21.** Optical microscopy of (a) 2 wt.% carboxyl polystyrene (PS) latex particles in the aqueous dispersion at pH 3, (b) 0.5 wt.% monodispersed silica particles ( $d = 2 \mu\text{m}$ ) in aqueous dispersion and (c) in dodecane.

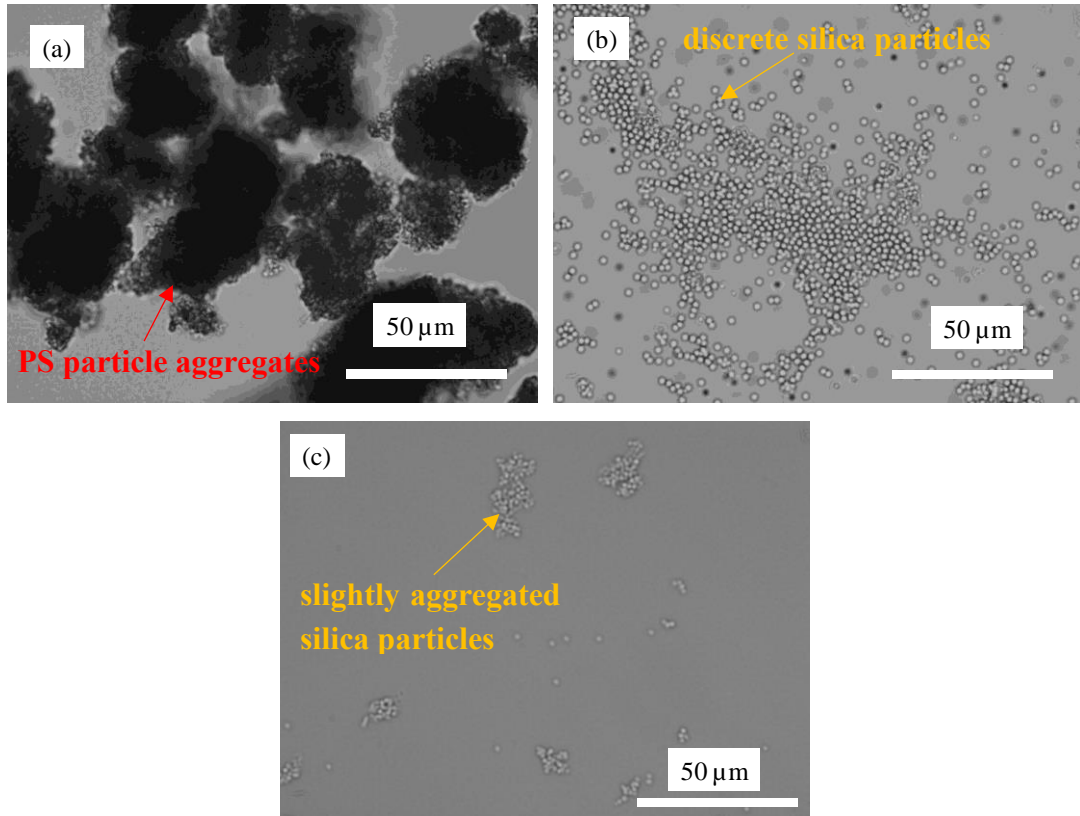


**Figure 5.22.** Optical microscopy of particles in the oil layers after breaking of emulsions ( $\phi_w = 0.5$ ) stabilized by 2 wt.% carboxyl PS latex particles ( $d = 0.2 \mu\text{m}$ ) at pH 3 by adding hydrophilic monodispersed silica particles ( $d = 2 \mu\text{m}$ ) and stirring at 300 rpm for 4.5 hours. Taken immediately after stirring. Scale bar = 50  $\mu\text{m}$ .

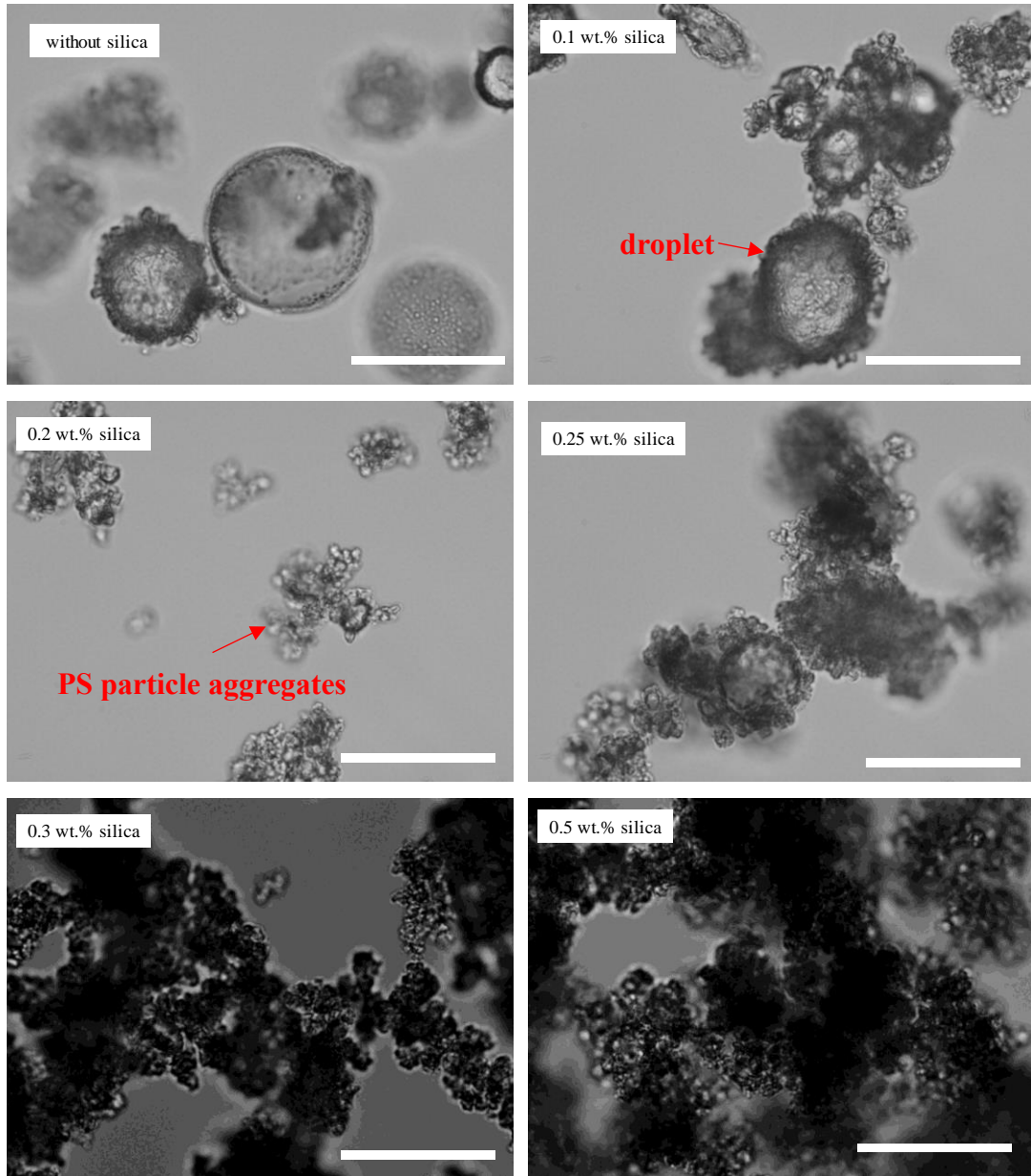
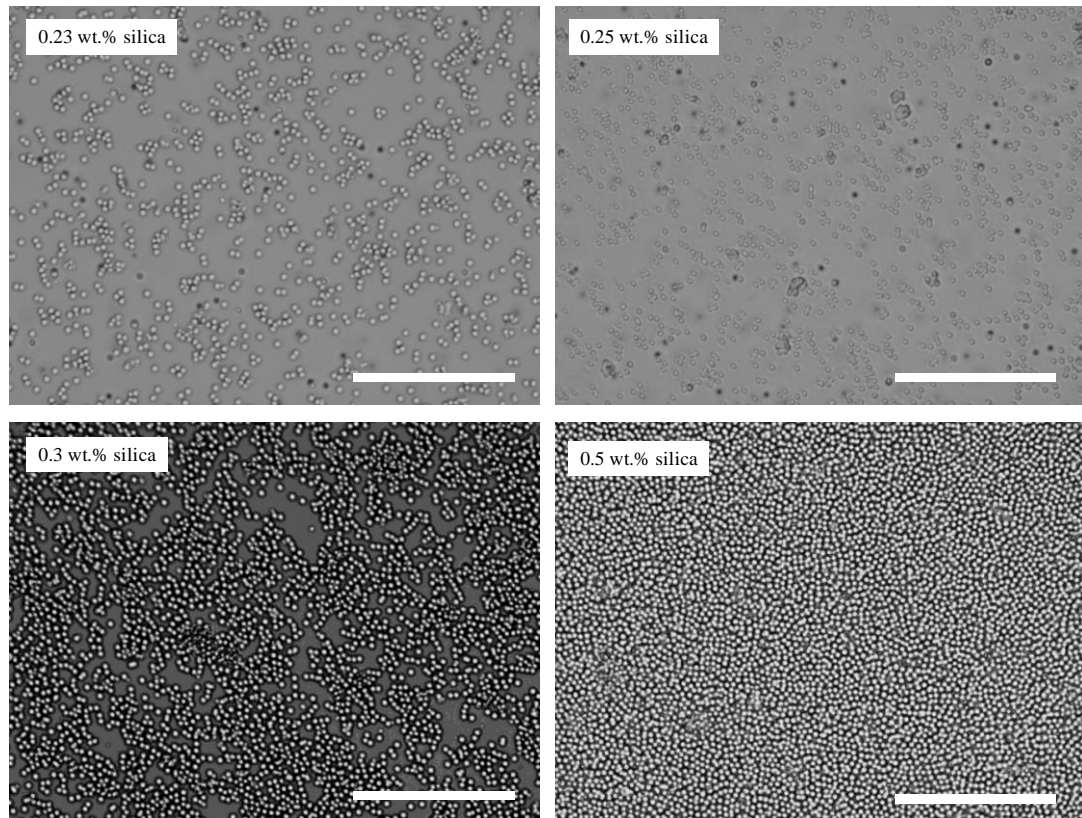


**Figure 5.23.** Optical microscopy images of particles in the released water after breaking of emulsions ( $\phi_w = 0.5$ ) stabilized by 2 wt.% carboxyl PS latex particles ( $d = 0.2 \mu\text{m}$ ) at pH 3 by adding hydrophilic monodispersed silica particles ( $d = 2 \mu\text{m}$ ) and stirring at 300 rpm for 4.5 hours. Taken immediately after stirring. Scale bar = 50  $\mu\text{m}$ .



### 5.2.3.2 Destabilization at $\phi_w = 0.7$

In the previous sections, the initial emulsions prepared at  $\phi_w = 0.5$  are partially unstable to sedimentation. For the destabilization process, initial emulsions completely stable to both sedimentation and coalescence were preferred. Therefore, an effort has been made to prepare emulsions with higher sedimentation stability. In this section, emulsions stabilized by 2 wt.% carboxyl latex particles at  $\phi_w = 0.7$  and pH 3 were prepared. Monodispersed silica particles ( $d = 2 \mu\text{m}$ ) were added to the model emulsions and rendered to stir for 4.5 hours. The appearance of the remaining emulsions is shown in Figure 5.24 (a). Water starts to release from the emulsion at a particle concentration of 0.13 wt.%, lower than the 0.23 wt.% in the case of emulsions prepared at  $\phi_w = 0.5$ . This indicates that silica particles are more effective in destabilising w/o emulsions at higher water content. The reason is possibly that these emulsions has less oil in the continuous phase, which results in thinner oil layers between droplets. Hence, droplets have more chance to collide and coalesce during stirring. Complete phase separation of emulsions occurs at silica particles concentrations  $\leq 0.3$  wt.%, the same as the emulsions prepared at  $\phi_w = 0.5$ . Figure 5.24 (b) represents the  $f_o$  and  $f_w$  of emulsions against silica particle concentration after stirring. Both  $f_o$  and  $f_w$  increase rapidly with particle concentration until reaching 1, indicating an increase in destabilisation efficiency at higher particle concentrations. Figure 5.25 shows the optical microscopy of the remaining emulsions and Figure 5.26 represents the average droplet diameter. Resembling the case of emulsions prepared at  $\phi_w = 0.5$ , 0.1 wt.% silica particles make no difference. While increase of silica concentration results in a significant increase in the emulsion droplet size, and in the samples with more than 0.3 wt.% of silica particles, carboxyl latex particle aggregations were observed instead of emulsion droplets. Carboxyl latex particles transferring to the oil phases while silica particles end up in resolved water after breaking of emulsion droplets were also observed, as illustrated in Figure 5.27 and Figure 5.28.

**Figure 5.24.** (a) Appearance of water-in-dodecane emulsions ( $\phi_w = 0.7$ ) stabilized by 2 wt.% carboxyl PS latex particles ( $d = 0.2 \mu\text{m}$ ) at pH 3 after adding monodispersed silica particles ( $d = 2 \mu\text{m}$ ) at different concentrations and stirred at 300 rpm. Taken immediately after 4.5 hours of stirring. (b)  $f_o$  and  $f_w$  of emulsions in (a) against particle concentration.

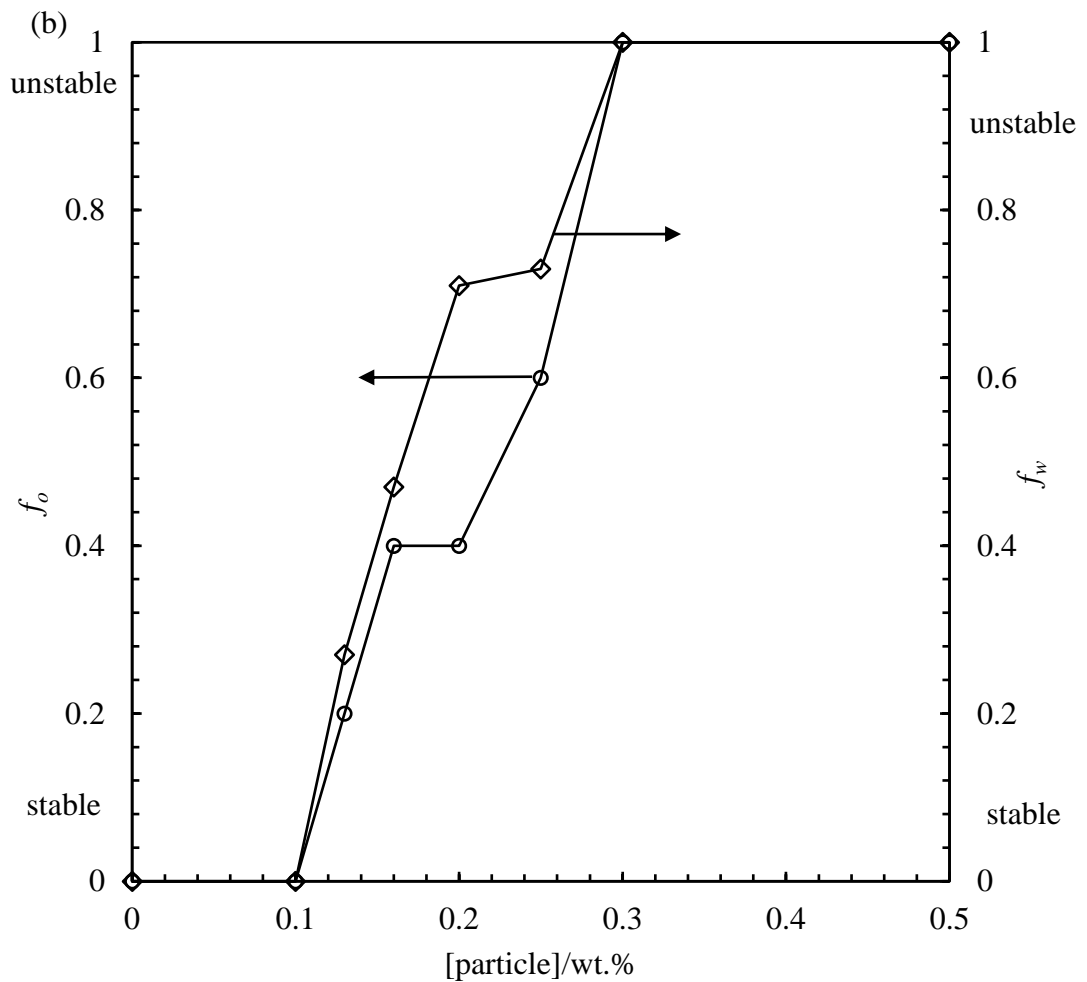
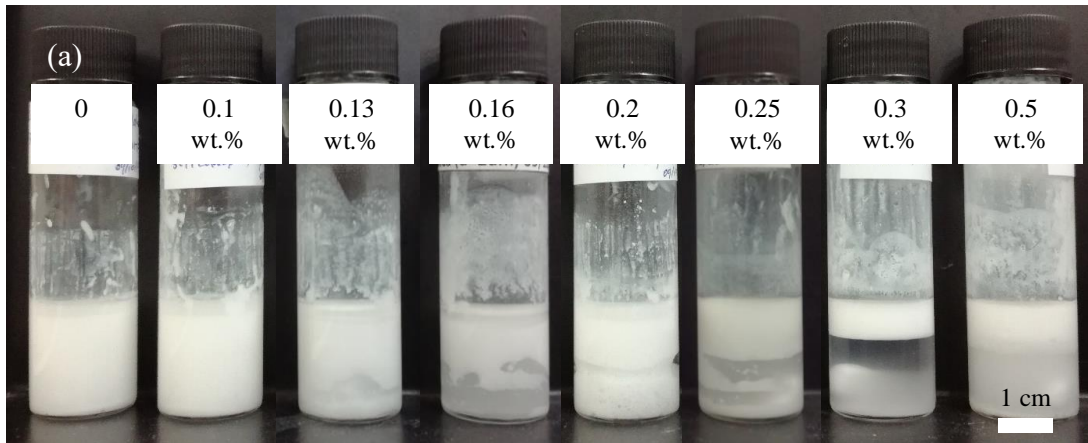


**Figure 5.25.** Optical microscopy of water-in-dodecane emulsions ( $\phi_w = 0.7$ ) stabilized by 2 wt.% carboxyl PS latex particles ( $d = 0.2 \mu\text{m}$ ) at pH 3 after adding monodispersed silica particles ( $d = 2 \mu\text{m}$ ) at different concentrations (given) and stirring at 300 rpm for 4.5 hours. Taken immediately after stirring. Scale bar =  $500 \mu\text{m}$ .

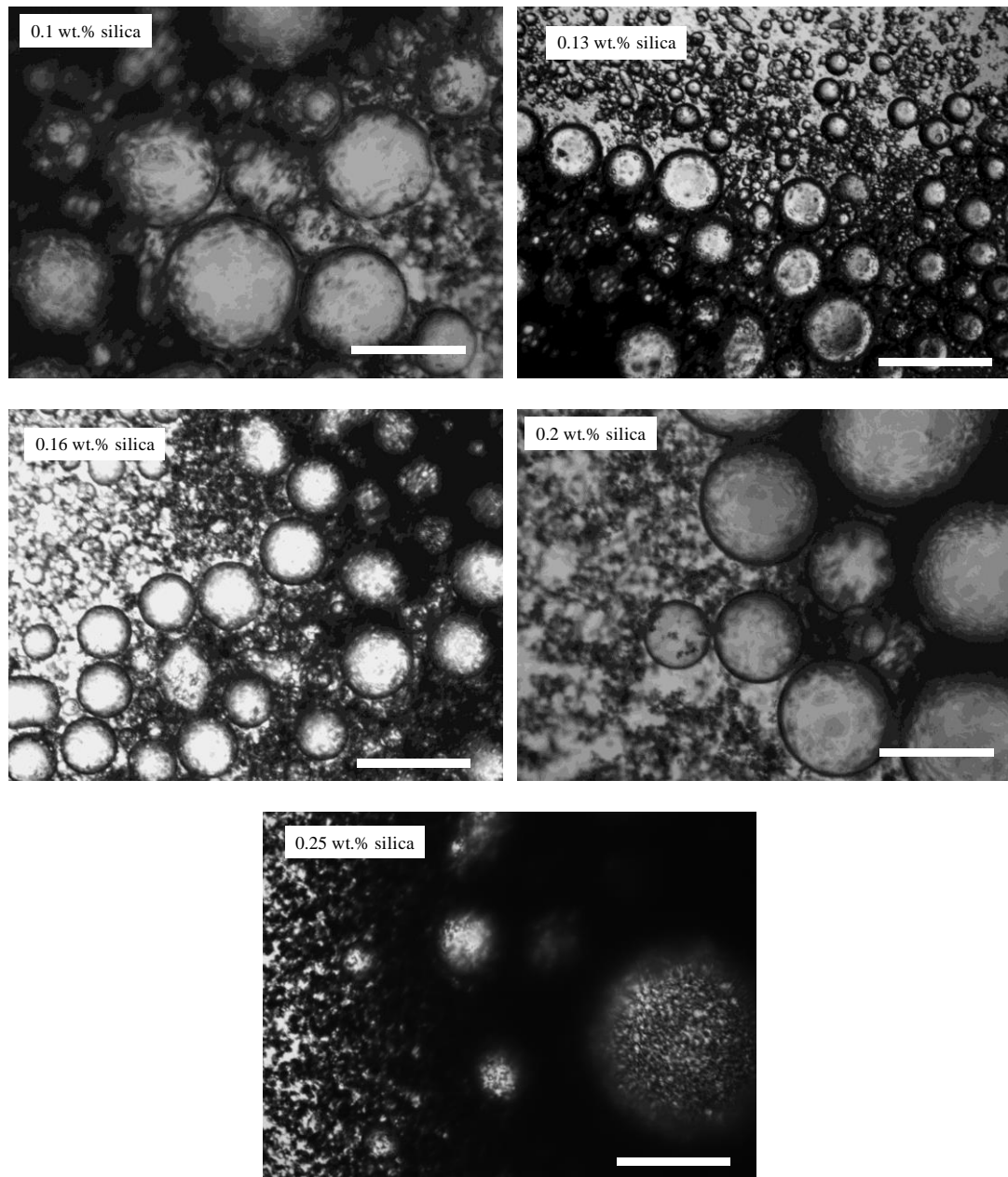


**Figure 5.26.** Average droplet diameter of water-in-dodecane emulsions ( $\phi_w = 0.7$ ) stabilized by 2 wt.% carboxyl PS latex particles ( $d = 0.2 \mu\text{m}$ ) at pH 3 after adding monodispersed silica particles ( $d = 2 \mu\text{m}$ ) and stirring at 300 rpm for 4.5 hours, plotted against silica particle concentration.

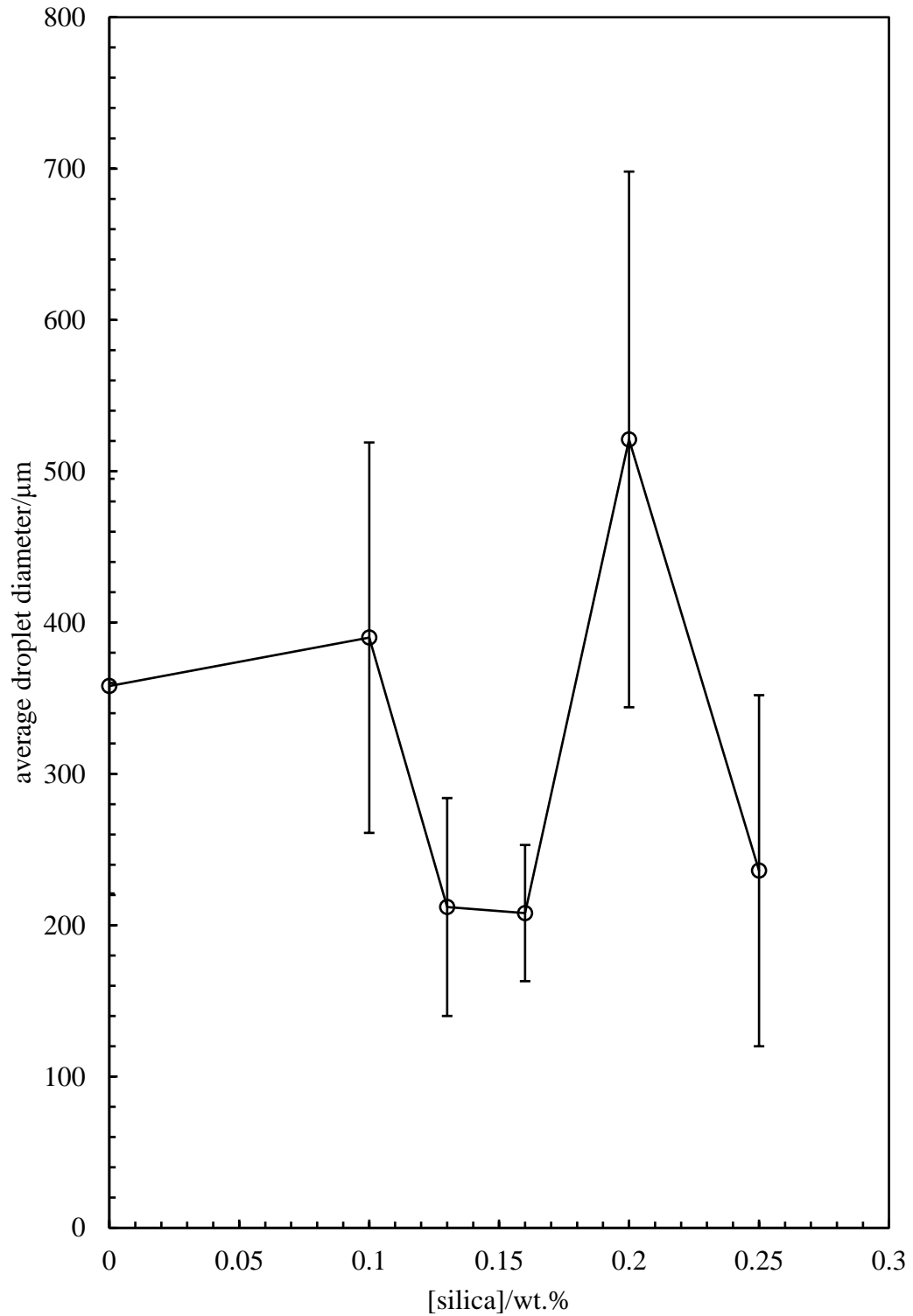


**Figure 5.27.** Optical microscopy images of particles in the oil layers after breaking of emulsions ( $\phi_w = 0.7$ ) stabilized by 2 wt.% carboxyl PS latex particles ( $d = 0.2 \mu\text{m}$ ) at pH 3 by adding hydrophilic monodispersed silica particles ( $d = 2 \mu\text{m}$ ) and stirring at 300 rpm for 4.5 hours. Taken immediately after stirring. Scale bar = 50  $\mu\text{m}$ .

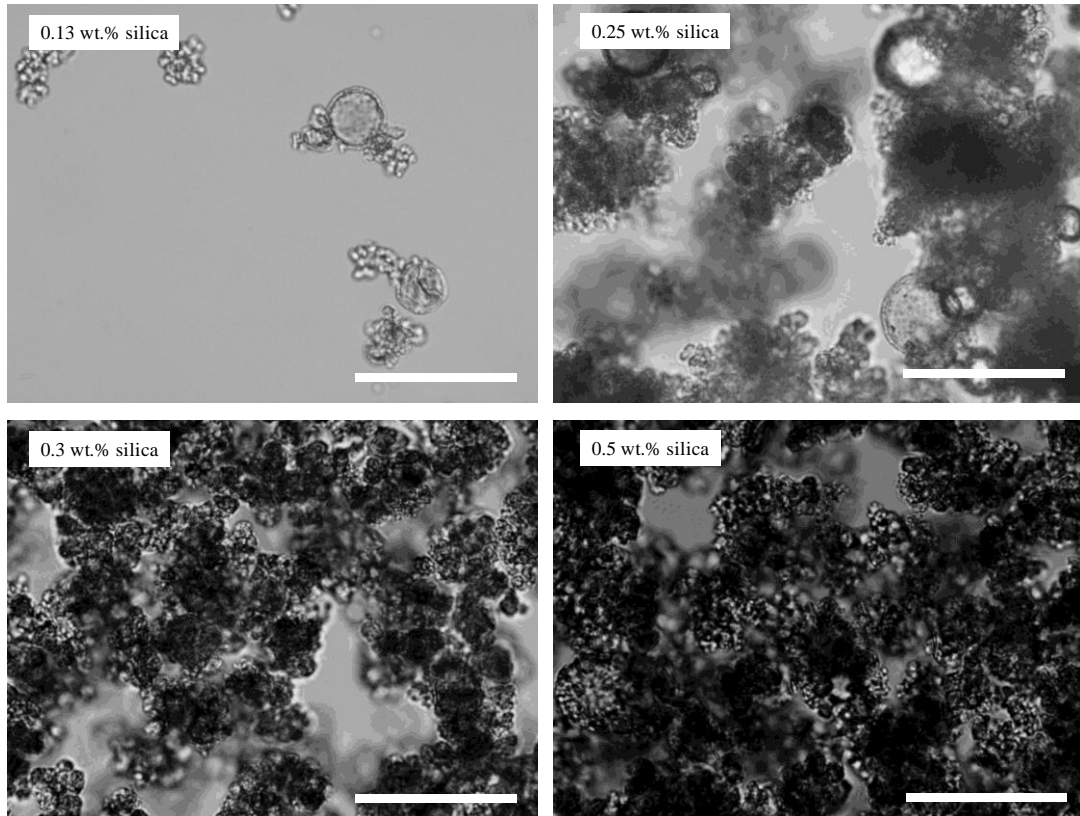
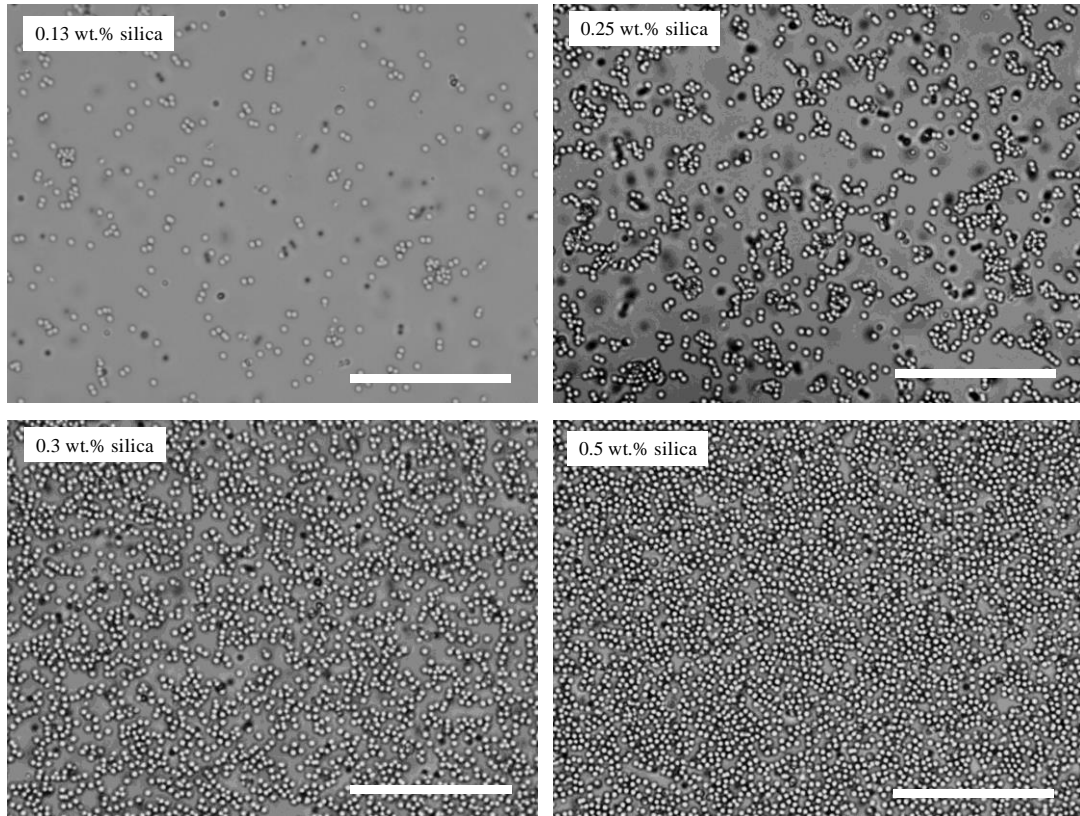


**Figure 5.28.** Optical microscopy images of particles in the released water after breaking of emulsions ( $\phi_w = 0.7$ ) stabilized by 2 wt.% carboxyl PS latex particles ( $d = 0.2 \mu\text{m}$ ) at pH 3 by adding hydrophilic monodispersed silica particles ( $d = 2 \mu\text{m}$ ) and stirring at 300 rpm for 4.5 hours. Taken immediately after stirring. Scale bar = 50  $\mu\text{m}$ .

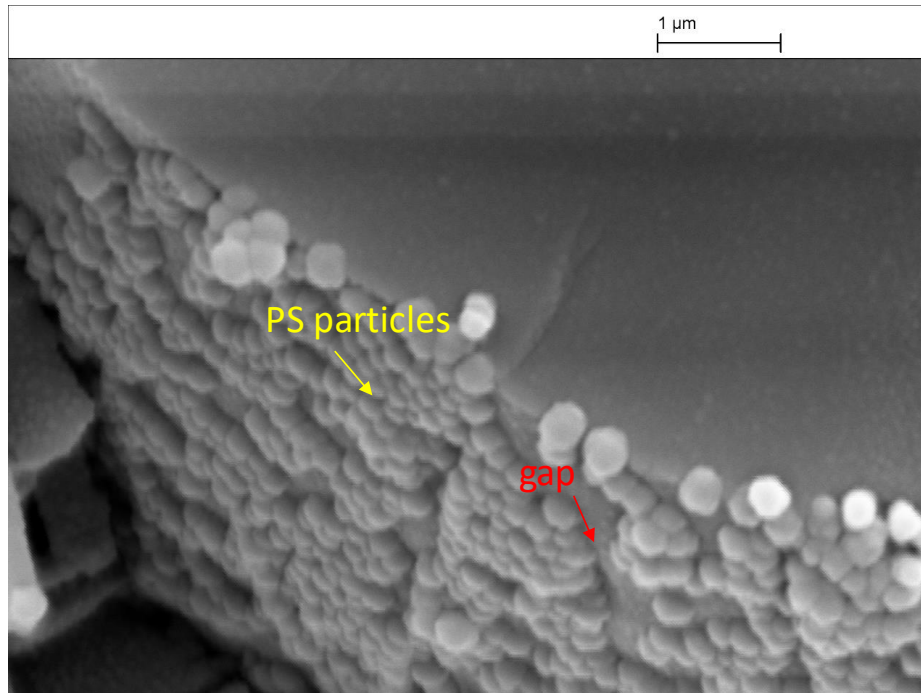


### 5.2.3.3 Possible mechanism of destabilization

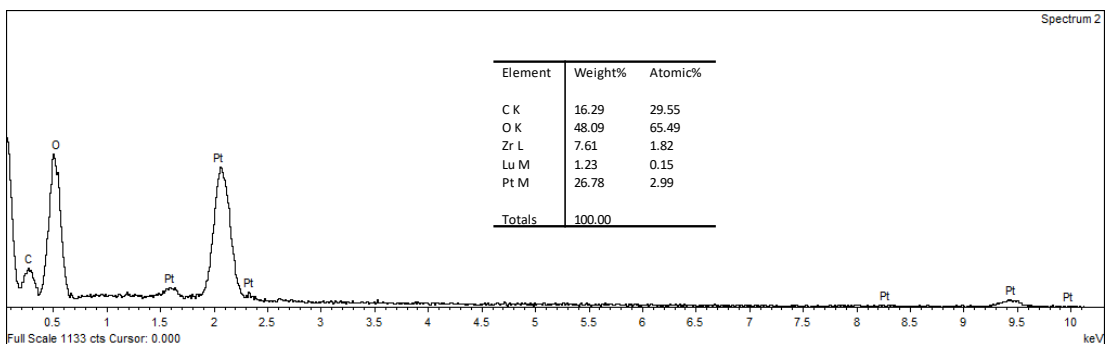
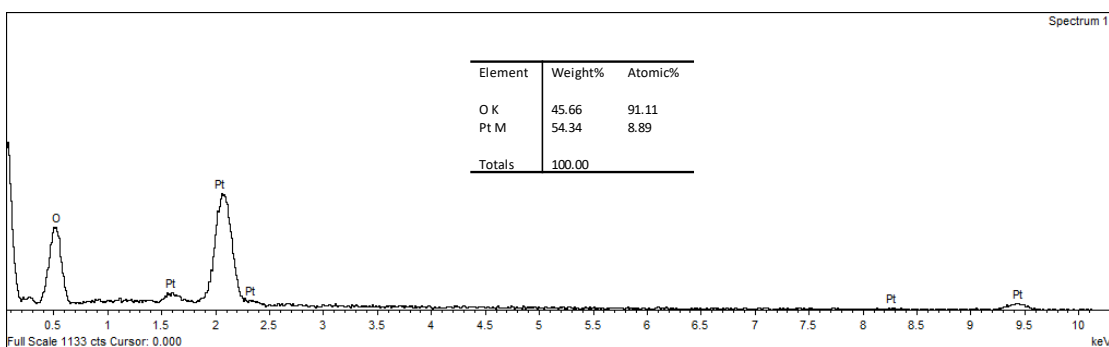
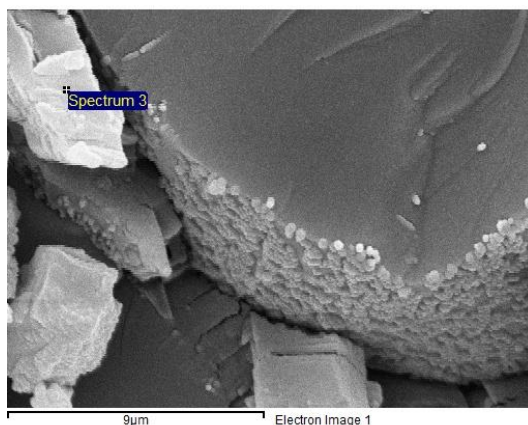
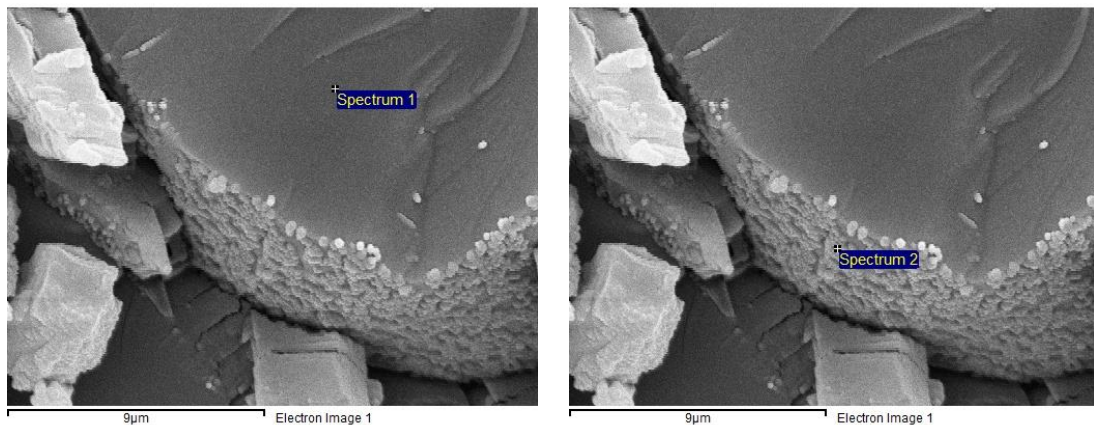
The results in the previous sections indicate that monodispersed silica particles are able to destabilize w/o emulsions stabilized by carboxyl latex particles after gentle stirring. However, the mechanism remains a mystery. It has been reported that silica particles are able to destabilize o/w Pickering emulsions if they are hydrophobic enough.<sup>10</sup> The hypothesis is that higher wettability of hydrophobic silica particles by the inner phase of droplets than that by the continuous phase promotes particles protruding the oil-water interface and wetted by the inner phase, which finally results in the breaking of droplets.

To trace the position of silica particles during the destabilisation process thus to explore the mechanism of destabilisation, Cryo-SEM with EDX spectrum were conducted on emulsions. Figure 5.29 shows the Cryo-SEM image of an initial water-in-dodecane emulsion stabilized by 2 wt.% carboxyl PS latex particles ( $d = 0.2 \mu\text{m}$ ) at  $\phi_w = 0.5$  and pH 3. As can be seen, monodispersed PS latex particles as well as particle clusters are adsorbing at the droplet surface. The droplet surface is loosely packed by the particles, gaps between particle-rich areas can be determined. We recall that in the aqueous dispersions at pH 3, carboxyl PS latex particles aggregates with diameter of  $\sim 20 \mu\text{m}$  were measured by Mastersizer 2000 (see Figure 4.16 in section 4.3.3). Therefore, the Cryo-SEM image implies that homogenization at 13,000 rpm for 2 minutes breaks large particle aggregates into much smaller clusters and single particles. Figure 5.30 shows corresponding EDX spectra of selected spots on the droplet. On spectrum 1 inside the droplet, only oxygen atoms were detected, indicating the presence of water inside the droplet. Spectrum 2 shows the information of carbon and oxygen atoms, with the percentage of oxygen much higher than that of carbon. This spectrum represents the information of a carboxyl PS latex particle, as there is co-existence of polystyrene (gives carbon atoms) and carboxyl groups (give oxygen atoms). In addition, as carboxyl PS latex particle initially dispersed in water, the weight percentage of oxygen can also be contributed by residues water on the particle surface. Spectrum 3 also shows the information of carbon and oxygen atoms. However, the weight percentage of carbon is much higher than that of oxygen. This is likely dodecane with a trace amount of water.

**Figure 5.29.** Cryo-scanning electron microscopy (Cryo-SEM) of a water-in-dodecane emulsion ( $\phi_w = 0.5$ ) stabilized by 2 wt.% carboxyl PS latex particles ( $d = 0.2 \mu\text{m}$ ) at pH 3, taken two days after preparation.



**Figure 5.30.** Cryo-SEM and corresponding energy dispersive X-ray spectrometry (EDX) spectrum of a water-in-dodecane emulsion ( $\phi_w = 0.5$ ) stabilized by 2 wt.% carboxyl PS latex particles ( $d = 0.2 \mu\text{m}$ ) at pH 3, taken two days after preparation.



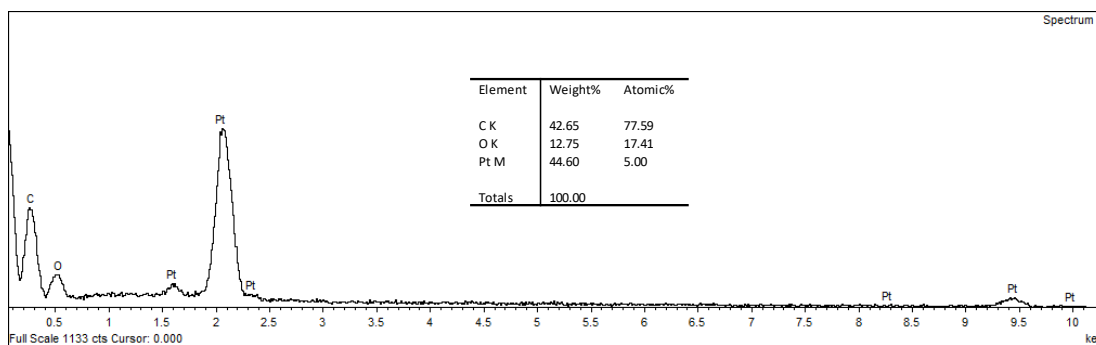
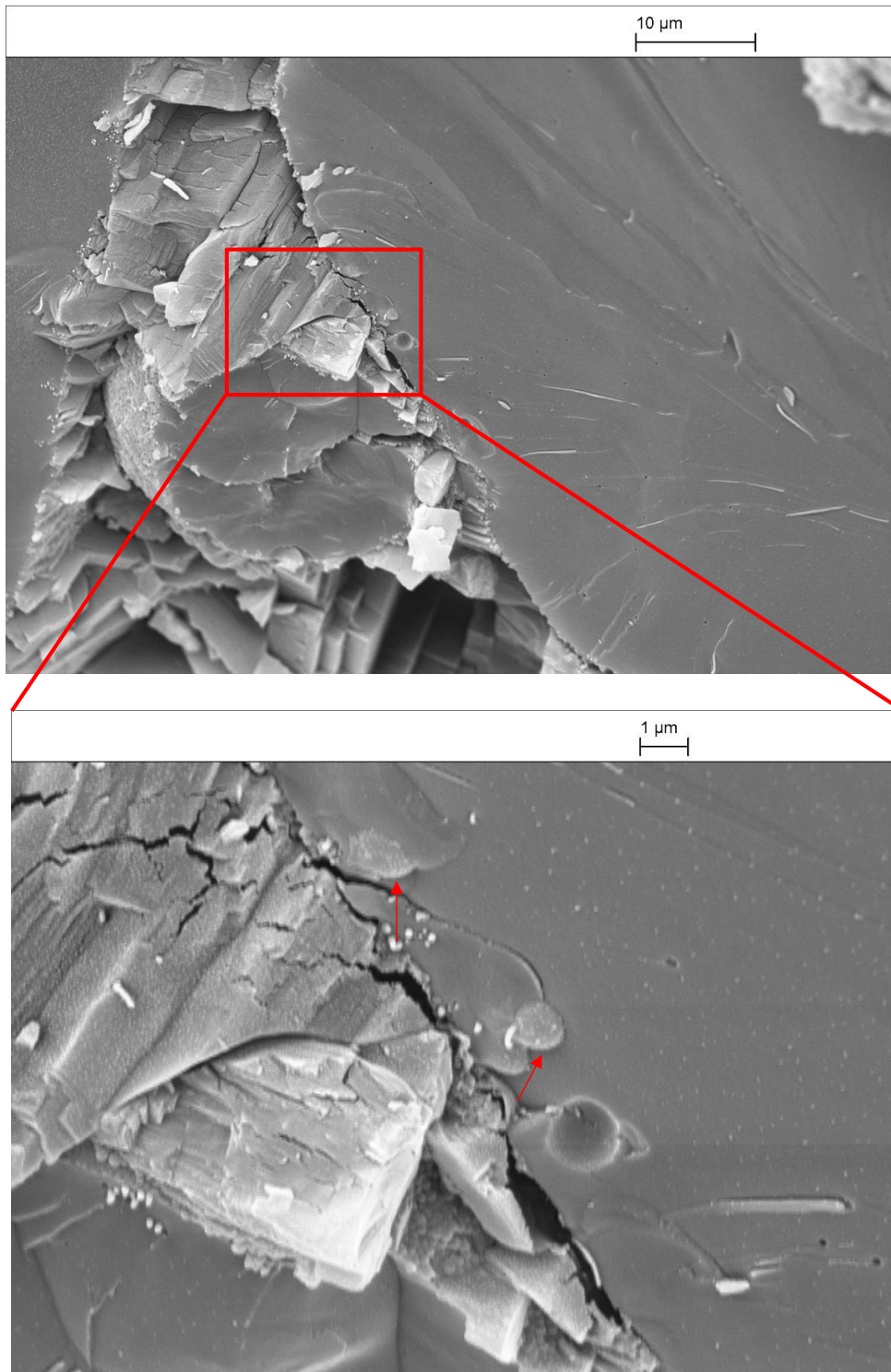
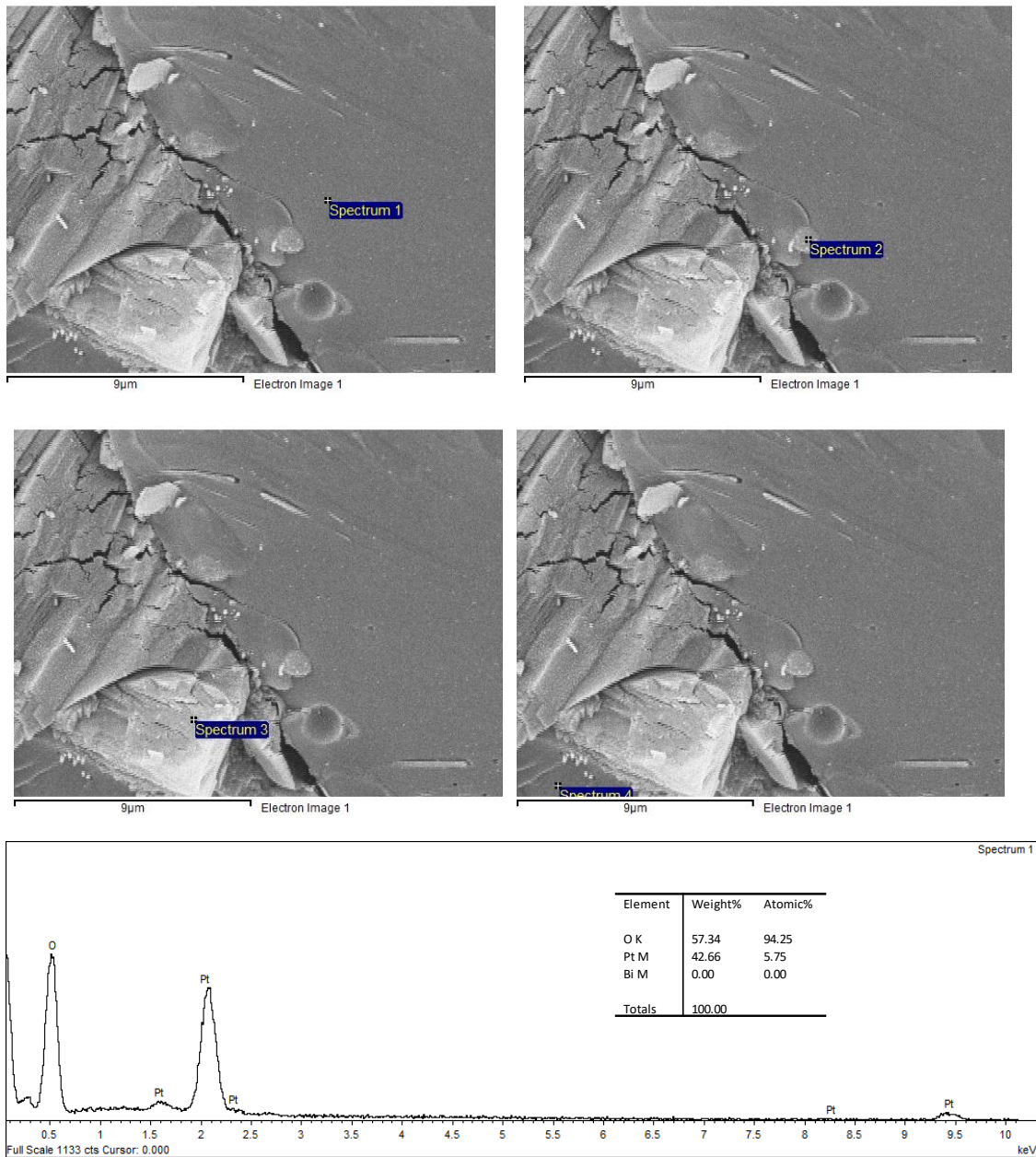


Figure 5.31 shows the Cryo-SEM of a water-in-dodecane emulsion stabilized by 2 wt.% carboxyl PS latex particles ( $d = 0.2 \mu\text{m}$ ) at  $\phi_w = 0.5$  and pH 3 after adding 0.25 wt.% (relative to the mass of emulsion) hydrophilic monodispersed silica particles ( $d = 2 \mu\text{m}$ ) and stirring at 300 rpm for 2 hours. This is the half-way of the destabilisation procedure, where a small volume of water is resolved but the majority of the droplets remain unbroken. The edges of two large droplets can be determined on the image, between which is a relatively smaller droplet. On the magnified image of the portion in the red frame, two spherical silica particles can be determined. Figure 5.32 shows the corresponding EDX spectrum of selected spots on the droplet. Spectrum 1 shows the information of oxygen atoms, indicating water inside the droplet. Spectrum 2 shows the information of silicone and oxygen atoms, which confirms the silica particle. Spectrum 3 and 4 illustrates the content of dodecane and inner water of a neighbour droplet, respectively. Figure 5.33 represents the EDX mapping of the same emulsion sample. Light spots represent the distribution of corresponding elements. The distribution of carbon atoms illustrates a dodecane layer between two droplets, that of oxygen atoms shows the frame of two neighbouring water droplets and that of silicone atoms illustrates the profile of silica particles. The Cryo-SEM images with the corresponding EDX spectrum and mapping imply that silica particles end up inside water droplets. It is worth to note that when silica particles were added to the emulsion, they were initially dispersed in the oil. This means silica particles entering into emulsion droplets through oil-water interfaces, which disturbs the oil-water interface and results in coalescence of emulsion droplets.

**Figure 5.31.** Cryo-SEM of a water-in-dodecane emulsion ( $\phi_w = 0.5$ ) stabilized by 2 wt.% carboxyl PS latex particles ( $d = 0.2 \mu\text{m}$ ) at pH 3 after adding 0.25 wt.% (relative to the mass of emulsion) hydrophilic monodispersed silica particles ( $d = 2 \mu\text{m}$ ) and stirring at 300 rpm for 2 hours. Red arrows point out the silica particles inside a droplet.



**Figure 5.32.** Cryo-Scanning electron microscopy images and corresponding EDX spectrum of a water-in-dodecane emulsion ( $\phi_w = 0.5$ ) stabilized by 2 wt.% carboxyl PS latex particles ( $d = 0.2 \mu\text{m}$ ) at pH 3 after adding 0.25 wt.% (relative to the mass of emulsion) hydrophilic monodispersed silica particles ( $d = 2 \mu\text{m}$ ) and stirring at 300 rpm for 2 hours.



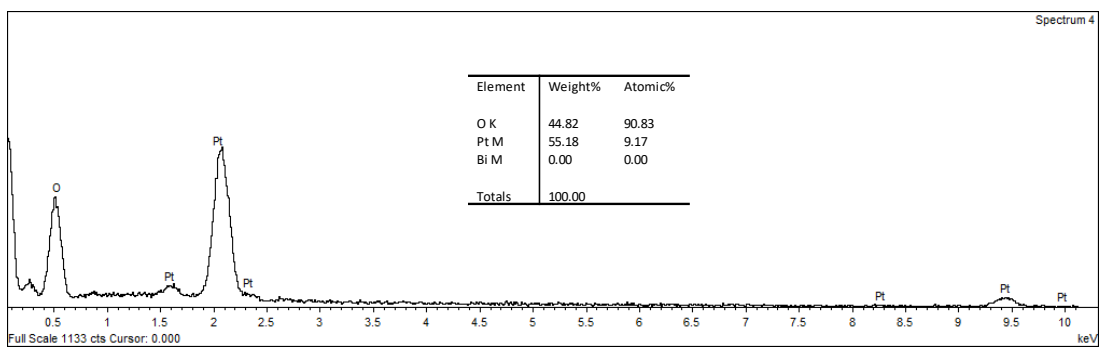
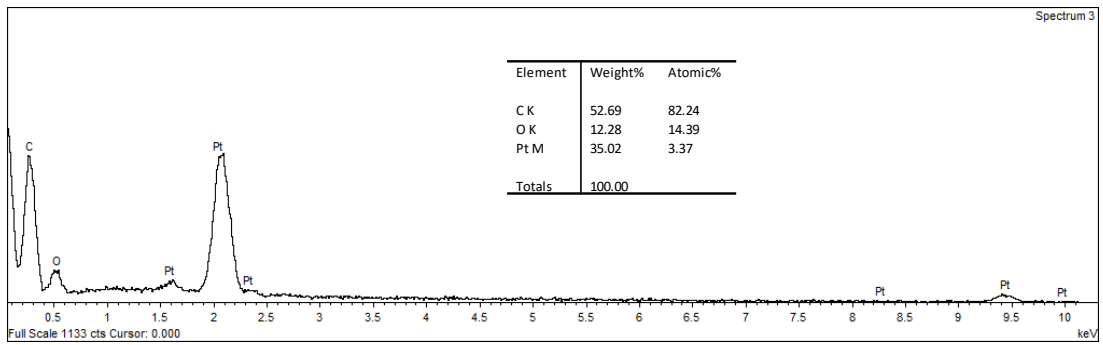
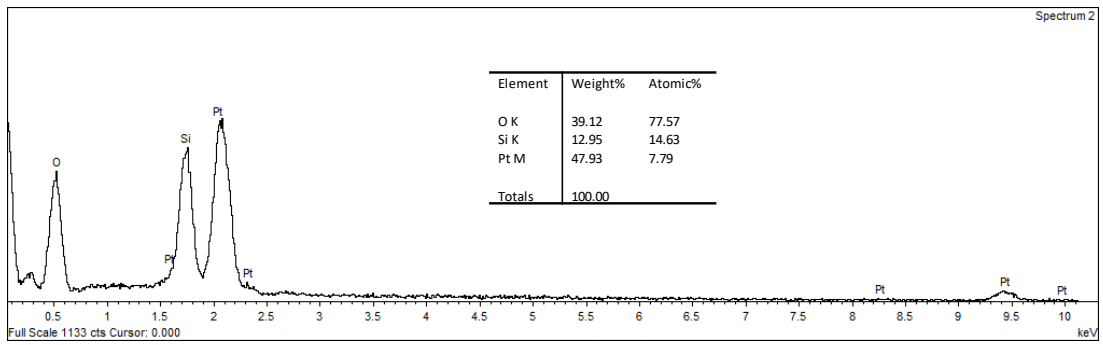


**Figure 5.33.** Energy dispersive X-ray spectrometry mapping on a water-in-dodecane emulsion ( $\phi_w = 0.5$ ) stabilized by 2 wt.% carboxyl PS latex particles ( $d = 0.2 \mu\text{m}$ ) at pH 3 after adding 0.25 wt.% (relative to the mass of emulsion) hydrophilic monodispersed silica particles ( $d = 2 \mu\text{m}$ ) and stirring at 300 rpm for 2 hours.

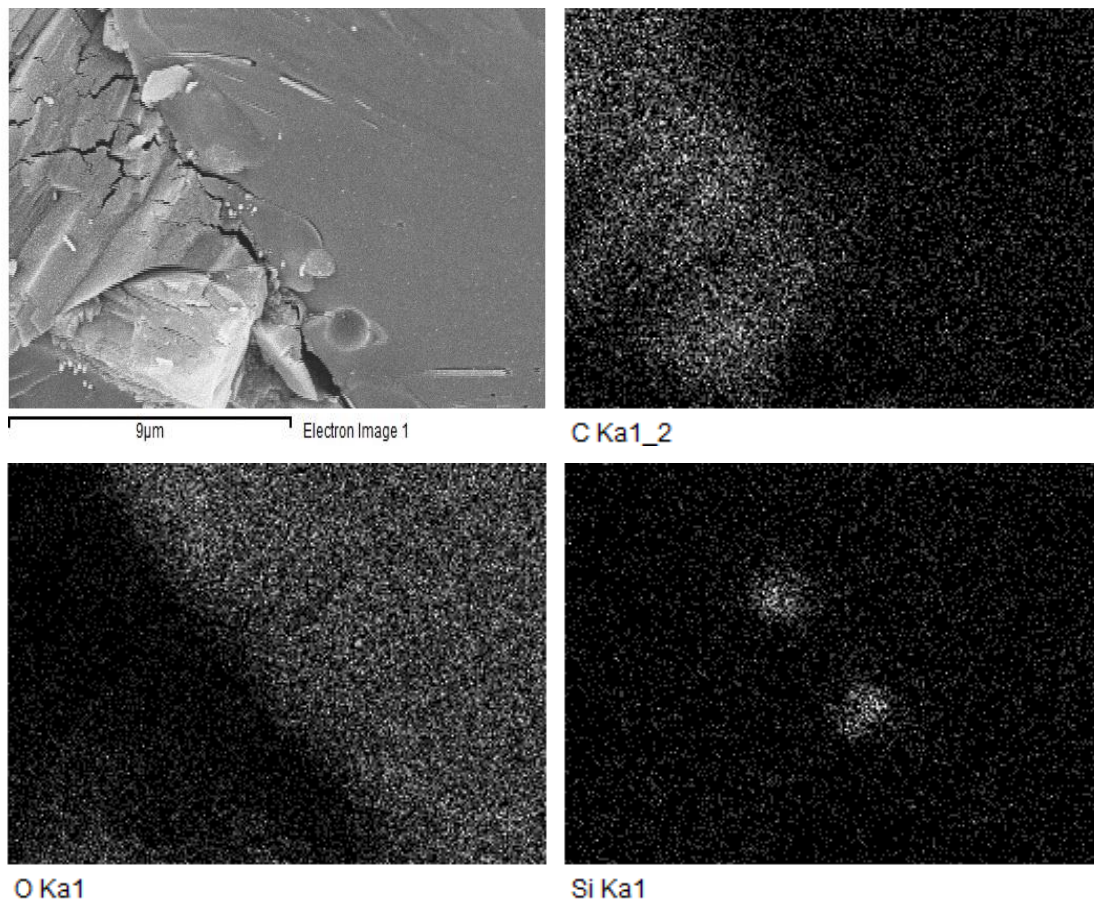
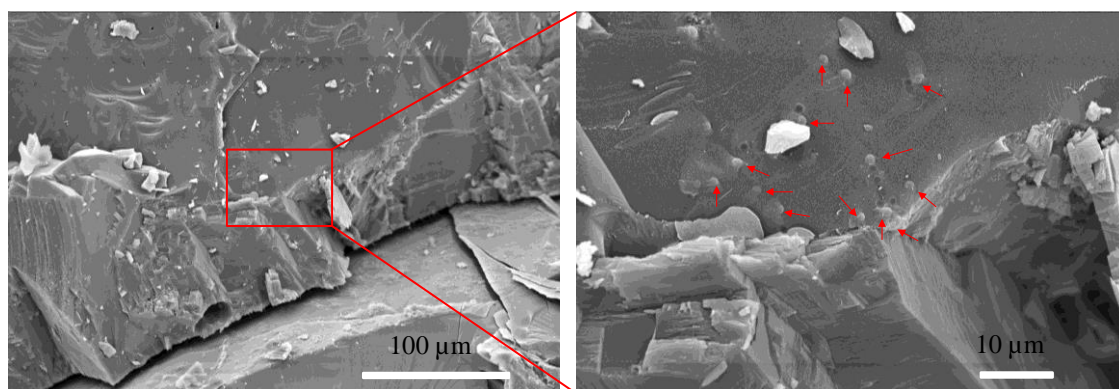
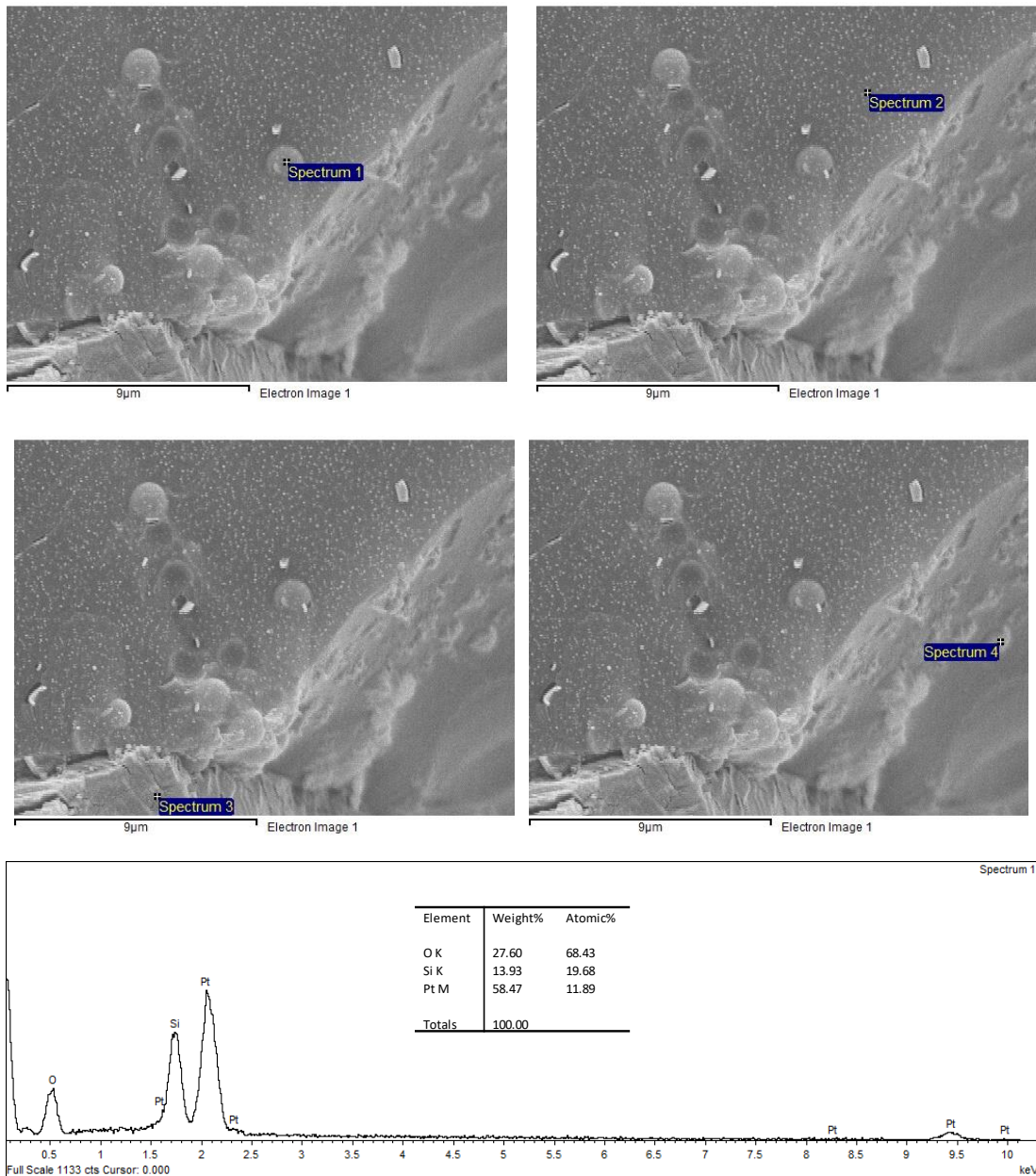


Figure 5.34 shows Cryo-SEM images of a parallel emulsion after adding 0.25 wt.% hydrophilic monodispersed silica particles ( $d = 2 \mu\text{m}$ ) and stirred at 300 rpm for 4.5 hours. As has been studied in last section (see Figure 5.18), the majority of initial water was released from the emulsion but there were several large water droplets left. Two neighbouring large droplets can be detected from the image and spherical silica particles can be observed from the magnified image. In addition, several silica particles are observed attaching at the frozen oil-water interface, which is convincing evidence of silica entering from the oil to the inner water phase by protruding into the oil-water interface. Figure 5.35 and Figure 5.36 show the EDX spectrum of selected spots and EDX mapping, respectively, confirming the distribution of water, dodecane and silica particles. In addition, compared with the parallel sample stirred for 2 hours, more silica particles are detected inside the water droplet after 4.5 hours of stirring, indicating that more silica particles protrude the oil-water interface, which should lead to more coalescence of emulsion, indeed consistent with the findings in Figure 5.18.

**Figure 5.34.** Cryo-Scanning electron microscopy images of a water-in-dodecane emulsion ( $\phi_w = 0.5$ ) stabilized by 2 wt.% carboxyl PS latex particles ( $d = 0.2 \mu\text{m}$ ) at pH 3 after adding 0.25 wt.% (relative to the mass of emulsion) hydrophilic monodispersed silica particles ( $d = 2 \mu\text{m}$ ) and stirring at 300 rpm for 4.5 hours. Red arrows point out the silica particles inside a droplet and adsorbing at oil-water interface.



**Figure 5.35.** Cryo-Scanning electron microscopy images and corresponding EDX spectrum of a water-in-dodecane emulsion ( $\phi_w = 0.5$ ) stabilized by 2 wt.% carboxyl PS latex particles ( $d = 0.2 \mu\text{m}$ ) at pH 3 after adding 0.25 wt.% (relative to the mass of emulsion) hydrophilic monodispersed silica particles ( $d = 2 \mu\text{m}$ ) and stirring at 300 rpm for 4.5 hours.



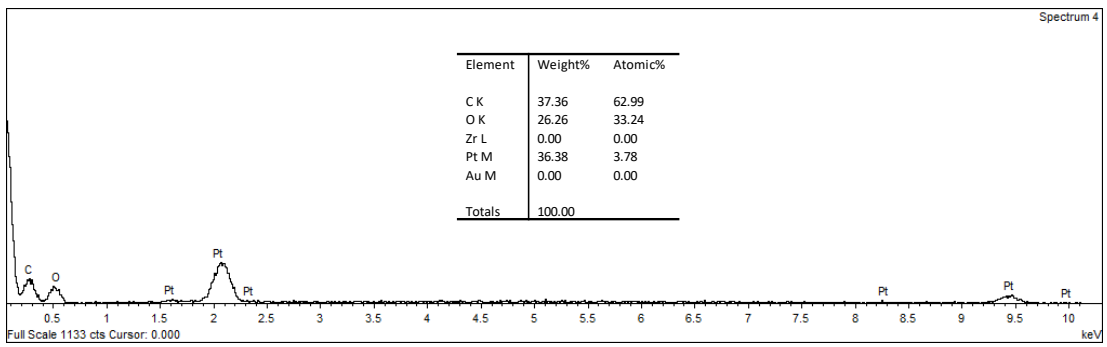
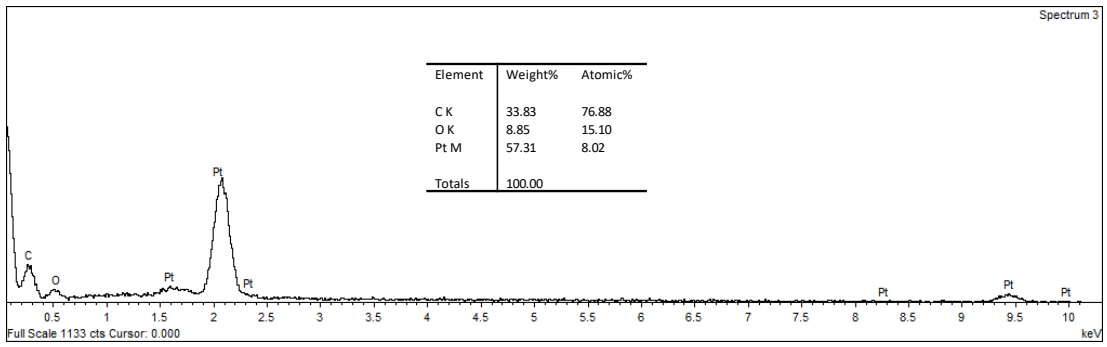
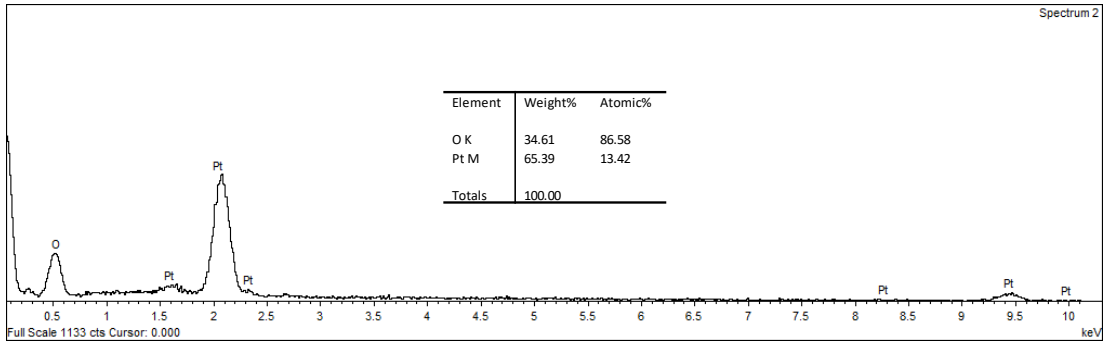
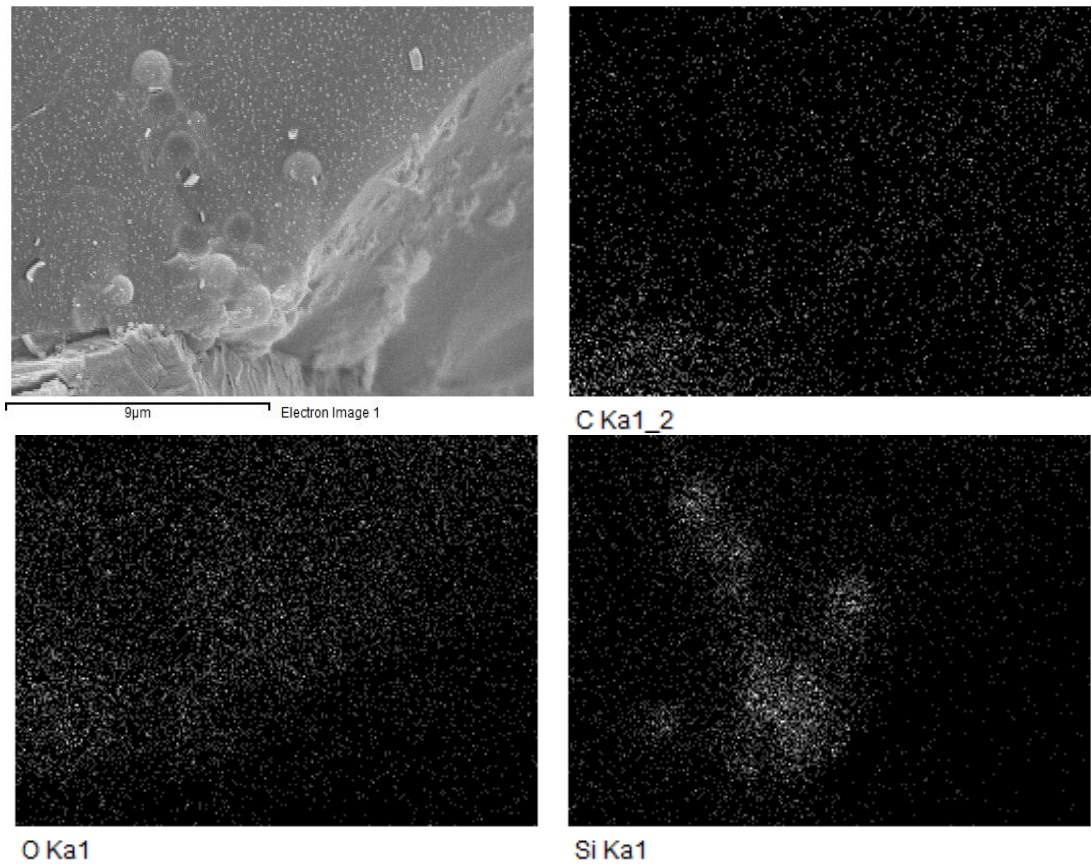


**Figure 5.36.** Energy dispersive X-ray spectrometry mapping on a water-in-dodecane emulsion ( $\phi_w = 0.5$ ) stabilized by 2 wt.% carboxyl PS latex particles ( $d = 0.2 \mu\text{m}$ ) at pH 3 after adding 0.25 wt.% (relative to the mass of emulsion) hydrophilic monodispersed silica particles ( $d = 2 \mu\text{m}$ ) and stirring at 300 rpm for 4.5 hours.

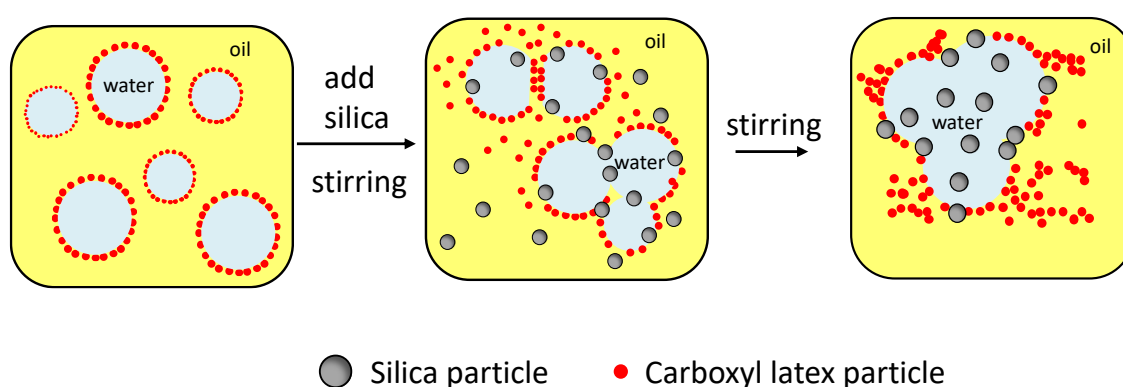


Regarding to the mechanism of solid particles destabilising Pickering emulsions, different possibilities have been taken into consideration. In the destabilisation of emulsions by drop flocculation and adhesion induced by adding poor-wetted solvent of particles, Whitby *et al.*<sup>13</sup> suggested that adhesive interactions between particles coating drops as the inducement for droplets merging. Strong flocculated particles detach from droplet surfaces which exposes the water menisci. Due to van der Waals attraction, drops merge once the oil film is thin enough to rupture. In the present study, the collision between droplet can be promoted by stirring and adhesive interaction between particles on neighbouring droplets is possible as van der Waals attraction dominates the interaction between particles at pH 3. In addition, the friable layers of the aggregated particles at droplet surfaces probably expose the water menisci and lead to the merging of droplets. However, the aggregation of droplets and macroscopic coalescence of emulsion must be induced by extra added silica particles. In the absence of silica particles, neither droplet aggregates nor free water was observed.

A conceptual bridging model has been proposed to explain the mechanism of destabilizing o/w Pickering emulsions by adding fresh oils,<sup>12, 17</sup> as has been described in section 1.4.1. Particles stabilising Pickering emulsions are biwettable by both oil and water phases, they should be able to attach to the interface of fresh created oil droplets. For hydrophilic particles ( $\theta < 90^\circ$ ), only a small portion of particle surface embeds in the oil phase of each droplet, the bridging created by these particles does not merge the droplets, hence, no coalescence of emulsion is favoured. This type of bridging was reported to enhance the stability of Pickering emulsions.<sup>18,19</sup> By contrast, for hydrophobic particles ( $\theta > 90^\circ$ ) which are more wetted by the inner oil phases, both the emulsion droplet and the fresh created oil droplet tend to engulf larger portion of the particle surface. Consequently, merging of oil droplets probably occurs which leads to coalescence of emulsion. (see Figure 1.13). The bridging model can be applied to explain the mechanism of partially hydrophilic silica particles destabilizing w/o emulsions. The schematic is shown in Figure 5.37. Fresh added particles attach at bare oil-water interfaces with the help of stirring. As particles are more wetted by inner water, they protrude into the droplets and break the oil-water interface, which results in destabilisation of emulsions. Completely hydrophilic particles directly enter into the inner phase of the droplet through the oil-water interface and give less chance for droplets to merge, which makes these particles less efficient in destabilising. In

addition, as highly hydrophobic particles repel water, it is difficult for them to be stirred into the continuous phase and contact with the droplet surface, which makes them less efficient in breaking w/o emulsions as well. Hence, partially hydrophilic particles ( $0^\circ < \theta < 90^\circ$ ) are preferred for the destabilisation of w/o emulsions. By contrast, for the destabilisation of o/w emulsions, partially hydrophobic ( $90^\circ < \theta < 180^\circ$ ) particles are predicted the most efficient.

**Figure 5.37.** Schematic showing possible mechanism of hydrophilic silica particles destabilizing a w/o emulsion stabilized by carboxyl latex particles.



#### 5.2.4 By adding fumed silica particles

##### 5.2.4.1 Effect of particle hydrophobicity

Fumed silica particles are also reported to destabilize Pickering emulsions.<sup>10</sup> In this section, a series of fumed silica particles at different hydrophobicity have been rendered as the destabilizers for w/o emulsions stabilized by carboxyl latex particles at  $\phi_w = 0.7$  and pH 3. The silica particles were hydrophobized to different extents by the manufacturer using dichlorodimethylsilane (DCDMS). The hydrophobicity of particles is represented by the density of SiOH groups on the surface of particles. Higher percentage of SiOH means particles are more hydrophilic. Figure 5.38 (a) shows the appearance of emulsion after adding 0.5 wt.% fumed silica particles at varied SiOH groups and stirring for 5 hours. Silica particles with 100% SiOH groups are not able to destabilize emulsions. By contrast, in the presence of particles with 79% and less SiOH groups, large volume of water is released from the emulsions. In several samples, a thin layer of oil was also observed on the top of the emulsion layer. Figure

5.38 (b) plots  $f_o$  and  $f_w$  of each sample after 5 hours of stirring. As can be seen, both  $f_o$  and  $f_w$  fluctuate as the SiOH group density increases. A maximum of  $f_w$  is observed at 79% SiOH while the values at 15% and 100% of SiOH are close to zero. The values for  $f_o$  keep low at all SiOH densities studied, with maxima of 0.17. Figure 5.39 shows optical microscopy images of remaining emulsion droplets after stirring, with the average droplet diameter represented in Figure 5.40. Wrinkled surfaces were observed on large and deformed droplets in the sample with particles of 65% SiOH. Deformation of droplets probably occurs during merging of droplets under stirring, which creates an enlarged surface area. Excess particles adsorb at this newly created surface, preventing the droplets from relaxing back to their spherical shape.<sup>20</sup> Wrinkling of droplets occurs because particles remain adsorbed at the oil-water interface whereas the volume of droplets shrinks.<sup>21,22</sup> The addition of highly hydrophilic particles (79%-100% SiOH) results in large droplets, whereas those with more hydrophobic particles give much smaller droplets after stirring. In the emulsions destabilized by particles with moderate hydrophilicity (61%-65% SiOH), the droplet diameter more or less equals to that of initial emulsions (without destabilisers and stirring). It seems that the presence of hydrophobic particles or particles with moderate hydrophobicity protects droplets from coalescence under stirring. This is interesting as monodispersed silica particles of moderate hydrophilicity was found the most efficient in destabilising w/o emulsions (section 5.2.2.3). The system with fumed silica particles as destabilizers is more complicated as they were reported to stabilise emulsions.<sup>23,24</sup>

**Figure 5.38.** (a) Appearance of water-in-dodecane emulsions ( $\phi_w = 0.7$ ) stabilized by 2 wt.% carboxyl PS latex particles ( $d = 0.2 \mu\text{m}$ ) at pH 3 after adding 0.5 wt.% of fumed silica particles at varied percentages of SiOH groups (given) and stirring at 300 rpm for 5 hours. Taken immediately after stirring. (b)  $f_o$  and  $f_w$  of emulsions in (a) against SiOH percentage.

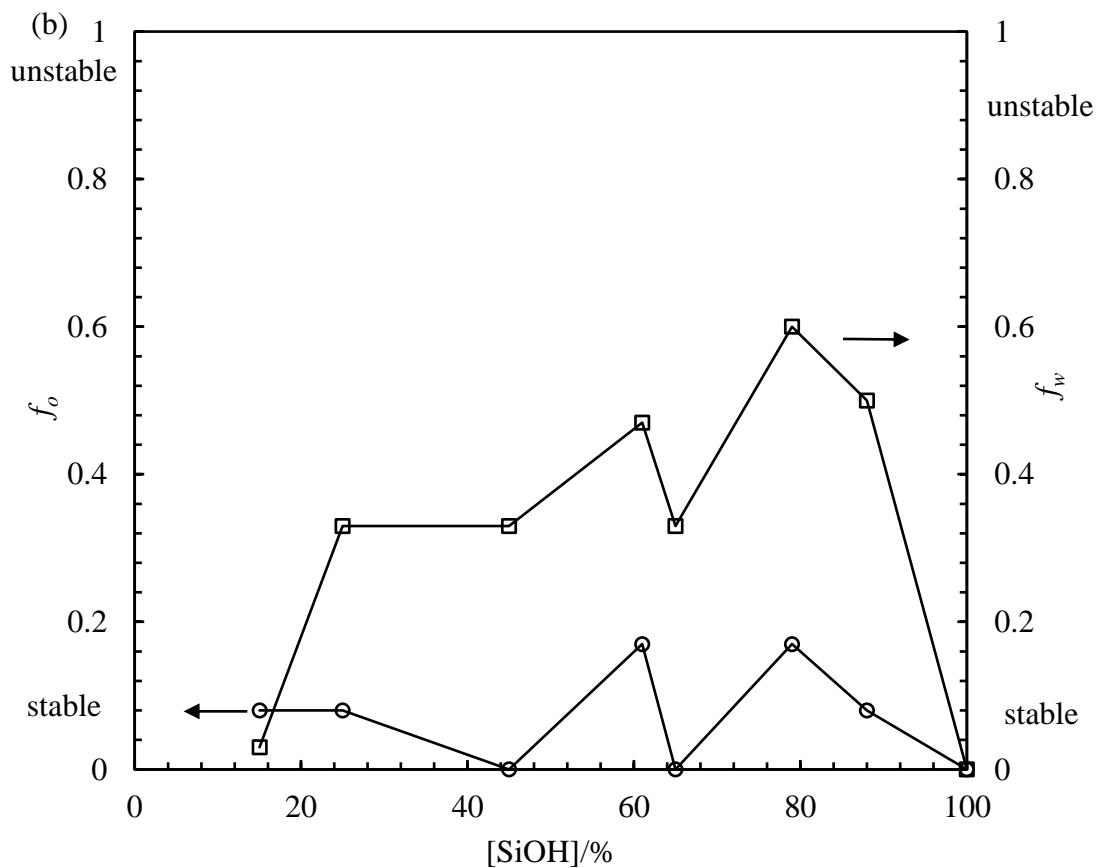
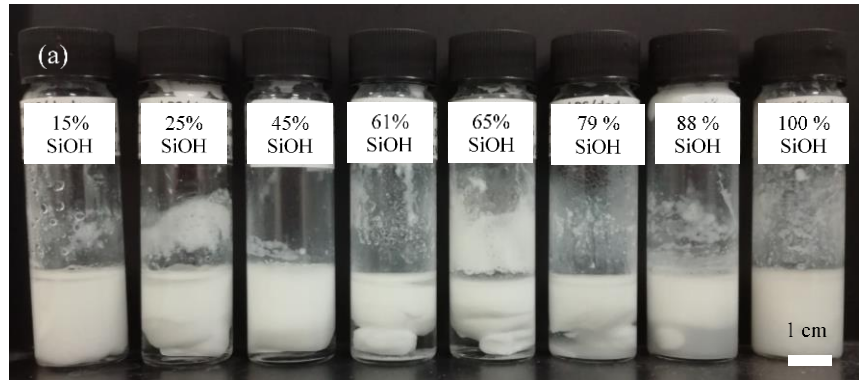


**Figure 5.39.** Optical microscopy images of water-in-dodecane emulsions ( $\phi_w = 0.7$ ) stabilized by 2 wt.% carboxyl PS latex particles ( $d = 0.2 \mu\text{m}$ ) at pH 3 after adding 0.5 wt.% of fumed silica particles at varied percentage of SiOH groups (given) and stirring at 300 rpm for 5 hours.

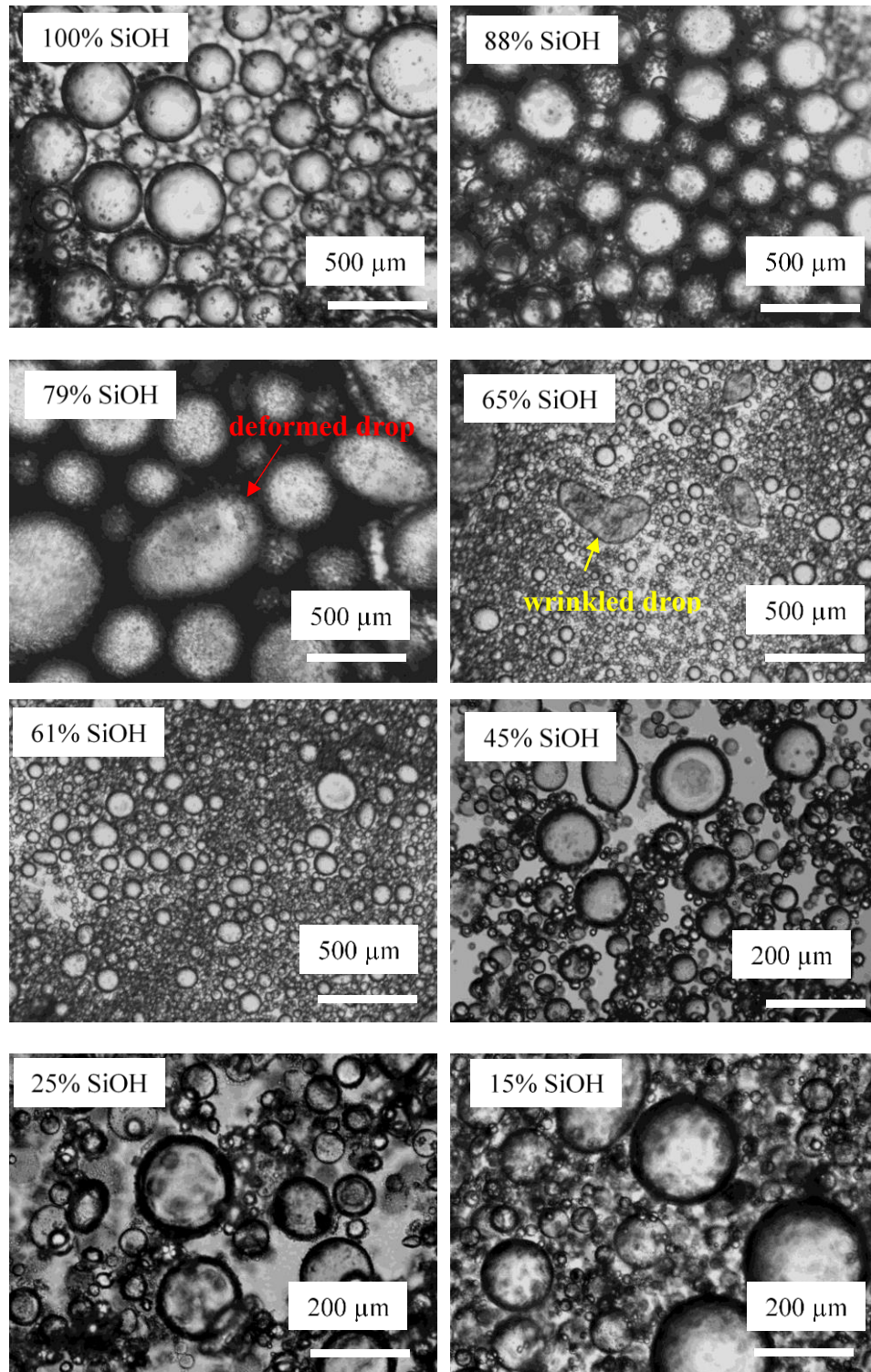
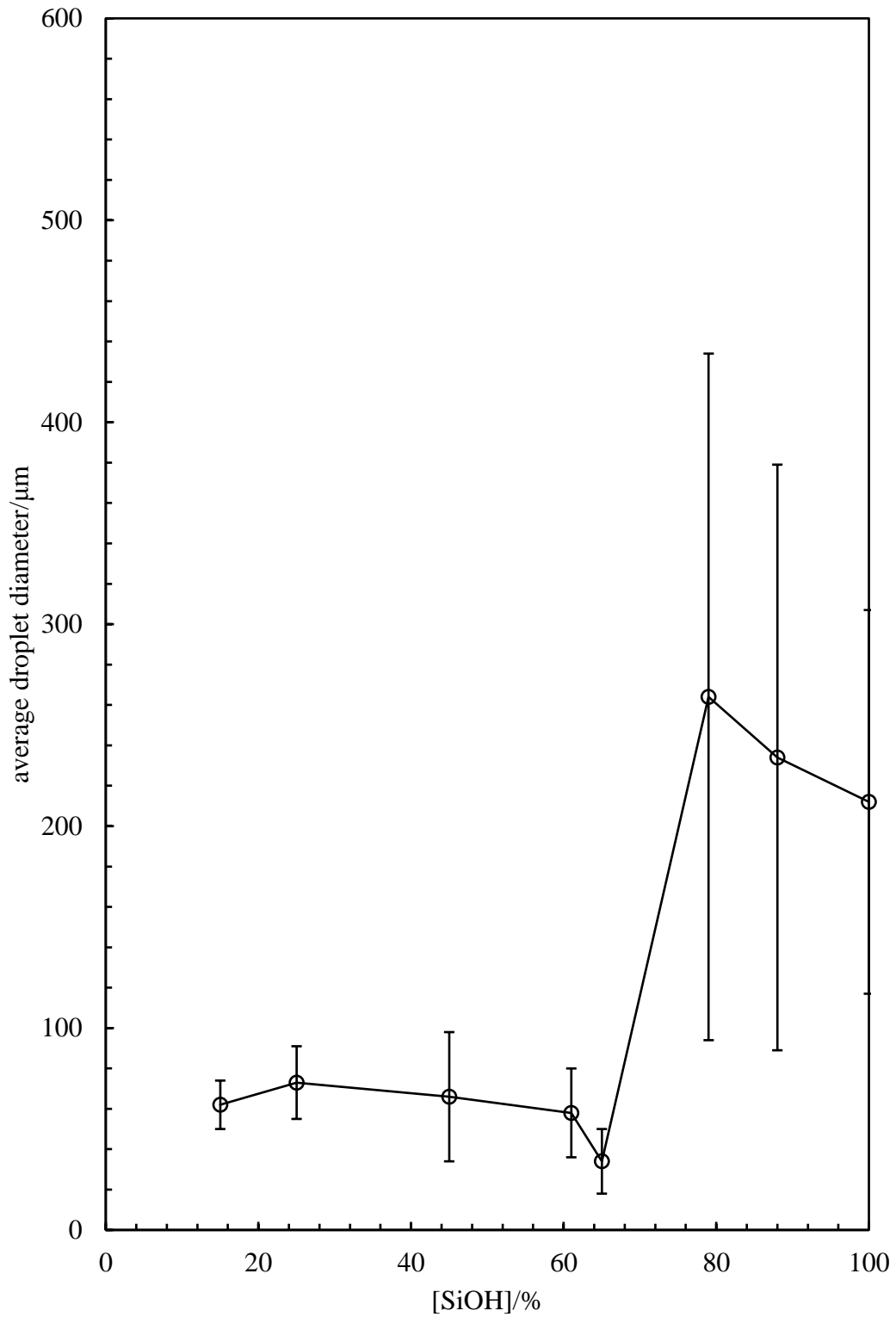


**Figure 5.40.** The average diameter of water-in-dodecane emulsions ( $\phi_w = 0.7$ ) stabilized by 2 wt.% carboxyl PS latex particles ( $d = 0.2 \mu\text{m}$ ) at pH 3 after adding 0.5 wt.% of fumed silica particles at varied percentage of SiOH groups (given) and stirring at 300 rpm for 5 hours.



A series of emulsions were prepared at particle concentration of 2 wt.%,  $\phi_w = 0.7$  and pH of 3 to confirm the ability of fumed particles in emulsion stabilisation, as shown in Figure 5.41. The emulsion stabilised by particles with 100% SiOH is unstable, complete phase separation occurs immediately after homogenisation. Oil-in-water emulsions were obtained with particles containing less SiOH groups, the volume of emulsion peaks at particles with 65% SiOH. Addition of these particles to an oil-water mixture might promote the formation of fresh emulsions. In addition, complete phase separation occurs again in the emulsions stabilised by highly hydrophobic particles (15%-25% SiOH), particles now end up in the oil phases. Therefore, what happens to model w/o emulsions during the destabilisation process after adding particles of 65% and 61% SiOH is possibly as following: at the beginning of stirring, silica particles attach to emulsion droplets and coalesce the droplets. When there is free water resolved, stirring promotes the formation of new droplets, which hinders further coalescence of initial water droplets. However, this needs further experimental confirmation.

As has been reported, in the destabilization of o/w Pickering emulsions by hydrophobic fumed silica particles, the most efficient silica particles have a three-phase contact angle of  $75^\circ$  at the toluene/water interface.<sup>10</sup> In fact, these silica particles are partially wetted by the continuous phases (water). Therefore, slightly hydrophobic silica particles should be the best choice to destabilise w/o emulsions, whereas completely hydrophilic particles are not effective as they cannot be wetted by the continuous phase (now with dodecane). They will keep as large agglomerates during stirring and have less chance to contact with the droplet surface. In contrast, highly hydrophobic particles are more wetted by the continuous phase. If the bridging model is true, these particles tend to bridge the droplets in the manner of enhancing the emulsion stability rather than breaking droplets.

**Figure 5.41.** Appearance of water-dodecane emulsions ( $\phi_w = 0.7$ ) stabilized by 2 wt.% fumed silica particles at varied SiOH percentages at pH 3.



#### 5.2.4.2 Effect of particle concentration

As has been studied above, fumed silica particles with 79% and lower density of SiOH groups partially destabilized emulsions at 0.5 wt.% of particles. It is worth to investigate effect of silica particle concentration on the destabilization efficiency. The SiOH group density was fixed at 79%. Figure 5.42 (a) represents the appearance of emulsions after adding fumed silica particles and stirring at 300 rpm for 5 hours. In the emulsion without and with 0.1 wt.% of silica, no water is released after stirring. By contrast, increasing volumes of water and oil are extracted from the emulsions at higher silica concentrations. Figure 5.42 (b) plots  $f_o$  and  $f_w$  of each emulsion against silica concentration. As can be seen,  $f_o$  peaks at 0.5 wt.% of particle while  $f_w$  gradually increase from 0 to 0.8 as particle concentration increases. Figure 5.43 shows the optical microscopy of the remaining emulsion droplets after stirring, and the average droplet diameter is represented in Figure 5.44. Large and deformed droplets were observed in the samples with fumed silica of 0.3 wt.% and above. Wrinkled surfaces were observed on the large and deformed droplets in the sample with 1 wt.% particles, resembling previous destabilisation of Pickering emulsions by shearing or drop flocculation.<sup>13, 25</sup> The droplet diameter fluctuates as particle concentration increases.

**Figure 5.42.** (a) Appearance of water-in-dodecane emulsions ( $\phi_w = 0.7$ ) stabilized by 2 wt.% carboxyl PS latex particles ( $d = 0.2 \mu\text{m}$ ) at pH 3 after adding fumed silica particles (79% SiOH) at different concentrations (given) and stirring at 300 rpm for 5 hours. Taken immediately after stirring. (b)  $f_o$  and  $f_w$  of emulsions in (a).

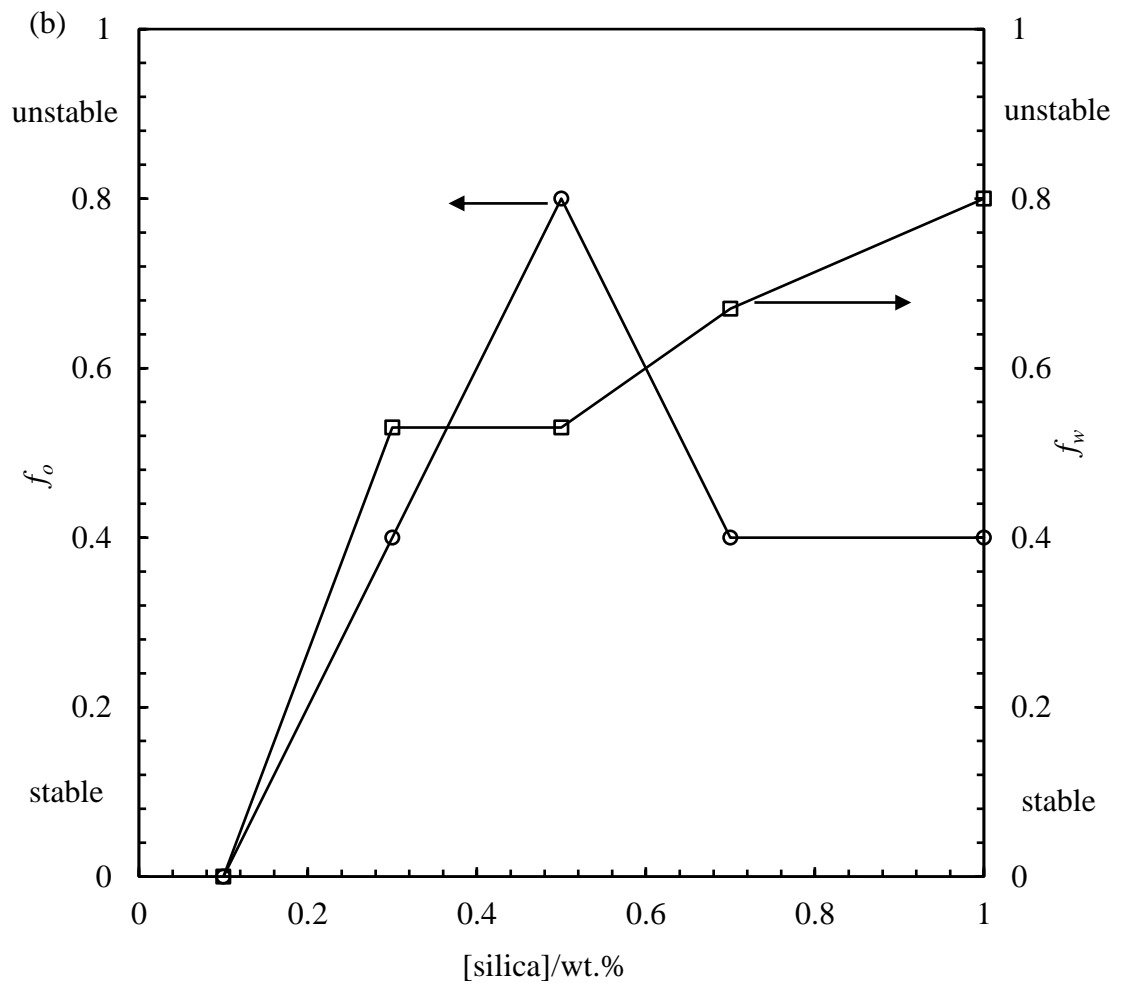


**Figure 5.43.** Optical microscopy of water-in-dodecane emulsions ( $\phi_w = 0.7$ ) stabilized by 2 wt.% carboxyl PS latex particles ( $d = 0.2 \mu\text{m}$ ) at pH 3 after adding fumed silica particles (79% SiOH) at varied concentrations and stirring at 300 rpm for 5 hours. Taken immediately after stirring. Scale bar = 500  $\mu\text{m}$ .

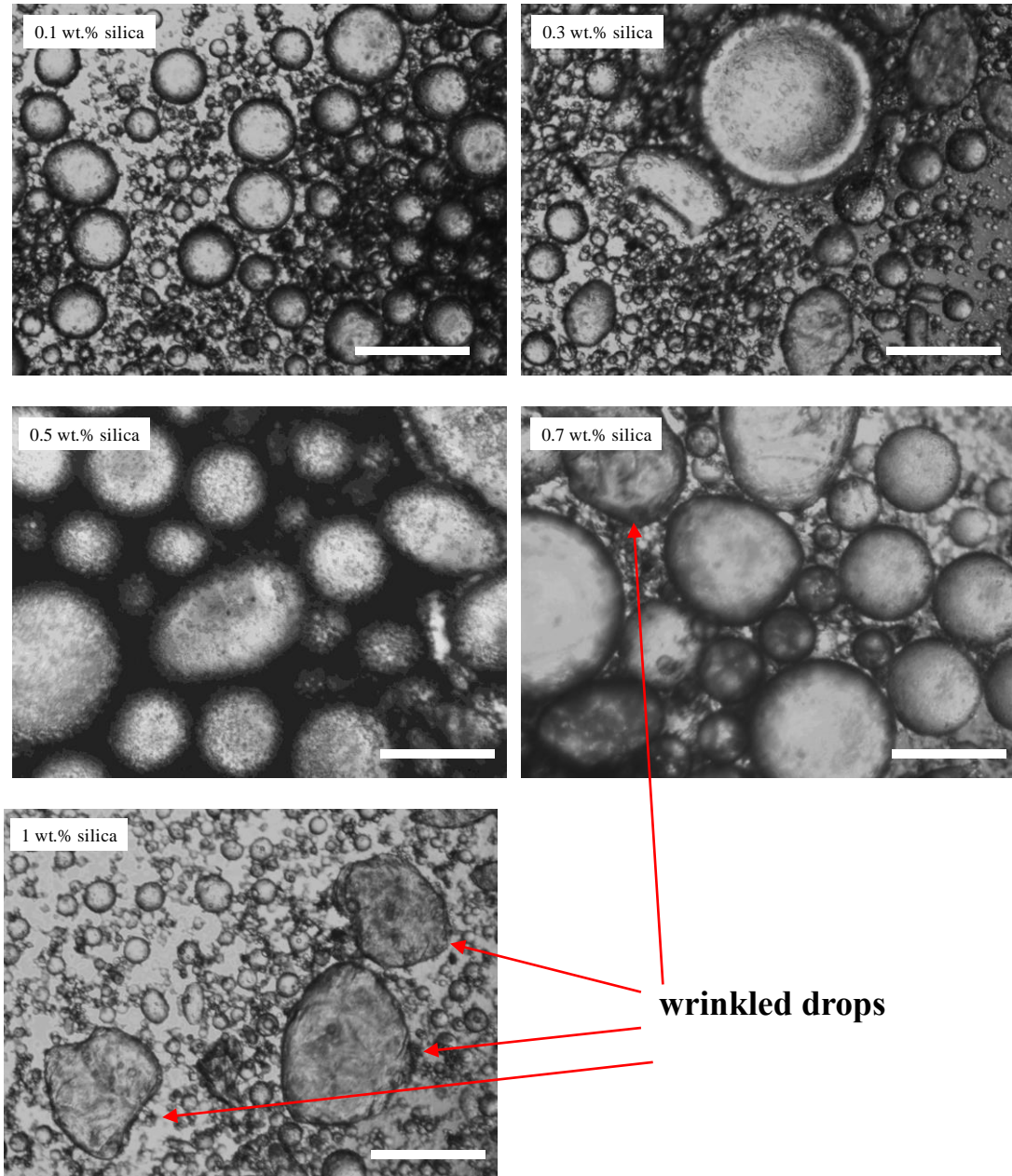


**Figure 5.44.** Average droplet diameter of water-in-dodecane emulsions ( $\phi_w = 0.7$ ) stabilized by 2 wt.% carboxyl PS latex particles ( $d = 0.2 \mu\text{m}$ ) at pH 3 after adding fumed silica particles (79% SiOH) at varied concentrations and stirring at 300 rpm for 5 hours.

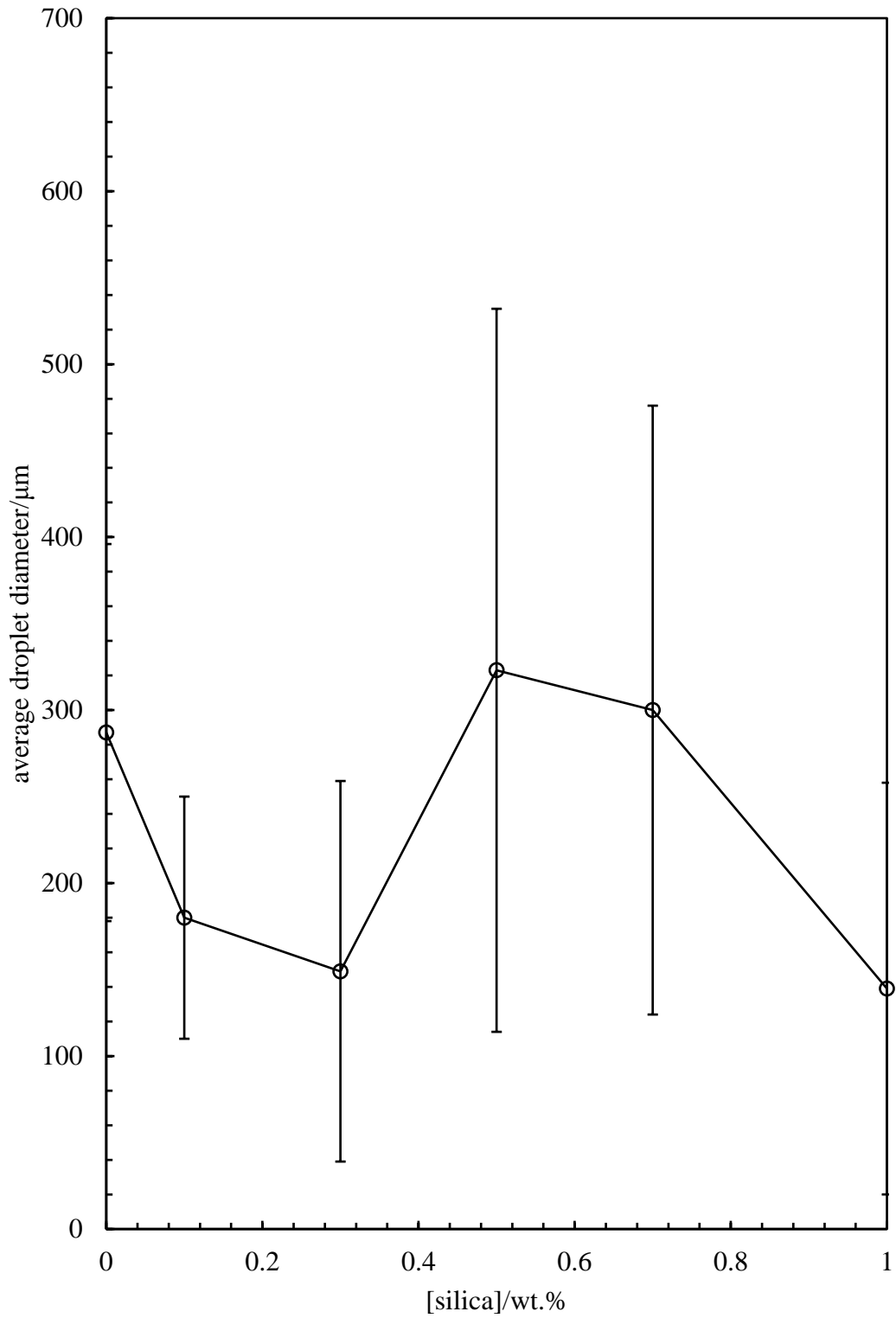
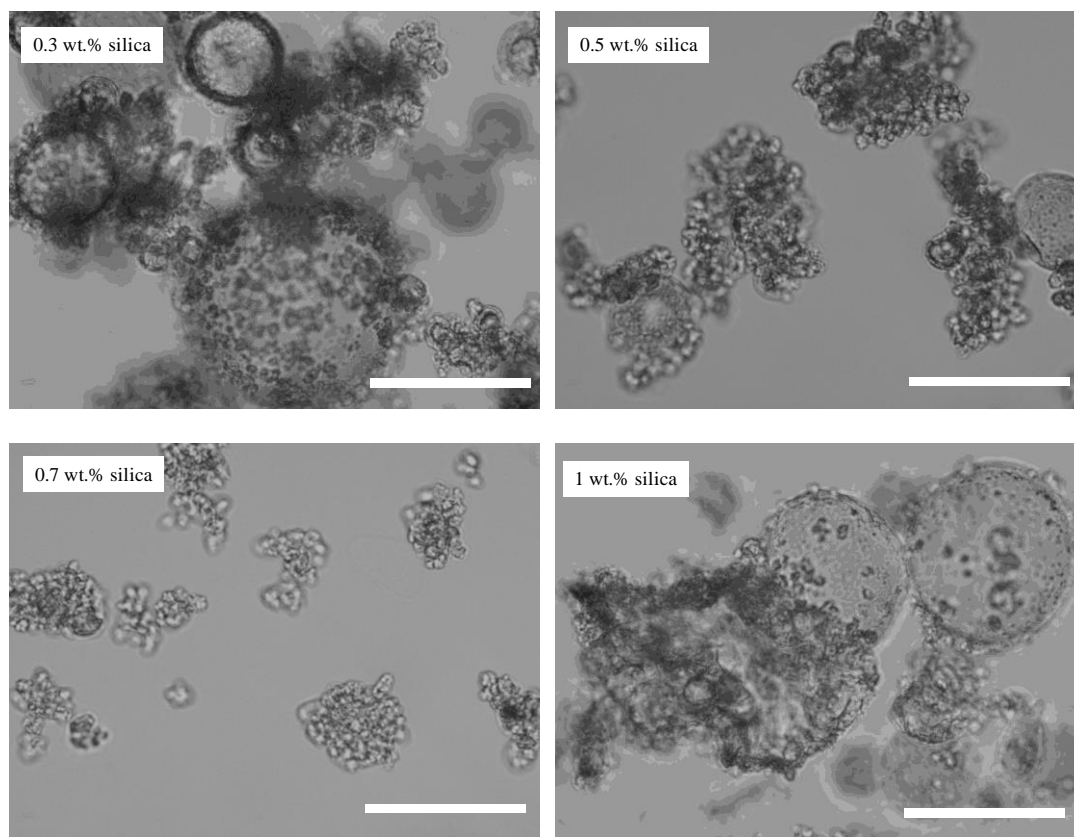
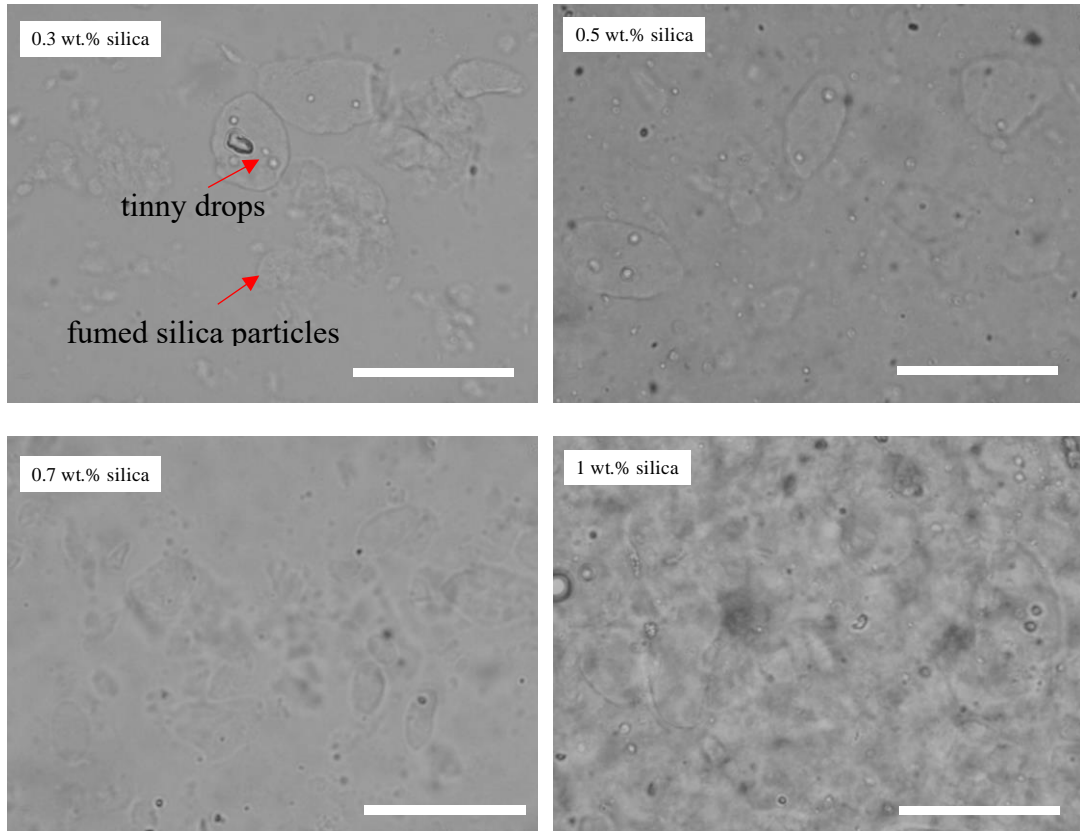


Figure 5.45 shows the optical microscopy of the oil layer after destabilization of emulsions, carboxyl latex particle aggregates along with water droplets were observed. Figure 5.46 shows the optical microscopy of resolved water after destabilization process. Large silica agglomerates and tinny drops of remaining emulsions were also observed. One may notice that fumed silica is much less efficient in destabilization than monodispersed particles at corresponding concentrations. Monodispersed silica particles are discrete in water and dodecane, they are easily dispersed between emulsion droplets by stirring. By contrast, fumed silica consists of large agglomerates. When they are added to emulsion as a dry powder, the perturbation induced by stirring is not strong enough to break agglomerates, which make them difficult to be stirred into the continuous phase between droplets.

**Figure 5.45.** Optical microscopy images of samples taken from the oil layers after breaking of water-in-dodecane emulsions ( $\phi_w = 0.7$ ) stabilized by 2 wt.% carboxyl PS latex particles ( $d = 0.2 \mu\text{m}$ ) at pH 3 by adding fumed silica particles (79% SiOH) at different concentrations and stirring at 300 rpm for 5 hours. Scale bar = 50  $\mu\text{m}$ .



**Figure 5.46.** Optical microscopy images of sample taken from the released water after breaking of water-in-dodecane emulsions ( $\phi_w = 0.7$ ) stabilized by 2 wt.% carboxyl PS latex particles ( $d = 0.2 \mu\text{m}$ ) at pH 3 by adding fumed silica particles (79% SiOH) at different concentrations and stirring at 300 rpm for 5 hours. Scale bar = 50  $\mu\text{m}$ .



### 5.3 Destabilization of oil-in-water emulsions stabilized by fumed silica particles

#### 5.3.1 Preparation of o/w emulsions stabilized by fumed silica particles

Before studying the destabilisation of o/w emulsions, an effort has been conducted on preparing model emulsions stable to coalescence. As has been roughly studied in section 5.2.4.1, fumed silica particles with 65% SiOH groups on the surface give the largest volume of o/w emulsions with dodecane. It is necessary to determine whether they are stable against stirring. Hence, four dodecane-in-water emulsions stabilised by 1 wt.% (relative to the aqueous dispersion) fumed silica particles at  $\phi_o = 0.5$  were prepared at neutral pH. The hydrophobicity of particles was selected ranging from 65% to 79% SiOH groups on particle surface. Figure 5.47 (a) shows the appearance of the emulsions immediately after homogenization. The emulsions are stable to coalescence but partially unstable to creaming. Water is extracted from each emulsion after 24 hours, as illustrated in Figure 5.47 (b). The volume of water extracted increases with SiOH density, meaning that emulsions stabilised by more hydrophilic silica particles are less stable to creaming. The emulsions were then stirred at 300 rpm for 3 hours to investigate their stability against stirring. Figure 5.47 (c) shows the appearance of emulsions 24 hours after stirring. Comparing with the emulsions before stirring, more water is extracted from the emulsions after stirring. In addition, large oil droplets were visually observed on top of the emulsion layer except the one with particles of 79% SiOH groups, where complete phase separation was observed. The stability of the emulsions to creaming ( $f_w$ ) and coalescence ( $f_o$ ) before and after stirring is represented in Figure 5.48 against SiOH density. As can be seen,  $f_w$  of emulsions after stirring is higher than that before stirring, with a difference larger than 0.3. There is no free oil released from emulsions with particles of 65, 69 and 75% SiOH groups. These results indicate that stirring increases the creaming of emulsions, but no macroscopic coalescence is induced. As has been explained in section 1.2.2, creaming of emulsions is proportional to the radius of the droplets and the density difference between the continuous phase and dispersed phase. Shearing induces inner coalescence of emulsions and results in larger droplets. Hence, lower creaming stability of emulsions after stirring is not surprising.

**Figure 5.47.** Appearance of dodecane-in-water emulsions ( $\phi_o = 0.5$ ) stabilized by 1 wt.% fumed silica particles with varied SiOH group densities, taken (a) immediately, (b) 24 hours after homogenization and (c) 24 hours after stirring at 300 rpm for 3 hours, red dashed lines mark the boundary between the large oil globules layer and the concentrated emulsion layer.

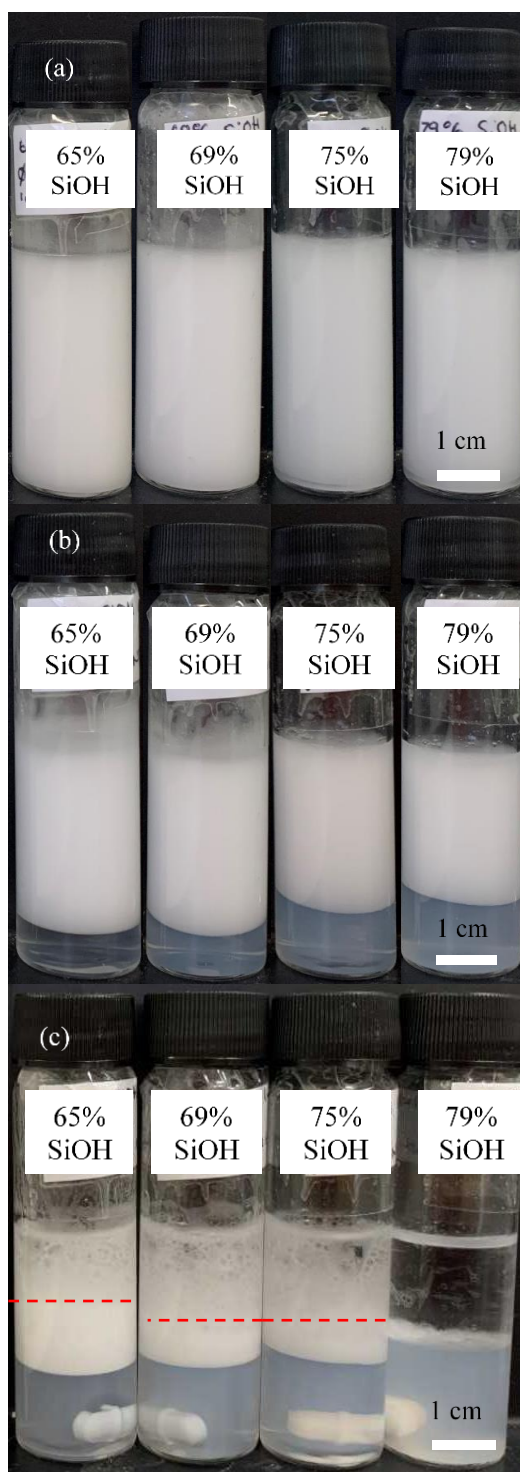
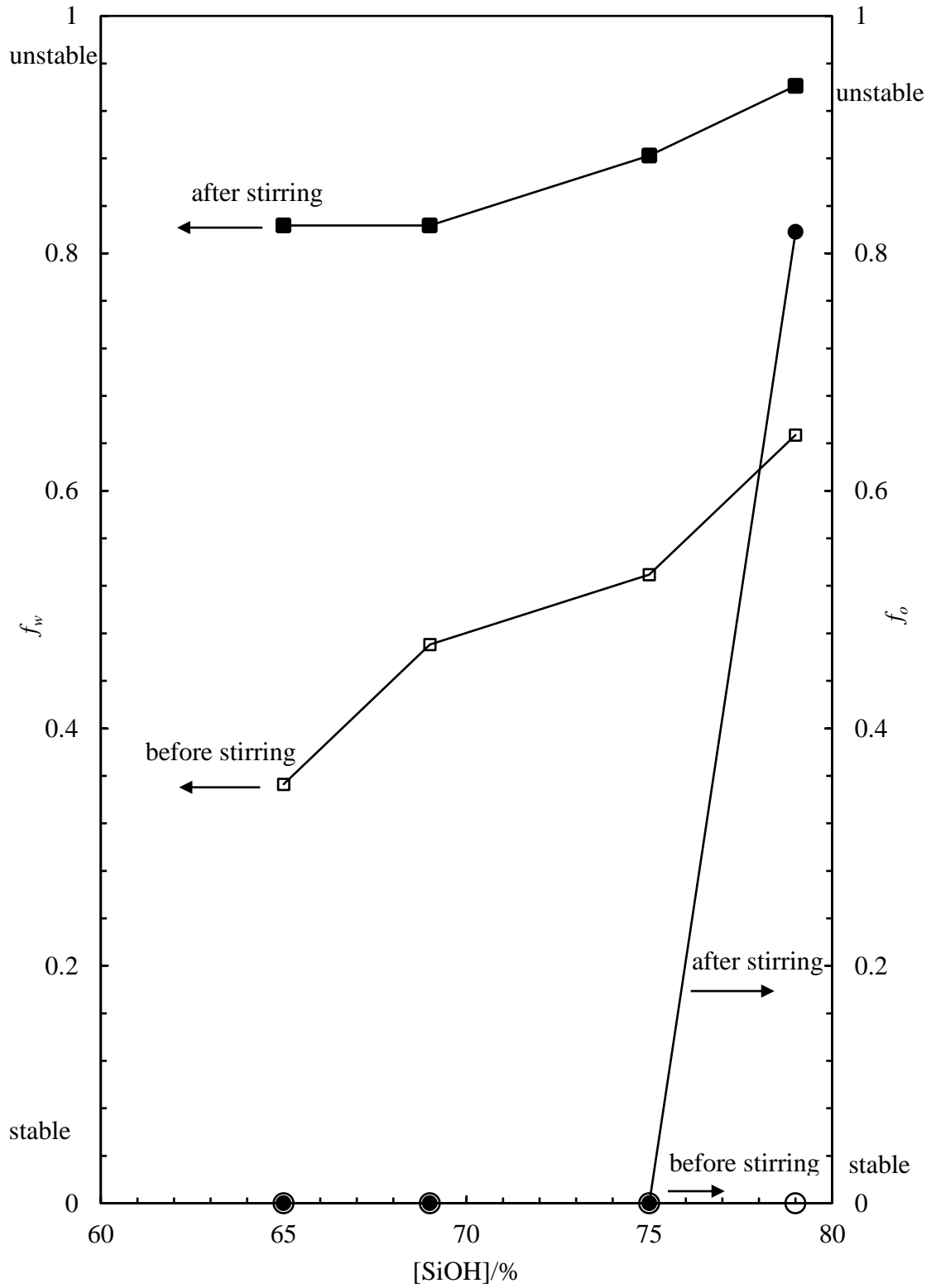


**Figure 5.48.** The  $f_w$  (squares) and  $f_o$  (circles) of dodecane-in-water emulsions ( $\phi_o = 0.5$ ) stabilized by 1 wt.% fumed silica particles with 65% SiOH groups before and after stirring at 300 rpm for 3 hours.



Optical microscopy images of emulsions before and after stirring are shown in Figure 5.49 and Figure 5.50, respectively. Before stirring, spherical droplets less than  $100\ \mu\text{m}$  were observed under the microscope. For the emulsions after stirring, different layers were observed in the sample vessel. A clear oil layer on the top, a layer with very large droplets, a concentrated emulsion layer and a water layer at the bottom. The microscopy images have been taken with samples from separated layers. Droplets taken from the concentrated emulsion layers are more or less the same as those without stirring, whereas droplets taken from the top oil layers are very large and deformed. Figure 5.51 plots the average droplet diameter of emulsions before and after stirring. The drop diameter of initial emulsions increases with the density of SiOH groups, the same as the concentrated emulsions after stirring. However, the droplet diameter of emulsions after stirring is smaller than that of the initial emulsions at corresponding SiOH densities. This might be due to that stirring coalesce the bigger droplets and leave the smaller ones, thus gives a lower average value. The emulsion stabilised with 79% SiOH was completely broken by stirring so no microscopy image was taken. These figures as well as emulsion stability results above consistently show that the emulsion stabilized by silica particles with 65% SiOH groups shows the highest stability to creaming and coalescence against stirring. Therefore, this emulsion was used as the model emulsion for further destabilisation experiments.

**Figure 5.49.** Optical microscopy of dodecane-in-water emulsions ( $\phi_o = 0.5$ ) stabilised by 1 wt.% fumed silica particles with different SiOH densities.

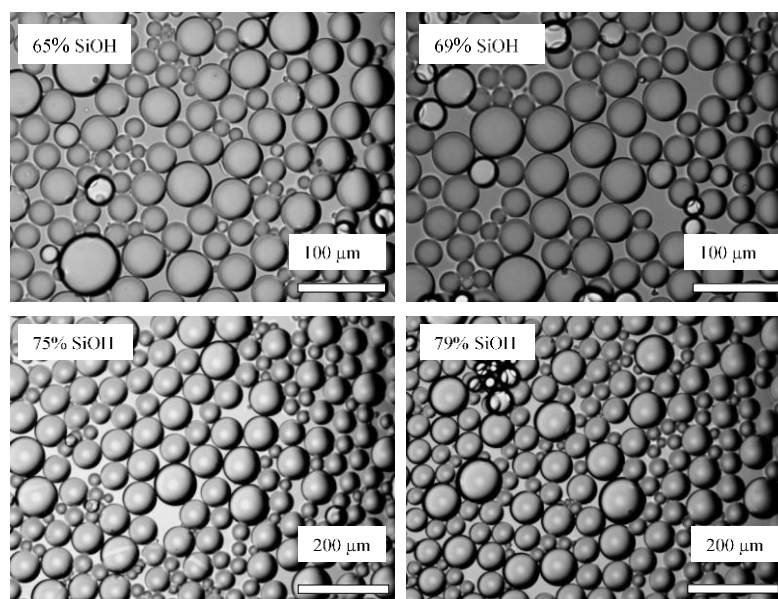


**Figure 5.50.** Optical microscopy of dodecane-in-water emulsions ( $\phi_o = 0.5$ ) stabilised by 1 wt.% fumed silica particles with varied SiOH group densities after stirring at 300 rpm for 3 hours, taken 24 hours after stirring. The left images were taken from the concentrated emulsion layers, the right images were taken from the large oil globule layers.

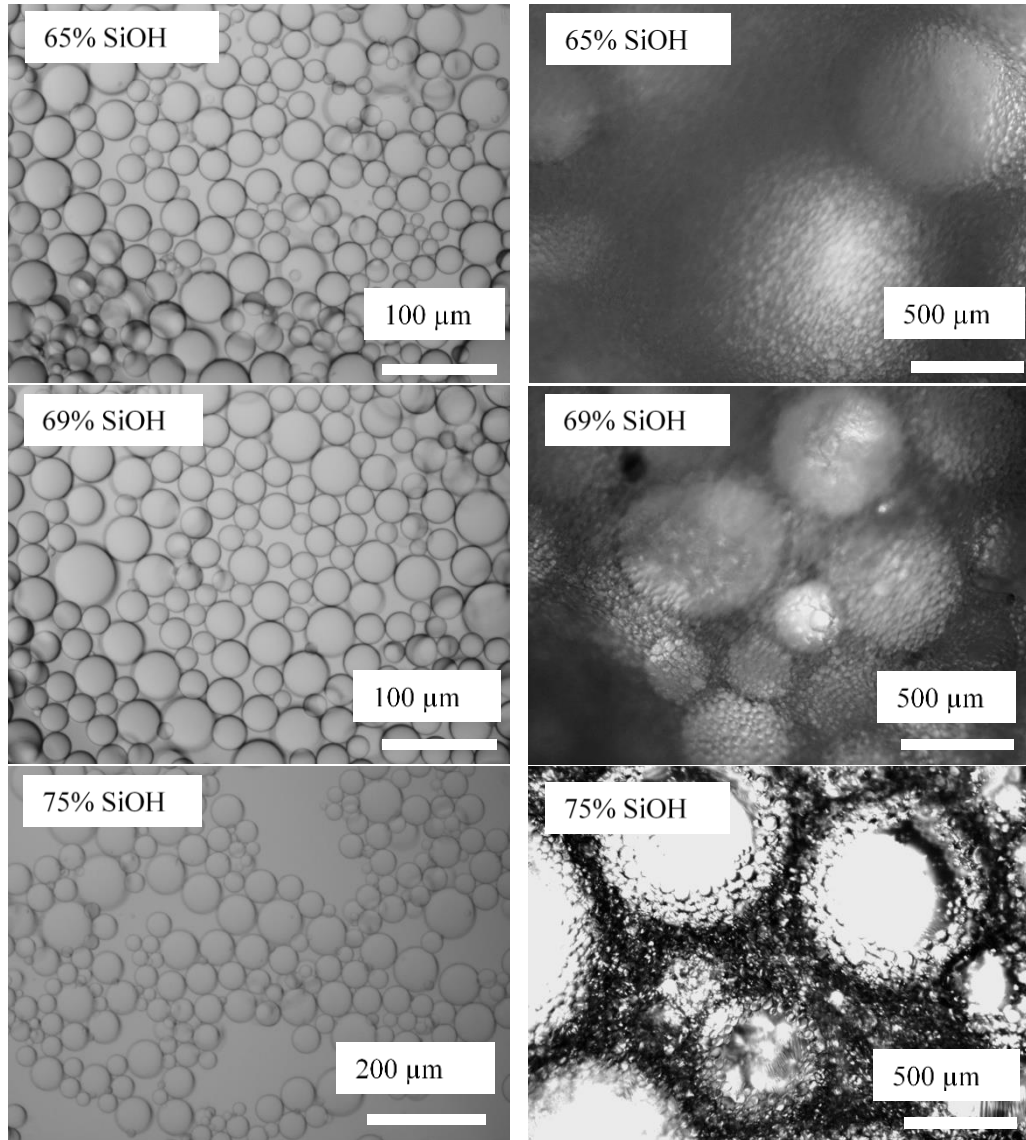
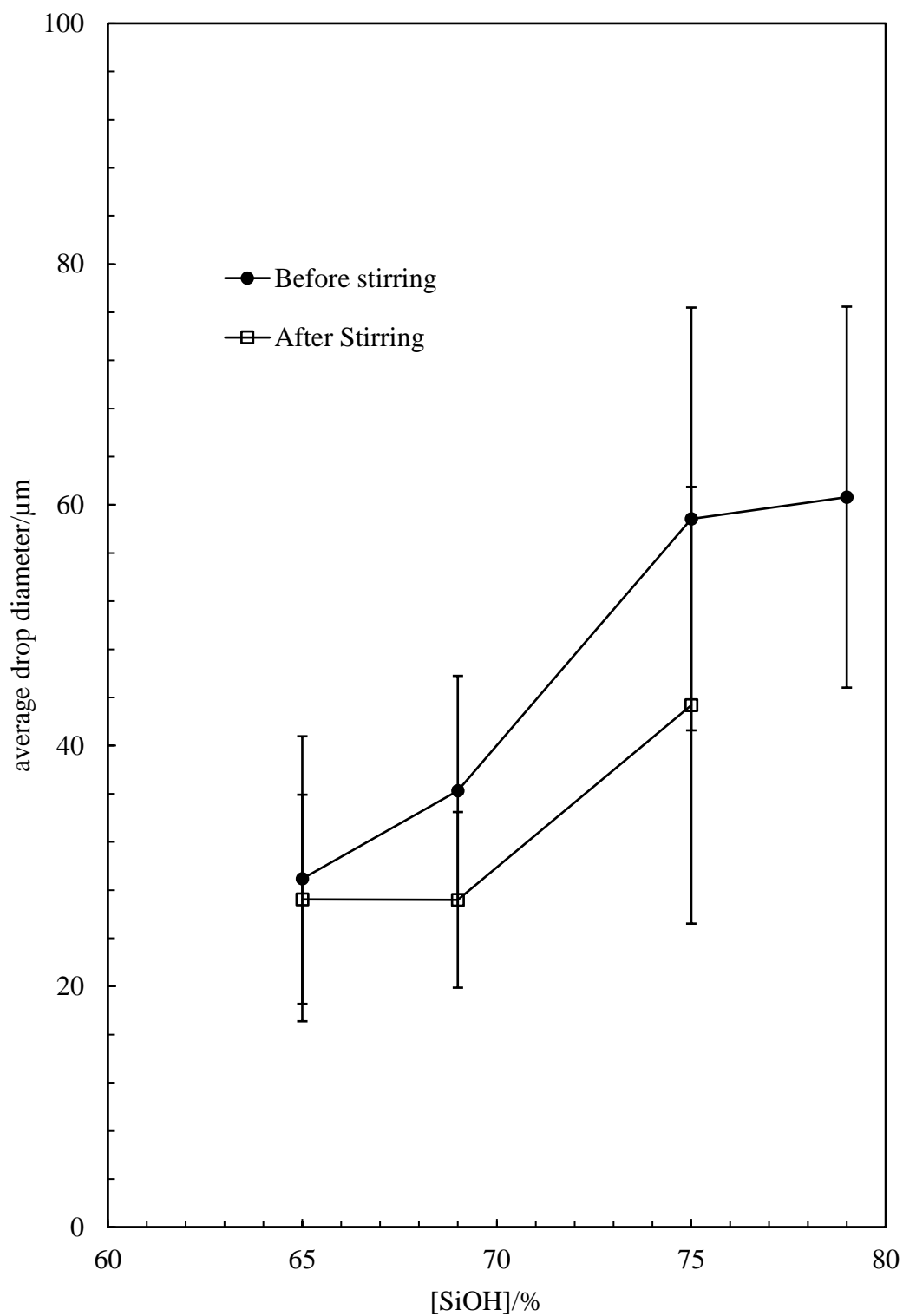


**Figure 5.51.** Average droplet diameter of dodecane-in-water emulsions ( $\phi_o = 0.5$ ) stabilized by 1 wt.% fumed silica particles with varied SiOH group densities before and after stirring at 300 rpm for 3 hours. The diameter after stirring was calculated from droplets taken from concentrated emulsion layers.

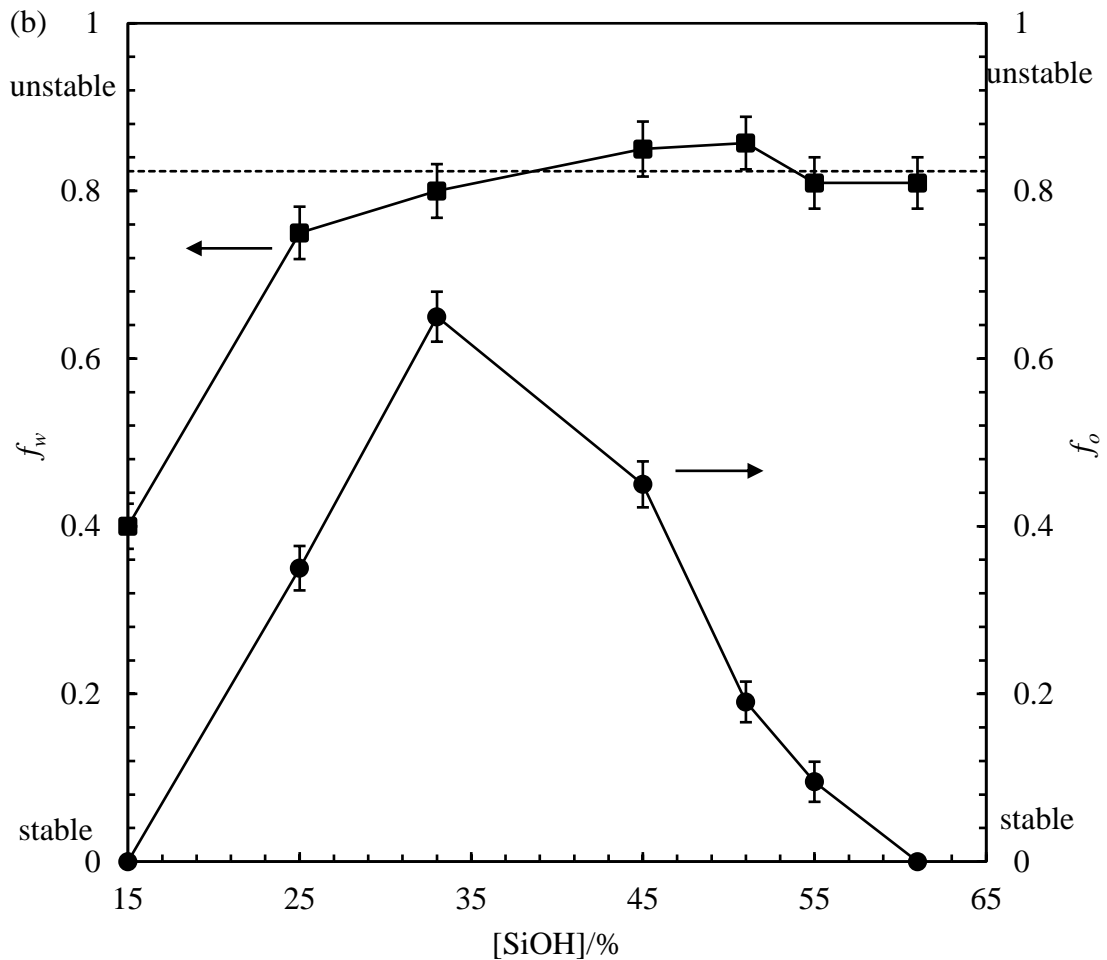
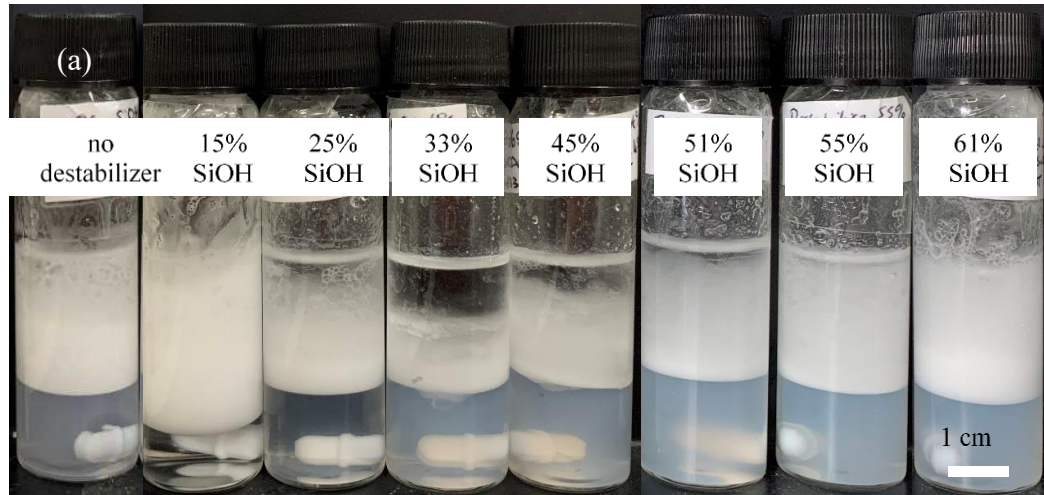


### 5.3.2 Destabilization by hydrophobic fumed silica particles

#### 5.3.2.1 Effect of particle hydrophobicity

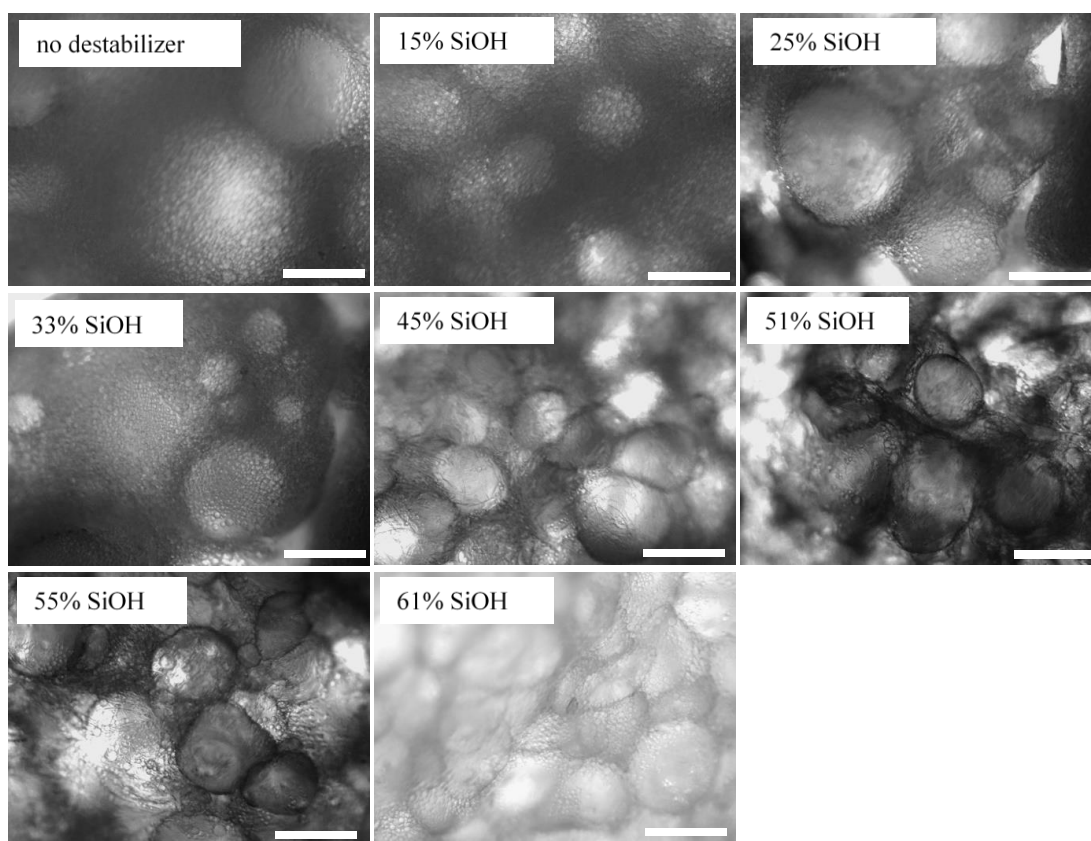
Batches of dodecane-in-water emulsions ( $\phi_o = 0.5$ ) stabilised with 1 wt.% fumed silica particles with 65% SiOH groups were prepared. These emulsions were then destabilised by adding 0.5 wt.% fumed silica (relative to the weight of the emulsion) with varied SiOH group densities and stirring at 300 rpm for 3 hours. As a control, an emulsion without extra destabilizers was rendered to stir under the same condition. Figure 5.52 (a) shows the appearance of the emulsions after stirring. Four layers were observed in each emulsion, *i.e.*, a water layer at the bottom, a concentrated emulsion layer in the middle, a layer of large oil droplets above the concentrated emulsion layer and a clear oil layer on the top. The volume of water increases with SiOH group densities of destabilising particles, indicating an increased creaming of the emulsions. In addition, the volume of oil released from the emulsion destabilised by particles with 33% SiOH groups is higher than all others, which implies the highest efficiency of destabilisation. Figure 5.52 (b) represents the  $f_w$  and  $f_o$  of emulsions against SiOH group percentage after stirring. As can be seen,  $f_w$  increases rapidly from 0.4 to 0.8, close to the control emulsion after stirring. However,  $f_o$  increases from zero to a peak at 0.65 then decreases gradually until back to zero. It is worth to note that the volume of remaining emulsion with the most hydrophobic silica particles (15% SiOH) after stirring is higher than the control (being stirred under the same condition but with extra added destabilizers), which means that the addition of extreme hydrophobic particles enhances the stabilization of emulsions instead of breaking them. It is probably that the hydrophobic particles combine with remaining hydrophilic particles in the aqueous phase to stabilise emulsions. This is possible as Binks and Lumsdon<sup>24</sup> reported that a combination of hydrophilic and hydrophobic particles give stable Pickering emulsions. Evidence can also be found in the aqueous phase of each sample after stirring. The aqueous phase of the control emulsion is bluish, indicating the presence of un-emulsified particles. By contrast, in the emulsion destabilised by particles with 15% SiOH, the aqueous layer is clear, implying that un-emulsified particles now all transfer to the emulsion layer. Similar phenomenon was observed in the emulsion destabilized by particles with 25% SiOH groups.

**Figure 5.52.** (a) Appearance of dodecane-in-water emulsions ( $\phi_o = 0.5$ ) stabilized by 1 wt.% fumed silica particles (65% SiOH) after adding 0.5 wt.% (relative to the mass of emulsions) fumed silica particles with varied SiOH group densities and stirring at 300 rpm for 3 hours, photos were taken 24 hours after stirring. (b)  $f_w$  (squares) and  $f_o$  (circles) emulsions in (a) against SiOH group percentage.



Optical microscopy has been taken on large droplet layers of each emulsion after stirring and the images are shown in Figure 5.53. In the samples with particles of SiOH  $\leq 33\%$ , droplets with diameters larger than 1  $\mu\text{m}$  were observed. In comparison, relatively smaller droplets were obtained in the emulsions destabilised by more hydrophilic particles. The droplets are deformed and aggregate into large clusters. The results illustrate that partially hydrophobic particles with a surface SiOH density of 33% are the most effective in destabilising o/w emulsions. Either extremes result in macroscopically coalescence-stable emulsions after gentle stirring.

**Figure 5.53.** Optical microscopy of dodecane-in-water emulsions ( $\phi_o = 0.5$ ) stabilized by 1 wt.% fumed silica particles with 65% SiOH groups after adding 0.5 wt.% (relative to the mass of emulsions) fumed silica particles with varied SiOH group densities and stirring at 300 rpm for 3 hours. Taken 24 hours after stirring. Scale bar = 500  $\mu\text{m}$ .



### 5.3.2.2 Effect of particle concentration

The study in the last section has shown that fumed silica particles with 33% SiOH groups are the most effective in destabilising o/w emulsions stabilised by fumed silica of 65% SiOH groups. However, complete phase separation was not observed when 0.5 wt.% silica was added as the destabilizer. In this section, the particle concentration of fumed silica with 33% SiOH groups was investigated to find the best destabiliser concentration for destabilisation. Batches of dodecane-in-water emulsions ( $\phi_o = 0.5$ ) were prepared with 1 wt.% (relative to the aqueous dispersion) 65% fumed silica. These emulsions were then destabilised by adding 33% SiOH fumed silica at varying concentrations (relative to the weight of the emulsion) and stirring at 300 rpm for 3 hours, after which the photos of the remaining emulsions were taken. Figure 5.54 (a) is the appearance of emulsions taken immediately after stirring. It is difficult to quantify the height of each phase immediately after stirring as the interface is fuzzy. The destabilised emulsions were left quiescently for 24 hours and the appearance of emulsions is shown in Figure 5.54 (b). Water is extracted from every sample. In the samples with 0.1 wt.% and 0.15 wt.% particles, the resolved water layer is clear. By contrast, the aqueous layer of other samples is bluish, implying the presence of particles. Oil starts to extract from the emulsion containing 0.15 wt.% particles, and the volume of free oil increases with increasing particle concentration. At high concentrations ( $\geq 0.7$  wt.%) of particles, white layers that look slightly different from an emulsion were observed in the middle of the vessels. A small sample has been taken from the white layer and observed under the optical microscope. The images are shown in Figure 5.54 (c). It looks like fumed silica particle aggregates dispersing in oil. It is likely that at high concentrations, hydrophobic (33% SiOH) fumed silica has been partially stirred into the continuous phase between droplets, and remained particles end up in the resolved oil. The stability of emulsions to creaming ( $f_w$ ) and coalescence ( $f_o$ ) was evaluated and the result is plotted in Figure 5.55. As extra added particles are dispersed in the oil phase of samples with 0.7 wt.% and 1 wt.% particles,  $f_o$  was determined by including the clear oil layer and the turbid particle layer. As shown in Figure 5.55, both  $f_w$  and  $f_o$  increases with increasing destabiliser concentrations. In the sample containing 1 wt.% particles as the destabiliser, about 95% of initial emulsion is broken.

**Figure 5.54.** Appearance of dodecane-in-water emulsions ( $\phi_o = 0.5$ ) stabilized by 1 wt.% fumed silica particles (65% SiOH) after adding 0.5 wt.% (relative to the mass of emulsions) partially hydrophobic fumed silica particles (33% SiOH) at varied concentrations (given) and stirring at 300 rpm for 3 hours, taken (a) immediately and (b) 24 hours after stirring. (c) Optical microscopy of samples taken from the white layers in the oil phases of emulsions destabilized by 0.7 wt.% and 1 wt.% particles.

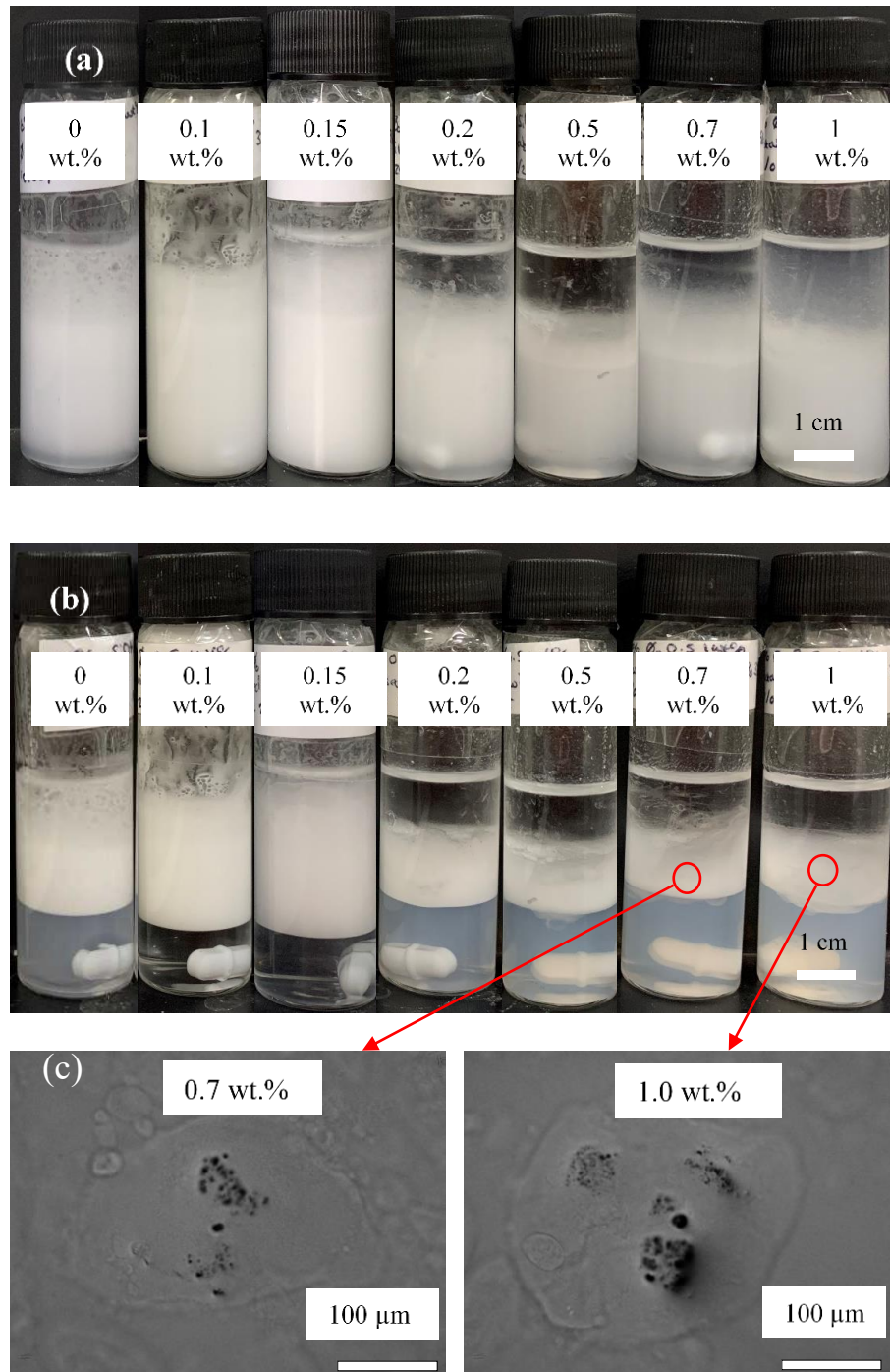
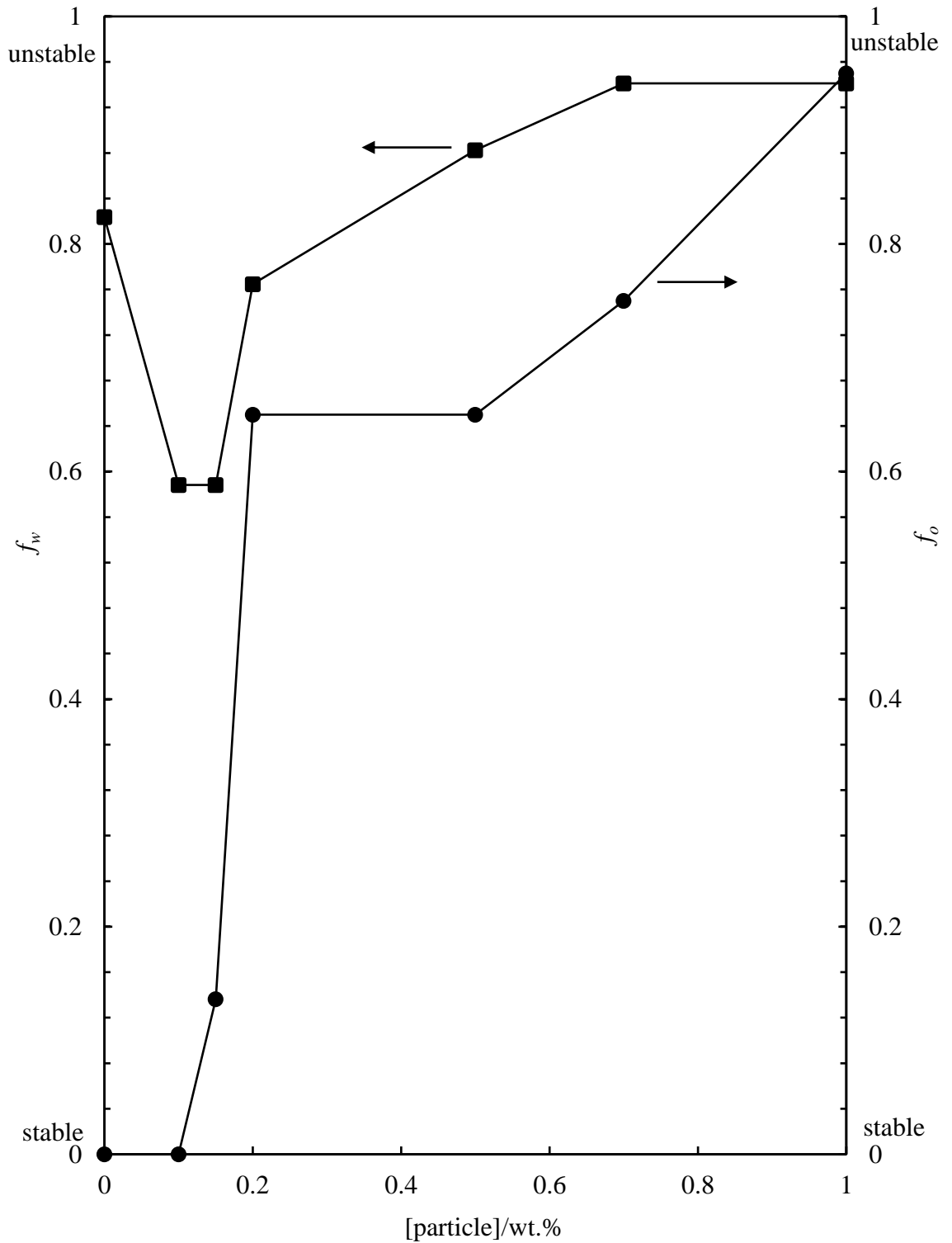


**Figure 5.55.** The  $f_w$  (squares) and  $f_o$  (circles) of dodecane-in-water emulsions ( $\phi_o = 0.5$ ) stabilized by 1 wt.% fumed silica particles (65% SiOH) after adding 0.5 wt.% (relative to the mass of emulsions) partially hydrophobic fumed silica particles (33% SiOH) at varied concentrations and stirring at 300 rpm for 3 hours.



### 5.3.3 Destabilization by other hydrophobic particles

As illustrated in the last section, when fumed silica particles were used as the destabiliser for o/w emulsions, at least 0.2 wt.% of particles were needed, and no complete phase separation was obtained even with 1 wt.% of silica particles. By contrast, in the destabilisation of w/o emulsions in section 5.2, it was suggested that monodispersed silica particles start to destabilise emulsions at lower particle concentrations. Hence, in this section, hydrophobic monodispersed particles, Zonyl MP1100 and oligotetrafluoroethylene (OTFE), were rendered as the destabilisers for model o/w emulsions. These two particles are of similar hydrophobicity but different in size. Zonyl MP1100 are spherical polytetrafluoroethylene (PTFE) particles with a diameter of  $\sim 0.3 \mu\text{m}$ , whereas OTFE particles are almost spherical with a diameter of  $\sim 1.3 \mu\text{m}$ .<sup>27</sup> Before use, the contact angle of these particles at dodecane-water interfaces was determined using the sessile droplet method on compressed particle disks. The measurement was described in section 2.2.6.1. The advancing contact angle ( $\theta_{w,o}$ ) of Zonyl MP 1100 particles at dodecane-water interface is  $157 \pm 1^\circ$  and the receding contact angle is  $165 \pm 5^\circ$ . The corresponding values for OTFE particles are  $161 \pm 6^\circ$  and  $162 \pm 1^\circ$ , respectively. Particles were added to dodecane-in-water emulsions ( $\phi_o = 0.5$ ) stabilised by 1 wt.% fumed silica (65% SiOH) and stirred at 300 rpm for 3 hours.

The appearance of emulsions destabilised by Zonyl MP 1100 particles is shown in Figure 5.56 (a), which is taken 24 hours after stirring. The stability of emulsions to creaming ( $f_w$ ) and coalescence ( $f_o$ ) is evaluated and represented against particle concentration in Figure 5.56 (b). The  $f_w$  in each sample appears to be remarkable the same while the  $f_o$  peaks at 0.1 wt.% of particles. Complete phase separation is not observed. Particles at 0.1 wt.% are determined as the best destabiliser. Optical microscopy of emulsions after destabilisation is shown in Figure 5.57. Large droplets in both spherical and non-spherical shape are observed. In the sample with 0.1 wt.% and 0.2 wt.% particles, large droplets almost disappear and small spots which are likely fumed silica aggregates are observed instead.

**Figure 5.56.** (a) Appearance of dodecane-in-water emulsions ( $\phi_o = 0.5$ ) stabilised with 1 wt. % fumed silica particles (65% SiOH) after adding 0.1 wt.% (relative to the mass of emulsions) Zonyl MP1100 particles at varied concentrations (given) and stirring at 300 rpm for three hours. Photos were taken 24 hours after stirring. (b) The  $f_w$  (squares) and  $f_o$  (circles) of emulsions in (a) against Zonyl MP1100 particle concentration.

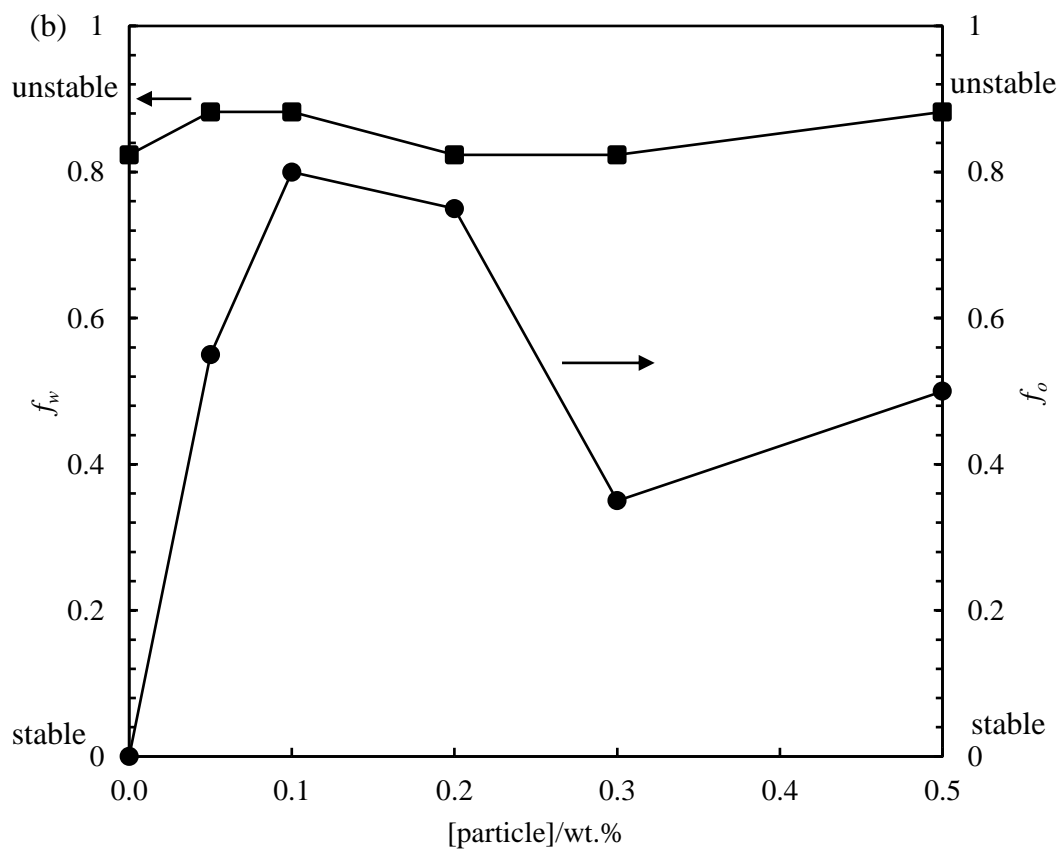
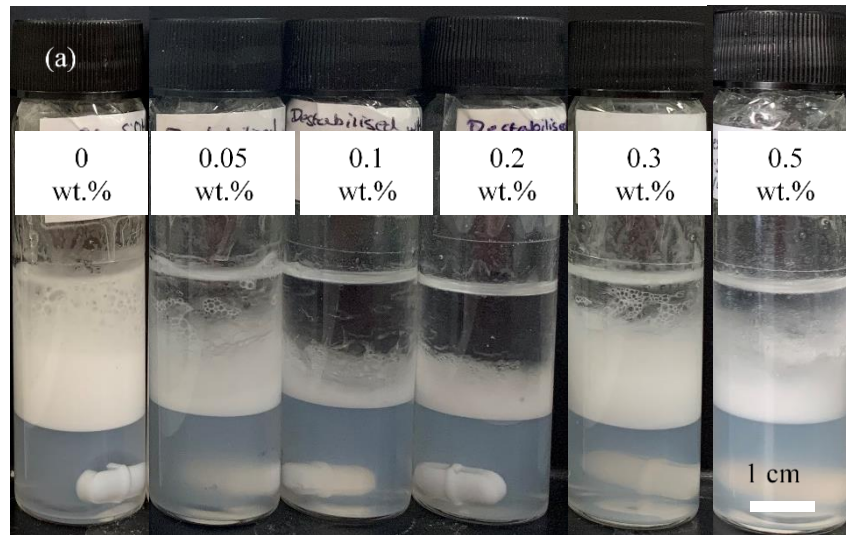
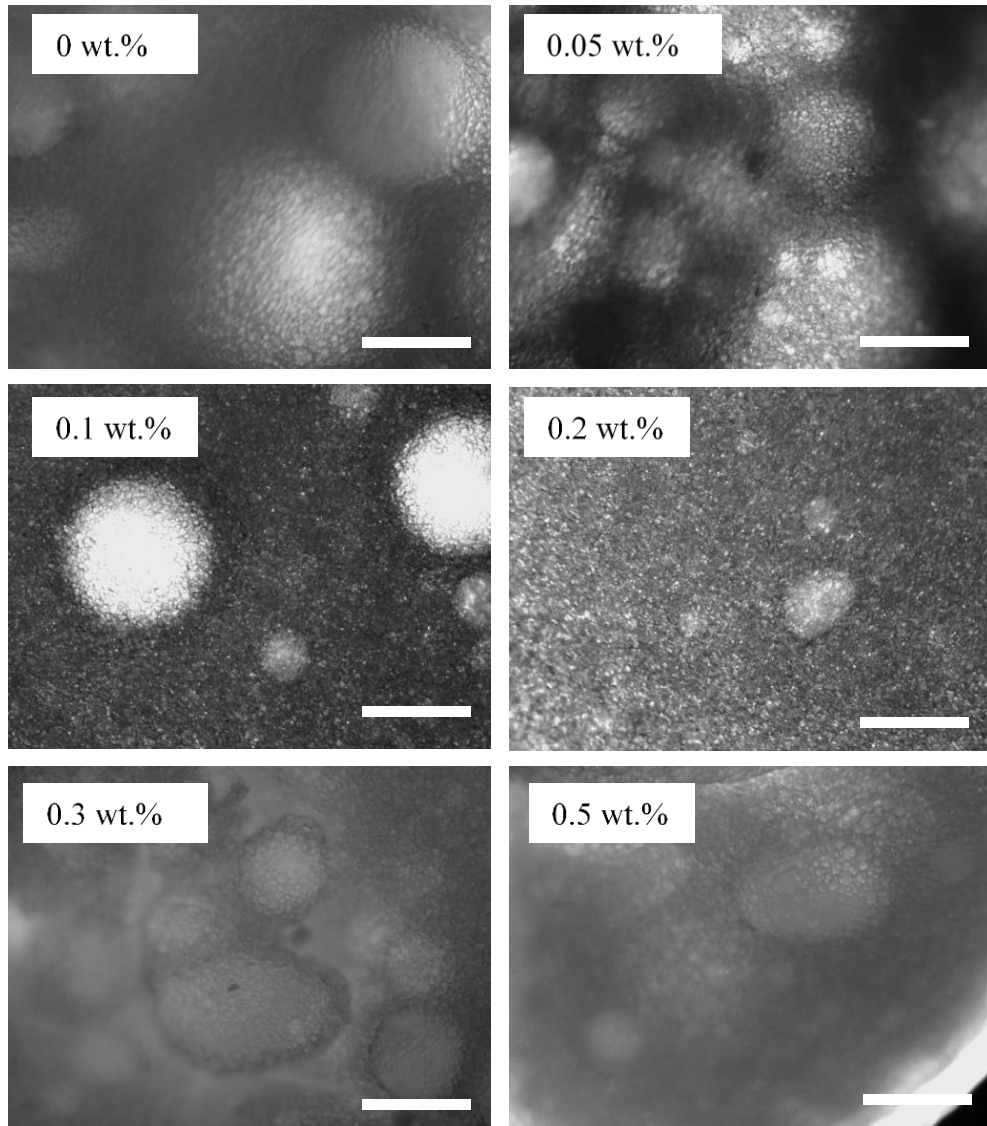


**Figure 5.57.** Optical microscopy of dodecane-in-water emulsions ( $\phi_o = 0.5$ ) stabilised by 1 wt. % fumed silica particles (65% SiOH) after adding 0.1 wt.% (relative to the mass of emulsions) Zonyl MP1100 particles at varied concentrations (given) and stirring at 300 rpm for three hours. Samples are taken from the large oil globules layer. Scale bar = 500  $\mu\text{m}$ .



The appearance of emulsions destabilised by OTFE particles is shown in Figure 5.58 (a), and  $f_w$  and  $f_o$  of these emulsions are represented in Figure 5.58 (b) against particle concentration after the destabilisation procedure. As can be seen,  $f_w$  increases from 0.65 to a maximum at 0.9 followed by decreasing to 0.77 as the particle concentration increases. By contrast,  $f_o$  keeps zero as no free oil is observed on top of the emulsion. However, a layer of oil globules with diameters larger than 1 mm are observed on the top of a concentrated emulsion layer except for the samples with 0.2 wt.% and 0.3 wt.% particles, where only large oil globules were observed above the resolved water layer. The boundary of large droplets layer and the concentrated emulsion layer is marked on the vessels using dashed lines. Although no free oil is observed, the height of large droplets layer shows maxima at 0.2 wt.% and 0.3 wt.% particles. Comparing emulsions destabilised by the two types of particles, one can easily conclude that larger particles are less efficient in destabilising o/w emulsions. The reason is probably that larger particles are more difficult to be stirred into the continuous phase between droplets. Evidence was found in Figure 5.58 (a) where extra added OTFE particles were clearly observed attaching at the inside surface of the vessels after stirring. Another possibility is that large droplets are favoured by OTFE particles. During the coalescence of droplets, OTFE particles might combine with detached silica particles and stabilise fresh droplets under stirring. In the sample containing 0.05 wt.% OTFE particles, the resolved water phase is clear, indicating un-emulsified silica particles transferring to the emulsion layer. Optical microscopy of emulsions after destabilisation is shown in Figure 5.59. Large spherical droplets were observed on all images. On the images with more than 0.2 wt.% particles, several black spots were observed on the surface of droplets, which are likely aggregated OTFE particles.

**Figure 5.58.** (a) Appearance of dodecane-in-water emulsions ( $\phi_o = 0.5$ ) stabilised with 1 wt. % fumed silica particles with 65% SiOH groups after adding 0.1 wt.% (relative to the mass of emulsions) OTFE particles at varied concentrations (given) and stirring at 300 rpm for three hours. Photos were taken 24 hours after stirring. Red dashed lines mark the boundary between the large oil globules layer and the concentrated emulsion layer. (b) The  $f_w$  (squares) and  $f_o$  (circles) of emulsions in (a) against OTFE particle concentration.

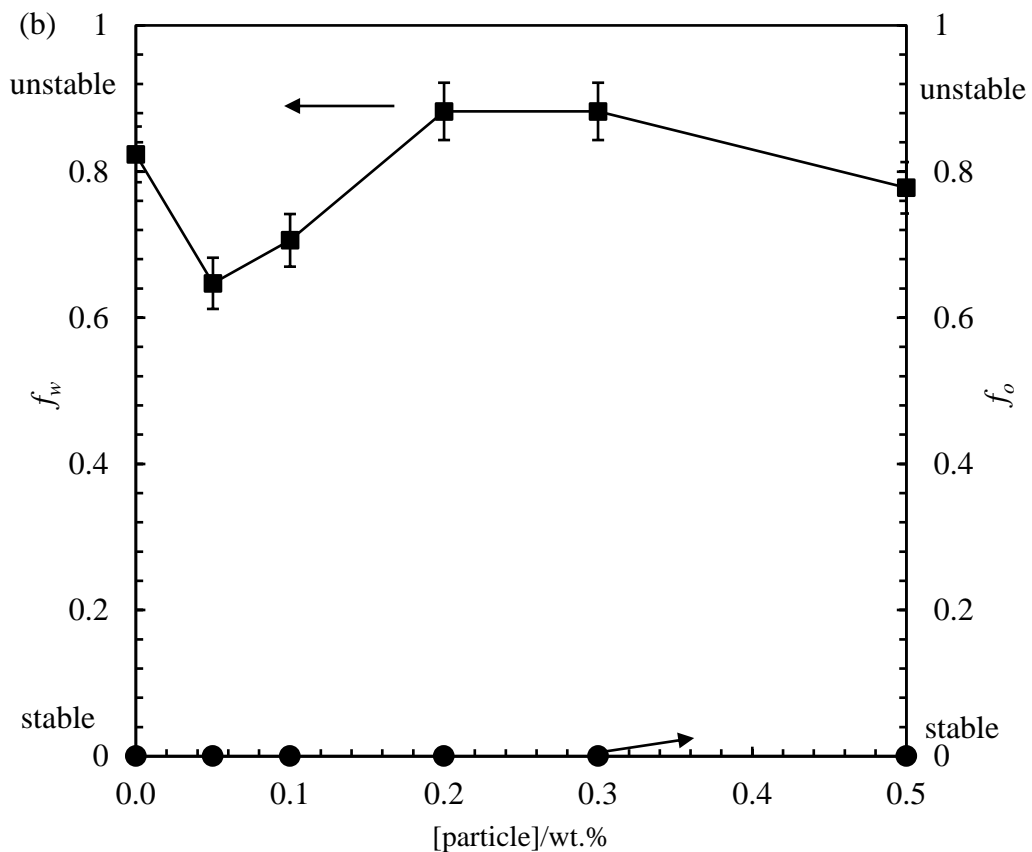
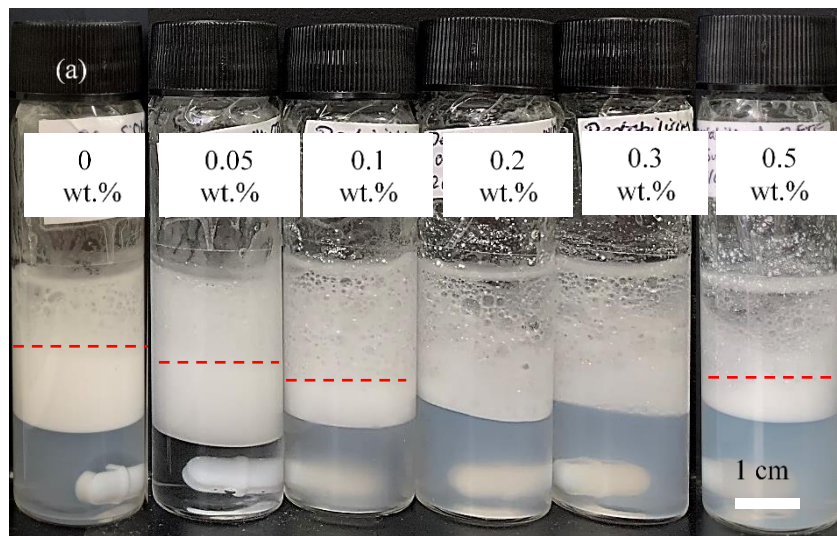
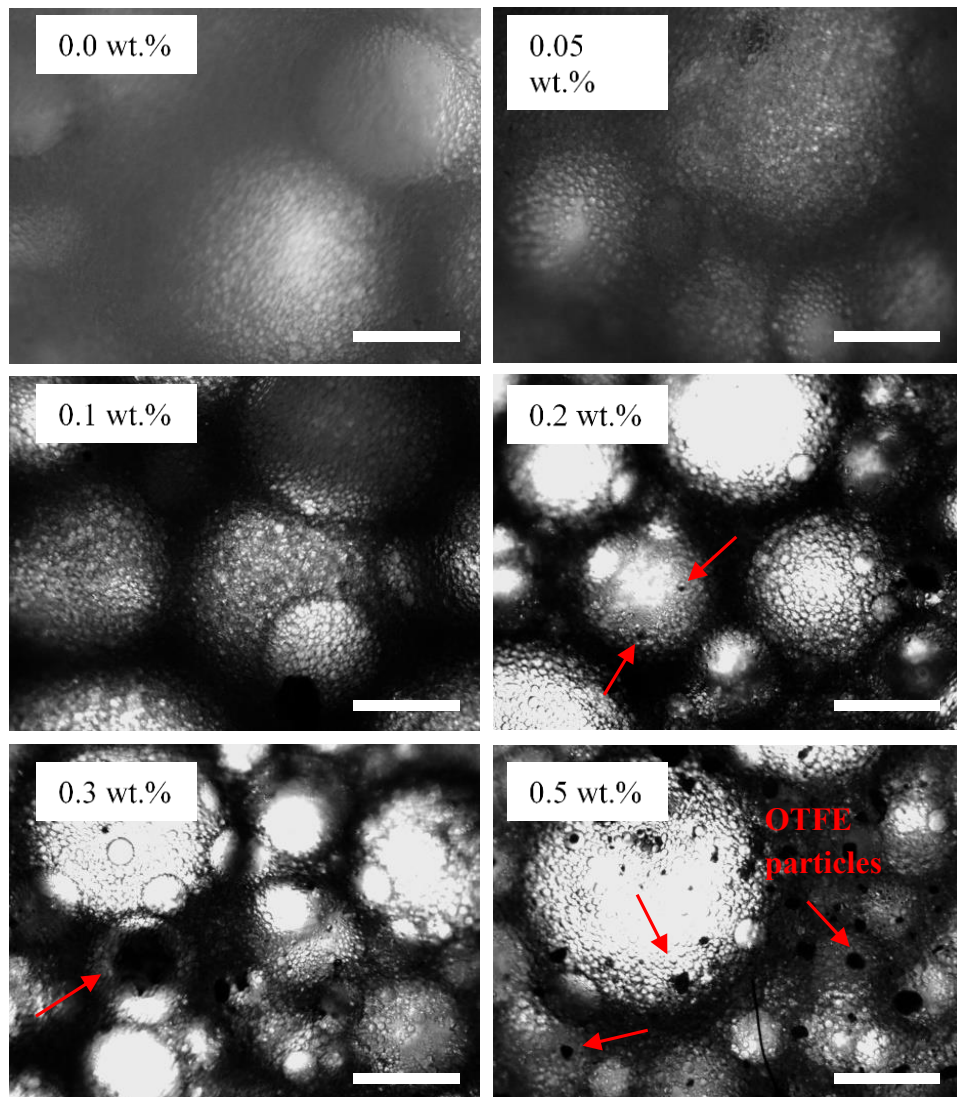


**Figure 5.59.** Optical microscopy of dodecane-in-water emulsions ( $\phi_o = 0.5$ ) stabilised with 1 wt. % fumed silica (65% SiOH) groups after adding 0.1 wt.% (relative to the mass of emulsions) OTFE particles at varied concentrations (given) and stirring at 300 rpm for three hours. Samples were taken from the large droplets layer. Red arrows point out aggregated OTFE particles at the surface of oil globules. Scale bar = 500  $\mu\text{m}$ .

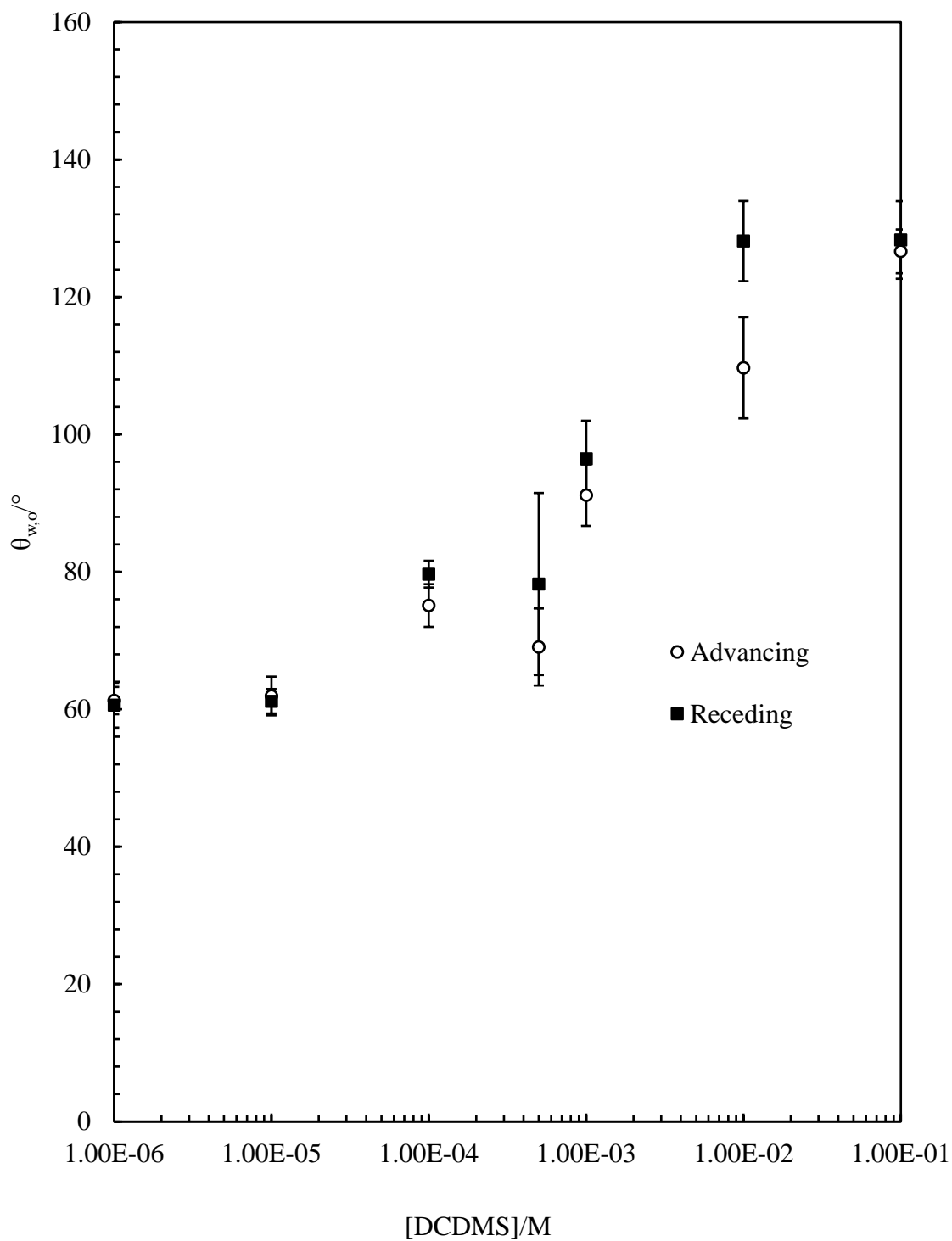


### 5.3.4 Destabilization by monodisperse silica particles

#### 5.3.4.1 Addition of 0.3 $\mu\text{m}$ silica particles of varied hydrophobicity

Monodispersed hydrophobic particles of sub-micron size have been proved more efficient in destabilising o/w emulsions stabilised by fumed silica particles. It is worth to study the effect of hydrophobicity of monodispersed particles on the destabilisation of these emulsions. In this section, hydrophilic monodispersed silica particles with a diameter of 0.3  $\mu\text{m}$  were hydrophobized by reacting with DCDMS, the hydrophobicity of particles was tuned by varying the concentration of DCDMS. The contact angle of glass slides hydrophobized with silica particles was measured at dodecane-water interfaces. As particles were added to continuous aqueous phases as destabilisers, the contact angle was measured by dropping a water on the glass slide followed by immersing the system in dodecane. Hence,  $\theta_{w,o}$  was determined. Figure 5.60 shows the advancing and receding contact angle of hydrophobized glass slides at dodecane-water interfaces against DCDMS concentration. As can be seen, higher concentrations of DCDMS give more hydrophobic substrates, and the highest  $\theta_{w,o}$  is about  $130^\circ$  for both advancing and receding results. It shows that  $\theta_{w,o}$  is about  $10^\circ$  lower than  $\theta_{o,w}$  at the same dodecane-water interfaces at corresponding DCDMS concentrations ( $\theta_{o,w}$  has been measured in section 5.2.2.3). It hints that the three-phase contact angle of particles is different depending on particles contacting with which phase first. This probably reflects on the type of emulsions stabilised by particles of intermediate hydrophobicity, o/w emulsions were preferentially stabilised for particles initially dispersed in water first, whereas w/o emulsions were obtained when particles are added from the oil phase.<sup>28</sup>

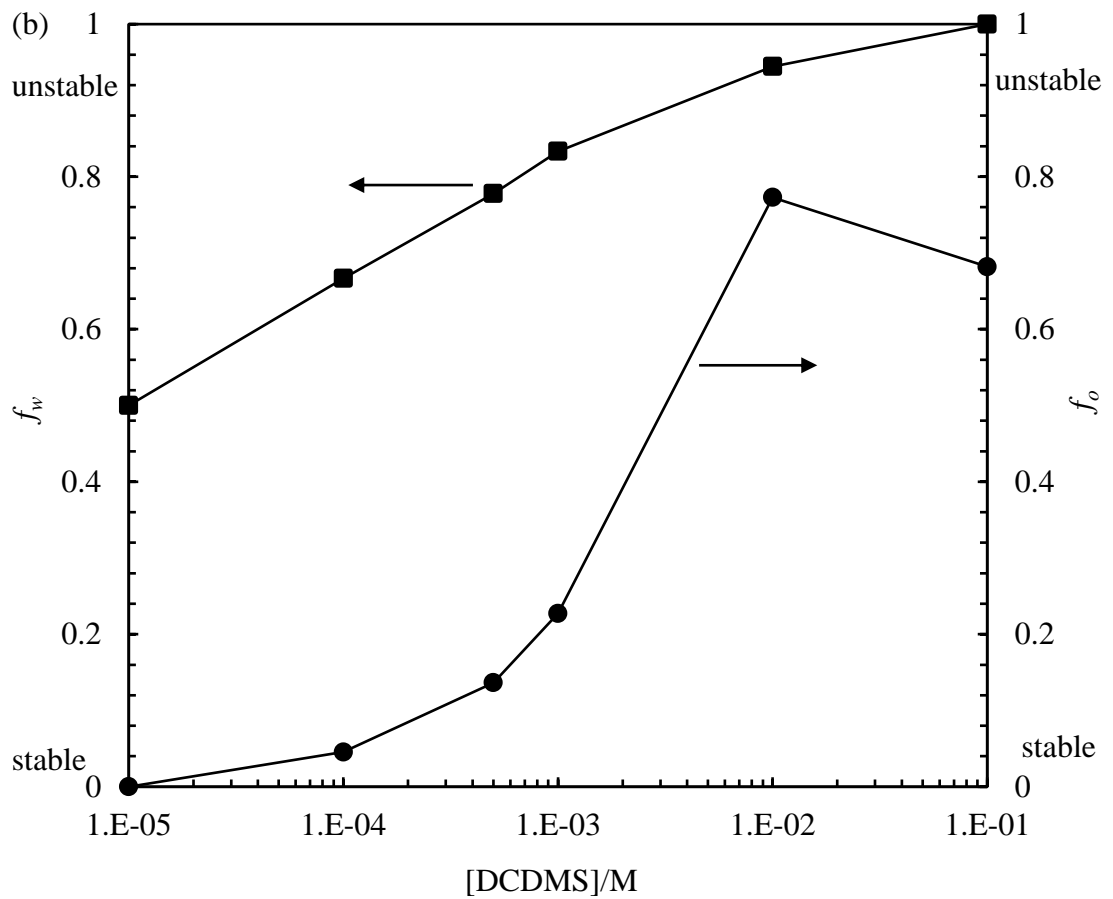
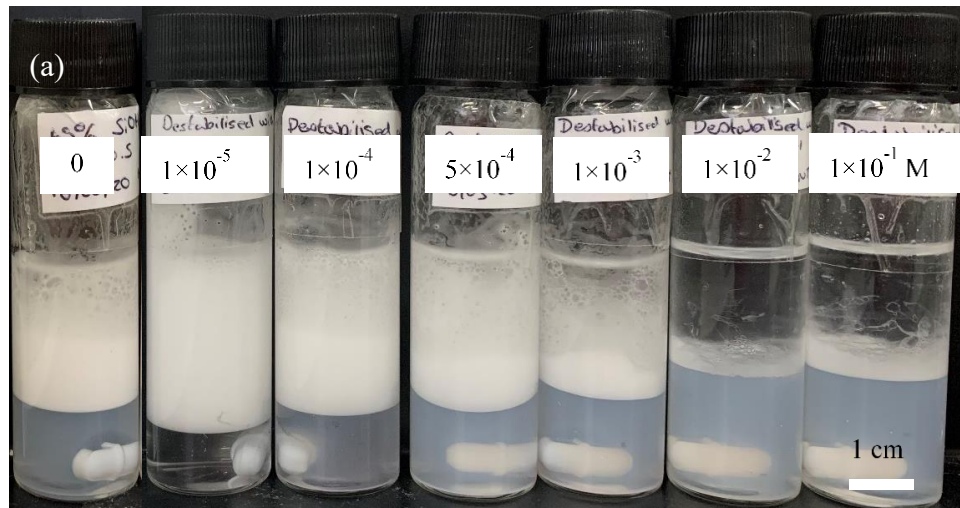
**Figure 5.60.** Three-phase contact angle ( $\theta_{w,o}$ ) of hydrophobized glass slides at dodecane-water interfaces. The glass slides were hydrophobized simultaneously with silica particles by DCDMS at varied concentrations. The advancing and receding angles are shown against DCDMS concentration.



The hydrophobized silica particles were used to destabilise o/w emulsions stabilised by 1 wt.% fumed silica particles of 65% SiOH groups. The appearance of remained emulsions after 3 hours of stirring is shown in Figure 5.61 (a), which was taken 24 hours after the stirring. Increasing of particle hydrophobicity results in higher efficiency of destabilisation. The emulsions containing the most hydrophobic particles are almost completely broken, although a thin layer of droplets is still observed. Figure 5.61 (b) represents the  $f_w$  and  $f_o$  of remained emulsions against [DCDMS]. The  $f_w$  increases gradually with [DCDMS] until 1, so does  $f_o$  until a plateau at  $1 \times 10^{-2}$  M DCDMS.

The reason why partially hydrophobic particles breaking o/w emulsions more effectively is explained as following. On one hand, highly hydrophobic particles are difficult to be stirred into the continuous phase (water) between droplets because they repel water. Particles are clearly seen attaching at the inside surface of the vessels supporting this hypothesis. In contrast, partially hydrophobic particles are wetted by both phases, which have bigger chance to be stirred into the continuous phase. Hence, higher efficiency in destabilization is obtained with partially hydrophobic particles. On the other hand, highly hydrophobic particles prefer to stay in oil. Once there is free oil released, particles would stay in the free oil and now they have to pass through two oil-water interfaces to destabilize the emulsions: the interface between free oil and continuous water and the oil-water interface of emulsion droplets. This probably explains initial fast then slow release of oil during stirring. Complete phase separation is predicted after longer stirring time. In addition, larger particles are more difficult to be stirred into the continuous phase than smaller ones. Thus, they are less efficient in the destabilization. As for hydrophobic fumed silica particles forming very big agglomerates, they are even more difficult to be stirred into the continuous phase and finally shows very low efficiency in destabilization.

**Figure 5.61.** (a) Appearance of dodecane-in-water emulsions ( $\phi_o = 0.5$ ) stabilized by 1 wt. % fumed silica particles (65% SiOH) after adding 0.1 wt.% (relative to the mass of emulsions) monodispersed silica particles ( $d = 0.3 \mu\text{m}$ ) hydrophobized by DCDMS at varied concentrations (given) and stirring at 300 rpm for three hours. Photos were taken 24 hours after stirring. (b) The  $f_w$  (squares) and  $f_o$  (circles) of emulsions in (a) against DCDMS concentration.



#### 5.3.4.2 Addition of 0.3 $\mu\text{m}$ silica particles of varied concentration

A set of dodecane-in-water emulsions ( $\phi_o = 0.5$ ) stabilised by 1 wt.% fumed silica particles (65% SiOH) were prepared. These emulsions were then destabilised by adding different concentrations of 0.3  $\mu\text{m}$  monodispersed silica particles treated with  $1 \times 10^{-2}$  M DCDMS and stirring at 300 rpm for 3 hours. The remaining emulsions can be seen in Figure 5.62 (a), photos were taken 24 hours after stirring. The  $f_w$  and  $f_o$  of remaining emulsions are represented in Figure 5.62 (b). Water is extracted from every emulsion and the volume generally increases with increasing particle concentrations. In the samples with particles at 0.3 wt.% and higher concentrations, the volume of water extracted equals to that initially added for the preparation of emulsions. Hence, almost complete phase separation occurs in these samples. Free oil starts to extract from the emulsion containing 0.025 wt.% of particles as the destabilizer. Increase of particle concentration results in a sharp increase of  $f_o$  followed by a plateau at particles higher than 0.1 wt.%. In the samples at low particle concentrations ( $\leq 0.1$  wt.%), three layers are observed in the upper oil phases, namely, a clear oil layer on the top, a layer consist of large droplets in the middle and a layer of concentrated emulsion with small droplets. By contrast, in the samples at higher particle concentrations, the concentrated emulsion droplet layers disappear, droplets in the remaining thin cloudy layers are very large. Optical microscopy of emulsions after destabilisation is shown in Figure 5.63. In the emulsions with particles  $\leq 0.05$  wt.%, samples were taken from the large droplets oil layer. Large droplets in both spherical and non-spherical shape were observed. By contrast, in the emulsions with particles  $\geq 0.1$  wt.%, samples were taken from the thin cloudy layers. globules are all deformed and aggregated. Tinny droplets adsorb on the surface of globules were observed.

**Figure 5.62.** (a) Appearance of dodecane-in-water emulsions ( $\phi_o = 0.5$ ) stabilised with 1 wt. % fumed silica particles (65% SiOH) after adding varied concentrations (given, relative to the mass of emulsions) of 0.3  $\mu\text{m}$  monodispersed silica particles hydrophobized by  $1 \times 10^{-2}$  M DCDMS and stirring at 300 rpm for three hours. Photos were taken 24 hours after stirring. (b) The  $f_w$  (squares) and  $f_o$  (circles) of emulsions in (a) against monodispersed silica particle concentration.

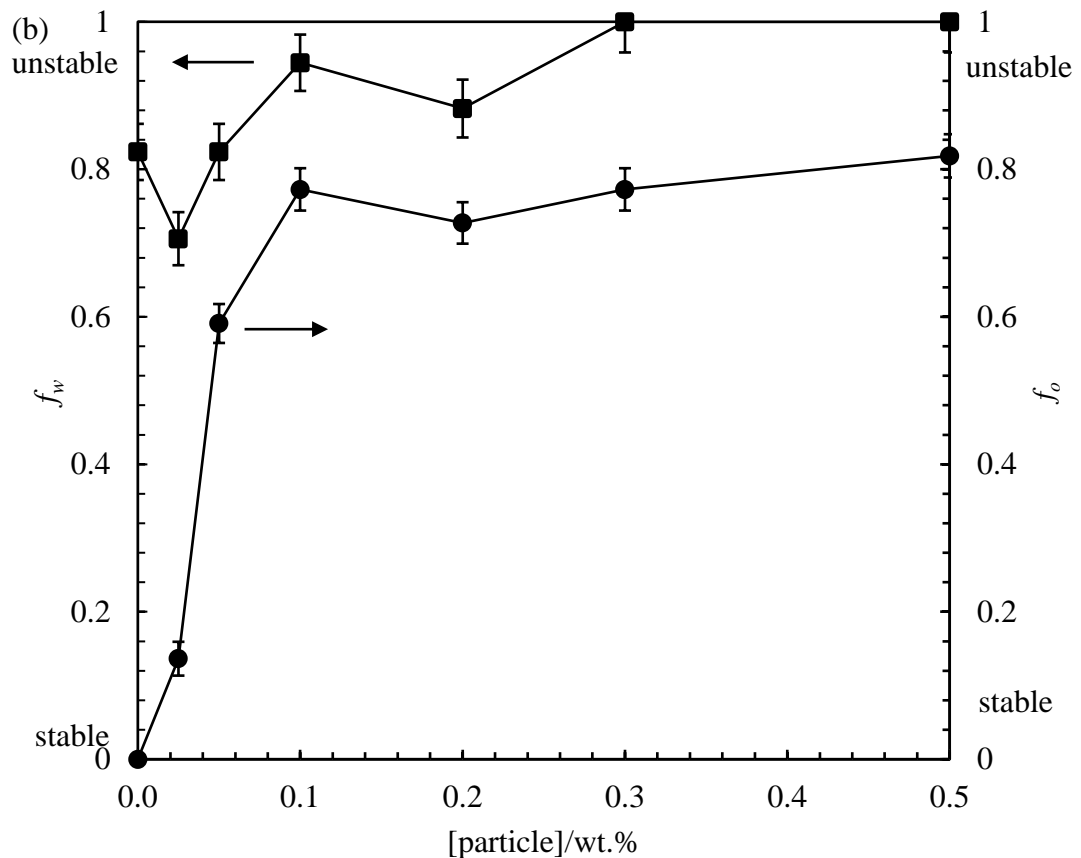
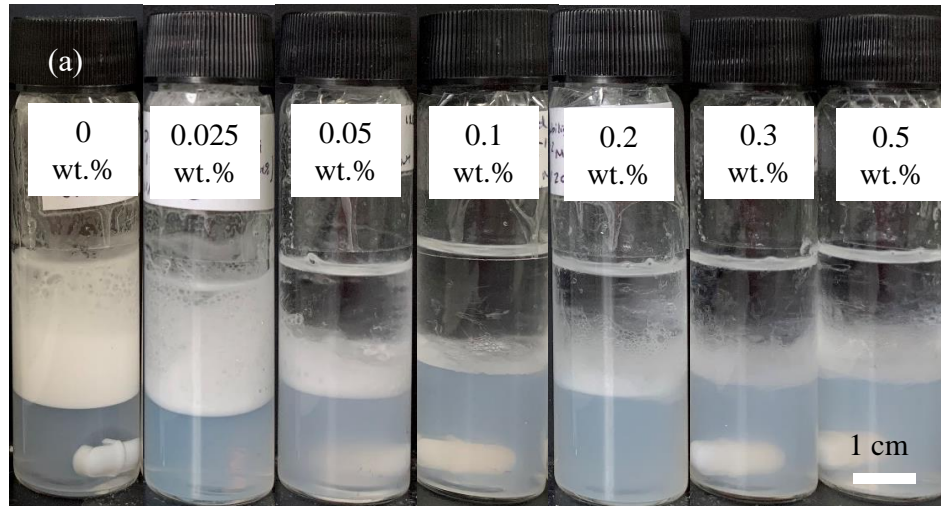
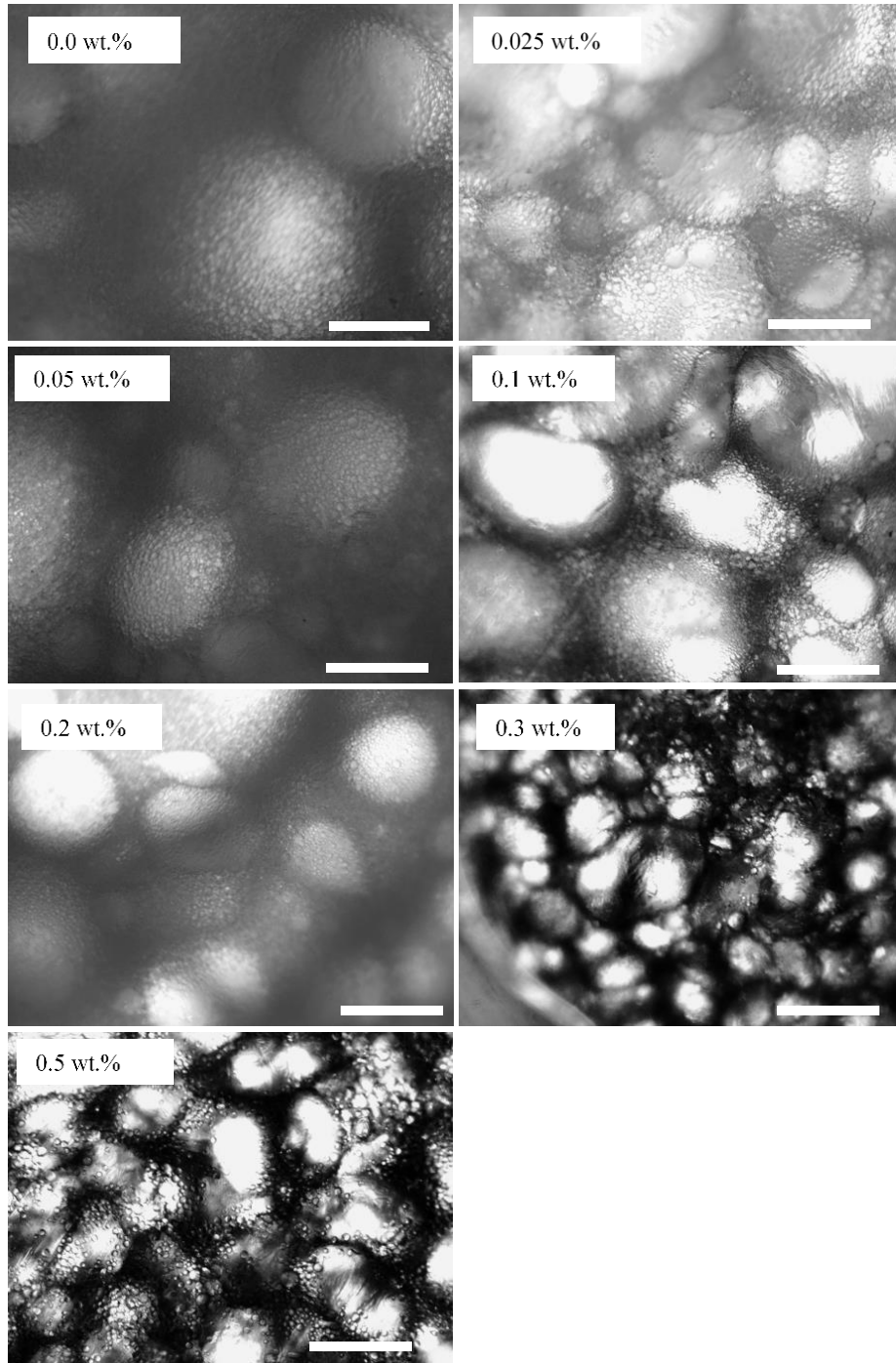


**Figure 5.63.** Optical microscopy of dodecane-in-water emulsions ( $\phi_o = 0.5$ ) stabilized by 1 wt. % fumed silica particles (65% SiOH) after adding different concentrations (given, relative to the mass of emulsions) of 0.3  $\mu\text{m}$  monodispersed silica particles treated with  $1 \times 10^{-2}$  M DCDMS and stirring at 300 rpm for 3 hours. Scale bar = 500  $\mu\text{m}$ .



## 5.4 Conclusions

In this chapter, Pickering emulsions have been destabilized by solid particles under gentle stirring. The destabilization described here is quite general since both w/o and o/w emulsions have been destabilized by different particles. The effects of size, type and concentration of particles on the destabilization efficiency have been investigated. For w/o emulsions stabilized by carboxyl latex particles, the most effective destabilizers are hydrophilic monodispersed silica particles with a diameter of 2  $\mu\text{m}$ . Complete phase separation of a model emulsion was observed by adding 0.3 wt.% of these particles after stirring at 300 rpm for 4.5 hours. In the case of sub-micron sized silica particles, 0.025 wt.% of 0.3  $\mu\text{m}$  silica particles were able to break 90% of model emulsions, although complete phase separation was not observed. Increase of particle size results in a slight decrease of destabilizing efficiency. Fumed silica particles are generally less effective than monodispersed ones in the destabilization. Complete hydrophilic fumed silica particles (100% SiOH) were unable to destabilize w/o emulsions, while those with moderate hydrophobicity (79% SiOH) result in a recovery of 80% initial water after 5 hours of gentle stirring.

The destabilization of o/w emulsions stabilized by fumed silica particles have also been studied. Partially hydrophobic particles are preferred for the destabilization. Addition of 0.5 wt.% partially hydrophobic fumed silica particles (33% SiOH) obtained a recovery of 65% initial oil, while highly hydrophobic (15 % SiOH) or hydrophilic (61% SiOH) silica particles were unable to destabilize model o/w emulsions at all. In addition, increase of particle concentration results in increase of destabilizing efficiency. Addition of 1 wt.% fumed silica particles (33% SiOH) results in a recovery of 90% initial oil. Monodispersed particles are relatively effective in the destabilization of o/w emulsions. Nearly complete phase separation occurs in the presence of 0.1 wt.% hydrophobic silica particles (hydrophobized by  $1 \times 10^{-2}$  M DCDMS) with a diameter of 0.3  $\mu\text{m}$  or Zonyl MP 1100 particles ( $d = 0.3 \mu\text{m}$ ). However, larger particles such as OTFE ( $d = 1.3 \mu\text{m}$ ) are less efficient in the destabilization, although the hydrophobicity of OTFE particles is almost the same as that of Zonyl MP 1100 particles. This is probably due to that large particles are difficult to be dispersed into the continuous phase between oil droplets, thus, get less chance to adsorb onto droplet surface, which is essential for the destabilization process.

The mechanism of Pickering emulsions stabilized by solid particles has been deduced. Fresh added particles are dispersed in the continuous phase between droplets, which enables them attach onto droplet surfaces. The preferred particles as the destabilizers are more wetted by the inner phase of emulsion droplets than the continuous phase. In this case, the adsorption of particles on droplet surface will induce particles to protrude into the inner phase of droplets through the oil/water interface, which breaks the droplet surface and finally result in the coalescence of emulsions. Hence, in order to achieve an ideal destabilization efficiency of Pickering emulsions, particles more wetted by the inner phase of droplets are preferred as the destabilizers. In the practical application, monodispersed particles with relatively small size are likely more effective than large particles or particle agglomerates.

## 5.5 References

1. Chevalier, Y. and Bolzinger, M.A. Emulsions stabilized with solid nanoparticles: Pickering emulsions. *Colloids Surf. A* **2013**, *439*, 23-34.
2. Yuan, S.; Tong, M. and Wu, G. Destabilization of emulsions by natural minerals. *J. Hazard. Mater.* **2011**, *192*, 1882-1885.
3. Furtado, G.F.; Picone, C.S.; Cuellar, M.C. and Cunha, R.L. Breaking oil-in-water emulsions stabilized by yeast. *Colloids Surf. B* **2015**, *128*, 568-576.
4. Tang, J.T.; Quinlan, P.J. and Tam, K.C. Stimuli-responsive Pickering emulsions: recent advances and potential applications. *Soft Matter* **2015**, *11*, 3512-3529.
5. Dyab, A.K. Destabilisation of Pickering emulsions using pH. *Colloids Surf. A* **2012**, *402*, 2-12.
6. Hwang, K.; Singh, P. and Aubry, N. Destabilization of Pickering emulsions using external electric fields. *Electrophoresis* **2010**, *31*, 850-859.
7. Melle, S.; Lask, M. and Fuller, G.G. Pickering emulsions with controllable stability. *Langmuir* **2005**, *21*, 2158-2162.
8. Whitby, C.P. and Wanless, E.J. Controlling pickering emulsion destabilisation: a route to fabricating new materials by phase inversion. *Materials* **2016**, *9*, 626.
9. Whitby, C.P.; Fornasiero, D. and Ralston, J. Structure of oil-in-water emulsions stabilised by silica and hydrophobised titania particles. *J. Colloid Interface Sci.* **2010**, *342*, 205-209.

10. Griffith, C. and Daigle, H. Destabilizing Pickering emulsions using fumed silica particles with different wettabilities. *J. Colloid Interface Sci.* **2019**, *547*, 117-126.
11. Vashisth, C.; Whitby, C.P.; Fornasiero, D. and Ralston, J. Interfacial displacement of nanoparticles by surfactant molecules in emulsions. *J. Colloid Interface Sci.* **2010**, *349*, 537-543.
12. Yan, N. and Masliyah, J.H. Characterization and demulsification of solids-stabilized oil-in-water emulsions Part 2. Demulsification by the addition of fresh oil. *Colloids Surf. A* **1995**, *96*, 243-252.
13. Whitby, C.P.; Anwar, H.K. and Hughes, J. Destabilising Pickering emulsions by drop flocculation and adhesion. *J. Colloid Interface Sci.* **2016**, *465*, 158-164.
14. Whitby, C.P.; Fischer, F.E.; Fornasiero, D. and Ralston, J. Shear-induced coalescence of oil-in-water Pickering emulsions. *J. Colloid Interface Sci.* **2011**, *361*, 170-177.
15. Kruglyakov, P.; Nushtayeva, A. and Vilкова, N. Experimental investigation of capillary pressure influence on breaking of emulsions stabilized by solid particles. *J. Colloid Interface Sci.* **2004**, *276*, 465-474.
16. Eral, H. and Oh, J. Contact angle hysteresis: a review of fundamentals and applications. *Colloid Polym. Sci.* **2013**, *291*, 247-260.
17. Yan, Y. and Masliyah, J.H. Solids-stabilized oil-in-water emulsions: scavenging of emulsion droplets by fresh oil addition. *Colloids Surf. A* **1993**, *75*, 123-132.
18. Horozov, T.S. and Binks, B.P. Particle-Stabilized Emulsions: A Bilayer or a Bridging Monolayer? *Angew. Chem. Int. Ed.* **2006**, *118*, 787-790.
19. French, D.J.; Taylor, P.; Fowler, J. and Clegg, P.S. Making and breaking bridges in a Pickering emulsion. *J. Colloid Interface Sci.* **2015**, *441*, 30-38.
20. Bon, S.A.; Mookhoek, S.D.; Colver, P.J.; Fischer, H.R. and van der Zwaag, S. Route to stable non-spherical emulsion droplets. *Eur. Polym. J.* **2007**, *43*, 4839-4842.
21. Nakagawa, N. and Nonomura, Y. Drying process of emulsions stabilized by solid particles. *Chem. Lett.* **2011**, *40*, 818-819.
22. Datta, S.S.; Shum, H.C. and Weitz, D.A. Controlled buckling and crumpling of nanoparticle-coated droplets. *Langmuir* **2010**, *26*, 18612-18616.

23. Binks, B.P.; Philip, J. and Rodrigues, J.A. Inversion of silica-stabilized emulsions induced by particle concentration. *Langmuir* **2005**, *21*, 3296-3302.
24. Binks, B.P. and Lumsdon, S.O. Transitional phase inversion of solid-stabilized emulsions using particle mixtures. *Langmuir* **2000**, *16*, 3748-3756.
25. Whitby, C.P. and Krebsz, M. Coalescence in concentrated Pickering emulsions under shear. *Soft Matter* **2014**, *10*, 4848-4854.
26. Vella, D.; Aussillous, P. and Mahadevan, L. Elasticity of an interfacial particle raft. *Europhys. Lett.* **2004**, *68*, 212-218.
27. Binks, B.P.; Rocher, A. and Kirkland, M. Oil foams stabilised solely by particles. *Soft Matter* **2011**, *7*, 1800-1808.
28. Binks, B.P. and Lumsdon, S.O. Effects of oil type and aqueous phase composition on oil-water mixtures containing particles of intermediate hydrophobicity. *Phys. Chem. Chem. Phys.* **2000**, *2*, 2959-2967.

## CHAPTER 6

### SUMMARY OF CONCLUSIONS AND FUTURE WORK

#### 6.1 Summary of conclusions

This thesis was aimed at understanding the behavior of solid particles at oil-water interfaces. Chapter 3 and Chapter 4 investigated the adsorption of particles onto oil-water interfaces in the presence of organic electrolytes, whereas chapter 5 investigated the desorption of particles from oil-water interfaces using added solid particles. The findings in this thesis suggest new methods to stabilize Pickering emulsions, *i.e.*, by using organic electrolytes to promote the adsorption of particles onto oil-water interfaces. This methodology applies to both hydrophilic silica particles and partially hydrophobic polystyrene particles. In addition, the outcomes in chapter 5 opens the potential application of destabilizing Pickering emulsions and recovering oils and particles from emulsions. The conclusions of each chapter are summarized as:

Chapter 3 investigated the properties of silica particles in aqueous dispersions and at oil-water interfaces in the presence of symmetrical tetraalkylammonium salts,  $R_4NX$ , where R represents a hydrophobic alkyl chain varying from methyl to butyl and X is an anion. Ludox HS-30 silica nanoparticles are highly charged and discrete in aqueous dispersions. Addition of  $R_4NX$  salts decreased the zeta potential of particles progressively with concentration, with an increase of R chain length being more effective. This was attributed to specific adsorption of  $R_4N^+$  ions on silica particle surfaces reducing the surface charge. However, unlike indifferent salts, the presence of these  $R_4NX$  salts did not coagulate the particles.

The adsorption of  $R_4N^+$  ions on silica particles also increased the particle hydrophobicity which enhanced the stability of emulsions. The methyl analogue did not promote emulsification of Ludox-HS 30 silica particles at any concentration studied, while the ethyl, propyl, and butyl analogues favoured the stabilisation of octane-in-water emulsions at certain concentrations. The stability of emulsions to both creaming and coalescence increased with salt concentration as well as R chain length. In addition, the butyl analogues behaved like a cationic surfactant with the same number of carbon atoms in the hydrophobic chains, *i.e.* cetyltrimethylammonium

bromide, in terms of its ability to enhance the stabilisation of emulsions.

The effect of particle concentration on the stability of emulsions was also studied. The stability of emulsions increased with particle concentration. The emulsion droplet size was consistent with the limited coalescence phenomenon: increase of particle concentration resulted in a decrease of droplet size until reaching a plateau. However, high concentrations of particles in the presence of 5 mM tetraethylammonium nitrate (TEANO<sub>3</sub>) failed to stabilise emulsions, which was attributed to limited adsorption of TEA<sup>+</sup> cations on particle surfaces. At a fixed salt concentration and high particle concentrations, limited TEA<sup>+</sup> ions adsorbed on particle surfaces such that particles were not hydrophobic enough to stabilise emulsions.

The enhanced stability of emulsions by adding the most hydrophobic analogue to Ludox HS-30 silica particles also applied to micron-sized silica particles. For emulsions prepared at a fixed particle concentration, their stability to coalescence gradually increased with salt concentration. The arrangement of the particles at the droplet surface changed from random loose packing to hexagonally closed packing then to multilayer aggregation as salt concentration increased. When spread at a planar oil-water interface, most particles transferred directly into water when pure water was used as the aqueous phase. By contrast, in the presence of salt, particles remain adsorbed at the interface forming loose packing - hexagonal close packing - loose packing as salt concentration increased.

Chapter 4 explored emulsions stabilised by partially hydrophobic polystyrene latex particles in the presence of oppositely charged ions to that of particles which were reported to induce charge reversal of particles. Particles with three types of surface groups (sulfate, amidine and carboxyl) were used. For systems with negatively charged particles (sulfate and carboxyl), tetrapentylammonium bromide (TPeAB) was used as the electrolyte, whereas for systems with positively charged particles (amidine), sodium thiocyanate (NaSCN) was used. The particles are partially hydrophobic but initially dispersed in water due to their surface charges.

In systems with sulfate latex particles, addition of  $1 \times 10^{-4}$  M TPeAB to aqueous dispersions caused significant aggregation of particles. Charge reversal of particles

occurred after addition of  $1 \times 10^{-3}$  M TPeAB. Emulsions with dodecane are w/o at all salt concentrations. Increase of salt concentration resulted in an increase of stability to sedimentation and coalescence while a decrease of droplet size. However, charge reversal of particles induced little specific influence on the stability or type of emulsions. The contact angles of particles at the planar dodecane-water interface measured by the gel trapping technique were all above  $90^\circ$ , consistent with w/o emulsions obtained. Addition of  $1 \times 10^{-4}$  M TPeAB increased the contact angle while increase of salt concentration resulted in a decrease of contact angle. This was attributed to the adsorption of  $\text{TPeA}^+$  ions on particle surfaces at low concentrations owing to the electrostatic attraction between  $\text{TPeA}^+$  ions and  $\text{SO}_4^-$  groups. Whereas at higher salt concentrations, the interaction was dominated by hydrophobic attraction between alkyl chains of  $\text{TPeA}^+$  ions and polystyrene surface, which resulted in the occupation of the polystyrene surface by alkyl chains probably leading to a decrease of surface hydrophobicity.

In systems with carboxyl latex particles, w/o emulsions were obtained when alkanes such as dodecane and heptane were used as the oil phase. However, when polydimethylsiloxane (PDMS) was used as the oil phase, emulsions inverted from w/o to o/w upon increasing TPeAB concentration. In addition, w/o/w emulsions were obtained at moderate TPeAB concentrations when 50 cS PDMS was used as the oil phase. The contact angles of particles at PDMS (1 cS and 50 cS)-water interfaces decreased from  $\sim 105^\circ$  to  $\sim 90^\circ$ . It seemed that a slight increase in the polarity of oil phase had a remarkable influence on the type of emulsions. However, this requires further confirmation by using even more polar oils.

The surface charge of amidine polystyrene latex particles reversed from positive to negative in the presence of  $1 \times 10^{-3}$  M NaSCN. Adsorption of  $\text{SCN}^-$  ions onto amidine latex particles was attributed to the ion specific effect. Poorly hydrated  $\text{SCN}^-$  ions adsorbed onto particle surfaces and broke the structure of water around particles, which increased their surface hydrophobicity. Emulsions of dodecane stabilised by these particles are w/o at all salt concentrations, whereas the contact angles increased from  $75^\circ$  to  $105^\circ$  with the increase of salt concentration.

It was initially predicted that o/w emulsions be stabilised at low electrolyte concentrations where particles were highly charged; w/o emulsions at moderate electrolyte concentrations where charge neutralization of particles occurred and o/w emulsions again at high electrolyte concentrations where particles were highly charged again after charge reversal. However, as summarized above, the experimental results turned out that w/o emulsions with dodecane were obtained from all the three types of particles. The surface charge of particles played a minor role in determining the type of emulsions. It appears that the emulsion type was dominated by the hydrophobic polystyrene portion since polystyrene occupied at least 90% of the particle surface.

Chapter 5 focused on the destabilisation of Pickering emulsions using solid particles. Emulsion stabilised by 2 wt.% carboxyl latex particles at pH 3 described in Chapter 4 was used the model w/o emulsions. Model o/w emulsions were stabilised by fumed silica particles of 65% SiOH groups. During the destabilization process, solid particles were added to the model emulsions followed by gentle stirring at 300 rpm.

For w/o emulsions stabilised by carboxyl latex particles, monodisperse silica particles as well as fumed silica particles were employed as destabilisers. It was found that monodisperse silica particles are generally more efficient than fumed silica particles in destabilising the model emulsion. In addition, smaller particles are more efficient than larger ones, and relatively lower particle concentrations are preferred. Complete phase separation of emulsions was observed after adding 0.3 wt.% hydrophilic monodisperse silica particles ( $d = 2 \mu\text{m}$ ) under stirring at 300 rpm for 4.5 hours. The hydrophobicity of monodisperse particles surprisingly showed little influence on the destabilising efficiency. By contrast, in systems with fumed silica particles, slightly hydrophilic particles were more efficient than hydrophobic ones. However, completely hydrophilic fumed silica particles showed no capability of destabilization.

By tracing the position of silica particles during the destabilisation process using cryo-SEM and EDX, the mechanism of Pickering emulsion destabilisation by solid particles was deduced. Fresh added destabiliser enters the inner phase of droplets from the continuous phase between droplets with the help of gentle stirring, which means they traverse the interface and disrupt the droplet surface causing droplet coalescence.

It was speculated that particles more wetted by the inner phase were preferred as the destabilisers.

The mechanism above also applies to the destabilisation of o/w emulsions stabilised by fumed silica particles. Partially hydrophobic particles were preferred for the destabilisation in the case of both monodisperse and fumed silica particles. Nearly complete phase separation was observed in the presence of 0.1 wt.% PTFE particles or monodisperse silica particles ( $d = 0.3 \mu\text{m}$ ) hydrophobized by  $1 \times 10^{-2}$  M of DCDMS. Larger monodisperse OTFE particles ( $d = 1.3 \mu\text{m}$ ) are less efficient than PTFE particles ( $d = 0.3 \mu\text{m}$ ) in destabilising the model emulsions, although their hydrophobicity is almost the same. In conclusion, for practical applications, monodispersed particles relatively more wetted by the inner phase of droplets are preferred for the destabilization of Pickering emulsions.

## 6.2 Future work

The following ideas are suggested from the work presented in the thesis.

Chapter 3 focused on systems containing negatively charged silica particles and positively charged tetraalkylammonium salts. As an idea of future work, it is suggested to extend the system to positively charged particles, *e.g.* alumina, and negatively charged ions, *e.g.* tetraphenylborate ions, to see whether the mechanism of organic electrolyte promoting hydrophilic particles to stabilise emulsions applies to other systems. In addition, it was reported that hydrophilic particles were able to stabilise emulsions if they were dispersed in the oil phase before emulsification.<sup>1</sup> It is worth exploring the stabilisation of Pickering emulsions by adding hydrophilic particles and organic electrolytes in the oil phase.

In Chapter 4, w/o emulsions were obtained for all the three types (sulfate, carboxyl and amidine) of polystyrene latex particles when dodecane is used as the oil phase. However, phase inversion was observed in emulsions stabilised by carboxyl latex particles when PDMS is used as oil. It is therefore worth further investigating the effect of oil polarity on the stability and type of emulsions stabilised by these particles. Chapter 4 has shown that organic electrolytes such as tetrapentylammonium bromide induced limited influence on the stability and type of emulsions. It is worth

trying with surfactants which are probably more strongly adsorbed on particle surfaces. Will they induce significant modification on the polystyrene surface and even induce phase inversion of emulsions stabilised by modified particles?

For the destabilisation of Pickering emulsions, further study is suggested on adding oppositely charged particles to those used for the preparation of emulsions. When oppositely charged particles are added, heteroaggregates of particles should form which may detach from droplet surfaces and result in emulsion destabilisation. On the other hand, it will be interesting to study other types of particles, for example, magnetic particles or electric field-responsive particles as the destabiliser, which make it possible to break general emulsions using a magnetic or electric field.

### 6.3 References

1. Marina, P.F.; Xu, J.; Wu, X. and Xu, H. Thinking outside the box: placing hydrophilic particles in an oil phase for the formation and stabilisation of Pickering emulsions. *Chem. Sci.* **2018**, *9*, 4821-4829.